

IN-39

30107

p. 172

NASA Contractor Report 195383

# Discrete-Layer Piezoelectric Plate and Shell Models for Active Tip-Clearance Control

P.R. Heyliger, G. Ramirez, and K.C. Pei  
*Colorado State University*  
*Fort Collins, Colorado*

October 1994

Prepared for  
Lewis Research Center  
Under Grant NAG3-1520



National Aeronautics and  
Space Administration

(NASA-CR-195383) DISCRETE-LAYER  
PIEZOELECTRIC PLATE AND SHELL  
MODELS FOR ACTIVE TIP-CLEARANCE  
CONTROL Final Report (Colorado  
State Univ.) 170 p

N95-14417

Unclass

G3/39 0030107

## TABLE OF CONTENTS

1. INTRODUCTION .....	1
Project Objectives .....	1
Structure of Report .....	1
2. BACKGROUND .....	3
Literature Review .....	3
Linear Theory of Piezoelectricity .....	8
3. SEMI-ANALYTIC SOLUTIONS .....	13
Governing Equations .....	13
Finite Element Approximation .....	16
4. THE PLATE ELEMENT .....	21
Governing Equations .....	21
Discrete-Layer Approximations .....	25
Transformation Matrices .....	31
5. THE SHELL ELEMENT .....	34
Variational Formulation in Cylindrical Coordinates .....	34
Variational Formulation in Curvilinear Coordinates .....	36
Discrete-Layer Theories .....	40
Dynamic Analysis .....	52
Computational Models .....	55
6. EXACT SOLUTIONS .....	56
Introduction .....	56
Exact Solution .....	57
7. NUMERICAL EXAMPLES AND RESULTS .....	68
The Plate Element .....	68
Semi-Analytic Solutions .....	76
Exact Solution .....	82
8. SUMMARY AND FUTURE WORK .....	91
COMPILATION OF FIGURES .....	93
REFERENCES .....	155
APPENDIX .....	158

## ACKNOWLEDGEMENT

The study that yielded the developments and results presented in this report was sponsored by a grant from NASA-Lewis Research Center (NAG3-1520). The authors gratefully acknowledge this support and that of the grant monitor, Dale Hopkins, and the technical monitor, Dimitris Saravanos.

## 1. INTRODUCTION

### Project Objectives

The primary objectives of this research project, as stated in the initial proposal by the first author of this report, were to develop the following computational tools for use in active tip-clearance control:

- A discrete-layer plate theory (both semi-analytic and finite element approximations) for laminated composites structures with embedded piezoelectric layers.
- A 3-D general discrete-layer element generated in curvilinear coordinates with constant out-of-plane displacement components for modeling laminated composite piezoelectric shells with curved surfaces. This tool will be used to represent the general geometries of the engine blades and the casing.

This report describes the theoretical developments and implementation of these models as well as additional work completed as part of this study. Conclusions regarding the nature and performance of these models are presented, and additional testing and applications are suggested.

### Structure of Report

The primary components of this research were the theoretical development and introduction of finite element models and semi-analytic solutions using discrete-layer approximations for the analysis of laminated piezoelectric plates and shells. These models form the basic thrust and results of the present study. However, as part of this development, it was found necessary to develop an additional component as both a check and a computational alternative for the plate geometry. This additional component involved the development of exact solutions for the static and dynamic behavior of simply-supported laminated piezoelectric plates. Although not included in the original proposal, the development of the exact solutions was critical to the successful development of the plate element because there are effectively no other results in the literature for laminated piezoelectric plates other than very simple approximate models. The exact solutions filled a needed gap in the understanding of these laminates, and because their development was completed under the auspices of this project, the results are included here.

The following chapter gives a brief review of the literature to describe the current state-of-the-art in the field of control using active materials, with emphasis given to piezoelectric

materials. Also given in this chapter is an overview of the linear theory of piezoelectricity and the governing equations to be used in the following chapters. In the third chapter, semi-analytic solutions developed for the plate geometry are described. The fourth and fifth chapters give the development of the plate and shell elements, respectively, for laminated piezoelectric solids using the discrete-layer theory. The sixth chapter details the development of the exact solutions for the static and dynamic behavior of simply-supported piezoelectric laminates. The seventh chapter contains representative example problems for the models developed in the previous chapters. A discussion of potential future work and summary are given in the eighth and final chapter.

## 2. BACKGROUND

This section includes a review of the literature regarding both discrete-layer theories and so-called smart structures as these topics apply to the present study. The fundamental equations related to the linear theory of piezoelectricity are also included in this section, and are provided as a useful foundation for the chapters that follow.

### Literature Review

#### *Piezoelectricity*

In 1880, Pierre and Jacques Curie discovered that the electrical charges on certain dielectric crystal could be produced by impressing mechanical stress. Later in 1881, Hankle named this direct and its converse effect "piezoelectricity". With the knowledge of solid mechanics and electricity, the mathematical foundations and governing equations were available and used in the original work of Voight [63]. In addition to this volume, two other classical works of Mason [64] and Cady [66], are cited frequently in latter studies of piezoelectricity. Both works gave a special attention in the physical properties of crystals, as well as practical applications.

Several works published in 1960's initiated the numerical solution of problems involving piezoelectric solids. In 1967, Eer Nisse introduced the variational calculus and a Ritz-approximation for analyzing electroelastic vibration problems [5, 6]. In his work, variational formulas were derived for the equations of motion of piezoelectric cylinders and were applied to find the resonant frequencies of thick discs. This application gave a beginning for latter studies using numerical approximation. The monograph of Tiersten [67], provides a comprehensive treatment and application of the linear theory of piezoelectricity. In this book, a systematic derivation of the governing equations of linear piezoelectricity were given, and results of homogeneous plate vibration problems were shown. In later works dealing with piezoelectric vibrations, this monograph is without question the most oft-cited reference.

On the basis of the works of Eer Nisse [5, 6], Holland [7] presented an application to rectilinear geometry. With specified trial functions, the resonant properties of piezoelectric ceramic rectangular parallelepipeds were discussed, as well as several mode shapes were contoured. To avoid the limitation of using Ritz-approximation under complicated boundary conditions, Allik and Hughes [9] introduced a finite element formulation for the

equations of piezoelectricity. A electroelastic tetrahedral element was also developed in this work but without further application and numerical results. This work began the efforts of using modern computational techniques to represent the behavior of piezoelectric solids.

Several studies have appeared using finite element approximations to the equations of linear piezoelectricity. Kagawa and Yamabuchi [14] developed a computer program to solve the axisymmetric vibrations of a piezoelectric circular rod of finite length. Later in the 1980's, several piezoelectric structures were analyzed by Naillon et al. [20], as well as three-dimensional structures by Ostergaard and Pawlak [25]. Being different from Eer Nisse's approximation [6], Kunkel et al. [38] used the finite element method to find the natural vibrational mode of axially symmetric piezoelectric ceramic disks.

Three volumes, which are not referred here but have been cited frequently in recent studies, are the works of Nye [68], Bottom [71] and Zelenka [72]. These books provide details and more recent information on the properties of (quartz) crystals. In Zelenka's book, Piezoelectric resonators and non-linear properties of crystal are an area of focus.

#### *Theories of Thick Laminates*

The classical laminated plate theory (CLPT), which is a direct extension of classical plate theory (CPT), has been used to solve many composite plate problems for years. Because the assumed Kirchhoff hypothesis remains in CLPT, the thickness effect, which is known to cause poor results when analyzing thick plates with the use of CPT, similarly occurs when using CLPT to analyze thick laminates. According to the literature reviews of several studies [32, 43, 44], the initial work to take into account the thickness effect could be credited to Basset [1] in 1890. After this work, several displacement-based refined theories developed by Hidebrand, Reissner and Thomas [2], as well as Mindlin [3], were extremely useful to later studies dealing with the transverse stresses in plates. Another commonly used book is that of Timoshenko [65], which gives development of a generalized plate theory and some elasticity solutions for specific plate geometries. In many later studies to refine the CLPT, the above works are frequently cited.

In Pagano's works [10, 11], limitations of the CLPT for laminated elastic plates were investigated. Solutions of several specific composite problems using CLPT were compared with the corresponding elasticity solutions (i.e. exact solutions). The conclusions pointed out the undesirable effects and limitations of CLPT, and motivated later re-

finment. To deal with the shear deformation and rotatory inertia effects in arbitrarily laminated anisotropic plates, the first-order shear deformation plate theory (FSDT) [2, 3] was generalized by Yang et al. [4]. In this generalized FSDT, the normals to the mid-plane before deformation remains straight (i.e. first-order formulation) but not necessarily normal to the mid-plane after deformation. However, a correction to transverse stiffness was required to satisfy the boundary conditions (i.e. the zero transverse shear stress on the top and bottom surfaces of plate). Several applications using this theory in bending, vibration and transient analyses were shown by Whitney et al. [12] and Reddy [17, 19]. Following the generalized FSDT, higher order formulations were given to obtain a better description for thick laminates. A variationally consistent high order shear deformation laminate plate theory was introduced by Reddy [22, 27]. Using this theory, the correction needed in the FSDT was not required. Later, for reasons of efficiency, Putchu and Reddy developed a mixed shear flexible finite element [27] to apply the high order theories. An analysis of stability and natural vibration for laminated plates were also represented. In addition to Reddy's studies, Khdeir presented several applications using his refined shear deformation theory [40]. Results available in the literature have been adapted frequently for comparisons in many later studies.

#### *Discrete-layer Theories*

Several works employed to develop so-called discrete-layer theories are specially introduced here for their usefulness in this research. The most initial work that use a layerwise displacement theory to analyze layered piezoelectric plates and layered anisotropic plates could be credited to Pauley [13] in 1974. In his dissertation, a layer-wise analysis was used to study the free vibration characteristics of infinite laminated piezoelectric plates using finite element thickness approximations. However, the analysis was limited under a condition of plane strain. Even though this work was a precursor to later development of discrete-layer theories and research in laminated piezoelectric structures, no later studies have cited this effort.

In the work of Reddy [32], a general two-dimensional shear deformation theory of laminate plates (GLPT) was represented. Based on GLPT, a desired degree of approximation of the displacements through the laminate thickness can be given. Additionally, this work indicated that the GLPT could represent a generalized form of many other laminate theories. The CLPT, the generalized FSDT, the higher order theory [22], and



several other refined laminate theories can be considered as special cases deduced from GLPT. The discrete-layer theories are also extended from the GLPT.

After GLPT was developed, Reddy et al. [43, 44] presented several applications and detailed discussion. In [43], a plate bending element was developed using GLPT. The accuracy of using this element was also evaluated by comparison with the exact solutions of the generalized plate theory [65] and 3D-elasticity solutions. When using the bending element, a layer-wise description of the inplane displacements and stresses of laminate can be given, and an improved approximation to the transverse shear deformation was obtained. Results of several examples showed that the thickness effect was effectively eliminated. Almost at the same time, another work [44] represented the exact analytic solutions of GLPT in two cases, cylindrical bending and simple support plate. By comparing with the 3D-elasticity solutions, this work confirmed that GLPT allowed accurate determination of interlaminar stresses.

In the work of Robbins and Reddy [53], the GLPT was adapted to laminated piezoelectric beams. This could be the first work that involved the GLPT into the analysis of the smart material. Four different displacement-based finite element models, which were derived from GLPT, were represented with numerical results. However, the piezoelectric effect was only modeled using an induced strain rather than the equation of piezoelectricity.

Finally, the recent work of Heyliger and Saravanos [59, 62] represented discrete-layer theories that can deal with the thick piezoelectric laminates. The kinematic assumptions were based on the GLPT. To describe the in-plane performance of plates or beams, piecewise linear variations of the components were used through the composite thickness. In addition, finite element and global/Ritz approximation in plane of laminate were involved to solve several test problems.

### *Intelligent Structures And Piezoelectric Laminate Theories*

In this section, the primary characteristics of piezoelectric beam, plate, and shell theories are introduced.

Compared with the use of piezoelectrics in transducer applications, the study of distributed piezoelectric actuators for all solids is quite recent, with most papers appearing after 1985. The work of Bailey and Hubbard [23] may be the first that introduced distributed piezoelectric polymers as actuators to control the bending vibration of cantilever

beams. Fanson and Chen [28, 29] also demonstrated that the use of piezoelectric materials as sensors/actuators in beam vibration control was feasible. The passive structure element for the control of large space structures can also be replaced by piezoelectric active members.

Later, Crawley and Luis [30] presented an analytic and experimental development of one-dimensional piezoelectric elements. These elements can be placed either on the surface or embedded within structural laminated beams, and function as actuators to excite the steady-state resonant vibrations in the cantilevered beams. The given conclusion emphasized that the existence of the embedded actuators may not affect the elastic modulus of the composite structures, but would reduce the ultimate strength of the laminate by 20%. Finally, the work of Robbins and Reddy [53] is repeated here for their analysis of simulated piezoelectric laminated beams.

Beginning in 1987, a series of publications by Lee et al. [39, 84, 47] initiated efforts to develop theoretical models for bending and torsional control in laminated piezoelectric plates. In [39], Lee and Moon presented a set of piezopolymer devices for the model control of piezoelectric laminates. Experimental results were followed and used to compare with the theoretical predictions. The latter work by Lee [84] introduced in detail the governing equations for piezoelectric laminate plates, as well as the reciprocal relationships of the piezoelectric sensor/actuator. The assumptions of CLPT were involved because only slender plates were considered.

Wang and Rogers [52] also used the assumptions of CLPT to model laminated plates with spatially distributed piezoelectric actuator patches. Using the Heaviside function that corresponding to the inplane location of patches, the strain induced by the actuators was represented. In addition, the equivalent external forces induced by the piezoceramic patches under some voltage field can be determined upon the assumption of free constraint for expansion or contraction of the patches.

In the work of Heyliger and Saravanos [59], discrete-layer theories were developed to analyze the laminated composite beams and plates which contain active piezoelectric layers or patches. The coupled relationship between the elastic and electric variables were explicitly represented in the governing equations. Both the static and dynamic behaviors were also considered. Later, Heyliger and Brooks [60] derived the exact solution for piezoelectric laminates in the two-dimensional configuration of cylindrical bending. These results provided useful information to evaluate the developed or future piezoelectric plate

theories.

Development of piezoelectric shell theories were initiated by a number of Russian authors, whose effort are summarized in the outstanding monograph of Kudrayavstev and Parton. Yet only recently have these been extended for active control problems. In 1989, Tzou et al. presented a numbers of works regarding piezoelectric shell theory [42, 49, 51, 55]. In [42], a laminated thin shell with piezoelectric layers was evaluated. The governing equations of the dynamic state were derived based on Love's hypothesis and Hamilton's principle. Later, Tzou [49] introduced a piezoelectric element to analyze the distributed sensing and active vibration control of flexible plates and shells. The finite element formulation was also given. However, only a zero-curvature shell problem was demonstrated. In [51], Tzou and Tseng developed a "thin" piezoelectric solid element with the internal degrees of freedom. This element was used in the finite element formulations to analyze the piezoelectric shell. In 1991, Tzou and Zhong [55] developed electromechanic equations of motion of generic piezoelectric shell using Hamilton's principle and linear piezoelectricity. Numerical results using finite difference technique were represented, as well as a comparison with the experimental results.

In addition to the works of Tzou et al., Lammering [54] developed a shell deformation finite element to analyze a shell structure with surface coated piezoelectric layers. In this work, a shear deformation elastic shell theory of the Reissner-Mindlin type was used to develop the finite element formulation.

## The Linear Theory of Piezoelectricity

To begin the analysis for laminated structures with embedded piezoelectric layers, the material properties and governing equations for piezoelectric media must to be defined. The behavior of piezoelectric material used in the composite is assumed to be linear. A brief introduction to the material behavior and related equations is given below.

### *Behavior of Piezoelectric Material*

In 1880, the Curie brothers discovered the piezoelectric effect on certain crystalline materials. When mechanical stresses are applied on a dielectric crystal, surface electric charges are instantaneously created. The converse effect is that the presence of an electric field results in changing the shape of the crystal. More than a hundred ferroelectric materials with the piezoelectric effect have been found. Conventional piezoelectric materials

are crystalline or polycrystalline style. Therefore, they are mostly produced in the form of ceramics or crystals. The brittle property leads to disadvantages in usage.

In 1969, a strong piezoelectric effect in PVDF, polyvinylidene fluoride polymer, was discovered by Kawai [84, 16]. PVDF-type materials are flexible. The polymeric properties are very different to the properties of the conventional piezoelectric materials. They can be produced and formed into thin-film sheets that are easy to cut or shape for complex configurations. Because of the convenience, structures with highly distributed sensors/actuators (intelligent structure) can be constructed.

In laminated structures, the embedded or coated piezoelectric layers function as distributed sensors and actuators. When applied forces result in strains within the structure, the surface charges on each layer can be collected through a surface electrode (i.e. it can be coated on the layer) to an outside detector. The deformation can therefore be measured. Conversely, if a voltage field is linked to a certain piezoelectric layer, the shape change within that layer can be used to actuate the structure. The surface electrode, which covers the piezoelectric layer, can be placed at any desired location. Only the portion of the piezoelectric layer covered by the electrode can initiate the effect.

In Figure 1, a piezoelectric film with covered electrodes, and the poling and rolling (stretching) directions are shown. Figure 2 presents three possible deformations of piezoelectric laminated plate when applying an electric field. Both figures are taken from the work of Lee [84].

#### *Equations to Describe the Piezoelectric Medium*

To describe the behavior of a piezoelectric medium, there are five mechanical and electromagnetic relations (or equations) involved :

- (1) the stress equations of motion/equilibrium,
- (2) the strain - displacement relations,
- (3) the charge equation of electrostatics,
- (4) the electric field - electric potential relations, and
- (5) the constitutive equations.

These are given sequentially as follows:

$$\tau_{ij,i} = \rho \ddot{u}_j \quad (f_j = 0) \quad (1)$$

Here  $\tau_{ij}$  are stress components,  $\rho$  is material density,  $\ddot{u}_j$  are components of acceleration,

and the body forces  $f_j$  are assumed to be zero.

$$S_{ij} = \frac{1}{2}(u_{i,j} + u_{j,i}) \quad (2)$$

Here  $S_{ij}$  are strain components and  $u_i$  are components of displacement.

$$D_{i,i} = 0 \quad (3)$$

Here  $D_i$  are the components of the electric displacement, or electric flux density, along the  $i$  direction.

$$E_k = -\phi_{,k} \quad (4)$$

Here  $E_k$  are electric field along  $k$  direction and  $\phi$  is electrostatic potential.

The piezoelectric constitutive equations present the relations among :

(1) the stress field, the strain field, and the electric field;

(2) the electric displacement, the strain field, and the electric field.

They can be written as follows.

$$\tau_{ij} = C_{ijkl}S_{kl} - e_{kij}E_k \quad (5)$$

$$D_i = e_{ikl}S_{kl} + \epsilon_{ik}E_k \quad (6)$$

The elements  $C_{ijkl}$  are elastic constants,  $e_{kij}$  are piezoelectric coefficients, and  $\epsilon_{ik}$  are dielectric constants. In this research, the constitutive relations of an orthotropic layer off-axis are followed. The elastic stiffness matrix and the matrix of piezoelectric coefficients are given as

$$\begin{bmatrix} C_{11} & C_{12} & C_{13} & 0 & 0 & C_{16} \\ C_{12} & C_{22} & C_{23} & 0 & 0 & C_{26} \\ C_{13} & C_{23} & C_{33} & 0 & 0 & C_{36} \\ 0 & 0 & 0 & C_{44} & C_{45} & 0 \\ 0 & 0 & 0 & C_{54} & C_{55} & 0 \\ C_{16} & C_{26} & C_{36} & 0 & 0 & C_{66} \end{bmatrix} \quad (7)$$

and

$$\begin{bmatrix} 0 & 0 & 0 & e_{14} & e_{15} & 0 \\ 0 & 0 & 0 & e_{24} & e_{25} & 0 \\ e_{31} & e_{32} & e_{33} & 0 & 0 & e_{36} \end{bmatrix} \quad (8)$$

The indicial notations  $C_{ijkl}$  change into  $C_{ab}$ , also  $e_{kij}$  change into  $e_{ku}$  ( $a, b = 1, 2, \dots, 6$ , and  $k = 1, 2, 3$ ).

The total set of 22 equations in 22 variables can fully define a given piezoelectric medium. Several additional equations related to linear piezoelectricity are briefly introduced here.

The equation to describe the total surface charges  $q(t)$  at time  $t$ , which are collected by a surface electrode and sensed by the outside detector, is given by

$$q(t) = \int_S \mathbf{D} \cdot \mathbf{n} dS = \int_S D_i n_i dS \quad (9)$$

Here  $\mathbf{n}$  is the normal vector of the small surface area  $dS$ , and  $\mathbf{D}$  is the electric displacement vector in the piezoelectric medium. This equation represents that the  $\mathbf{D}$  passing through the surface with electrode are collected. The internal energy function can be written as

$$U = \int_V \left( \frac{1}{2} C_{ijkl} S_{ij} S_{kl} + \frac{1}{2} \varepsilon_{ij} E_i E_j \right) dV \quad (10)$$

The first item of right hand side is the strain energy per unit volume. The second is electrostatic energy density. Finally, the electric enthalpy  $H$  per unit volume is defined as

$$\begin{aligned} H(\mathbf{S}, \mathbf{E}) &= U - \mathbf{E} \cdot \mathbf{D} = U - E_i D_i \\ &= \frac{1}{2} C_{ijkl} S_{ij} S_{kl} - e_{kij} E_k S_{ij} - \frac{1}{2} \varepsilon_{ij} E_i E_j \end{aligned} \quad (11)$$

The electric enthalpy will be used in Hamilton's principle in the next section.

### *Hamilton's Principle for Linear Piezoelectricity*

In this section, the generalized Hamilton's principle for a piezoelectric medium is presented. The variational formulations developed in subsequent chapters depend critically on this expression. For the plate geometry, this expression will be given in terms of rectangular Cartesian coordinates. For the shell, the variational formulation will be developed in both the cylindrical and the curvilinear coordinates.

In this research, the generalized Hamilton's principle is used as

$$\int_{t_0}^{t_1} \delta(\mathcal{K} - U) dt + \int_{t_0}^{t_1} \delta\mathcal{W} dt = 0 \quad (12)$$

Where

$$\mathcal{K} = \int_V \frac{1}{2} \rho \dot{\mathbf{u}} \cdot \dot{\mathbf{u}} dV \quad (13)$$

$$\delta\mathcal{W} = \int_V (\mathbf{f} \cdot \delta \mathbf{u} + \delta(\mathbf{E} \cdot \mathbf{D})) dV + \int_S (\mathbf{t} \cdot \delta \mathbf{u} - \bar{\sigma} \delta \phi) dS \quad (14)$$

Here  $\mathcal{K}$  is the kinetic energy of the system,  $U$  is the internal energy of the piezoelectric medium, and  $\delta\mathcal{W}$ , virtual work done to the system. The four items on the right hand side of equation 14 represent the virtual work done by (1) body force in a virtual displacement, (2) variation of electric field in a electric displacement, as well as variation of electric displacement in a electric field, (3) the prescribed surface tractions in a virtual displacement on medium surface, and (4) the prescribed surface charge  $\bar{\sigma}$  in a small variation of electrical potential  $\phi$ .

Since the applied electric field  $\mathbf{E}$  and electric displacement  $\mathbf{D}$  are interdependent, the system is not conservative. The body force  $\mathbf{f}$  is assumed to be zero here. The expression of equation 14 is the governing equation used in this research, and is written as

$$\delta \int_{t_0}^{t_1} dt \int_V \left[ \frac{1}{2} \rho \dot{u}_i \dot{u}_i - H(S_{kl}, E_k) \right] dV + \int_{t_0}^{t_1} dt \int_S (\bar{t}_i \delta u_i - \bar{\sigma} \delta \phi) dS = 0 \quad (15)$$

Here  $H(S_{kl}, E_k)$  is the electric enthalpy, which replaces the terms of internal energy and  $\mathbf{E} \cdot \mathbf{D}$  in equation 14. The value will not be changed due to the coordinate transformation. The variational form of  $H$  is expressed as

$$\begin{aligned} \delta H &= \delta(U - \mathbf{E} \cdot \mathbf{D}) = \delta U - \delta(\mathbf{E} \cdot \mathbf{D}) \\ &= C_{ijkl} S_{ij} \delta S_{kl} - e_{kij} E_k \delta S_{ij} - e_{kij} \delta E_k S_{ij} - \varepsilon_{ij} E_i \delta E_j \end{aligned} \quad (16)$$

These equations will be used extensively in later chapters. Depending on the problem geometry and coordinate system used, the form of these equations will be different and are detailed for each case in the following chapters.

### 3. SEMI-ANALYTIC SOLUTIONS

This section details a discussion of what are termed semi-analytic solutions for simply-supported laminated piezoelectric plates. This work was an extension of work completed by the principal investigator and the technical monitor of this research project (DAS). The phrase "semi-analytic" denotes the fact that use of Navier-type displacement fields will identically satisfy the in-plane requirements of a simply supported plate for the exact solution of the equations of linear piezoelectricity. In this case, as for the exact solution included in a later chapter, the problem effectively becomes one-dimensional.

The new and major thrust of this section is to detail 1) the relative accuracy of the two major out-of-plane displacement approximations used in previous work in comparison with exact solutions, and 2) description of an alternative displacement field that was found necessary to accurately model piezoelectric plates. This field uses piecewise linear variation of the out-of-plane displacement components that are different than those for the in-plane and potential components. This is discussed to some extent in the chapters on the plate and shell elements, but is included here because it was for this class of problem that a preliminary numerical algorithm has been completed and results computed.

#### Governing Equations

##### *Geometry*

The geometrical configuration of the laminate is such that the thickness dimension of the laminate coincides with the  $z$ -direction, with the lengths of the plate in the  $x$  and  $y$  directions denoted as  $L_x$  and  $L_y$ , respectively. The general problem considered in this study is to determine the behavior of the elastic and electric field components throughout the laminate under an applied mechanical or electrical loading. Each layer of the laminate can be composed of a purely elastic, piezoelectric, or conducting material. The forcing function is introduced through either an applied surface displacement, traction, potential, or electric charge.

##### *Variational Formulation*

A single piezoelectric layer has the constitutive equations given by [67]

$$\begin{aligned}\sigma_{ij} &= C_{ij}S_j - e_{ji}E_j \\ D_i &= e_{ij}S_j + \epsilon_{ij}E_j\end{aligned}\tag{17}$$



Here  $\sigma_{ij}$  are the components of the stress tensor,  $C_{ij}$  are the elastic stiffness components,  $S_j$  are the components of infinitesimal strain,  $e_{ij}$  are the piezoelectric coefficients,  $E_i$  are the components of the electric field,  $D_i$  are the components of the electric displacement, and  $\epsilon_{ij}$  are the dielectric constants. The poling direction in this study is coincident with the  $x_3$  or  $z$  axis.

The strain-displacement relations are given by

$$S_{ij} = \frac{1}{2} \left( \frac{\partial u_i}{\partial x_j} + \frac{\partial u_j}{\partial x_i} \right) \quad (18)$$

Here  $S_{ij}$  are the components of the infinitesimal strain tensor and  $u_i$  represent the displacement components. To be consistent with equation 17, the conventional notation for the strain indices has been used, i.e.  $S_{11} = S_1$ ,  $S_{23} = S_4$ , etc. The electric field components  $E_i$  are related to the electrostatic potential  $\phi$  using the relation

$$E_i = -\frac{\partial \phi}{\partial x_i} \quad (19)$$

For the materials used in this study, it is assumed that the non-zero components of the rotated piezoelectric tensor  $e_{ij}$  are  $e_{31}$ ,  $e_{32}$ ,  $e_{33}$ ,  $e_{24}$ ,  $e_{15}$ ,  $e_{25}$ ,  $e_{14}$ , and  $e_{36}$ . The elastic stiffnesses  $C_{ij}$  are those of an orthotropic material rotated about the  $z$  axis, and the dielectric constants are given by  $\epsilon_{11}$ ,  $\epsilon_{12}$ ,  $\epsilon_{22}$ , and  $\epsilon_{33}$ .

The starting point for the variational formulation is Hamilton's principle for a piezoelectric medium [67], expressed as

$$\delta \int_{t_0}^t dt \int_V \left[ \frac{1}{2} \rho \dot{u}_i \dot{u}_i - H(S_{kl}, E_k) \right] dV + \int_{t_0}^t dt \int_S (\bar{t}_k \delta u_k - \bar{\sigma} \delta \phi) dS = 0 \quad (20)$$

Here  $t$  is time,  $V$  and  $S$  are the volume and surface occupied by and bounding the solid,  $\bar{t}$  and  $\bar{\sigma}$  are the specified surface tractions and surface charge, respectively,  $\delta$  is the variational operator, the  $\dot{\phantom{x}}$  superscript represents differentiation with respect to time, and  $H$  represents the electric enthalpy. The electric enthalpy is given by

$$H = \frac{1}{2} C_{ijkl} S_{ij} S_{kl} - e_{ijk} E_i S_{jk} - \frac{1}{2} \epsilon_{ij} E_i E_j \quad (21)$$

The weak form of the governing equations, as well as the governing differential equations themselves, can be found by applying the variational operator in equation 20 over a typical element. For the material constants of a typical lamina used in this study, the first variation of the electric enthalpy is

$$\begin{aligned}
\delta H = & C_{11} \frac{\partial u}{\partial x} \frac{\partial \delta u}{\partial x} + C_{12} \frac{\partial u}{\partial x} \frac{\partial \delta v}{\partial y} + C_{13} \frac{\partial u}{\partial x} \frac{\partial \delta w}{\partial z} + C_{16} \frac{\partial u}{\partial x} \left( \frac{\partial \delta u}{\partial y} + \frac{\partial \delta v}{\partial x} \right) + \\
& C_{12} \frac{\partial v}{\partial y} \frac{\partial \delta u}{\partial x} + C_{22} \frac{\partial v}{\partial y} \frac{\partial \delta v}{\partial y} + C_{23} \frac{\partial v}{\partial y} \frac{\partial \delta w}{\partial z} + C_{26} \frac{\partial v}{\partial y} \left( \frac{\partial \delta u}{\partial y} + \frac{\partial \delta v}{\partial x} \right) + \\
& C_{13} \frac{\partial w}{\partial z} \frac{\partial \delta u}{\partial x} + C_{23} \frac{\partial w}{\partial z} \frac{\partial \delta v}{\partial y} + C_{33} \frac{\partial w}{\partial z} \frac{\partial \delta w}{\partial z} + C_{36} \frac{\partial w}{\partial z} \left( \frac{\partial \delta u}{\partial y} + \frac{\partial \delta v}{\partial x} \right) + \\
& C_{44} \left( \frac{\partial v}{\partial z} + \frac{\partial w}{\partial y} \right) \left( \frac{\partial \delta v}{\partial z} + \frac{\partial \delta w}{\partial y} \right) + C_{45} \left( \frac{\partial v}{\partial z} + \frac{\partial w}{\partial y} \right) \left( \frac{\partial \delta u}{\partial z} + \frac{\partial \delta w}{\partial x} \right) + \\
& C_{45} \left( \frac{\partial u}{\partial z} + \frac{\partial w}{\partial x} \right) \left( \frac{\partial \delta v}{\partial z} + \frac{\partial \delta w}{\partial y} \right) + C_{55} \left( \frac{\partial u}{\partial z} + \frac{\partial w}{\partial x} \right) \left( \frac{\partial \delta u}{\partial z} + \frac{\partial \delta w}{\partial x} \right) + \\
& C_{16} \left( \frac{\partial u}{\partial y} + \frac{\partial v}{\partial x} \right) \frac{\partial \delta u}{\partial x} + C_{26} \left( \frac{\partial u}{\partial y} + \frac{\partial v}{\partial x} \right) \frac{\partial \delta v}{\partial y} + \\
& C_{36} \left( \frac{\partial u}{\partial y} + \frac{\partial v}{\partial x} \right) \frac{\partial \delta w}{\partial z} + C_{66} \left( \frac{\partial u}{\partial y} + \frac{\partial v}{\partial x} \right) \left( \frac{\partial \delta u}{\partial y} + \frac{\partial \delta v}{\partial x} \right) - \\
& e_{14} \delta E_1 \left( \frac{\partial v}{\partial z} + \frac{\partial w}{\partial y} \right) - e_{15} \delta E_1 \left( \frac{\partial u}{\partial z} + \frac{\partial w}{\partial x} \right) - e_{24} \delta E_2 \left( \frac{\partial v}{\partial z} + \frac{\partial w}{\partial y} \right) - e_{25} \delta E_2 \left( \frac{\partial u}{\partial z} + \frac{\partial w}{\partial x} \right) - \\
& e_{31} \delta E_3 \frac{\partial u}{\partial x} - e_{32} \delta E_3 \frac{\partial v}{\partial y} - e_{33} \delta E_3 \frac{\partial w}{\partial z} - e_{36} \delta E_3 \left( \frac{\partial u}{\partial y} + \frac{\partial v}{\partial x} \right) - \\
& \epsilon_{11} E_1 \delta E_1 - \epsilon_{22} E_2 \delta E_2 - \epsilon_{33} E_3 \delta E_3 - \epsilon_{12} E_1 \delta E_2 - \epsilon_{12} E_2 \delta E_1 - \\
& e_{14} E_1 \left( \frac{\partial \delta v}{\partial z} + \frac{\partial \delta w}{\partial y} \right) - e_{15} E_1 \left( \frac{\partial \delta u}{\partial z} + \frac{\partial \delta w}{\partial x} \right) - e_{24} E_2 \left( \frac{\partial \delta v}{\partial z} + \frac{\partial \delta w}{\partial y} \right) - e_{25} E_2 \left( \frac{\partial \delta u}{\partial z} + \frac{\partial \delta w}{\partial x} \right) - \\
& e_{31} E_3 \frac{\partial \delta u}{\partial x} - e_{32} E_3 \frac{\partial \delta v}{\partial y} - e_{33} E_3 \frac{\partial \delta w}{\partial z} - e_{36} E_3 \left( \frac{\partial \delta u}{\partial y} + \frac{\partial \delta v}{\partial x} \right) \quad (22)
\end{aligned}$$

Using the assumption of periodic motion, the substitution of this expression into equation 20 yields the final weak form, which provides the basis for the finite-element approximations over an element. It is possible to integrate this expression by parts to give the three equilibrium equations and the conservation of charge equation. For brevity, results of this step are not included here.

### Displacement Functions

There are several cases in both static behavior and free-vibration analysis for which

either exact solutions are available or global in-plane functions can represent the elastic and electric fields within the laminate. One such case is for simply-supported plates. In this case, the Navier-type boundary conditions along the edges of the plate are given as

$$\begin{aligned}
 w(x, 0, z) = w(x, L_y, z) = w(0, y, z) = w(L_x, y, z) &= 0 \\
 \phi(x, 0, z) = \phi(x, L_y, z) = \phi(0, y, z) = \phi(L_x, y, z) &= 0 \\
 u(x, 0, z) = u(x, L_y, z) &= 0 \\
 v(0, y, z) = v(L_x, y, z) &= 0
 \end{aligned} \tag{23}$$

$$\tag{24}$$

These conditions are satisfied exactly for the functions

$$\begin{aligned}
 u(x, y, z) &= U(z) \cos px \sin qy = \bar{U} \exp(sz) \cos px \sin qy \\
 v(x, y, z) &= V(z) \sin px \cos qy = \bar{V} \exp(sz) \sin px \cos qy \\
 w(x, y, z) &= W(z) \sin px \sin qy = \bar{W} \exp(sz) \sin px \sin qy \\
 \phi(x, y, z) &= \Phi(z) \sin px \sin qy = \bar{\Phi} \exp(sz) \sin px \sin qy
 \end{aligned} \tag{25}$$

#### *Finite Element Approximation*

The through-thickness approximation for each displacement component and the electrostatic potential can be given as

$$\begin{aligned}
 u(z, t) &= \sum_{j=1}^n U_j(t) \bar{\Psi}_j^u(z) \\
 v(z, t) &= \sum_{j=1}^n V_j(t) \bar{\Psi}_j^v(z) \\
 w(z, t) &= \sum_{j=1}^n W_j(t) \bar{\Psi}_j^w(z) \\
 \phi(z, t) &= \sum_{j=1}^n \Phi_j(t) \bar{\Psi}_j^\phi(z)
 \end{aligned} \tag{26}$$

Hence the variables are represented by linear combinations of a known through-thickness distribution described using the one-dimensional Lagrangian interpolation polynomials

$\bar{\Psi}_j(z)$  [14,16]. The in-plane distributions are already included in the total approximation. Here  $(n-1)$  is the number of subdivisions through the laminate thickness (typically taken equal to or greater than the number of layers in the laminate), and  $U_{ji}$  is the value of component  $u$  at height  $j$  corresponding to the  $i$ -th in-plane approximation function.

The difference between the two theories considered here is in the form of  $\bar{\Psi}_j^\psi$ . For the case of constant transverse displacement through the thickness, this function is equal to 1. For a variable- $w$  approximation, this function can be any Lagrangian interpolation polynomial. It is also possible to use functions in the  $z$ -direction which are non-zero only over specified regions. This would be most useful for the functions  $\Psi_j^\phi$  for conducting materials, in which case the potential is a constant. Also, independent approximations for all variables can be used by denoting different ranges and limits of integration for each component.

Substituting these approximations into the weak form and collecting the coefficients allows the governing equations to be expressed in matrix form as

$$\begin{bmatrix} [M^{11}] & [0] & [0] & [0] \\ [0] & [M^{22}] & [0] & [0] \\ [0] & [0] & [M^{33}] & [0] \\ [0] & [0] & [0] & [0] \end{bmatrix} \begin{Bmatrix} \{\ddot{U}\} \\ \{\ddot{V}\} \\ \{\ddot{W}\} \\ \{\ddot{\Phi}\} \end{Bmatrix} + \begin{bmatrix} [K^{11}] & [K^{12}] & [K^{13}] & [K^{14}] \\ [K^{21}] & [K^{22}] & [K^{23}] & [K^{24}] \\ [K^{31}] & [K^{32}] & [K^{33}] & [K^{34}] \\ [K^{41}] & [K^{42}] & [K^{43}] & [K^{44}] \end{bmatrix} \begin{Bmatrix} \{U\} \\ \{V\} \\ \{W\} \\ \{\Phi\} \end{Bmatrix} = \begin{Bmatrix} \{F^1\} \\ \{F^2\} \\ \{F^3\} \\ \{Q\} \end{Bmatrix}$$

The elements of these matrices contain additional submatrices whose elements are determined by evaluating the pre-integrated elastic stiffnesses, piezoelectric coefficient, or dielectric constant through the thickness multiplied by the various shape functions or their derivatives as determined by the variational statement. These are identical to those of the plate element, and as such are not stated here. They are documented in the next chapter.

The nature of the submatrices depends on the approximation used for  $w$ . For variable  $w$ , the structure of  $[K^{j3}]$  are similar to those of the other matrices. Depending on the approximation functions used, this type of model is either similar or identical to a three-dimensional finite element model of the equations of piezoelectricity. This aspect and other computational issues regarding these types of models for elastic laminates are discussed in [61]. For constant  $w$ , the submatrices within  $[K^{13}]$ ,  $[K^{23}]$ , and  $[K^{43}]$  are column vectors and those in  $[K^{33}]$  become scalars. In general, the submatrices within  $[K^{ij}]$  are each of order  $(n+1)$ , while the  $[K^{ij}]$  themselves depend on the order of in-plane approximation. These

can be defined by the subscripts  $\alpha$  and  $\beta$ . The final representation of these elements can be expressed in fairly compact form and are given in the chapter on the plate element. In matrix form, they are written as

$$\begin{bmatrix} [M] & [0] \\ [0] & [0] \end{bmatrix} \begin{Bmatrix} \{\ddot{\Delta}\} \\ \{\ddot{\phi}\} \end{Bmatrix} + \begin{bmatrix} [K^{\Delta\Delta}] & [K^{\Delta\phi}] \\ [K^{\phi\Delta}] & [K^{\phi\phi}] \end{bmatrix} \begin{Bmatrix} \{\Delta\} \\ \{\phi\} \end{Bmatrix} = \begin{Bmatrix} \{0\} \\ \{0\} \end{Bmatrix} \quad (28)$$

Assuming periodic motion and eliminating the potentials results in the eigenvalue problem

$$([\bar{K}] - \omega^2[M])\{\Delta\} = \{0\}$$

where

$$[\bar{K}] = [K_{\Delta\Delta}] - [K_{\Delta\phi}][K_{\phi\phi}]^{-1}[K_{\phi\Delta}] \quad (29)$$

The numerical results for the preceding theories are given in a later chapter. However, it is necessary to note at this point that the case of a constant transverse displacement gave results for both the static and dynamic cases that was wholly inadequate for most geometries. Part of the reason for this was the fact that the transverse strain must be zero in this case, which implies that the actuation strain is also zero. For any dimension plate, this is a hindrance far more severe than for the pure elastic case, as this strain figures significantly in the stress computation and in the evaluation of the electric enthalpy terms.

This type of behavior can be asauaged by introducing approximations for  $w$  that are at least linear through the thickness of the entire laminate. This is accomplished using an approximation function for  $w$  through the thickness of the laminate that is completely independent of the two in-plane components and the electrostatic potential.

This type of approximation can be thought of in the following fashion. Each individual layer can be described by one or more "real" layers for purposes of finite element discretization through the lamina thickness, composed in this study of linear Lagrangian interpolation polynomials. Spanning over these layers is one or more "pseudo-layers" (see Figure 3), which is the range of layers encompassed by the linear approximation for any of the variables, which in this case will be the transverse displacement  $w$ . For example,

consider a plate with three physical layers, which is modeled using three layers (and 4 nodes) for  $u$ ,  $v$ , and  $\phi$  but a single pseudo-layer for  $w$ . Each of the linear basis functions for  $u$ ,  $v$ , and  $\phi$  has support only over two layers, with the basis function for  $w$  spanning over all layers.

The shape functions for the  $i$ -th layer for each of the true layers are given in terms of the global  $z$ -coordinate as

$$\begin{aligned}\psi_1^t &= \frac{z_q - z}{h_i} \\ \psi_2^t &= \frac{z - z_p}{h_i}\end{aligned}\quad (30)$$

Here  $h_i$  is the thickness of each of the true layers, and the  $t$  superscript indicates "true" and corresponds to the approximations for  $u$ ,  $v$ , and  $\phi$  (and any, all, or none of these may have this type of approximation).

The approximation functions for the transverse displacement component are given by

$$\begin{aligned}\psi_1^p &= \beta_i - \alpha_i \frac{z}{L_k} \\ \psi_2^p &= \gamma_i + \alpha_i \frac{z}{L_k}\end{aligned}\quad (31)$$

Here  $L_k$  is the thickness of the  $k$ -th pseudo-layer, and the values for  $\alpha$ ,  $\gamma$ , and  $\beta$  change for each true layer, with their values being given by

$$\alpha_i = \frac{h_i}{L_i} \quad (32)$$

$$\gamma_i = \sum_{j=1}^i \alpha_j \quad (33)$$

$$\beta_i = 1 - \sum_{j=1}^i \alpha_j \quad (34)$$

By analytically integrating the products of the appropriate shape functions and their derivatives, the appropriate sub-matrices similar to those computed earlier for the original

two theories can be obtained. This approach has the significant advantage of allowing a transverse normal strain through the laminate thickness but introducing only (potentially) one new degree of freedom. By allowing a transverse normal strain, the difficulties of the constant- $w$  theory disappear. Examples of this type of behavior are given in a later chapter, but indicate one of the major conclusions of this study: it appears that the constant- $w$  theory is wholly inadequate for modeling the behavior of piezoelectric solids because of the inability to model the normal actuation strain.

#### 4. THE PLATE ELEMENT

In this chapter, the theoretical formulation for piezoelectrically laminated composite plates are presented. The variational form is obtained using Hamilton's principle for a linear piezoelectric solid [67]. The equations resulting from this variational statement will be solved using the discrete-layer theory similar to that described in the preceding chapter, in which the three-dimensional elasticity theory is reduced to a two-dimensional laminate theory by assuming an approximation of the displacements through the thickness.

In this study, a piece-wise linear variation is assumed for the in-plane displacement and for the electrostatic potential components through the thickness. Regarding the transverse displacement components, three theories will be presented: 1) a constant transverse displacement through the thickness, 2) a piece-wise linear variation through the thickness, and 3) an independent piece-wise linear variation through the thickness different than that of the in-plane and potential components.

#### Governing Equations

##### *Electric Field-Potential and Strain-Displacement Relations*

The electric field components are related to the electrostatic potential by [67] :

$$E_k = -\varphi_{,k} \quad (35)$$

In Cartesian coordinates, the above expression yields:

$$E_1 = -\frac{\partial\varphi}{\partial x} \quad E_2 = -\frac{\partial\varphi}{\partial y} \quad E_3 = -\frac{\partial\varphi}{\partial z} \quad (36)$$

In addition, the strain-displacement relations are given by:

$$S_{ij} = \frac{1}{2}(u_{i,j} + u_{j,i}) \quad (37)$$

which turns into the following six components when is expressed in cartesian coordinates:

$$\begin{aligned} S_{xx} &= \frac{\partial u}{\partial x} & S_{xy} &= \frac{1}{2}\left(\frac{\partial u}{\partial y} + \frac{\partial v}{\partial x}\right) \\ S_{yy} &= \frac{\partial v}{\partial y} & S_{yz} &= \frac{1}{2}\left(\frac{\partial v}{\partial z} + \frac{\partial w}{\partial y}\right) \\ S_{zz} &= \frac{\partial w}{\partial z} & S_{zx} &= \frac{1}{2}\left(\frac{\partial u}{\partial z} + \frac{\partial w}{\partial x}\right) \end{aligned}$$



### Constitutive Relations for a Piezoelectric Material

For a piezoelectric material, the mechanical behavior is coupled together with the electrical behavior. This electromechanical coupling is described by [67]:

$$\sigma_{ij} = C_{ijkl}S_{kl} - e_{kij}E_k \quad (38)$$

$$D_i = e_{ikl}S_{kl} + \epsilon_{ik}E_k \quad (39)$$

Here  $\sigma_{ij}$  represent the components of the stress tensor,  $e_{kij}$  are the components of the piezoelectric constants of the solid,  $\epsilon_{ik}$  are the components of the dielectric tensor,  $D_i$  are the components of the electric displacement tensor, and  $C_{ijkl}$  are the components of the elastic stiffness tensor.

Since we are interested in a linear theory, it is important to note that:

$$C_{ijkl} = C_{ijlk} = C_{jikl} = C_{klij}$$

$$e_{ijk} = e_{ikj}$$

$$\epsilon_{ij} = \epsilon_{ji}$$

Taking into account this symmetry of the material, Nye [68] compressed this notation by replacing  $ij$  or  $kl$  by  $p$  or  $q$ , where  $i, j, k$ , and  $l$  take the values 1, 2, and 3, and  $p$  and  $q$  take the values 1, 2, 3, 4, 5, and 6. Hence the equations can be rewritten as:

$$\sigma_p = C_{pq}S_q - e_{kp}E_k \quad p = 1, 2, \dots, 6 \quad q = 1, 2, \dots, 6 \quad (40)$$

$$D_i = e_{iq}S_q + \epsilon_{ik}E_k \quad i = 1, 2, 3 \quad k = 1, 2, 3 \quad (41)$$

Now that the elastic, piezoelectric, and dielectric constants are specified by two indices, they can be written in matrix form as follows:

$$C_{ij} = \begin{bmatrix} C_{11} & C_{12} & C_{13} & C_{14} & C_{15} & C_{16} \\ C_{12} & C_{22} & C_{23} & C_{24} & C_{25} & C_{26} \\ C_{13} & C_{23} & C_{33} & C_{34} & C_{35} & C_{36} \\ C_{14} & C_{24} & C_{34} & C_{44} & C_{45} & C_{46} \\ C_{15} & C_{25} & C_{35} & C_{45} & C_{55} & C_{56} \\ C_{16} & C_{26} & C_{36} & C_{46} & C_{56} & C_{66} \end{bmatrix} \quad (42)$$

$$e_{kp} = \begin{bmatrix} e_{11} & e_{12} & e_{13} & e_{14} & e_{15} & e_{16} \\ e_{21} & e_{22} & e_{23} & e_{24} & e_{25} & e_{26} \\ e_{31} & e_{32} & e_{33} & e_{34} & e_{35} & e_{36} \end{bmatrix} \quad (43)$$

$$\epsilon_{ij} = \begin{bmatrix} \epsilon_{11} & \epsilon_{12} & \epsilon_{13} \\ \epsilon_{12} & \epsilon_{22} & \epsilon_{23} \\ \epsilon_{13} & \epsilon_{23} & \epsilon_{33} \end{bmatrix} \quad (44)$$

At this point, we have 21 independent elastic constants, 18 independent piezoelectric constants, and 6 independent dielectric constants. Because of the symmetric properties of some piezoelectric materials, these matrices can be further simplified. For instance, for a monoclinic material, which can represent an orthotropic layer oriented off-axis, these matrices can be reduced to:

$$C_{ij} = \begin{bmatrix} C_{11} & C_{12} & C_{13} & 0 & 0 & C_{16} \\ C_{12} & C_{22} & C_{23} & 0 & 0 & C_{26} \\ C_{13} & C_{23} & C_{33} & 0 & 0 & C_{36} \\ 0 & 0 & 0 & C_{44} & C_{45} & 0 \\ 0 & 0 & 0 & C_{45} & C_{55} & 0 \\ C_{16} & C_{26} & C_{36} & 0 & 0 & C_{66} \end{bmatrix} \quad (45)$$

$$e_{kp} = \begin{bmatrix} 0 & 0 & 0 & e_{14} & e_{15} & 0 \\ 0 & 0 & 0 & e_{24} & e_{25} & 0 \\ e_{31} & e_{32} & e_{33} & 0 & 0 & e_{36} \end{bmatrix} \quad (46)$$

$$\epsilon_{ij} = \begin{bmatrix} \epsilon_{11} & 0 & 0 \\ 0 & \epsilon_{22} & 0 \\ 0 & 0 & \epsilon_{33} \end{bmatrix} \quad (47)$$

Thus the material with this type of symmetry is described by 13 independent elastic constants, 8 independent piezoelectric constants, and 2 dielectric constants.

#### *Variational Form of the Governing Equations*

In classical mechanics, the Hamilton's principle for a system with nonconservative forces states that:

$$\delta \int_{t_0}^t L dt + \int_{t_0}^t \delta W dt = 0 \quad (48)$$

where

$$L = T(\dot{x}_k) - V(x_k, t) = L(\dot{x}_k, x_k, t)$$

In the above expressions,  $t$  is time,  $L$  is the Lagrangian energy function,  $T$  is the kinetic energy,  $V$  is the potential energy,  $\delta W$  is the work done by the nonconservative forces in a virtual displacement, and  $\delta$  is the variational operator.

As noted in earlier chapters, Hamilton's principle for a zero body and surface forces is given by

$$\delta \int_{t_0}^t dt \int_v \left[ \frac{1}{2} \rho \dot{u}_j \dot{u}_j - \left( \frac{1}{2} C_{ij} S_i S_j - e_{ij} E_i S_j - \frac{1}{2} \epsilon_{ij} E_i E_j \right) \right] dv = 0 \quad (49)$$

The weak form of the governing equations can be found by substituting the elastic strain-displacement and the electric field-electric potential relations and by operating the variational operator  $\delta$  on Hamilton's principle. Assuming static conditions, the above procedure yields the following for an off-axis, orthotropic piezoelectric layer:

$$\begin{aligned} \delta H = & C_{11} \frac{\partial u}{\partial x} \frac{\partial \delta u}{\partial x} + C_{12} \frac{\partial u}{\partial x} \frac{\partial \delta v}{\partial y} + C_{13} \frac{\partial u}{\partial x} \frac{\partial \delta w}{\partial z} + C_{16} \left( \frac{\partial u}{\partial x} \frac{\partial \delta u}{\partial y} + \frac{\partial u}{\partial x} \frac{\partial \delta v}{\partial x} \right) + \\ & C_{12} \frac{\partial v}{\partial y} \frac{\partial \delta u}{\partial x} + C_{22} \frac{\partial v}{\partial y} \frac{\partial \delta v}{\partial y} + C_{23} \frac{\partial v}{\partial y} \frac{\partial \delta w}{\partial z} + C_{26} \left( \frac{\partial v}{\partial y} \frac{\partial \delta u}{\partial y} + \frac{\partial v}{\partial y} \frac{\partial \delta v}{\partial x} \right) + \\ & C_{13} \frac{\partial w}{\partial z} \frac{\partial \delta u}{\partial x} + C_{23} \frac{\partial w}{\partial z} \frac{\partial \delta v}{\partial y} + C_{33} \frac{\partial w}{\partial z} \frac{\partial \delta w}{\partial z} + C_{36} \left( \frac{\partial w}{\partial z} \frac{\partial \delta u}{\partial y} + \frac{\partial w}{\partial z} \frac{\partial \delta v}{\partial x} \right) + \\ & C_{44} \left( \frac{\partial v}{\partial z} \frac{\partial \delta v}{\partial z} + \frac{\partial v}{\partial z} \frac{\partial \delta w}{\partial y} + \frac{\partial w}{\partial y} \frac{\partial \delta v}{\partial z} + \frac{\partial w}{\partial y} \frac{\partial \delta w}{\partial y} \right) + \\ & C_{45} \left( \frac{\partial v}{\partial z} \frac{\partial \delta w}{\partial x} + \frac{\partial v}{\partial z} \frac{\partial \delta u}{\partial z} + \frac{\partial w}{\partial y} \frac{\partial \delta w}{\partial x} + \frac{\partial w}{\partial y} \frac{\partial \delta u}{\partial z} \right) + \\ & C_{45} \left( \frac{\partial w}{\partial x} \frac{\partial \delta v}{\partial z} + \frac{\partial w}{\partial x} \frac{\partial \delta w}{\partial y} + \frac{\partial u}{\partial z} \frac{\partial \delta v}{\partial z} + \frac{\partial u}{\partial z} \frac{\partial \delta w}{\partial y} \right) + \\ & C_{55} \left( \frac{\partial w}{\partial x} \frac{\partial \delta w}{\partial x} + \frac{\partial w}{\partial x} \frac{\partial \delta u}{\partial z} + \frac{\partial u}{\partial z} \frac{\partial \delta w}{\partial x} + \frac{\partial u}{\partial z} \frac{\partial \delta u}{\partial z} \right) + \\ & C_{16} \left( \frac{\partial u}{\partial y} \frac{\partial \delta u}{\partial x} + \frac{\partial v}{\partial x} \frac{\partial \delta u}{\partial x} \right) + C_{26} \left( \frac{\partial u}{\partial y} \frac{\partial \delta v}{\partial y} + \frac{\partial v}{\partial x} \frac{\partial \delta v}{\partial y} \right) + C_{36} \left( \frac{\partial u}{\partial y} \frac{\partial \delta w}{\partial z} + \frac{\partial v}{\partial x} \frac{\partial \delta w}{\partial z} \right) + \\ & C_{66} \left( \frac{\partial u}{\partial y} \frac{\partial \delta u}{\partial y} + \frac{\partial u}{\partial y} \frac{\partial \delta v}{\partial x} + \frac{\partial v}{\partial x} \frac{\partial \delta u}{\partial y} + \frac{\partial v}{\partial x} \frac{\partial \delta v}{\partial x} \right) + \\ & e_{14} \left( \frac{\partial v}{\partial z} \frac{\partial \delta \varphi}{\partial x} + \frac{\partial w}{\partial y} \frac{\partial \delta \varphi}{\partial x} \right) + e_{15} \left( \frac{\partial w}{\partial x} \frac{\partial \delta \varphi}{\partial x} + \frac{\partial u}{\partial z} \frac{\partial \delta \varphi}{\partial x} \right) + \\ & e_{24} \left( \frac{\partial v}{\partial z} \frac{\partial \delta \varphi}{\partial y} + \frac{\partial w}{\partial y} \frac{\partial \delta \varphi}{\partial y} \right) + e_{25} \left( \frac{\partial w}{\partial x} \frac{\partial \delta \varphi}{\partial y} + \frac{\partial u}{\partial z} \frac{\partial \delta \varphi}{\partial y} \right) + \\ & e_{31} \frac{\partial u}{\partial x} \frac{\partial \delta \varphi}{\partial z} + e_{32} \frac{\partial v}{\partial y} \frac{\partial \delta \varphi}{\partial z} + e_{33} \frac{\partial w}{\partial z} \frac{\partial \delta \varphi}{\partial z} + e_{36} \left( \frac{\partial u}{\partial y} \frac{\partial \delta \varphi}{\partial z} + \frac{\partial v}{\partial x} \frac{\partial \delta \varphi}{\partial z} \right) + \\ & e_{14} \left( \frac{\partial \varphi}{\partial x} \frac{\partial \delta v}{\partial z} + \frac{\partial \varphi}{\partial x} \frac{\partial \delta w}{\partial y} \right) + e_{15} \left( \frac{\partial \varphi}{\partial x} \frac{\partial \delta w}{\partial x} + \frac{\partial \varphi}{\partial x} \frac{\partial \delta u}{\partial z} \right) + \end{aligned}$$

$$\begin{aligned}
& e_{24} \left( \frac{\partial \varphi}{\partial y} \frac{\partial \delta v}{\partial z} + \frac{\partial \varphi}{\partial y} \frac{\partial \delta w}{\partial y} \right) + e_{25} \left( \frac{\partial \varphi}{\partial y} \frac{\partial \delta w}{\partial x} + \frac{\partial \varphi}{\partial y} \frac{\partial \delta u}{\partial z} \right) + \\
& e_{31} \frac{\partial \varphi}{\partial z} \frac{\partial \delta u}{\partial x} + e_{32} \frac{\partial \varphi}{\partial z} \frac{\partial \delta v}{\partial y} + e_{33} \frac{\partial \varphi}{\partial z} \frac{\partial \delta w}{\partial z} + e_{36} \left( \frac{\partial \varphi}{\partial z} \frac{\partial \delta u}{\partial y} + \frac{\partial \varphi}{\partial z} \frac{\partial \delta v}{\partial x} \right) - \\
& \epsilon_{11} \frac{\partial \varphi}{\partial x} \frac{\partial \delta \varphi}{\partial x} - \epsilon_{22} \frac{\partial \varphi}{\partial y} \frac{\partial \delta \varphi}{\partial y} - \epsilon_{33} \frac{\partial \varphi}{\partial z} \frac{\partial \delta \varphi}{\partial z} \quad (50)
\end{aligned}$$

## Discrete-Layer Approximation

Three theories are presented in this work. The first assumes a piece-wise linear variation of the transverse displacement through the thickness. The second yields a constant transverse displacement through the thickness. The last uses independent piece-wise linear approximations for  $w$  and the remaining in-plane and potential components. All theories are based on the general laminate theory of Reddy [32] for elastic laminates, with the added feature that the electric potential is included as an additional variable.

### *A piece-wise transverse displacement model*

This theory is based on approximations of the displacement and potential variables in the following form:

$$\begin{aligned}
u(x, y, z, t) &= \sum_{j=1}^n U_j(x, y, t) \bar{\Psi}_j^u(z) = \sum_{i=1}^m \sum_{j=1}^n U_{ji}(t) \Psi_i^u(x, y) \bar{\Psi}_j^u(z) \\
v(x, y, z, t) &= \sum_{j=1}^n V_j(x, y, t) \bar{\Psi}_j^v(z) = \sum_{i=1}^m \sum_{j=1}^n V_{ji}(t) \Psi_i^v(x, y) \bar{\Psi}_j^v(z) \\
w(x, y, z, t) &= \sum_{j=1}^n W_j(x, y, t) \bar{\Psi}_j^w(z) = \sum_{i=1}^m \sum_{j=1}^n W_{ji}(t) \Psi_i^w(x, y) \bar{\Psi}_j^w(z) \quad (51)
\end{aligned}$$

In similar way, the approximation for the potential can be written as:

$$\varphi(x, y, z, t) = \sum_{j=1}^n \Phi_j(x, y, t) \bar{\Psi}_j^\varphi(z) = \sum_{i=1}^m \sum_{j=1}^n \Phi_{ji}(t) \Psi_i^\varphi(x, y) \bar{\Psi}_j^\varphi(z) \quad (52)$$

where  $u, v$ , and  $w$  represent the displacement components in the  $x, y$ , and  $z$  directions respectively of a material in the underformed laminate, and  $\varphi$  represents the electric potential. In the above equations, two approximations have been made. In the first one, the transverse variation of the displacement field is defined in terms of the one-dimensional Lagrangian interpolation polynomials  $\bar{\Psi}_j(z)$  which are associated with the  $j^{\text{th}}$  interface of the layers through the laminate thickness and are defined only on two adjacent layers.

The laminate is divided into  $n$  nodes distributed through the thickness at the  $j^{\text{th}}$  level, defined by  $z = z_j$  in the undeformed laminate. At this level of approximation, the functions  $U_j(x, y, t), V_j(x, y, t), W_j(x, y, t)$ , and  $\Phi_j(x, y, t)$  represent the displacement and potential components of all points located at the  $j^{\text{th}}$  plane. In the second approximation, the in-plane displacement and electric potential field have been defined in terms of the two-dimensional Lagrangian interpolation polynomials  $\Psi(x, y)$ . The  $j^{\text{th}}$  plane is divided into two-dimensional finite elements and  $m$  represents the number of nodes per every one of these elements. At this level of approximation, the functions  $U_{ji}, V_{ji}, W_{ji}$ , and  $\Phi_{ji}$  represent the values of the components  $u, v$ , and  $w$ , and  $\varphi$  at height  $j$  corresponding to the  $i^{\text{th}}$  node of the two-dimensional finite element.

Now substituting equation 51 and 52 into the variational form of Hamilton's principle 50, integrating with respect to the thickness coordinate  $z$ , and collecting terms, the final equation in matrix form can be expressed as:

$$[K]_e \{\Delta\}_e = \{F\}_e \quad (53)$$

or

$$\begin{bmatrix} [K^{11}] & [K^{12}] & [K^{13}] & [K^{14}] \\ [K^{12}] & [K^{22}] & [K^{23}] & [K^{24}] \\ [K^{13}] & [K^{23}] & [K^{33}] & [K^{34}] \\ [K^{14}] & [K^{24}] & [K^{34}] & [K^{44}] \end{bmatrix}_e \begin{Bmatrix} \{u\} \\ \{v\} \\ \{w\} \\ \{\Phi\} \end{Bmatrix}_e = \begin{Bmatrix} \{f^1\} \\ \{f^2\} \\ \{f^3\} \\ \{f^4\} \end{Bmatrix}_e \quad (54)$$

The elements of the stiffness matrix  $[K]_e$  and force vector  $\{F\}_e$  are given below:

$$[K^{11}]_{\alpha\beta} = \int_A \left[ [A^{11}] \frac{\partial \Psi_\alpha^u}{\partial x} \frac{\partial \Psi_\beta^u}{\partial x} + [A^{16}] \left( \frac{\partial \Psi_\alpha^u}{\partial y} \frac{\partial \Psi_\beta^u}{\partial x} + \frac{\partial \Psi_\alpha^u}{\partial x} \frac{\partial \Psi_\beta^u}{\partial y} \right) + [D^{55}] \Psi_\alpha^u \Psi_\beta^u + [A^{66}] \frac{\partial \Psi_\alpha^u}{\partial y} \frac{\partial \Psi_\beta^u}{\partial y} \right] dx dy$$

$$[K^{12}]_{\alpha\beta} = \int_A \left[ [A^{12}] \frac{\partial \Psi_\alpha^u}{\partial x} \frac{\partial \Psi_\beta^v}{\partial y} + [A^{26}] \frac{\partial \Psi_\alpha^u}{\partial y} \frac{\partial \Psi_\beta^v}{\partial y} + [A^{16}] \frac{\partial \Psi_\alpha^u}{\partial x} \frac{\partial \Psi_\beta^v}{\partial x} + [D^{45}] \Psi_\alpha^u \Psi_\beta^v + [A^{66}] \frac{\partial \Psi_\alpha^u}{\partial y} \frac{\partial \Psi_\beta^v}{\partial x} \right] dx dy$$

$$[K^{13}]_{\alpha\beta} = \int_A \left[ [B^{13}] \frac{\partial \Psi_\alpha^u}{\partial x} \Psi_\beta^w + [B^{36}] \frac{\partial \Psi_\alpha^u}{\partial y} \Psi_\beta^w + [\bar{B}^{45}] \Psi_\alpha^u \frac{\partial \Psi_\beta^w}{\partial y} + \right]$$

$$\begin{aligned}
& [\bar{B}^{55}] \Psi_\alpha^u \frac{\partial \Psi_\beta^w}{\partial x} \Big] dx dy \\
[K^{14}]_{\alpha\beta} &= \int_A \left[ [\bar{E}^{25}] \Psi_\alpha^u \frac{\partial \Psi_\beta^\varphi}{\partial y} + [\bar{E}^{15}] \Psi_\alpha^u \frac{\partial \Psi_\beta^\varphi}{\partial x} + [E^{31}] \frac{\partial \Psi_\alpha^u}{\partial x} \Psi_\beta^\varphi + \right. \\
& \quad \left. [E^{36}] \frac{\partial \Psi_\alpha^u}{\partial y} \Psi_\beta^\varphi \right] dx dy \\
[K^{22}]_{\alpha\beta} &= \int_A \left[ [A^{22}] \frac{\partial \Psi_\alpha^v}{\partial y} \frac{\partial \Psi_\beta^v}{\partial y} + [A^{26}] \left( \frac{\partial \Psi_\alpha^v}{\partial x} \frac{\partial \Psi_\beta^v}{\partial y} + \frac{\partial \Psi_\alpha^v}{\partial y} \frac{\partial \Psi_\beta^v}{\partial x} \right) + \right. \\
& \quad \left. [D^{44}] \Psi_\alpha^v \Psi_\beta^v + [A^{66}] \frac{\partial \Psi_\alpha^v}{\partial x} \frac{\partial \Psi_\beta^v}{\partial x} \right] dx dy \\
[K^{23}]_{\alpha\beta} &= \int_A \left[ [B^{23}] \frac{\partial \Psi_\alpha^v}{\partial y} \Psi_\beta^w + [B^{36}] \frac{\partial \Psi_\alpha^v}{\partial x} \Psi_\beta^w + [\bar{B}^{44}] \Psi_\alpha^v \frac{\partial \Psi_\beta^w}{\partial y} + \right. \\
& \quad \left. [\bar{B}^{45}] \Psi_\alpha^v \frac{\partial \Psi_\beta^w}{\partial x} \right] dx dy \\
[K^{24}]_{\alpha\beta} &= \int_A \left[ \bar{E}^{14} \Psi_\alpha^v \frac{\partial \Psi_\beta^\varphi}{\partial x} + [\bar{E}^{24}] \Psi_\alpha^v \frac{\partial \Psi_\beta^\varphi}{\partial y} + [E^{32}] \frac{\partial \Psi_\alpha^v}{\partial y} \Psi_\beta^\varphi + \right. \\
& \quad \left. [E^{36}] \frac{\partial \Psi_\alpha^v}{\partial x} \Psi_\beta^\varphi \right] dx dy \\
[K^{33}]_{\alpha\beta} &= \int_A \left[ [A^{44}] \frac{\partial \Psi_\alpha^w}{\partial y} \frac{\partial \Psi_\beta^w}{\partial y} + [A^{45}] \left( \frac{\partial \Psi_\alpha^w}{\partial x} \frac{\partial \Psi_\beta^w}{\partial y} + \frac{\partial \Psi_\alpha^w}{\partial y} \frac{\partial \Psi_\beta^w}{\partial x} \right) + \right. \\
& \quad \left. [D^{33}] \Psi_\alpha^w \Psi_\beta^w + [A^{55}] \frac{\partial \Psi_\alpha^w}{\partial x} \frac{\partial \Psi_\beta^w}{\partial x} \right] dx dy \\
[K^{34}]_{\alpha\beta} &= \int_A \left[ [\hat{E}^{14}] \frac{\partial \Psi_\alpha^w}{\partial y} \frac{\partial \Psi_\beta^\varphi}{\partial x} + [\hat{E}^{15}] \frac{\partial \Psi_\alpha^w}{\partial x} \frac{\partial \Psi_\beta^\varphi}{\partial x} + [\hat{E}^{24}] \frac{\partial \Psi_\alpha^w}{\partial y} \frac{\partial \Psi_\beta^\varphi}{\partial y} + \right. \\
& \quad \left. [\hat{E}^{25}] \frac{\partial \Psi_\alpha^w}{\partial x} \frac{\partial \Psi_\beta^\varphi}{\partial y} + [\hat{E}^{33}] \Psi_\alpha^w \Psi_\beta^\varphi \right] dx dy \\
[K^{44}]_{\alpha\beta} &= \int_A \left[ [G^{11}] \frac{\partial \Psi_\alpha^\varphi}{\partial x} \frac{\partial \Psi_\beta^\varphi}{\partial x} + [G^{22}] \frac{\partial \Psi_\alpha^\varphi}{\partial y} \frac{\partial \Psi_\beta^\varphi}{\partial y} + [\bar{G}^{33}] \Psi_\alpha^\varphi \Psi_\beta^\varphi \right] dx dy \quad (55)
\end{aligned}$$

$$\{q\} = \int_A D_i \Psi_i dx dy \quad (56)$$

$$\{f^\alpha\} = \int_A f_i \Psi_i dx dy \quad (57)$$

The matrices involved in the above equations result from the evaluation of the integration of the elastic and dielectric constants through the thickness of the laminate. These matrices can be written as follows:

$$A_{ij}^{km} = \sum_{l=1}^N \int_{z_l}^{z_{l+1}} C_{km} \bar{\Psi}_i(z) \bar{\Psi}_j(z) dz \quad (58)$$

$$D_{ij}^{km} = \sum_{l=1}^N \int_{z_l}^{z_{l+1}} C_{km} \frac{d\bar{\Psi}_i(z)}{dz} \frac{d\bar{\Psi}_j(z)}{dz} dz \quad (59)$$

$$B_{ij}^{km} = \sum_{l=1}^N \int_{z_l}^{z_{l+1}} C_{km} \bar{\Psi}_i(z) \frac{d\bar{\Psi}_j(z)}{dz} dz \quad (60)$$

$$\bar{B}_{ij}^{km} = \sum_{l=1}^N \int_{z_l}^{z_{l+1}} C_{km} \frac{d\bar{\Psi}_i(z)}{dz} \bar{\Psi}_j(z) dz \quad (61)$$

$$\bar{E}_{ij}^{km} = \sum_{l=1}^N \int_{z_l}^{z_{l+1}} e_{km} \frac{d\bar{\Psi}_i(z)}{dz} \bar{\Psi}_j(z) dz \quad (62)$$

$$E_{ij}^{km} = \sum_{l=1}^N \int_{z_l}^{z_{l+1}} e_{km} \bar{\Psi}_i(z) \frac{d\bar{\Psi}_j(z)}{dz} dz \quad (63)$$

$$\hat{E}_{ij}^{km} = \sum_{l=1}^N \int_{z_l}^{z_{l+1}} e_{km} \bar{\Psi}_i(z) \bar{\Psi}_j(z) dz \quad (64)$$

$$\check{E}_{ij}^{km} = \sum_{l=1}^N \int_{z_l}^{z_{l+1}} e_{km} \frac{d\bar{\Psi}_i(z)}{dz} \frac{d\bar{\Psi}_j(z)}{dz} dz \quad (65)$$

$$G_{ij}^{km} = \sum_{l=1}^N \int_{z_l}^{z_{l+1}} \epsilon_{km} \frac{d\bar{\Psi}_i(z)}{dz} \frac{d\bar{\Psi}_j(z)}{dz} dz \quad (66)$$

$$\bar{G}_{ij}^{km} = \sum_{l=1}^N \int_{z_l}^{z_{l+1}} \epsilon_{km} \bar{\Psi}_i(z) \bar{\Psi}_j(z) dz \quad (67)$$

where N is the number of subdivisions through the thickness and, in general, it will be taken equal or greater than the number of layers in the laminate.

The theory which allows independent piece-wise linear approximations for w and the remaining components can be represented by the above discussion, with the provision that

now the through-thickness linear Lagrangian interpolation polynomials will differ.

*A constant transverse displacement model*

The following approximations for the the displacement and potential variables are assumed:

$$u(x, y, z, t) = \sum_{j=1}^n U_j(x, y, t) \bar{\Psi}_j^u(z) = \sum_{i=1}^m \sum_{j=1}^n U_{ji}(t) \Psi_i^u(x, y) \bar{\Psi}_j^u(z)$$

$$v(x, y, z, t) = \sum_{j=1}^n V_j(x, y, t) \bar{\Psi}_j^v(z) = \sum_{i=1}^m \sum_{j=1}^n V_{ji}(t) \Psi_i^v(x, y) \bar{\Psi}_j^v(z)$$

$$w(x, y, t) = \sum_{i=1}^m W_i(t) \Psi_i^w(x, y)$$

$$\varphi(x, y, z, t) = \sum_{j=1}^n \Phi_j(x, y, t) \bar{\Psi}_j^\varphi(z) = \sum_{i=1}^m \sum_{j=1}^n \Phi_{ji}(t) \Psi_i^\varphi(x, y) \bar{\Psi}_j^\varphi(z) \quad (68)$$

The only difference between these approximations and those assumed in the other models is found in the approximation used for the transverse displacement in the  $z$  direction. In this model, the transverse displacement is considered constant through the thickness and therefore the one-dimensional Lagrangian interpolation polynomials  $\bar{\Psi}^j(z)$  used before is equal to one. The  $W_i$  represents the transverse displacement corresponding to the  $i$ -th node of the two-dimensional finite element used in the approximations through the  $x-y$  plane.

Proceeding in the same way as that used in the other model, the following element stiffness submatrices of  $[K]_e$  and the force vector  $\{F\}_e$  are obtained and may be written as:

$$[K^{11}]_{\alpha\beta} = \int_A \left[ [A^{11}] \frac{\partial \Psi_\alpha^u}{\partial x} \frac{\partial \Psi_\beta^u}{\partial x} + [A^{16}] \left( \frac{\partial \Psi_\alpha^u}{\partial y} \frac{\partial \Psi_\beta^u}{\partial x} + \frac{\partial \Psi_\alpha^u}{\partial x} \frac{\partial \Psi_\beta^u}{\partial y} \right) + [D^{55}] \Psi_\alpha^u \Psi_\beta^u + [A^{66}] \frac{\partial \Psi_\alpha^u}{\partial y} \frac{\partial \Psi_\beta^u}{\partial y} \right] dx dy$$

$$[K^{12}]_{\alpha\beta} = \int_A \left[ [A^{12}] \frac{\partial \Psi_\alpha^u}{\partial x} \frac{\partial \Psi_\beta^v}{\partial y} + [A^{26}] \frac{\partial \Psi_\alpha^u}{\partial y} \frac{\partial \Psi_\beta^v}{\partial y} + [A^{16}] \frac{\partial \Psi_\alpha^u}{\partial x} \frac{\partial \Psi_\beta^v}{\partial x} + [D^{45}] \Psi_\alpha^u \Psi_\beta^v + [A^{66}] \frac{\partial \Psi_\alpha^u}{\partial y} \frac{\partial \Psi_\beta^v}{\partial x} \right] dx dy$$



$$[K^{13}]_{\alpha\beta} = \int_A \left[ \{AB^{45}\} \Psi_\alpha^u \frac{\partial \Psi_\beta^w}{\partial y} + \{AB^{55}\} \Psi_\alpha^u \frac{\partial \Psi_{w\beta}}{\partial x} \right] dx dy$$

$$[K^{14}]_{\alpha\beta} = \int_A \left[ [\bar{E}^{25}] \Psi_\alpha^u \frac{\partial \Psi_\beta^\varphi}{\partial y} + [\bar{E}^{15}] \Psi_\alpha^u \frac{\partial \Psi_\beta^\varphi}{\partial x} + [E^{31}] \frac{\partial \Psi_\alpha^u}{\partial x} \Psi_\beta^\varphi + \right. \\ \left. [E^{36}] \frac{\partial \Psi_\alpha^u}{\partial y} \Psi_\beta^\varphi \right] dx dy$$

$$[K^{22}]_{\alpha\beta} = \int_A \left[ [A^{22}] \frac{\partial \Psi_\alpha^v}{\partial y} \frac{\partial \Psi_\beta^v}{\partial y} + [A^{26}] \left( \frac{\partial \Psi_\alpha^v}{\partial x} \frac{\partial \Psi_\beta^v}{\partial y} + \frac{\partial \Psi_\alpha^v}{\partial y} \frac{\partial \Psi_\beta^v}{\partial x} \right) + \right. \\ \left. [D^{44}] \Psi_\alpha^v \Psi_\beta^v + [A^{66}] \frac{\partial \Psi_\alpha^v}{\partial x} \frac{\partial \Psi_\beta^v}{\partial x} \right] dx dy$$

$$[K^{23}]_{\alpha\beta} = \int_A \left[ \{AB^{44}\} \Psi_\alpha^v \frac{\partial \Psi_\beta^w}{\partial y} + \{AB^{45}\} \Psi_\alpha^v \frac{\partial \Psi_{w\beta}}{\partial x} \right] dx dy$$

$$[K^{24}]_{\alpha\beta} = \int_A \left[ \bar{E}^{14} \Psi_\alpha^v \frac{\partial \Psi_\beta^\varphi}{\partial x} + [\bar{E}^{24}] \Psi_\alpha^v \frac{\partial \Psi_\beta^\varphi}{\partial y} + [E^{32}] \frac{\partial \Psi_\alpha^v}{\partial y} \Psi_\beta^\varphi + \right. \\ \left. [E^{36}] \frac{\partial \Psi_\alpha^v}{\partial x} \Psi_\beta^\varphi \right] dx dy$$

$$[K^{33}]_{\alpha\beta} = \int_A \left[ AA^{44} \frac{\partial \Psi_\alpha^w}{\partial y} \frac{\partial \Psi_\beta^w}{\partial y} + AA^{45} \left( \frac{\partial \Psi_\alpha^w}{\partial x} \frac{\partial \Psi_\beta^w}{\partial y} + \frac{\partial \Psi_\alpha^w}{\partial y} \frac{\partial \Psi_\beta^w}{\partial x} \right) + \right. \\ \left. AA^{55} \frac{\partial \Psi_\alpha^w}{\partial x} \frac{\partial \Psi_\beta^w}{\partial x} \right] dx dy$$

$$[K^{34}]_{\alpha\beta} = \int_A \left[ (EE^{14}) \frac{\partial \Psi_\alpha^w}{\partial y} \frac{\partial \Psi_\beta^\varphi}{\partial y} + (EE^{15}) \frac{\partial \Psi_\alpha^w}{\partial x} \frac{\partial \Psi_\beta^\varphi}{\partial x} + (EE^{14}) \frac{\partial \Psi_\alpha^w}{\partial y} \frac{\partial \Psi_\beta^\varphi}{\partial y} + \right. \\ \left. (EE^{25}) \frac{\partial \Psi_\alpha^w}{\partial x} \frac{\partial \Psi_\beta^\varphi}{\partial y} \right] dx dy$$

$$[K^{44}]_{\alpha\beta} = \int_A \left[ [G^{11}] \frac{\partial \Psi_\alpha^\varphi}{\partial x} \frac{\partial \Psi_\beta^\varphi}{\partial x} + [G^{22}] \frac{\partial \Psi_\alpha^\varphi}{\partial y} \frac{\partial \Psi_\beta^\varphi}{\partial y} + [\bar{G}^{33}] \Psi_\alpha^\varphi \Psi_\beta^\varphi \right] dx dy \quad (69)$$

$$(70)$$

As before, the matrices and vectors involved in the above equations result from the integration of the elastic and dielectric constants through the thickness of the laminate. These matrices and vectors can be expressed as :

$$A_{ij}^{km} = \sum_{l=1}^N \int_{z_l}^{z_{l+1}} C_{km} \bar{\Psi}_i(z) \bar{\Psi}_j(z) dz \quad (71)$$

$$D_{ij}^{km} = \sum_{l=1}^N \int_{z_l}^{z_{l+1}} C_{km} \frac{d\bar{\Psi}_i(z)}{dz} \frac{d\bar{\Psi}_j(z)}{dz} dz \quad (72)$$

$$AB_i^{km} = \sum_{l=1}^N \int_{z_l}^{z_{l+1}} C_{km} \frac{d\bar{\Psi}_i(z)}{dz} dz \quad (73)$$

$$\bar{E}_{ij}^{km} = \sum_{l=1}^N \int_{z_l}^{z_{l+1}} e_{km} \frac{d\bar{\Psi}_i(z)}{dz} \bar{\Psi}_j(z) dz \quad (74)$$

$$E_{ij}^{km} = \sum_{l=1}^N \int_{z_l}^{z_{l+1}} e_{km} \bar{\Psi}_i(z) \frac{d\bar{\Psi}_j(z)}{dz} dz \quad (75)$$

$$AA^{km} = \sum_{l=1}^N \int_{z_l}^{z_{l+1}} C_{km} dz \quad (76)$$

$$EE_j^{km} = \sum_{l=1}^N \int_{z_l}^{z_{l+1}} e_{km} \bar{\Psi}_j(z) dz \quad (77)$$

### Transformation Matrices

In this work, it is desirable to simulate the behavior of a shell element derived from the plate element using an assemblage of flat plates. In this sections it is assumed that the behavior of a continuously curved surface can be adequately represented by the behavior of a surface built up of small plate elements.

Consider a typical plate element as derived in this section of the report. In general, there are four degrees of freedom per node in the  $j^{th}$  level, and depending on the approximation used for the transverse displacement,  $w$ , in the  $z$  direction we would have either  $4*(\text{number of layers} + 1)$  when  $w$  is a linear function through the thickness of the laminate or  $3*(\text{number of layers} + 1) + 1$  when  $w$  is considered constant through the thickness of the laminate as the total number of degrees of freedom per node through the thickness. The independent approximation case can be considered in this section as well.

The stiffness matrix derived before was based on a system of local coordinates, therefore a transformation of coordinates from a local system,  $(x', y', z')$  to a global system  $(x, y, z)$  will be necessary in order to assemble the elements and to write the appropriate

equilibrium equations. Moreover, it will be convenient to read the element node coordinates in the global system and get from these the local coordinates.

Therefore according to figure 14, we have that:

$$\{V'\} = [T]\{V\} \quad (78)$$

where  $V'_i$  are the components of a vector on the local system,  $V_i$  are the components of a vector on the global system, and  $T_{ij}$  are the cosine angles between the local and global axes and the matrix is given by:

$$T_{ij} = \begin{bmatrix} 1 & 0 & 0 \\ 0 & \cos\beta & \sin\beta \\ 0 & -\sin\beta & \cos\beta \end{bmatrix} \quad (79)$$

The cosine angles can be calculated by the following expressions:

$$\cos\beta = \frac{y_j - y_i}{\sqrt{((z_j - z_i)^2 + (y_j - y_i)^2)}} \quad \sin\beta = \frac{z_j - z_i}{\sqrt{((z_j - z_i)^2 + (y_j - y_i)^2)}} \quad (80)$$

Since we have to transform both the forces and displacements by using the equation 78 and taking into account that  $[k_{local}^e]\{\Delta_{local}\} = \{F_{local}\}$ , we get the final relationship:

$$([T]^T[k_{local}^e][T])\{\Delta_{global}\} = \{F_{global}\} \quad (81)$$

but

$$[K_{global}^e] = [T]^T[k_{local}^e][T] \quad (82)$$

therefore we can write equation 81 as:

$$[K_{global}^e]\{\Delta_{global}\} = \{F_{global}\} \quad (83)$$

where  $\Delta_i$  are the components of the displacement vector,  $F_i$  are the components of the force vector,  $k_{ij}$  are the components of element stiffness matrix in local coordinates, and  $K_{ij}$  are the components of the element stiffness matrix in the global coordinates.

Therefore for one node in a linear plate element and for both theories, with  $w$  varying and  $w$  constant through the thickness, the corresponding displacement vectors will appear as

$$\left\{ \begin{array}{c} U_{11} \\ U_{12} \\ V_{11} \\ V_{12} \\ W_{11} \\ W_{12} \\ \Phi_{11} \\ \Phi_{12} \end{array} \right\} \quad (84)$$

$$\begin{Bmatrix} U_{11} \\ U_{12} \\ V_{11} \\ V_{12} \\ W_1 \\ \Phi_{11} \\ \Phi_{12} \end{Bmatrix} \quad (85)$$

and the corresponding transformation matrix [T] will be:

$$T_{ij} = \begin{bmatrix} 1 & 0 & 0 & 0 & 0 & 0 & 0 & 0 \\ 0 & 1 & 0 & 0 & 0 & 0 & 0 & 0 \\ 0 & 0 & \cos\beta & 0 & \sin\beta & 0 & 0 & 0 \\ 0 & 0 & 0 & \cos\beta & 0 & \sin\beta & 0 & 0 \\ 0 & 0 & -\sin\beta & 0 & \cos\beta & 0 & 0 & 0 \\ 0 & 0 & 0 & -\sin\beta & 0 & \cos\beta & 0 & 0 \\ 0 & 0 & 0 & 0 & 0 & 0 & 1 & 0 \\ 0 & 0 & 0 & 0 & 0 & 0 & 0 & 1 \end{bmatrix}$$

Examples of applications of this element are included in the results chapter of this report. As of this writing, only the flat plate case had been investigated with the assembly of plates remaining to be studied.

## 5. THE SHELL ELEMENT

In this chapter, the formulation for two laminated piezoelectric shell elements is given: the cylindrical shell and the general curvilinear shell. Both are based on solutions of the weak form of the equations of motion using the discrete-layer type theories described in the two preceding chapters.

### Variational Formulation in Cylindrical Coordinates

A special case of a laminated shell is the cylindrical shell geometry, which is best formulated in cylindrical coordinates. Let  $u, v, w$  be the components of displacement along the  $r, \theta$ , and  $z$  directions in cylindrical coordinates, respectively. The strain-displacement relations and the stress equations of motion are given as

$$\epsilon_{rr} = \frac{\partial u}{\partial r} \quad \epsilon_{\theta\theta} = \frac{1}{r} \frac{\partial v}{\partial \theta} + \frac{u}{r} \quad \epsilon_{zz} = \frac{\partial w}{\partial z} \quad (86)$$

$$\gamma_{\theta z} = \frac{\partial v}{\partial z} + \frac{1}{r} \frac{\partial w}{\partial \theta} \quad \gamma_{rz} = \frac{\partial w}{\partial r} + \frac{\partial u}{\partial z} \quad \gamma_{r\theta} = \frac{1}{r} \frac{\partial u}{\partial \theta} + \frac{\partial v}{\partial r} - \frac{v}{r} \quad (87)$$

$$\rho \ddot{u} = \frac{1}{r} \frac{\partial(r\sigma_{rr})}{\partial r} + \frac{1}{r} \frac{\partial\sigma_{r\theta}}{\partial \theta} + \frac{\partial\sigma_{rz}}{\partial z} - \frac{\sigma_{\theta\theta}}{r} \quad (88)$$

$$\rho \ddot{v} = \frac{1}{r^2} \frac{\partial(r^2\sigma_{\theta r})}{\partial r} + \frac{1}{r} \frac{\partial\sigma_{\theta\theta}}{\partial \theta} + \frac{\partial\sigma_{\theta z}}{\partial z} \quad (89)$$

$$\rho \ddot{w} = \frac{1}{r} \frac{\partial(r\sigma_{zr})}{\partial r} + \frac{1}{r} \frac{\partial\sigma_{z\theta}}{\partial \theta} + \frac{\partial\sigma_{zz}}{\partial z} \quad (90)$$

Because the normal vector of layer surface will be taken along the  $r$ -direction, also this direction is assumed to be the poling direction of each layer, the matrix of piezoelectric coefficient is given as

$$\begin{bmatrix} e_{11} & e_{12} & e_{13} & 0 & 0 & e_{16} \\ 0 & 0 & 0 & e_{24} & e_{25} & 0 \\ 0 & 0 & 0 & e_{34} & e_{35} & 0 \end{bmatrix} \quad (91)$$

Also, the electric field can be written as

$$E(r, \theta, z) = -\frac{\partial\phi}{\partial r} \vec{e}_r - \frac{1}{r} \frac{\partial\phi}{\partial \theta} \vec{e}_\theta - \frac{\partial\phi}{\partial z} \vec{e}_z \quad (92)$$

Hamilton's principle as written in equation 14 can be expressed as

$$\begin{aligned} & \delta \int_{t_0}^{t_1} dt \int_V \left[ \frac{1}{2} \rho \dot{u}_i \dot{u}_i - H(S_{kl}, E_k) \right] dV + \int_{t_0}^{t_1} dt \int_S (\bar{t}_i \delta u_i - \bar{\sigma} \delta \phi) dS \\ & = \int_{t_0}^{t_1} dt \int_V \left\{ -[\rho \ddot{u} \delta u + \rho \ddot{v} \delta v + \rho \ddot{w} \delta w] - C_{11} \frac{\partial u}{\partial r} \frac{\partial \delta u}{\partial r} \right. \end{aligned}$$

$$\begin{aligned}
& -\frac{1}{r}C_{12} \left[ \frac{\partial u}{\partial r} (\delta u + \frac{\partial \delta v}{\partial \theta}) + (u + \frac{\partial v}{\partial \theta}) \frac{\partial \delta u}{\partial r} \right] - C_{13} \left( \frac{\partial u}{\partial r} \frac{\partial \delta w}{\partial z} + \frac{\partial \delta u}{\partial r} \frac{\partial w}{\partial z} \right) \\
& -C_{16} \left[ \frac{\partial u}{\partial r} \left( \frac{1}{r} \frac{\partial \delta u}{\partial \theta} + \frac{\partial \delta v}{\partial r} - \frac{\delta v}{r} \right) + \left( \frac{1}{r} \frac{\partial u}{\partial \theta} + \frac{\partial v}{\partial r} - \frac{v}{r} \right) \frac{\partial \delta u}{\partial r} \right] \\
& -\frac{1}{r^2}C_{22} \left( \frac{\partial v}{\partial \theta} \frac{\partial \delta v}{\partial \theta} + \frac{\partial v}{\partial \theta} \delta u + \frac{\partial \delta v}{\partial \theta} u + u \delta u \right) \\
& -\frac{1}{r}C_{23} \left( \frac{\partial w}{\partial z} \frac{\partial \delta v}{\partial \theta} + \frac{\partial \delta w}{\partial z} \frac{\partial v}{\partial \theta} + \frac{\partial w}{\partial z} \delta u + \frac{\partial \delta w}{\partial z} u \right) \\
& -\frac{1}{r}C_{26} \left( \frac{\partial v}{\partial \theta} + u \right) \left( \frac{1}{r} \frac{\partial \delta u}{\partial \theta} + \frac{\partial \delta v}{\partial r} - \frac{\delta v}{r} \right) \\
& -\frac{1}{r}C_{26} \left( \frac{1}{r} \frac{\partial u}{\partial \theta} + \frac{\partial v}{\partial r} - \frac{v}{r} \right) \left( \frac{\partial \delta v}{\partial \theta} + \delta u \right) - C_{33} \frac{\partial w}{\partial z} \frac{\partial \delta w}{\partial z} \\
& -C_{36} \left[ \frac{\partial w}{\partial z} \left( \frac{1}{r} \frac{\partial \delta u}{\partial \theta} + \frac{\partial \delta v}{\partial r} - \frac{\delta v}{r} \right) + \left( \frac{1}{r} \frac{\partial u}{\partial \theta} + \frac{\partial v}{\partial r} - \frac{v}{r} \right) \frac{\partial \delta w}{\partial z} \right] \\
& -C_{44} \left( \frac{\partial v}{\partial z} + \frac{1}{r} \frac{\partial w}{\partial \theta} \right) \left( \frac{\partial \delta v}{\partial z} + \frac{1}{r} \frac{\partial \delta w}{\partial \theta} \right) \\
& -C_{45} \left[ \left( \frac{\partial v}{\partial z} + \frac{1}{r} \frac{\partial w}{\partial \theta} \right) \left( \frac{\partial \delta w}{\partial r} + \frac{\partial \delta u}{\partial z} \right) + \left( \frac{\partial w}{\partial r} + \frac{\partial u}{\partial z} \right) \left( \frac{\partial \delta v}{\partial z} + \frac{1}{r} \frac{\partial \delta w}{\partial \theta} \right) \right] \\
& -C_{55} \left( \frac{\partial w}{\partial r} + \frac{\partial u}{\partial z} \right) \left( \frac{\partial \delta w}{\partial r} + \frac{\partial \delta u}{\partial z} \right) \\
& -C_{66} \left( \frac{1}{r} \frac{\partial u}{\partial \theta} + \frac{\partial v}{\partial r} - \frac{v}{r} \right) \left( \frac{1}{r} \frac{\partial \delta u}{\partial \theta} + \frac{\partial \delta v}{\partial r} - \frac{\delta v}{r} \right) \\
& -e_{11} \left( \frac{\partial \phi}{\partial r} \frac{\partial \delta u}{\partial r} + \frac{\partial u}{\partial r} \frac{\partial \delta \phi}{\partial r} \right) - \frac{1}{r} e_{12} \left[ \frac{\partial \phi}{\partial r} (\delta u + \frac{\partial \delta v}{\partial \theta}) + (u + \frac{\partial v}{\partial \theta}) \frac{\partial \delta \phi}{\partial r} \right] \\
& -e_{13} \left( \frac{\partial \phi}{\partial r} \frac{\partial \delta w}{\partial z} + \frac{\partial \delta \phi}{\partial r} \frac{\partial w}{\partial z} \right) \\
& -e_{16} \left[ \frac{\partial \phi}{\partial r} \left( \frac{1}{r} \frac{\partial \delta u}{\partial \theta} + \frac{\partial \delta v}{\partial r} - \frac{\delta v}{r} \right) + \left( \frac{1}{r} \frac{\partial u}{\partial \theta} + \frac{\partial v}{\partial r} - \frac{v}{r} \right) \frac{\partial \delta \phi}{\partial r} \right] \\
& -\frac{1}{r} e_{24} \left[ \left( \frac{\partial v}{\partial z} + \frac{1}{r} \frac{\partial w}{\partial \theta} \right) \frac{\partial \delta \phi}{\partial \theta} + \frac{\partial \phi}{\partial \theta} \left( \frac{\partial \delta v}{\partial z} + \frac{1}{r} \frac{\partial \delta w}{\partial \theta} \right) \right] \\
& -\frac{1}{r} e_{25} \left[ \left( \frac{\partial w}{\partial r} + \frac{\partial u}{\partial z} \right) \frac{\partial \delta \phi}{\partial \theta} + \frac{\partial \phi}{\partial \theta} \left( \frac{\partial \delta w}{\partial r} + \frac{\partial \delta u}{\partial z} \right) \right] \\
& -e_{34} \left[ \left( \frac{\partial v}{\partial z} + \frac{1}{r} \frac{\partial w}{\partial \theta} \right) \frac{\partial \delta \phi}{\partial z} + \frac{\partial \phi}{\partial z} \left( \frac{\partial \delta v}{\partial z} + \frac{1}{r} \frac{\partial \delta w}{\partial \theta} \right) \right] \\
& -e_{35} \left[ \left( \frac{\partial w}{\partial r} + \frac{\partial u}{\partial z} \right) \frac{\partial \delta \phi}{\partial z} + \frac{\partial \phi}{\partial z} \left( \frac{\partial \delta w}{\partial r} + \frac{\partial \delta u}{\partial z} \right) \right] \\
& + \left[ \varepsilon_{11} \frac{\partial \phi}{\partial r} \frac{\partial \delta \phi}{\partial r} + \frac{1}{r^2} \varepsilon_{22} \frac{\partial \phi}{\partial \theta} \frac{\partial \delta \phi}{\partial \theta} + \varepsilon_{33} \frac{\partial \phi}{\partial z} \frac{\partial \delta \phi}{\partial z} \right] dV \\
& + \int_{t_0}^{t_1} dt \int_S (\bar{t}_r \delta u + \bar{t}_\theta \delta v + \bar{t}_z \delta w - \bar{\sigma} \delta \phi) dS = 0 \tag{93}
\end{aligned}$$

This state provides the basis for finite element approximations to the equations of

motion as formulated in cylindrical coordinates, and are a special case of that described below. This more general case is described thoroughly and has a corresponding numerical algorithm that was completed as part of this proposal.

### Variational Formulation in Curvilinear Coordinates

To analyze the laminated piezoelectric shell with arbitrary geometry, curvilinear coordinates ( see Figures 4 and 11) will be used here to overcome the disadvantage from the integration directly using the global coordinate system. The local and global systems can be related using mapping technique. Let  $u, v, w$  be the components of displacement along the  $x$ -,  $y$ -, and  $z$ -coordinate directions of a Cartesian coordinate system, respectively. This coordinate represents the global coordinate system. The curvilinear coordinate system, described by  $\xi$ -,  $\eta$ -, and  $\zeta$ -coordinate directions, is the local system for the general shell. Let  $\bar{u}, \bar{v}, \bar{w}$  be the components of displacement along the  $\xi, \eta, \zeta$ -coordinate directions. A laminated shell with complicated geometry can be separated into several small parts that function as shell elements, and described using more but simpler curvilinear coordinates. In this section, the variational formulation will be expressed in terms of the local coordinate system.

The strain-displacement relations and the stress equations of motion using the global coordinate are given as

$$\epsilon_{xx} = \frac{\partial u}{\partial x} \quad \epsilon_{yy} = \frac{\partial v}{\partial y} \quad \epsilon_{zz} = \frac{\partial w}{\partial z} \quad (94)$$

$$\gamma_{yz} = \frac{\partial v}{\partial z} + \frac{\partial w}{\partial y} \quad \gamma_{xz} = \frac{\partial w}{\partial x} + \frac{\partial u}{\partial z} \quad \gamma_{xy} = \frac{\partial u}{\partial y} + \frac{\partial v}{\partial x} \quad (95)$$

$$\rho \ddot{u} = \frac{\partial \sigma_{xx}}{\partial x} + \frac{\partial \sigma_{xy}}{\partial y} + \frac{\partial \sigma_{xz}}{\partial z} \quad (96)$$

$$\rho \ddot{v} = \frac{\partial \sigma_{yx}}{\partial x} + \frac{\partial \sigma_{yy}}{\partial y} + \frac{\partial \sigma_{yz}}{\partial z} \quad (97)$$

$$\rho \ddot{w} = \frac{\partial \sigma_{zx}}{\partial x} + \frac{\partial \sigma_{zy}}{\partial y} + \frac{\partial \sigma_{zz}}{\partial z} \quad (98)$$

The electric field can be written as

$$E(x, y, z) = -\frac{\partial \phi}{\partial x} \vec{e}_x - \frac{\partial \phi}{\partial y} \vec{e}_y - \frac{\partial \phi}{\partial z} \vec{e}_z \quad (99)$$

The strain components in global coordinate system can be changed into the local system

with the coordinate transformations given by

$$\begin{bmatrix} \bar{\epsilon}_{\xi\xi} & \bar{\epsilon}_{\xi\eta} & \bar{\epsilon}_{\xi\zeta} \\ \bar{\epsilon}_{\eta\xi} & \bar{\epsilon}_{\eta\eta} & \bar{\epsilon}_{\eta\zeta} \\ \bar{\epsilon}_{\zeta\xi} & \bar{\epsilon}_{\zeta\eta} & \bar{\epsilon}_{\zeta\zeta} \end{bmatrix} = \begin{bmatrix} \frac{\partial x}{\partial \xi} & \frac{\partial y}{\partial \xi} & \frac{\partial z}{\partial \xi} \\ \frac{\partial x}{\partial \eta} & \frac{\partial y}{\partial \eta} & \frac{\partial z}{\partial \eta} \\ \frac{\partial x}{\partial \zeta} & \frac{\partial y}{\partial \zeta} & \frac{\partial z}{\partial \zeta} \end{bmatrix} \begin{bmatrix} \epsilon_{xx} & \epsilon_{xy} & \epsilon_{xz} \\ \epsilon_{yx} & \epsilon_{yy} & \epsilon_{yz} \\ \epsilon_{zx} & \epsilon_{zy} & \epsilon_{zz} \end{bmatrix} \begin{bmatrix} \frac{\partial x}{\partial \xi} & \frac{\partial x}{\partial \eta} & \frac{\partial x}{\partial \zeta} \\ \frac{\partial y}{\partial \xi} & \frac{\partial y}{\partial \eta} & \frac{\partial y}{\partial \zeta} \\ \frac{\partial z}{\partial \xi} & \frac{\partial z}{\partial \eta} & \frac{\partial z}{\partial \zeta} \end{bmatrix} \quad (100)$$

It can be written as :  $[\bar{\epsilon}]_{\xi\eta\zeta} = [J(\frac{x,y,z}{\xi,\eta,\zeta})] [\epsilon]_{xyz} [J(\frac{x,y,z}{\xi,\eta,\zeta})]^T$ , here

$$\left[ J\left(\frac{xyz}{\xi\eta\zeta}\right) \right] = \begin{bmatrix} \frac{\partial x}{\partial \xi} & \frac{\partial y}{\partial \xi} & \frac{\partial z}{\partial \xi} \\ \frac{\partial x}{\partial \eta} & \frac{\partial y}{\partial \eta} & \frac{\partial z}{\partial \eta} \\ \frac{\partial x}{\partial \zeta} & \frac{\partial y}{\partial \zeta} & \frac{\partial z}{\partial \zeta} \end{bmatrix} = \begin{bmatrix} J_{11} & J_{12} & J_{13} \\ J_{21} & J_{22} & J_{23} \\ J_{31} & J_{32} & J_{33} \end{bmatrix} \quad (101)$$

Equation 100 can be further expressed as :

$$\{\bar{\epsilon}\}_{\xi\eta\zeta} = \begin{bmatrix} \bar{\epsilon}_{\xi\xi} \\ \bar{\epsilon}_{\eta\eta} \\ \bar{\epsilon}_{\zeta\zeta} \\ \bar{\epsilon}_{\eta\zeta} \\ \bar{\epsilon}_{\xi\zeta} \\ \bar{\epsilon}_{\xi\eta} \end{bmatrix} = [T] \begin{bmatrix} \epsilon_{xx} \\ \epsilon_{yy} \\ \epsilon_{zz} \\ \epsilon_{yz} \\ \epsilon_{xz} \\ \epsilon_{xy} \end{bmatrix} = \quad (102)$$

$$\begin{bmatrix} J_{11}^2 & J_{12}^2 & J_{13}^2 & 2J_{12}J_{13} & 2J_{11}J_{13} & 2J_{11}J_{12} \\ J_{21}^2 & J_{22}^2 & J_{23}^2 & 2J_{22}J_{23} & 2J_{21}J_{23} & 2J_{21}J_{22} \\ J_{31}^2 & J_{32}^2 & J_{33}^2 & 2J_{32}J_{33} & 2J_{31}J_{33} & 2J_{31}J_{32} \\ J_{21}J_{31} & J_{22}J_{32} & J_{23}J_{33} & J_{22}J_{33} + J_{23}J_{32} & J_{21}J_{33} + J_{23}J_{31} & J_{21}J_{32} + J_{22}J_{31} \\ J_{11}J_{31} & J_{12}J_{32} & J_{13}J_{33} & J_{12}J_{33} + J_{13}J_{32} & J_{11}J_{33} + J_{13}J_{31} & J_{11}J_{32} + J_{12}J_{31} \\ J_{11}J_{21} & J_{12}J_{22} & J_{13}J_{23} & J_{12}J_{23} + J_{13}J_{22} & J_{11}J_{23} + J_{13}J_{21} & J_{11}J_{22} + J_{12}J_{21} \end{bmatrix} \begin{bmatrix} \epsilon_{xx} \\ \epsilon_{yy} \\ \epsilon_{zz} \\ \epsilon_{yz} \\ \epsilon_{xz} \\ \epsilon_{xy} \end{bmatrix}$$

The  $(u, v, w)$  in  $x, y, z$  system and  $(\bar{u}, \bar{v}, \bar{w})$  in  $\xi, \eta, \zeta$  system can be related using

$$\begin{bmatrix} \bar{u} \\ \bar{v} \\ \bar{w} \end{bmatrix} = \left[ J\left(\frac{x, y, z}{\xi, \eta, \zeta}\right) \right] \begin{bmatrix} u \\ v \\ w \end{bmatrix} \quad (103)$$

The electric field  $(E_x, E_y, E_z)$  and  $(\bar{E}_\xi, \bar{E}_\eta, \bar{E}_\zeta)$  can be related using

$$\begin{bmatrix} \bar{E}_\xi \\ \bar{E}_\eta \\ \bar{E}_\zeta \end{bmatrix} = \left[ J\left(\frac{x, y, z}{\xi, \eta, \zeta}\right) \right] \begin{bmatrix} E_x \\ E_y \\ E_z \end{bmatrix} \quad (104)$$

The first differential of  $(u, v, w, \phi)_{global}$  to  $(x, y, z)$  and  $(u, v, w, \phi)_{global}$  to  $(\xi, \eta, \zeta)$  can be related using the matrix,  $[J^{-1}(\frac{x,y,z}{\xi,\eta,\zeta})]^T$ .

$$\begin{bmatrix} u_x & u_y & u_z \\ v_x & v_y & v_z \\ w_x & w_y & w_z \\ \phi_x & \phi_y & \phi_z \end{bmatrix} = \begin{bmatrix} u_\xi & u_\eta & u_\zeta \\ v_\xi & v_\eta & v_\zeta \\ w_\xi & w_\eta & w_\zeta \\ \phi_\xi & \phi_\eta & \phi_\zeta \end{bmatrix} \begin{bmatrix} \frac{\partial \xi}{\partial x} & \frac{\partial \xi}{\partial y} & \frac{\partial \xi}{\partial z} \\ \frac{\partial \eta}{\partial x} & \frac{\partial \eta}{\partial y} & \frac{\partial \eta}{\partial z} \\ \frac{\partial \zeta}{\partial x} & \frac{\partial \zeta}{\partial y} & \frac{\partial \zeta}{\partial z} \end{bmatrix} \quad (105)$$



The  $\zeta$ -direction is located along the normal direction (also the poling direction) of the layer surface, and the  $\xi$ - and  $\eta$ - direction parallel to the layer surface. Hence equations 100 and 102 can be used to present the elastic stiffness matrix and the matrix of piezoelectric coefficient in the curvilinear coordinate system. The variation of electric enthalpy,  $\delta H$ , can be expressed as the following equation.

$$\begin{aligned}
\delta H &= \delta[\bar{\epsilon}_{ij}, \bar{E}_i]_{local} [R] [C]_{local} [R] [\bar{\epsilon}_{ij}, \bar{E}_i]_{local}^T \\
&= \delta[\epsilon_{lm}, E_l]_{global} [T^*]^T [R] [C]_{local} [R] [T^*] [\epsilon_{lm}, E_l]_{global}^T \\
&= \delta[\epsilon_{lm}, E_l]_{global} [R] ([\bar{T}^*]^T [R] [C]_{local} [R] [\bar{T}^*]) [R] [\epsilon_{lm}, E_l]_{global}^T \\
&= \delta[\epsilon_{lm}, E_l]_{global} [R] ([C]_{global}) [R] [\epsilon_{lm}, E_l]_{global}^T \\
&= \delta[u_{l,m}, \phi_{,l}]_{xyz} [B] [C]_{global} [B]^T [u_{l,m}, \phi_{,l}]_{xyz}^T \\
&= \delta[u_{i,j}, \phi_{,i}]_{\xi\eta\zeta} [\bar{J}^*] [B] [C]_{global} [B]^T [\bar{J}^*]^T [u_{i,j}, \phi_{,i}]_{\xi\eta\zeta}^T
\end{aligned} \tag{106}$$

Where

$$[\epsilon_{lm}, E_l]_{global} = \begin{bmatrix} \epsilon_{xx} & \epsilon_{yy} & \epsilon_{zz} & \epsilon_{yz} & \epsilon_{zx} & \epsilon_{xy} & E_x & E_y & E_z \end{bmatrix} \tag{107}$$

$$[\bar{\epsilon}_{ij}, \bar{E}_i]_{local} = \begin{bmatrix} \bar{\epsilon}_{\xi\xi} & \bar{\epsilon}_{\eta\eta} & \bar{\epsilon}_{\zeta\zeta} & \bar{\epsilon}_{\eta\zeta} & \bar{\epsilon}_{\xi\zeta} & \bar{\epsilon}_{\xi\eta} & \bar{E}_\xi & \bar{E}_\eta & \bar{E}_\zeta \end{bmatrix} \tag{108}$$

$$[u_{l,m}, \phi_{,l}]_{xyz} = \begin{bmatrix} \frac{\partial u}{\partial x} & \frac{\partial u}{\partial y} & \frac{\partial u}{\partial z} & \frac{\partial v}{\partial x} & \frac{\partial v}{\partial y} & \frac{\partial v}{\partial z} & \frac{\partial w}{\partial x} & \frac{\partial w}{\partial y} & \frac{\partial w}{\partial z} & \frac{-\partial\phi}{\partial x} & \frac{-\partial\phi}{\partial y} & \frac{-\partial\phi}{\partial z} \end{bmatrix} \tag{109}$$

$$[u_{i,j}, \phi_{,i}]_{\xi\eta\zeta} = \begin{bmatrix} \frac{\partial u}{\partial \xi} & \frac{\partial u}{\partial \eta} & \frac{\partial u}{\partial \zeta} & \frac{\partial v}{\partial \xi} & \frac{\partial v}{\partial \eta} & \frac{\partial v}{\partial \zeta} & \frac{\partial w}{\partial \xi} & \frac{\partial w}{\partial \eta} & \frac{\partial w}{\partial \zeta} & \frac{-\partial\phi}{\partial \xi} & \frac{-\partial\phi}{\partial \eta} & \frac{-\partial\phi}{\partial \zeta} \end{bmatrix} \tag{110}$$

$$[\bar{J}^*] = \begin{bmatrix} J^{-1}\left(\frac{xyz}{\xi\eta\zeta}\right) & 0 & 0 & 0 \\ 0 & J^{-1}\left(\frac{xyz}{\xi\eta\zeta}\right) & 0 & 0 \\ 0 & 0 & J^{-1}\left(\frac{xyz}{\xi\eta\zeta}\right) & 0 \\ 0 & 0 & 0 & J^{-1}\left(\frac{xyz}{\xi\eta\zeta}\right) \end{bmatrix}_{12 \times 12}^T \tag{111}$$

$$[R] = \begin{bmatrix} 1 & 0 & 0 & 0 & 0 & 0 & 0 & 0 & 0 \\ 0 & 1 & 0 & 0 & 0 & 0 & 0 & 0 & 0 \\ 0 & 0 & 1 & 0 & 0 & 0 & 0 & 0 & 0 \\ 0 & 0 & 0 & 2 & 0 & 0 & 0 & 0 & 0 \\ 0 & 0 & 0 & 0 & 2 & 0 & 0 & 0 & 0 \\ 0 & 0 & 0 & 0 & 0 & 2 & 0 & 0 & 0 \\ 0 & 0 & 0 & 0 & 0 & 0 & 1 & 0 & 0 \\ 0 & 0 & 0 & 0 & 0 & 0 & 0 & 1 & 0 \\ 0 & 0 & 0 & 0 & 0 & 0 & 0 & 0 & 1 \end{bmatrix}_{9 \times 9} \tag{112}$$

$$[B] = \begin{bmatrix} 1 & 0 & 0 & 0 & 0 & 0 & 0 & 0 & 0 \\ 0 & 0 & 0 & 0 & 0 & 1 & 0 & 0 & 0 \\ 0 & 0 & 0 & 0 & 1 & 0 & 0 & 0 & 0 \\ 0 & 0 & 0 & 0 & 0 & 1 & 0 & 0 & 0 \\ 0 & 1 & 0 & 0 & 0 & 0 & 0 & 0 & 0 \\ 0 & 0 & 0 & 1 & 0 & 0 & 0 & 0 & 0 \\ 0 & 0 & 0 & 0 & 1 & 0 & 0 & 0 & 0 \\ 0 & 0 & 0 & 1 & 0 & 0 & 0 & 0 & 0 \\ 0 & 0 & 1 & 0 & 0 & 0 & 0 & 0 & 0 \\ 0 & 0 & 0 & 0 & 0 & 0 & 1 & 0 & 0 \\ 0 & 0 & 0 & 0 & 0 & 0 & 0 & 1 & 0 \\ 0 & 0 & 0 & 0 & 0 & 0 & 0 & 0 & 1 \end{bmatrix}_{12 \times 9} \quad (113)$$

$$[T^*] = \begin{bmatrix} [T]_{6 \times 6} & 0 \\ 0 & [J(\frac{x,y,z}{\xi,\eta,\zeta})]_{3 \times 3} \end{bmatrix}_{9 \times 9} \quad (114)$$

$$[T^*] = [\bar{T}^*] [R] \quad (115)$$

$$[C]_{global} = [\bar{T}^*]^T [R] [C]_{local} [R] [\bar{T}^*] \quad (116)$$

The matrix  $[C]_{local}$  that include the elastic constants, piezoelectric coefficients, and dielectric constants can be written as

$$[C]_{local} = \begin{bmatrix} C_{11} & C_{12} & C_{13} & 0 & 0 & C_{16} & 0 & 0 & -e_{31} \\ C_{21} & C_{22} & C_{23} & 0 & 0 & C_{26} & 0 & 0 & -e_{32} \\ C_{31} & C_{32} & C_{33} & 0 & 0 & C_{36} & 0 & 0 & -e_{33} \\ 0 & 0 & 0 & C_{44} & C_{45} & 0 & -e_{14} & -e_{24} & 0 \\ 0 & 0 & 0 & C_{54} & C_{55} & 0 & -e_{15} & -e_{25} & 0 \\ C_{61} & C_{62} & C_{63} & 0 & 0 & C_{66} & 0 & 0 & -e_{36} \\ 0 & 0 & 0 & -e_{14} & -e_{15} & 0 & -\epsilon_1 & 0 & 0 \\ 0 & 0 & 0 & -e_{24} & -e_{25} & 0 & 0 & -\epsilon_2 & 0 \\ -e_{31} & -e_{32} & -e_{33} & 0 & 0 & -e_{36} & 0 & 0 & -\epsilon_3 \end{bmatrix}_{9 \times 9} \quad (117)$$

Here the moduli and material axes of each layer,  $[C]_{local}$ , can be obtained.

The variational formulation using curvilinear coordinate can be derived using the above relationships, and can be expressed in compact notation as

$$0 = \int_{t_0}^{t_1} \left\{ - \int_S (\delta [u, \phi]_{\xi\eta\zeta} \{\bar{t}\}_{\xi\eta\zeta}) dS + \int_v (\delta [u, \phi]_{\xi\eta\zeta} \rho [\ddot{u}, \ddot{\phi}]_{\xi\eta\zeta}^T + \delta [u_{i,j}, \phi_{,i}]_{\xi\eta\zeta} [D] [u_{i,j}, \phi_{,j}]_{\xi\eta\zeta}^T) \det \left[ J \left( \frac{x,y,z}{\xi,\eta,\zeta} \right) \right] dV_{\xi\eta\zeta} \right\} dt \quad (118)$$

$$[D] = [\bar{J}^*] [B] [C]_{global} [B]^T [\bar{J}^*]^T \quad (119)$$

$$\delta [u, \phi]_{\xi\eta\zeta} = [ \delta u \quad \delta v \quad \delta w \quad \delta \phi ] \quad (120)$$

$$\left[ \begin{array}{cc} \ddot{u} & \ddot{\phi} \end{array} \right]_{\xi\eta\zeta} = \left[ \begin{array}{cccc} \ddot{u} & \ddot{v} & \ddot{w} & \ddot{\phi} \end{array} \right] \quad (121)$$

$$\{\bar{t}\}_{\xi\eta\zeta} = \left\{ \begin{array}{c} \bar{t}_\xi \\ \bar{t}_\eta \\ \bar{t}_\zeta \\ -\bar{\sigma} \end{array} \right\} \quad (122)$$

## Discrete-Layer Theories

To analyze thick laminated piezoelectric shells, discrete-layer theories are used in creating the numerical models. The governing equations in matrix form are available for both cylindrical and general shells.

### *Background And Motivation*

Most theories developed for analyzing laminated piezoelectric composites include limitations which may not represent the true behavior for certain applications. For the analysis of thick laminates under small deflection, the use of Kirchhoff hypothesis as theoretical background causes an undesirable approximation of both interlaminar and intralaminar stress components. In addition to this limitation, many previous studies have made use of an equivalent force representation of induced strain actuation in the piezoelectric laminate. This kind of approach does not solve the coupled equation of piezoelectricity. To analyze thick laminated piezoelectric shells, cylindrical or general, the above limitations need considerable refinement. This is the direction of this research.

In this research, discrete-layer theories developed by Pauley [81], Reddy, Barbero, Tply [32, 43, 44], Robbins [53], and Heyliger and Saravanos [59] are used. The main reason for using these approximations is that the coupled relationship between elastic and electric variables can be exactly represented. Additionally, the limitations from the Kirchhoff hypothesis can be avoided.

In discrete-layer theories, the kinematic assumptions as shown in Figure 5 defined for the laminated plate element are :

1. Through the thickness of composite elements, arbitrary variations are allowed within the in-plane displacement components and the electrostatic potential (i.e.  $u, v$ , and  $\phi$ ), and
2. There are three assumed forms of the transverse displacement component  $w$ , which are used to develop two separate theories.

- A constant transverse displacement through the thickness,
- A distributed transverse displacement which is identical in form to the other variable through the thickness.
- A distributed transverse displacement of which the form is not completely layer-wise like the other variable through the thickness as shown in Figure 6.

Within the laminated cylindrical shell element, the first assumption yields reference-surface displacement components and electrostatic potential that are assumed to have arbitrary variations through the thickness (r-direction for cylindrical shell,  $\zeta$ -direction for general shell). In the second assumption, the transverse displacement component,  $w(r, \theta, z)$  or  $w(\xi, \eta, \zeta)$ , is with the direction normal to the shell surface (r- or  $\zeta$ - direction).

The theory developed with a constant transverse displacement (i.e.  $w(r, \theta, z) = w(\theta, z)$  or  $w(\xi, \eta, \zeta) = w(\xi, \eta)$ ) is for simpler and more economical in computation. However, poor accuracy is given when calculating the interlaminar stress or analyzing thick laminates. As with the case of the constant  $w$  formulation for the plate, it is impossible to capture the through-thickness actuation strain using this form of approximation. With the second assumed form (i.e.  $w$  is function of  $r, \theta, z$  or function of  $\xi, \eta, \zeta$ ), the approach is more complex and more expensive, yet much more accurate. Both approaches will be investigated in this research. With the use of discrete-layer theories, the variational formulation is further derived for the type of approximation used in this approach.

#### *Governing Equation in Matrix Form for Cylindrical Shell*

In this section, a re-arranged variational formulation of governing equation is presented where a configuration of simultaneous equations is obtained. Secondly, an approximation of displacement and potential variables is given. The development of the discrete-layer theory for piezoelectric laminated shell begins with this. Finally, a matrix form is expressed for further computational models.

Equation 100 can be rewritten as

$$\begin{aligned}
& \int_{t_0}^{t_1} dt \int_v [\rho \ddot{u} \delta u + \rho \ddot{v} \delta v + \rho \ddot{w} \delta w] r dr d\theta dz \\
& + \int_{t_0}^{t_1} dt \int_v \left\{ \frac{\partial \delta u}{\partial r} \left[ C_{11} \frac{\partial u}{\partial r} + C_{12} \frac{u}{r} + \frac{C_{16}}{r} \frac{\partial u}{\partial \theta} \right] + \frac{\delta u}{r} \left[ C_{12} \frac{\partial u}{\partial r} + C_{22} \frac{u}{r} + \frac{C_{26}}{r} \frac{\partial u}{\partial \theta} \right] \right. \\
& \left. + \frac{\partial \delta u}{\partial \theta} \left[ \frac{C_{16}}{r} \frac{\partial u}{\partial r} + \frac{C_{26}}{r^2} + \frac{C_{66}}{r^2} \frac{\partial u}{\partial \theta} \right] + \frac{\partial \delta u}{\partial z} C_{55} \frac{\partial u}{\partial z} \right\}_{[K_{11}]}
\end{aligned}$$

$$\begin{aligned}
& + \left\{ \frac{\partial \delta u}{\partial r} \left[ \frac{C_{12}}{r} \frac{\partial v}{\partial \theta} - C_{16} \frac{v}{r} + C_{16} \frac{\partial v}{\partial r} \right] + \frac{\delta u}{r} \left[ \frac{C_{22}}{r} \frac{\partial v}{\partial \theta} - C_{26} \frac{v}{r} + C_{26} \frac{\partial v}{\partial r} \right] \right. \\
& + \left. \frac{\partial \delta u}{\partial \theta} \left[ \frac{C_{26}}{r^2} \frac{\partial v}{\partial \theta} - C_{66} \frac{v}{r^2} + \frac{C_{66}}{r} \frac{\partial v}{\partial r} \right] + \frac{\partial \delta u}{\partial z} C_{45} \frac{\partial v}{\partial z} \right\}_{[K_{12}]} \\
& + \left\{ \frac{\partial \delta u}{\partial r} C_{13} \frac{\partial w}{\partial z} + \frac{\delta u}{r} C_{23} \frac{\partial w}{\partial z} + \frac{\partial \delta u}{\partial \theta} \frac{C_{36}}{r} \frac{\partial w}{\partial z} + \frac{\partial \delta u}{\partial z} \left[ \frac{C_{45}}{r} \frac{\partial w}{\partial \theta} + C_{55} \frac{\partial w}{\partial r} \right] \right\}_{[K_{13}]} \\
& + \left\{ \frac{\partial \delta u}{\partial r} e_{11} \frac{\partial \phi}{\partial r} + \frac{\delta u}{r} e_{12} \frac{\partial \phi}{\partial r} + \frac{\partial \delta u}{\partial \theta} \frac{e_{16}}{r} \frac{\partial \phi}{\partial r} + \frac{\partial \delta u}{\partial z} \left[ \frac{e_{25}}{r} \frac{\partial \phi}{\partial \theta} + e_{35} \frac{\partial \phi}{\partial z} \right] \right\}_{[K_{14}]} \\
& + \left\{ \frac{\partial \delta v}{\partial r} \left[ C_{16} \frac{\partial u}{\partial r} + C_{26} \frac{u}{r} + \frac{C_{66}}{r} \frac{\partial u}{\partial \theta} \right] - \frac{\delta v}{r} \left[ C_{16} \frac{\partial u}{\partial r} + C_{26} \frac{u}{r} + \frac{C_{66}}{r} \frac{\partial u}{\partial \theta} \right] \right. \\
& + \left. \frac{\partial \delta v}{\partial \theta} \left[ \frac{C_{12}}{r} \frac{\partial u}{\partial r} + \frac{C_{22}}{r^2} + \frac{C_{26}}{r^2} \frac{\partial u}{\partial \theta} \right] + \frac{\partial \delta v}{\partial z} C_{45} \frac{\partial u}{\partial z} \right\}_{[K_{21}]} \\
& + \left\{ \frac{\partial \delta v}{\partial r} \left[ \frac{C_{26}}{r} \frac{\partial v}{\partial \theta} - C_{66} \frac{v}{r} + C_{66} \frac{\partial v}{\partial r} \right] - \frac{\delta v}{r} \left[ \frac{C_{26}}{r} \frac{\partial v}{\partial \theta} - C_{66} \frac{v}{r} + C_{66} \frac{\partial v}{\partial r} \right] \right. \\
& + \left. \frac{\partial \delta v}{\partial \theta} \left[ \frac{C_{22}}{r^2} \frac{\partial v}{\partial \theta} - C_{26} \frac{v}{r^2} + \frac{C_{26}}{r} \frac{\partial v}{\partial \theta} \right] + \frac{\partial \delta v}{\partial z} C_{44} \frac{\partial v}{\partial z} \right\}_{[K_{22}]} \\
& + \left\{ \frac{\partial \delta v}{\partial r} C_{36} \frac{\partial w}{\partial z} - \frac{\delta v}{r} C_{36} \frac{\partial w}{\partial z} + \frac{\partial \delta v}{\partial \theta} \frac{C_{23}}{r} \frac{\partial w}{\partial z} + \frac{\partial \delta v}{\partial z} \left[ \frac{C_{44}}{r} \frac{\partial w}{\partial \theta} + C_{45} \frac{\partial w}{\partial r} \right] \right\}_{[K_{23}]} \\
& + \left\{ \frac{\partial \delta v}{\partial r} e_{16} \frac{\partial \phi}{\partial r} - \frac{\delta v}{r} e_{16} \frac{\partial \phi}{\partial r} + \frac{\partial \delta v}{\partial \theta} \frac{e_{12}}{r} \frac{\partial \phi}{\partial r} + \frac{\partial \delta v}{\partial z} \left[ \frac{e_{24}}{r} \frac{\partial \phi}{\partial \theta} + e_{34} \frac{\partial \phi}{\partial z} \right] \right\}_{[K_{24}]} \\
& + \left\{ \frac{\partial \delta w}{\partial r} C_{55} \frac{\partial u}{\partial z} + \frac{\partial \delta w}{\partial \theta} \frac{C_{55}}{r} \frac{\partial u}{\partial z} + \frac{\partial \delta w}{\partial z} \left[ C_{13} \frac{\partial u}{\partial r} + C_{23} \frac{u}{r} + \frac{C_{36}}{r} \frac{\partial u}{\partial \theta} \right] \right\}_{[K_{31}]} \\
& + \left\{ \frac{\partial \delta w}{\partial r} C_{45} \frac{\partial v}{\partial z} + \frac{\partial \delta w}{\partial \theta} \frac{C_{44}}{r} \frac{\partial v}{\partial z} + \frac{\partial \delta w}{\partial z} \left[ C_{23} \frac{\partial v}{\partial r} - C_{36} \frac{v}{r} + \frac{C_{36}}{r} \frac{\partial v}{\partial \theta} \right] \right\}_{[K_{32}]} \\
& + \left\{ \frac{\partial \delta w}{\partial r} \left[ \frac{C_{45}}{r} \frac{\partial w}{\partial \theta} + C_{55} \frac{\partial w}{\partial r} \right] + \frac{\partial \delta w}{\partial \theta} \left[ \frac{C_{44}}{r^2} \frac{\partial w}{\partial \theta} + \frac{C_{45}}{r} \frac{\partial w}{\partial r} \right] + \frac{\partial \delta w}{\partial z} C_{33} \frac{\partial w}{\partial z} \right\}_{[K_{33}]} \\
& + \left\{ \frac{\partial \delta w}{\partial r} \left[ \frac{e_{25}}{r} \frac{\partial \phi}{\partial \theta} + e_{35} \frac{\partial \phi}{\partial z} \right] + \frac{\partial \delta w}{\partial \theta} \left[ \frac{e_{24}}{r^2} \frac{\partial \phi}{\partial \theta} + \frac{e_{34}}{r} \frac{\partial \phi}{\partial z} \right] + \frac{\partial \delta w}{\partial z} e_{13} \frac{\partial \phi}{\partial r} \right\}_{[K_{34}]} \\
& + \left\{ \frac{\partial \delta \phi}{\partial r} \left[ e_{11} \frac{\partial u}{\partial r} + e_{12} \frac{u}{r} + \frac{e_{16}}{r} \frac{\partial u}{\partial \theta} \right] + \frac{\partial \delta \phi}{\partial \theta} \frac{e_{25}}{r} \frac{\partial u}{\partial z} + \frac{\partial \delta \phi}{\partial z} e_{35} \frac{\partial u}{\partial z} \right\}_{[K_{41}]} \\
& + \left\{ \frac{\partial \delta \phi}{\partial r} \left[ e_{16} \frac{\partial v}{\partial r} - e_{16} \frac{v}{r} + \frac{e_{12}}{r} \frac{\partial v}{\partial \theta} \right] + \frac{\partial \delta \phi}{\partial \theta} \frac{e_{24}}{r} \frac{\partial v}{\partial z} + \frac{\partial \delta \phi}{\partial z} e_{34} \frac{\partial v}{\partial z} \right\}_{[K_{42}]} \\
& + \left\{ \frac{\partial \delta \phi}{\partial r} e_{13} \frac{\partial w}{\partial z} + \frac{\partial \delta \phi}{\partial \theta} \left[ \frac{e_{24}}{r^2} \frac{\partial w}{\partial \theta} + \frac{e_{25}}{r} \frac{\partial w}{\partial r} \right] + \frac{\partial \delta \phi}{\partial z} \left[ \frac{e_{34}}{r} \frac{\partial w}{\partial \theta} + e_{35} \frac{\partial w}{\partial r} \right] \right\}_{[K_{43}]} \\
& - \left\{ \frac{\partial \delta \phi}{\partial r} e_{11} \frac{\partial \phi}{\partial r} + \frac{\partial \delta \phi}{\partial \theta} \frac{e_{22}}{r^2} \frac{\partial \phi}{\partial \theta} + \frac{\partial \delta \phi}{\partial z} e_{33} \frac{\partial \phi}{\partial z} \right\}_{[K_{44}]} r dr d\theta dz
\end{aligned}$$

$$- \int_{t_0}^{t_1} dt \int_S (\bar{t}_r \delta u + \bar{t}_\theta \delta v + \bar{t}_z \delta w - \bar{\sigma} \delta \phi) dS = 0 \quad (123)$$

Here each subscript behind the right brace shows the connection between the variational form and the matrix form that is going to be derived.

The displacement and potential variables are approximated using linear combinations of the form

$$u(r, \theta, z, t) = \sum_{j=1}^n U_j(\theta, z, t) \psi_j(r) = \sum_{a=1}^m \sum_{j=1}^n U_{ja}(t) \Psi_a^u(\theta, z) \psi_j^u(r) \quad (124)$$

$$v(r, \theta, z, t) = \sum_{j=1}^n V_j(\theta, z, t) \psi_j(r) = \sum_{a=1}^m \sum_{j=1}^n V_{ja}(t) \Psi_a^v(\theta, z) \psi_j^v(r) \quad (125)$$

$$w(r, \theta, z, t) = \sum_{j=1}^n W_j(\theta, z, t) \psi_j(r) = \sum_{a=1}^m \sum_{j=1}^n W_{ja}(t) \Psi_a^w(\theta, z) \psi_j^w(r) \quad (126)$$

$$\phi(r, \theta, z, t) = \sum_{j=1}^n \Phi_j(\theta, z, t) \psi_j(r) = \sum_{a=1}^m \sum_{j=1}^n \Phi_{ja}(t) \Psi_a^\phi(\theta, z) \psi_j^\phi(r) \quad (127)$$

If a distributed transverse displacement is assumed in the discrete-layer theory, one-dimensional Lagrangian interpolation polynomials  $\psi_j(r)$  can be used for the through thickness approximation in the above ( $\psi_j^u(r) = \psi_j^v(r) = \psi_j^w(r) = \psi_j^\phi(r) = \psi_j(r)$ ). Thus,  $n - 1$  is defined as the number of subdivisions through the thickness. For better results, the number of subdivisions should be larger or equal to the number of layers in the laminate. The in-surface approximation for the cylindrical shell is assumed using two-dimensional functions  $(\theta, z)$ . The related number  $m$  is the total number of functions for the in-surface approximation. By replacing the variables with the approximations, the governing equations can be expressed in matrix form as

$$\begin{bmatrix} [M_{11}] & [0] & [0] & [0] \\ [0] & [M_{22}] & [0] & [0] \\ [0] & [0] & [M_{33}] & [0] \\ [0] & [0] & [0] & [0] \end{bmatrix} \begin{Bmatrix} \{\ddot{u}\} \\ \{\ddot{v}\} \\ \{\ddot{w}\} \\ \{\ddot{\phi}\} \end{Bmatrix} + \begin{bmatrix} [K_{11}] & [K_{12}] & [K_{13}] & [K_{14}] \\ [K_{21}] & [K_{22}] & [K_{23}] & [K_{24}] \\ [K_{31}] & [K_{32}] & [K_{33}] & [K_{34}] \\ [K_{41}] & [K_{42}] & [K_{43}] & [K_{44}] \end{bmatrix} \begin{Bmatrix} \{u\} \\ \{v\} \\ \{w\} \\ \{\phi\} \end{Bmatrix} = \begin{Bmatrix} \{F_1\} \\ \{F_2\} \\ \{F_3\} \\ \{Q\} \end{Bmatrix} \quad (128)$$

Both the  $[M]$  and  $[K]$  matrices are symmetric, so,  $[K_{12}] = [K_{21}]^T$ ,  $[K_{13}] = [K_{31}]^T$ ,  $[K_{14}] = [K_{41}]^T$ ,  $[K_{23}] = [K_{32}]^T$ ,  $[K_{24}] = [K_{42}]^T$ , and  $[K_{34}] = [K_{43}]^T$ . The structure of the submatrices ( $[K_{11}], [K_{12}], \dots$ ) is explained in Figure 7. Here the boxes drawn in the

submatrix locates the members of submatrix using certain approximate functions  $\Psi_a$  and  $\Psi_b$ . Those box areas are noted as  $[K_{11}]_{11}$ ,  $[K_{12}]_{13}$ , etc. The expressions in these cases are given as follows.

$$[M_{11}]_{ab} = \int_{\mathcal{A}} \{ [I] \Psi_a^u \Psi_b^u \} d\theta dz \quad (129)$$

$$[M_{22}]_{ab} = \int_{\mathcal{A}} \{ [I] \Psi_a^v \Psi_b^v \} d\theta dz \quad (130)$$

$$[M_{33}]_{ab} = \int_{\mathcal{A}} \{ [I] \Psi_a^w \Psi_b^w \} d\theta dz \quad (131)$$

$$\begin{aligned} [K_{11}]_{ab} = \int_{\mathcal{A}} \left\{ [A^{11}] \Psi_a^u \Psi_b^u + [B^{12}] \Psi_a^u \Psi_b^u + [B^{16}] \Psi_a^u \frac{\partial \Psi_b^u}{\partial \theta} + [\bar{B}^{12}] \Psi_a^u \Psi_b^u \right. \\ \left. + [D^{22}] \Psi_a^u \Psi_b^u + [D^{26}] \Psi_a^u \frac{\partial \Psi_b^u}{\partial \theta} + [\bar{B}^{16}] \frac{\partial \Psi_a^u}{\partial \theta} \Psi_b^u + [D^{26}] \frac{\partial \Psi_a^u}{\partial \theta} \Psi_b^u \right. \\ \left. + [D^{66}] \frac{\partial \Psi_a^u}{\partial \theta} \frac{\partial \Psi_b^u}{\partial \theta} + [\bar{D}^{55}] \frac{\partial \Psi_a^u}{\partial z} \frac{\partial \Psi_b^u}{\partial z} \right\} d\theta dz \end{aligned} \quad (132)$$

$$\begin{aligned} [K_{12}]_{ab} = \int_{\mathcal{A}} \left\{ [B^{12}] \Psi_a^u \frac{\partial \Psi_b^v}{\partial \theta} - [B^{16}] \Psi_a^u \Psi_b^v + [A^{16}] \Psi_a^u \Psi_b^v + [D^{22}] \Psi_a^u \frac{\partial \Psi_b^v}{\partial \theta} \right. \\ \left. + [D^{26}] \left( \frac{\partial \Psi_a^u}{\partial \theta} \frac{\partial \Psi_b^v}{\partial \theta} - \Psi_a^u \Psi_b^v \right) + [\bar{B}^{26}] \Psi_a^u \Psi_b^v - [D^{66}] \frac{\partial \Psi_a^u}{\partial \theta} \Psi_b^v \right. \\ \left. + [\bar{B}^{66}] \frac{\partial \Psi_a^u}{\partial \theta} \Psi_b^v + [\bar{D}^{45}] \frac{\partial \Psi_a^u}{\partial \theta} \frac{\partial \Psi_b^v}{\partial \theta} \right\} d\theta dz \end{aligned} \quad (133)$$

$$\begin{aligned} [K_{13}]_{ab} = \int_{\mathcal{A}} \left\{ [\hat{B}^{13}] \Psi_a^u \frac{\partial \Psi_b^w}{\partial z} + [\hat{D}^{23}] \Psi_a^u \frac{\partial \Psi_b^w}{\partial z} + [\hat{D}^{36}] \frac{\partial \Psi_a^u}{\partial \theta} \frac{\partial \Psi_b^w}{\partial z} \right. \\ \left. + [\hat{D}^{45}] \frac{\partial \Psi_a^u}{\partial z} \frac{\partial \Psi_b^w}{\partial \theta} + [\hat{B}^{55}] \frac{\partial \Psi_a^u}{\partial z} \Psi_b^w \right\} d\theta dz \end{aligned} \quad (134)$$

$$\begin{aligned} [K_{14}]_{ab} = \int_{\mathcal{A}} \left\{ [E^{11}] \Psi_a^u \Psi_b^\phi + [\bar{F}^{12}] \Psi_a^u \Psi_b^\phi + [\bar{F}^{16}] \frac{\partial \Psi_a^u}{\partial \theta} \Psi_b^\phi \right. \\ \left. + [\hat{G}^{25}] \frac{\partial \Psi_a^u}{\partial z} \frac{\partial \Psi_b^\phi}{\partial \theta} + [\bar{G}^{35}] \frac{\partial \Psi_a^u}{\partial z} \frac{\partial \Psi_b^\phi}{\partial z} \right\} d\theta dz \end{aligned} \quad (135)$$

$$\begin{aligned} [K_{22}]_{ab} = \int_{\mathcal{A}} \left\{ [B^{26}] \Psi_a^v \frac{\partial \Psi_b^v}{\partial \theta} - [B^{66}] \Psi_a^v \Psi_b^v + [A^{66}] \Psi_a^v \Psi_b^v - [D^{26}] \Psi_a^v \frac{\partial \Psi_b^v}{\partial \theta} \right. \\ \left. + [D^{66}] \Psi_a^v \Psi_b^v - [\bar{B}^{66}] \Psi_a^v \Psi_b^v + [D^{22}] \frac{\partial \Psi_a^v}{\partial \theta} \frac{\partial \Psi_b^v}{\partial \theta} - [D^{26}] \frac{\partial \Psi_a^v}{\partial \theta} \Psi_b^v \right. \\ \left. + [\bar{B}^{26}] \frac{\partial \Psi_a^v}{\partial \theta} \Psi_b^v + [\bar{D}^{44}] \frac{\partial \Psi_a^v}{\partial z} \frac{\partial \Psi_b^v}{\partial z} \right\} d\theta dz \end{aligned} \quad (136)$$

$$\begin{aligned} [K_{23}]_{ab} = \int_{\mathcal{A}} \left\{ [\hat{B}^{36}] \Psi_a^v \frac{\partial \Psi_b^w}{\partial z} - [\hat{D}^{36}] \Psi_a^v \frac{\partial \Psi_b^w}{\partial z} + [\hat{D}^{23}] \frac{\partial \Psi_a^v}{\partial \theta} \frac{\partial \Psi_b^w}{\partial z} \right. \\ \left. + [\hat{D}^{44}] \frac{\partial \Psi_a^v}{\partial z} \frac{\partial \Psi_b^w}{\partial \theta} + [\hat{B}^{45}] \frac{\partial \Psi_a^v}{\partial z} \Psi_b^w \right\} d\theta dz \end{aligned} \quad (137)$$

$$[K_{24}]_{ab} = \int_{\mathcal{A}} \left\{ [E^{16}] \Psi_a^v \Psi_b^\phi - [\bar{F}^{16}] \Psi_a^v \Psi_b^\phi + [\bar{F}^{12}] \frac{\partial \Psi_a^v}{\partial \theta} \Psi_b^\phi \right. \\ \left. + [\hat{G}^{24}] \frac{\partial \Psi_a^v}{\partial z} \frac{\partial \Psi_b^\phi}{\partial \theta} + [\bar{G}^{34}] \frac{\partial \Psi_a^v}{\partial z} \frac{\partial \Psi_b^\phi}{\partial z} \right\} d\theta dz \quad (138)$$

$$[K_{33}]_{ab} = \int_{\mathcal{A}} \left\{ [B^{45}] \Psi_a^w \frac{\partial \Psi_b^w}{\partial \theta} + [A^{55}] \Psi_a^w \Psi_b^w + [D^{44}] \frac{\partial \Psi_a^w}{\partial \theta} \frac{\partial \Psi_b^w}{\partial \theta} \right. \\ \left. + [\bar{B}^{45}] \frac{\partial \Psi_a^w}{\partial \theta} \Psi_b^w + [\bar{D}^{33}] \frac{\partial \Psi_a^w}{\partial z} \frac{\partial \Psi_b^w}{\partial z} \right\} d\theta dz \quad (139)$$

$$[K_{34}]_{ab} = \int_{\mathcal{A}} \left\{ [F^{25}] \Psi_a^w \frac{\partial \Psi_b^\phi}{\partial \theta} + [\hat{F}^{35}] \Psi_a^w \frac{\partial \Psi_b^\phi}{\partial z} + [G^{24}] \frac{\partial \Psi_a^w}{\partial \theta} \frac{\partial \Psi_b^\phi}{\partial \theta} \right. \\ \left. + [\hat{G}^{34}] \frac{\partial \Psi_a^w}{\partial \theta} \frac{\partial \Psi_b^\phi}{\partial z} + [\check{F}^{13}] \frac{\partial \Psi_a^w}{\partial z} \Psi_b^\phi \right\} d\theta dz \quad (140)$$

$$[K_{44}]_{ab} = - \int_{\mathcal{A}} \left\{ [H^{11}] \Psi_a^\phi \Psi_b^\phi + [\hat{H}^{22}] \frac{\partial \Psi_a^\phi}{\partial \theta} \frac{\partial \Psi_b^\phi}{\partial \theta} + [\check{H}^{33}] \frac{\partial \Psi_a^\phi}{\partial z} \frac{\partial \Psi_b^\phi}{\partial z} \right\} d\theta dz \quad (141)$$

The sub-matrices  $[A_{ij}]$ ,  $[B_{ij}]$ , ... are expressed as

$$I_{ij} = \sum_{l=1}^N \int_{r_l}^{r_{l+1}} \rho \psi_i \psi_j r dr \quad (142)$$

$$A_{ij}^{km} = \sum_{l=1}^N \int_{r_l}^{r_{l+1}} C_{km} \frac{\partial \psi_i}{\partial r} \frac{\partial \psi_j}{\partial r} r dr \quad (143)$$

$$B_{ij}^{km} = \sum_{l=1}^N \int_{r_l}^{r_{l+1}} C_{km} \frac{\partial \psi_i}{\partial r} \psi_j dr \quad (144)$$

$$\bar{B}_{ij}^{km} = \sum_{l=1}^N \int_{r_l}^{r_{l+1}} C_{km} \psi_i \frac{\partial \psi_j}{\partial r} dr \quad (145)$$

$$\hat{B}_{ij}^{km} = \sum_{l=1}^N \int_{r_l}^{r_{l+1}} C_{km} \frac{\partial \psi_i}{\partial r} \psi_j r dr \quad (146)$$

$$\check{B}_{ij}^{km} = \sum_{l=1}^N \int_{r_l}^{r_{l+1}} C_{km} \psi_i \frac{\partial \psi_j}{\partial r} r dr \quad (147)$$

$$D_{ij}^{km} = \sum_{l=1}^N \int_{r_l}^{r_{l+1}} \frac{C_{km}}{r} \psi_i \psi_j dr \quad (148)$$

$$\hat{D}_{ij}^{km} = \sum_{l=1}^N \int_{r_l}^{r_{l+1}} C_{km} \psi_i \psi_j dr \quad (149)$$

$$\bar{D}_{ij}^{km} = \sum_{l=1}^N \int_{r_l}^{r_{l+1}} C_{km} \psi_i \psi_j r dr \quad (150)$$

$$E_{ij}^{km} = \sum_{l=1}^N \int_{r_l}^{r_{l+1}} e_{km} \frac{\partial \psi_i}{\partial r} \frac{\partial \psi_j}{\partial r} r dr \quad (151)$$



$$F_{ij}^{km} = \sum_{l=1}^N \int_{r_l}^{r_{l+1}} e_{km} \frac{\partial \psi_i}{\partial r} \psi_j dr \quad (152)$$

$$\bar{F}_{ij}^{km} = \sum_{l=1}^N \int_{r_l}^{r_{l+1}} e_{km} \psi_i \frac{\partial \psi_j}{\partial r} dr \quad (153)$$

$$\hat{F}_{ij}^{km} = \sum_{l=1}^N \int_{r_l}^{r_{l+1}} e_{km} \frac{\partial \psi_i}{\partial r} \psi_j r dr \quad (154)$$

$$\bar{\hat{F}}_{ij}^{km} = \sum_{l=1}^N \int_{r_l}^{r_{l+1}} e_{km} \psi_i \frac{\partial \psi_j}{\partial r} r dr \quad (155)$$

$$G_{ij}^{km} = \sum_{l=1}^N \int_{r_l}^{r_{l+1}} \frac{e_{km}}{r} \psi_i \psi_j dr \quad (156)$$

$$\hat{G}_{ij}^{km} = \sum_{l=1}^N \int_{r_l}^{r_{l+1}} e_{km} \psi_i \psi_j dr \quad (157)$$

$$\bar{G}_{ij}^{km} = \sum_{l=1}^N \int_{r_l}^{r_{l+1}} e_{km} \psi_i \psi_j r dr \quad (158)$$

$$H_{ij}^{km} = \sum_{l=1}^N \int_{r_l}^{r_{l+1}} e_{km} \frac{\partial \psi_i}{\partial r} \frac{\partial \psi_j}{\partial r} r dr \quad (159)$$

$$\hat{H}_{ij}^{km} = \sum_{l=1}^N \int_{r_l}^{r_{l+1}} \frac{\epsilon_{km}}{r} \psi_i \psi_j dr \quad (160)$$

$$\bar{\hat{H}}_{ij}^{km} = \sum_{l=1}^N \int_{r_l}^{r_{l+1}} \epsilon_{km} \psi_i \psi_j r dr \quad (161)$$

Here  $N$  is the total number of layers ( $N = n - 1$ ).

However, if a constant transverse displacement is assumed, then  $\psi_j^u(r) = \psi_j^v(r) = \psi_j^\phi(r) = \psi_j(r)$  but  $\psi_j^w(r) = \text{constant}$ , say  $\kappa$ , and several of the above equations must be changed.

$$[M_{33}]_{ab} = \int_{\mathcal{A}} \{ [\bar{I}] \Psi_a^w \Psi_b^w \} d\theta dz \quad (162)$$

$$[K_{13}]_{ab} = \int_{\mathcal{A}} \left\{ [\hat{O}^{13}] \Psi_a^u \frac{\partial \Psi_b^w}{\partial z} + [\hat{P}^{23}] \Psi_a^u \frac{\partial \Psi_b^w}{\partial z} + [\hat{P}^{36}] \frac{\partial \Psi_a^u}{\partial \theta} \frac{\partial \Psi_b^w}{\partial z} + [\hat{P}^{45}] \frac{\partial \Psi_a^u}{\partial z} \frac{\partial \Psi_b^w}{\partial \theta} \right\} d\theta dz \quad (163)$$

$$[K_{23}]_{ab} = \int_{\mathcal{A}} \left\{ [\hat{O}^{36}] \Psi_a^v \frac{\partial \Psi_b^w}{\partial z} - [\hat{P}^{36}] \Psi_a^v \frac{\partial \Psi_b^w}{\partial z} + [\hat{P}^{23}] \frac{\partial \Psi_a^v}{\partial \theta} \frac{\partial \Psi_b^w}{\partial z} + [\hat{P}^{44}] \frac{\partial \Psi_a^v}{\partial z} \frac{\partial \Psi_b^w}{\partial \theta} \right\} d\theta dz \quad (164)$$

$$[K_{33}]_{ab} = \int_{\mathcal{A}} \left\{ [P^{44}] \frac{\partial \Psi_a^w}{\partial \theta} \frac{\partial \Psi_b^w}{\partial \theta} + [\bar{P}^{33}] \frac{\partial \Psi_a^w}{\partial z} \frac{\partial \Psi_b^w}{\partial z} \right\} d\theta dz \quad (165)$$

$$[K_{34}]_{ab} = \int_{\mathcal{A}} \left\{ [S^{24}] \frac{\partial \Psi_a^w}{\partial \theta} \frac{\partial \Psi_b^\phi}{\partial \theta} + [\hat{S}^{34}] \frac{\partial \Psi_a^w}{\partial \theta} \frac{\partial \Psi_b^\phi}{\partial z} + [\check{Q}^{13}] \frac{\partial \Psi_a^w}{\partial z} \Psi_b^\phi \right\} d\theta dz \quad (166)$$

Here the sub-matrices  $[O_{ij}]$ ,  $[P_{ij}]$ , ... , are expressed as

$$\bar{I}_{ij} = \sum_{l=1}^N \int_{r_l}^{r_{l+1}} \rho \kappa^2 r dr \quad (167)$$

$$\hat{O}_{ij}^{km} = \sum_{l=1}^N \int_{r_l}^{r_{l+1}} C_{km} \frac{\partial \psi_i}{\partial r} \kappa r dr \quad (168)$$

$$P_{ij}^{km} = \sum_{l=1}^N \int_{r_l}^{r_{l+1}} \frac{C_{km}}{r} \kappa^2 dr \quad (169)$$

$$\hat{P}_{ij}^{km} = \sum_{l=1}^N \int_{r_l}^{r_{l+1}} C_{km} \psi_i \kappa dr \quad (170)$$

$$\bar{P}_{ij}^{km} = \sum_{l=1}^N \int_{r_l}^{r_{l+1}} C_{km} \kappa^2 r dr \quad (171)$$

$$\check{Q}_{ij}^{km} = \sum_{l=1}^N \int_{r_l}^{r_{l+1}} e_{km} \kappa \frac{\partial \psi_j}{\partial r} r dr \quad (172)$$

$$S_{ij}^{km} = \sum_{l=1}^N \int_{r_l}^{r_{l+1}} \frac{e_{km}}{r} \kappa \psi_j dr \quad (173)$$

$$\hat{S}_{ij}^{km} = \sum_{l=1}^N \int_{r_l}^{r_{l+1}} e_{km} \kappa \psi_j dr \quad (174)$$

### *A Discrete-layer Element for General Shell*

To model the laminated shell with arbitrary geometry, a curvilinear representation of a discrete-layer shell element is developed using the kinematic assumptions of discrete-layer theories. This is shown schematically in Figure 8. Within the shell, continuity of the in-surface displacement components at a number of locations through the thickness (i.e. usually at the joint between layers) is required as shown in Figure 9. For the two different forms of the transverse displacement (out-of-surface displacement), different requirements need to be satisfied. If a distributed out-of-surface displacement is assumed, the same continuity of this displacement component is required as that of the in-surface components. However, if a constant out-of-surface displacement is assumed, the continuity of this displacement component is necessary at only one location through the thickness, such as the bottom or top surface of the shell.

The weak form of the governing equation using curvilinear coordinates was shown earlier and is used to allow a much easier integration for the shell with arbitrary geometries.

To impose continuity across the interface of adjoining elements with no loss of generality, the resulting degrees of freedom are maintained at the local level throughout the analysis. This type of formulation can give a much more accurate representation of adjoining element sides. With the defined Gauss points, the numerical integration can be accomplished by mapping the discrete-layer shell element into a parent element that is similar to the discrete-layer plate element described for the plate earlier in this report. Quadratic in-surface approximations will be used in the calculations to allow representation of the curved edges. This order of approximation can be easily modified if necessary.

To define the geometry of a laminated shell element and to determine the Jacobian matrices  $[J]$  and  $[\bar{J}^*]$  matrices, the geometry of shell element [69] is described in standard fashion as

$$\begin{Bmatrix} x \\ y \\ z \end{Bmatrix} = \sum_{i=1}^n N_i(\xi, \eta, \zeta) \begin{Bmatrix} x_i \\ y_i \\ z_i \end{Bmatrix} \quad (175)$$

Here  $(x, y, z)$  represents the location of a generic point within the shell element, and  $(x_i, y_i, z_i)$  are the locations of element nodes. The function  $N_i$  indicates the shape function corresponding to the node  $i$ . If the curvilinear coordinate systems used in all layers are same, then the geometry of this element can be defined using only the locations of the nodal points on any two layer surfaces, usually the top and bottom surfaces of the element. However, if more than one curvilinear coordinate systems is required, more nodes are needed for the approximation. The displacement components  $(u, v, w)$  and electric potential  $\phi$  in local system can be approximated in this fashion by the following equations,

$$u(x, y, z, t) = u(\xi, \eta, \zeta, t) = \sum_{a=1}^m \sum_{j=1}^n U_{ja}(t) \Psi_a^u(\xi, \eta) \psi_j^u(\zeta) \quad (176)$$

$$v(x, y, z, t) = v(\xi, \eta, \zeta, t) = \sum_{a=1}^m \sum_{j=1}^n V_{ja}(t) \Psi_a^v(\xi, \eta) \psi_j^v(\zeta) \quad (177)$$

$$w(x, y, z, t) = w(\xi, \eta, \zeta, t) = \sum_{a=1}^m \sum_{j=1}^n W_{ja}(t) \Psi_a^w(\xi, \eta) \psi_j^w(\zeta) \quad (178)$$

$$\phi(x, y, z, t) = \phi(\xi, \eta, \zeta, t) = \sum_{a=1}^m \sum_{j=1}^n \Phi_{ja}(t) \Psi_a^\phi(\xi, \eta) \psi_j^\phi(\zeta) \quad (179)$$

The  $J^{-1}\left(\frac{xyz}{\xi\eta\zeta}\right)$  can be expressed as :

$$\left[ J^{-1}\left(\frac{xyz}{\xi\eta\zeta}\right) \right]^T = \begin{bmatrix} \frac{\partial \xi}{\partial x} & \frac{\partial \xi}{\partial y} & \frac{\partial \xi}{\partial z} \\ \frac{\partial \eta}{\partial x} & \frac{\partial \eta}{\partial y} & \frac{\partial \eta}{\partial z} \\ \frac{\partial \zeta}{\partial x} & \frac{\partial \zeta}{\partial y} & \frac{\partial \zeta}{\partial z} \end{bmatrix} = \begin{bmatrix} \bar{J}_{11} & \bar{J}_{12} & \bar{J}_{13} \\ \bar{J}_{21} & \bar{J}_{22} & \bar{J}_{23} \\ \bar{J}_{31} & \bar{J}_{32} & \bar{J}_{33} \end{bmatrix} \quad (180)$$

The member  $D_{ij}$  of the  $[D]_{12 \times 12}$  matrix can be calculated by

$$D_{(i)(j)} = \bar{J}_{ik} C_{(k)(l)} \bar{J}_{jl} \quad (181)$$

$$D_{(i)(j+3)} = \bar{J}_{ik} C_{(k)(l+3)} \bar{J}_{jl} \quad (182)$$

$$D_{(i)(j+6)} = \bar{J}_{ik} C_{(k)(l+6)} \bar{J}_{jl} \quad (183)$$

$$D_{(i)(j+9)} = \bar{J}_{ik} C_{(k)(l+9)} \bar{J}_{jl} \quad (184)$$

$$D_{(i+3)(j)} = \bar{J}_{ik} C_{(k+3)(l)} \bar{J}_{jl} \quad (185)$$

$$D_{(i+3)(j+3)} = \bar{J}_{ik} C_{(k+3)(l+3)} \bar{J}_{jl} \quad (186)$$

$$D_{(i+3)(j+6)} = \bar{J}_{ik} C_{(k+3)(l+6)} \bar{J}_{jl} \quad (187)$$

$$D_{(i+3)(j+9)} = \bar{J}_{ik} C_{(k+3)(l+9)} \bar{J}_{jl} \quad (188)$$

$$D_{(i+6)(j)} = \bar{J}_{ik} C_{(k+6)(l)} \bar{J}_{jl} \quad (189)$$

$$D_{(i+6)(j+3)} = \bar{J}_{ik} C_{(k+6)(l+3)} \bar{J}_{jl} \quad (190)$$

$$D_{(i+6)(j+6)} = \bar{J}_{ik} C_{(k+6)(l+6)} \bar{J}_{jl} \quad (191)$$

$$D_{(i+6)(j+9)} = \bar{J}_{ik} C_{(k+6)(l+9)} \bar{J}_{jl} \quad (192)$$

$$D_{(i+9)(j)} = \bar{J}_{ik} C_{(k+9)(l)} \bar{J}_{jl} \quad (193)$$

$$D_{(i+9)(j+3)} = \bar{J}_{ik} C_{(k+9)(l+3)} \bar{J}_{jl} \quad (194)$$

$$D_{(i+9)(j+6)} = \bar{J}_{ik} C_{(k+9)(l+6)} \bar{J}_{jl} \quad (195)$$

$$D_{(i+9)(j+9)} = \bar{J}_{ik} C_{(k+9)(l+9)} \bar{J}_{jl} \quad (196)$$

$$(i, j, k, l = 1, 2, 3)$$

By replacing the variables with the approximations, the governing equations can be rewritten in matrix form. Let  $\psi_j^u(\zeta) = \psi_j^v(\zeta) = \psi_j^\phi(\zeta) = \psi_j(\zeta)$  but  $\psi_j^w(\zeta)$  is not necessarily equal to  $\psi_j(\zeta)$ . The expressions of the  $[M]$  and  $[K]$  for the general shell are given as follows.

$$[M_{11}]_{ab} = \int_{\mathcal{A}} \{ [I] \Psi_a^u \Psi_b^u \} \det j d\xi d\eta \quad (197)$$

$$[M_{22}]_{ab} = \int_{\mathcal{A}} \{ [I] \Psi_a^v \Psi_b^v \} \det j d\xi d\eta \quad (198)$$

$$[M_{33}]_{ab} = \int_{\mathcal{A}} \{ [\bar{I}] \Psi_a^w \Psi_b^w \} \det j d\xi d\eta \quad (199)$$

$$\begin{aligned} [K_{11}]_{ab} = \int_{\mathcal{A}} \left\{ [A^{11}] \frac{\partial \Psi_a^u}{\partial \xi} \frac{\partial \Psi_b^u}{\partial \xi} + [A^{12}] \frac{\partial \Psi_a^u}{\partial \xi} \frac{\partial \Psi_b^u}{\partial \eta} + [\hat{A}^{13}] \frac{\partial \Psi_a^u}{\partial \xi} \Psi_b^u \right. \\ + [A^{21}] \frac{\partial \Psi_a^u}{\partial \eta} \frac{\partial \Psi_b^u}{\partial \xi} + [A^{22}] \frac{\partial \Psi_a^u}{\partial \eta} \frac{\partial \Psi_b^u}{\partial \eta} + [\hat{A}^{23}] \frac{\partial \Psi_a^u}{\partial \eta} \Psi_b^u \\ \left. + [\hat{A}^{31}] \Psi_a^u \frac{\partial \Psi_b^u}{\partial \xi} + [\hat{A}^{32}] \Psi_a^u \frac{\partial \Psi_b^u}{\partial \eta} + [\bar{A}^{33}] \Psi_a^u \Psi_b^u \right\} \det j d\xi d\eta \quad (200) \end{aligned}$$

$$\begin{aligned}
[K_{12}]_{ab} = \int_{\mathcal{A}} \left\{ [A^{14}] \frac{\partial \Psi_a^u}{\partial \xi} \frac{\partial \Psi_b^v}{\partial \xi} + [A^{15}] \frac{\partial \Psi_a^u}{\partial \xi} \frac{\partial \Psi_b^v}{\partial \eta} + [\hat{A}^{16}] \frac{\partial \Psi_a^u}{\partial \xi} \Psi_b^v \right. \\
+ [A^{24}] \frac{\partial \Psi_a^u}{\partial \eta} \frac{\partial \Psi_b^v}{\partial \xi} + [A^{25}] \frac{\partial \Psi_a^u}{\partial \eta} \frac{\partial \Psi_b^v}{\partial \eta} + [\hat{A}^{26}] \frac{\partial \Psi_a^u}{\partial \eta} \Psi_b^v \\
\left. + [\check{A}^{34}] \Psi_a^u \frac{\partial \Psi_b^v}{\partial \xi} + [\check{A}^{35}] \Psi_a^u \frac{\partial \Psi_b^v}{\partial \eta} + [\bar{A}^{36}] \Psi_a^u \Psi_b^v \right\} \det j d\xi d\eta \quad (201)
\end{aligned}$$

$$\begin{aligned}
[K_{13}]_{ab} = \int_{\mathcal{A}} \left\{ [B^{17}] \frac{\partial \Psi_a^u}{\partial \xi} \frac{\partial \Psi_b^w}{\partial \xi} + [B^{18}] \frac{\partial \Psi_a^u}{\partial \xi} \frac{\partial \Psi_b^w}{\partial \eta} + [\hat{B}^{19}] \frac{\partial \Psi_a^u}{\partial \xi} \Psi_b^w \right. \\
+ [B^{27}] \frac{\partial \Psi_a^u}{\partial \eta} \frac{\partial \Psi_b^w}{\partial \xi} + [B^{28}] \frac{\partial \Psi_a^u}{\partial \eta} \frac{\partial \Psi_b^w}{\partial \eta} + [\hat{B}^{29}] \frac{\partial \Psi_a^u}{\partial \eta} \Psi_b^w \\
\left. + [\check{B}^{37}] \Psi_a^u \frac{\partial \Psi_b^w}{\partial \xi} + [\check{B}^{38}] \Psi_a^u \frac{\partial \Psi_b^w}{\partial \eta} + [\bar{B}^{39}] \Psi_a^u \Psi_b^w \right\} \det j d\xi d\eta \quad (202)
\end{aligned}$$

$$\begin{aligned}
[K_{14}]_{ab} = \int_{\mathcal{A}} - \left\{ [A^{110}] \frac{\partial \Psi_a^u}{\partial \xi} \frac{\partial \Psi_b^\phi}{\partial \xi} + [A^{111}] \frac{\partial \Psi_a^u}{\partial \xi} \frac{\partial \Psi_b^\phi}{\partial \eta} + [\hat{A}^{112}] \frac{\partial \Psi_a^u}{\partial \xi} \Psi_b^\phi \right. \\
+ [A^{210}] \frac{\partial \Psi_a^u}{\partial \eta} \frac{\partial \Psi_b^\phi}{\partial \xi} + [A^{211}] \frac{\partial \Psi_a^u}{\partial \eta} \frac{\partial \Psi_b^\phi}{\partial \eta} + [\hat{A}^{212}] \frac{\partial \Psi_a^u}{\partial \eta} \Psi_b^\phi \\
\left. + [\check{A}^{310}] \Psi_a^u \frac{\partial \Psi_b^\phi}{\partial \xi} + [\check{A}^{311}] \Psi_a^u \frac{\partial \Psi_b^\phi}{\partial \eta} + [\bar{A}^{312}] \Psi_a^u \Psi_b^\phi \right\} \det j d\xi d\eta \quad (203)
\end{aligned}$$

$$\begin{aligned}
[K_{22}]_{ab} = \int_{\mathcal{A}} \left\{ [A^{44}] \frac{\partial \Psi_a^v}{\partial \xi} \frac{\partial \Psi_b^v}{\partial \xi} + [A^{45}] \frac{\partial \Psi_a^v}{\partial \xi} \frac{\partial \Psi_b^v}{\partial \eta} + [\hat{A}^{46}] \frac{\partial \Psi_a^v}{\partial \xi} \Psi_b^v \right. \\
+ [A^{54}] \frac{\partial \Psi_a^v}{\partial \eta} \frac{\partial \Psi_b^v}{\partial \xi} + [A^{55}] \frac{\partial \Psi_a^v}{\partial \eta} \frac{\partial \Psi_b^v}{\partial \eta} + [\hat{A}^{56}] \frac{\partial \Psi_a^v}{\partial \eta} \Psi_b^v \\
\left. + [\check{A}^{64}] \Psi_a^v \frac{\partial \Psi_b^v}{\partial \xi} + [\check{A}^{65}] \Psi_a^v \frac{\partial \Psi_b^v}{\partial \eta} + [\bar{A}^{66}] \Psi_a^v \Psi_b^v \right\} \det j d\xi d\eta \quad (204)
\end{aligned}$$

$$\begin{aligned}
[K_{23}]_{ab} = \int_{\mathcal{A}} \left\{ [B^{47}] \frac{\partial \Psi_a^v}{\partial \xi} \frac{\partial \Psi_b^w}{\partial \xi} + [B^{48}] \frac{\partial \Psi_a^v}{\partial \xi} \frac{\partial \Psi_b^w}{\partial \eta} + [\hat{B}^{49}] \frac{\partial \Psi_a^v}{\partial \xi} \Psi_b^w \right. \\
+ [B^{57}] \frac{\partial \Psi_a^v}{\partial \eta} \frac{\partial \Psi_b^w}{\partial \xi} + [B^{58}] \frac{\partial \Psi_a^v}{\partial \eta} \frac{\partial \Psi_b^w}{\partial \eta} + [\hat{B}^{59}] \frac{\partial \Psi_a^v}{\partial \eta} \Psi_b^w \\
\left. + [\check{B}^{67}] \Psi_a^v \frac{\partial \Psi_b^w}{\partial \xi} + [\check{B}^{68}] \Psi_a^v \frac{\partial \Psi_b^w}{\partial \eta} + [\bar{B}^{69}] \Psi_a^v \Psi_b^w \right\} \det j d\xi d\eta \quad (205)
\end{aligned}$$

$$\begin{aligned}
[K_{24}]_{ab} = \int_{\mathcal{A}} - \left\{ [A^{410}] \frac{\partial \Psi_a^v}{\partial \xi} \frac{\partial \Psi_b^\phi}{\partial \xi} + [A^{411}] \frac{\partial \Psi_a^v}{\partial \xi} \frac{\partial \Psi_b^\phi}{\partial \eta} + [\hat{A}^{412}] \frac{\partial \Psi_a^v}{\partial \xi} \Psi_b^\phi \right. \\
+ [A^{510}] \frac{\partial \Psi_a^v}{\partial \eta} \frac{\partial \Psi_b^\phi}{\partial \xi} + [A^{511}] \frac{\partial \Psi_a^v}{\partial \eta} \frac{\partial \Psi_b^\phi}{\partial \eta} + [\hat{A}^{512}] \frac{\partial \Psi_a^v}{\partial \eta} \Psi_b^\phi \\
\left. + [\check{A}^{610}] \Psi_a^v \frac{\partial \Psi_b^\phi}{\partial \xi} + [\check{A}^{611}] \Psi_a^v \frac{\partial \Psi_b^\phi}{\partial \eta} + [\bar{A}^{612}] \Psi_a^v \Psi_b^\phi \right\} \det j d\xi d\eta \quad (206)
\end{aligned}$$

$$[K_{33}]_{ab} = \int_{\mathcal{A}} \left\{ [C^{77}] \frac{\partial \Psi_a^w}{\partial \xi} \frac{\partial \Psi_b^w}{\partial \xi} + [C^{78}] \frac{\partial \Psi_a^w}{\partial \xi} \frac{\partial \Psi_b^w}{\partial \eta} + [\hat{C}^{79}] \frac{\partial \Psi_a^w}{\partial \xi} \Psi_b^w \right.$$

$$\begin{aligned}
& + [C^{87}] \frac{\partial \Psi_a^w}{\partial \eta} \frac{\partial \Psi_b^w}{\partial \xi} + [C^{88}] \frac{\partial \Psi_a^w}{\partial \eta} \frac{\partial \Psi_b^w}{\partial \eta} + [\hat{C}^{89}] \frac{\partial \Psi_a^w}{\partial \eta} \Psi_b^w \\
& + [\check{C}^{97}] \Psi_a^w \frac{\partial \Psi_b^w}{\partial \xi} + [\check{C}^{98}] \Psi_a^w \frac{\partial \Psi_b^w}{\partial \eta} + [\bar{C}^{99}] \Psi_a^w \Psi_b^w \} \det j d\xi d\eta \quad (207)
\end{aligned}$$

$$\begin{aligned}
[K_{34}]_{ab} = \int_{\mathcal{A}} - \left\{ [B^{710}] \frac{\partial \Psi_a^w}{\partial \xi} \frac{\partial \Psi_b^\phi}{\partial \xi} + [B^{711}] \frac{\partial \Psi_a^w}{\partial \xi} \frac{\partial \Psi_b^\phi}{\partial \eta} + [\hat{B}^{712}] \frac{\partial \Psi_a^w}{\partial \xi} \Psi_b^\phi \right. \\
+ [B^{810}] \frac{\partial \Psi_a^w}{\partial \eta} \frac{\partial \Psi_b^\phi}{\partial \xi} + [B^{811}] \frac{\partial \Psi_a^w}{\partial \eta} \frac{\partial \Psi_b^\phi}{\partial \eta} + [\hat{B}^{812}] \frac{\partial \Psi_a^w}{\partial \eta} \Psi_b^\phi \\
\left. + [\check{B}^{910}] \Psi_a^w \frac{\partial \Psi_b^\phi}{\partial \xi} + [\check{B}^{911}] \Psi_a^w \frac{\partial \Psi_b^\phi}{\partial \eta} + [\bar{B}^{912}] \Psi_a^w \Psi_b^\phi \right\} \det j d\xi d\eta \quad (208)
\end{aligned}$$

$$\begin{aligned}
[K_{44}]_{ab} = \int_{\mathcal{A}} \left\{ [A^{1010}] \frac{\partial \Psi_a^\phi}{\partial \xi} \frac{\partial \Psi_b^\phi}{\partial \xi} + [A^{1011}] \frac{\partial \Psi_a^\phi}{\partial \xi} \frac{\partial \Psi_b^\phi}{\partial \eta} + [\hat{A}^{1012}] \frac{\partial \Psi_a^\phi}{\partial \xi} \Psi_b^\phi \right. \\
+ [A^{1110}] \frac{\partial \Psi_a^\phi}{\partial \eta} \frac{\partial \Psi_b^\phi}{\partial \xi} + [A^{1111}] \frac{\partial \Psi_a^\phi}{\partial \eta} \frac{\partial \Psi_b^\phi}{\partial \eta} + [\hat{A}^{1112}] \frac{\partial \Psi_a^\phi}{\partial \eta} \Psi_b^\phi \\
\left. + [\check{A}^{1210}] \Psi_a^\phi \frac{\partial \Psi_b^\phi}{\partial \xi} + [\check{A}^{1211}] \Psi_a^\phi \frac{\partial \Psi_b^\phi}{\partial \eta} + [\bar{A}^{1212}] \Psi_a^\phi \Psi_b^\phi \right\} \det j d\xi d\eta \quad (209)
\end{aligned}$$

Where the members of  $[A_{ij}]$ ,  $[B_{ij}]$ , ... , are expressed as

$$I_{ij} = \sum_{l=1}^N \int_{\zeta_l}^{\zeta_{l+1}} \rho \psi_i \psi_j d\zeta \quad (210)$$

$$\bar{I}_{ij} = \sum_{l=1}^N \int_{\zeta_l}^{\zeta_{l+1}} \rho \psi_i^w \psi_j^w d\zeta \quad (211)$$

$$A_{ij}^{km} = \sum_{l=1}^N \int_{\zeta_l}^{\zeta_{l+1}} D_{km} \psi_i \psi_j d\zeta \quad (212)$$

$$\check{A}_{ij}^{km} = \sum_{l=1}^N \int_{\zeta_l}^{\zeta_{l+1}} D_{km} \frac{\partial \psi_i}{\partial \zeta} \psi_j d\zeta \quad (213)$$

$$\hat{A}_{ij}^{km} = \check{A}_{ji}^{km} \quad (214)$$

$$\bar{A}_{ij}^{km} = \sum_{l=1}^N \int_{\zeta_l}^{\zeta_{l+1}} D_{km} \frac{\partial \psi_i}{\partial \zeta} \frac{\partial \psi_j}{\partial \zeta} d\zeta \quad (215)$$

$$B_{ij}^{km} = \sum_{l=1}^N \int_{\zeta_l}^{\zeta_{l+1}} D_{km} \psi_i \psi_j^w d\zeta \quad (216)$$

$$\check{B}_{ij}^{km} = \sum_{l=1}^N \int_{\zeta_l}^{\zeta_{l+1}} D_{km} \frac{\partial \psi_i}{\partial \zeta} \psi_j^w d\zeta \quad (217)$$

$$\hat{B}_{ij}^{km} = \sum_{l=1}^N \int_{\zeta_l}^{\zeta_{l+1}} D_{km} \psi_i \frac{\partial \psi_j^w}{\partial \zeta} d\zeta \quad (218)$$

$$\bar{B}_{ij}^{km} = \sum_{l=1}^N \int_{\zeta_l}^{\zeta_{l+1}} D_{km} \frac{\partial \psi_i}{\partial \zeta} \frac{\partial \psi_j^w}{\partial \zeta} d\zeta \quad (219)$$

$$C_{ij}^{km} = \sum_{l=1}^N \int_{\zeta_l}^{\zeta_{l+1}} D_{km} \psi_i^w \psi_j^w d\zeta \quad (220)$$

$$\check{C}_{ij}^{km} = \sum_{l=1}^N \int_{\zeta_l}^{\zeta_{l+1}} D_{km} \frac{\partial \psi_i^w}{\partial \zeta} \psi_j^w d\zeta \quad (221)$$

$$\hat{C}_{ij}^{km} = \check{C}_{ji}^{km} \quad (222)$$

$$\bar{C}_{ij}^{km} = \sum_{l=1}^N \int_{\zeta_l}^{\zeta_{l+1}} D_{km} \frac{\partial \psi_i^w}{\partial \zeta} \frac{\partial \psi_j^w}{\partial \zeta} d\zeta \quad (223)$$

If a distributed transverse displacement is assumed in the approximation, then  $\psi_j = \psi_j^w$ . Therefore,  $[A] = [B] = [C]$ ,  $[\hat{A}] = [\hat{A}]^T = [\hat{B}] = [\hat{B}]^T = [\hat{C}] = [\hat{C}]^T$ , and  $[\bar{A}] = [\bar{B}] = [\bar{C}]$ . However, if a constant transverse displacement is assumed ( $\psi_j^w(\zeta) = \text{constant}$ ), then  $[\hat{B}] = [\bar{B}] = 0$  and  $[\hat{C}] = [\bar{C}] = 0$ . The fundamental behavior of the shell is shown for several layers in Figure 11.

Static solutions to problems involving this type of approximation are fairly straightforward. However, there are several difficulties involved in dynamic analyses. These are described separately below.

### Dynamic Analyses

The kinetic energy of the system is involved when developing the Hamilton's principle into the matrix formulations. Hence, piezoelectric vibration analysis is possible using solutions of equation 128. The primary problem in this research to find the free vibration characteristics (i.e. natural frequencies and corresponding mode shapes) for given arbitrary shells and cylindrical shells, as well as the behavior of shells under a forced vibration.

#### Free Vibrations

Since no external force term is assumed in free vibration problems, equation 128 can be rewritten as [59]

$$\begin{bmatrix} [M] & [0] \\ [0] & [0] \end{bmatrix} \begin{Bmatrix} \{\ddot{\Delta}\} \\ \{\ddot{\phi}\} \end{Bmatrix} + \begin{bmatrix} [K^{\Delta\Delta}] & [K^{\Delta\phi}] \\ [K^{\phi\Delta}] & [K^{\phi\phi}] \end{bmatrix} \begin{Bmatrix} \{\Delta\} \\ \{\phi\} \end{Bmatrix} = \begin{Bmatrix} \{0\} \\ \{0\} \end{Bmatrix} \quad (224)$$

Here

$$[K^{\Delta\phi}] = [K^{\phi\Delta}]^T = \begin{bmatrix} [K_{14}] \\ [K_{24}] \\ [K_{34}] \end{bmatrix} \quad (225)$$

$$\{\Delta\} = \begin{Bmatrix} \{u\} \\ \{v\} \\ \{w\} \end{Bmatrix} \quad (226)$$

If periodic motion is assumed, equation 128 becomes an eigenvalue problem, expressed as

$$\{[\bar{K}] - \omega^2 [M]\} \{\Delta\} = \{0\} \quad (227)$$

Here  $[\bar{K}]$  is formed using static condensation, which is necessary to eliminate the potential variables. This matrix is given by

$$[\bar{K}] = [K^{\Delta\Delta}] - [K^{\Delta\phi}] [K^{\phi\phi}]^{-1} [K^{\phi\Delta}] \quad (228)$$

Here  $\omega$  is the natural frequency and the corresponding  $\{\Delta\}$  presents the mode shape.

### Forced Vibrations

It is possible to analyze the behavior of a laminated piezoelectric shell under a forced vibration, especially a harmonic excitation. According to the governing equation in matrix form, there are several ways to cause excitation in the system : (1) applying traction forces  $\{f(t)\}$ , (2) applying an electric field  $\{\phi(t)\}$ , (3) increasing / decreasing charges in the surface electrode, (4) mix of (1) and (2), and (5) mix of (1) and (3).

If the system is excited by surface traction forces which are harmonic, and no electric field is applied, equation 224 can be rewritten as

$$\begin{bmatrix} [M] & [0] \\ [0] & [0] \end{bmatrix} \begin{Bmatrix} \{\ddot{\Delta}\} \\ \{0\} \end{Bmatrix} + \begin{bmatrix} [K^{\Delta\Delta}] & [K^{\Delta\phi}] \\ [K^{\phi\Delta}] & [K^{\phi\phi}] \end{bmatrix} \begin{Bmatrix} \{\Delta\} \\ \{0\} \end{Bmatrix} = \begin{Bmatrix} \{f(t)\} \\ \{unknown\} \end{Bmatrix} \quad (229)$$

The equation of motion of this system can be expressed to the form that is the same as the equation of general laminates.

$$[M] \{\ddot{\Delta}\} + [K^{\Delta\Delta}] \{\Delta\} = \{f(t)\} \quad (230)$$

After the displacements,  $\{\Delta\}$ , are solved,  $[K^{\phi\Delta}] \{\Delta\}$  can be used to predict the surface charge created by shape change of the structure. The displacements can be discovered by measuring the surface charges which are collected through a surface electrode to the outside detector. Furthermore, if a static electric field is applied, the equation of motion becomes

$$[M] \{\ddot{\Delta}\} + [K^{\Delta\Delta}] \{\Delta\} = \{f(t)\} - [K^{\Delta\phi}] \{\phi\} \quad (231)$$

The surface charges can be predicted by solving  $[K^{\phi\Delta}] \{\Delta\} + [K^{\phi\phi}] \{\phi\}$ .



If the system is excited by an applied electric field that is changed harmonically, and no traction force is applied, equation 224 can be rewritten as

$$\begin{bmatrix} [M] & [0] \\ [0] & [0] \end{bmatrix} \begin{Bmatrix} \{\ddot{\Delta}\} \\ \{\dot{\phi}(t)\} \end{Bmatrix} + \begin{bmatrix} [K^{\Delta\Delta}] & [K^{\Delta\phi}] \\ [K^{\phi\Delta}] & [K^{\phi\phi}] \end{bmatrix} \begin{Bmatrix} \{\Delta\} \\ \{\phi(t)\} \end{Bmatrix} = \begin{Bmatrix} \{0\} \\ \{unknown\} \end{Bmatrix} \quad (232)$$

The equation of motion of this system can be written as

$$[M] \{\ddot{\Delta}\} + [K^{\Delta\Delta}] \{\Delta\} = - [K^{\Delta\phi}] \{\phi(t)\} \quad (233)$$

The equation of surface charges becomes  $\{Q\} = [K^{\phi\Delta}] \{\Delta\} + [K^{\phi\phi}] \{\phi(t)\}$ .

The third way to excite the system is harmonically increasing / decreasing the charges that store in the surface electrode. Equation 224 can be rewritten as

$$\begin{bmatrix} [M] & [0] \\ [0] & [0] \end{bmatrix} \begin{Bmatrix} \{\ddot{\Delta}\} \\ \{\ddot{\phi}\} \end{Bmatrix} + \begin{bmatrix} [K^{\Delta\Delta}] & [K^{\Delta\phi}] \\ [K^{\phi\Delta}] & [K^{\phi\phi}] \end{bmatrix} \begin{Bmatrix} \{\Delta\} \\ \{\phi\} \end{Bmatrix} = \begin{Bmatrix} \{0\} \\ \{Q(t)\} \end{Bmatrix} \quad (234)$$

Above equation can be expressed as

$$[M] \{\ddot{\Delta}\} + [\bar{K}] \{\Delta\} = - [K^{\Delta\phi}] [K^{\phi\phi}]^{-1} \{Q(t)\} \quad (235)$$

$$[\bar{K}] = [K^{\Delta\Delta}] - [K^{\Delta\phi}] [K^{\phi\phi}]^{-1} [K^{\phi\Delta}] \quad (236)$$

The corresponding voltage can be found using

$$\{\phi\} = [K^{\phi\phi}]^{-1} \{[Q(t)] - [K^{\phi\Delta}] \{\Delta\}\} \quad (237)$$

If the system is excited by traction forces and an applied electric field, which are both changed harmonically but not necessarily in the same frequency, equation 224 can be rewritten as

$$\begin{bmatrix} [M] & [0] \\ [0] & [0] \end{bmatrix} \begin{Bmatrix} \{\ddot{\Delta}\} \\ \{\dot{\phi}(t)\} \end{Bmatrix} + \begin{bmatrix} [K^{\Delta\Delta}] & [K^{\Delta\phi}] \\ [K^{\phi\Delta}] & [K^{\phi\phi}] \end{bmatrix} \begin{Bmatrix} \{\Delta\} \\ \{\phi(t)\} \end{Bmatrix} = \begin{Bmatrix} \{f(t)\} \\ \{unknown\} \end{Bmatrix} \quad (238)$$

The equation of motion becomes

$$[M] \{\ddot{\Delta}\} + [K^{\Delta\Delta}] \{\Delta\} = \{f(t)\} - [K^{\Delta\phi}] \{\phi\} \quad (239)$$

The surface charges can be predicted using  $[K^{\phi\Delta}] \{\Delta\} + [K^{\phi\phi}] \{\phi(t)\}$ . Since the motion of the intelligent structure can be sensed, it is possible to apply a required electric field to create or change the damping mechanism of this structure system. This effect is proposed to control (fully or partially) the vibration in this structure.

If the system is excited by traction forces which is harmonic and increasing / decreasing the surface charges in the electrode harmonically, equation 224 can be rewritten as

$$\begin{bmatrix} [M] & [0] \\ [0] & [0] \end{bmatrix} \begin{Bmatrix} \{\ddot{\Delta}\} \\ \{\ddot{\phi}\} \end{Bmatrix} + \begin{bmatrix} [K^{\Delta\Delta}] & [K^{\Delta\phi}] \\ [K^{\phi\Delta}] & [K^{\phi\phi}] \end{bmatrix} \begin{Bmatrix} \{\Delta\} \\ \{\phi\} \end{Bmatrix} = \begin{Bmatrix} \{f(t)\} \\ \{Q(t)\} \end{Bmatrix} \quad (240)$$

The equation of motion becomes

$$[M] \{\ddot{\Delta}\} + [\bar{K}] \{\Delta\} = \{f(t)\} - [K^{\Delta\phi}] [K^{\phi\phi}]^{-1} \{Q(t)\} \quad (241)$$

The corresponding voltage can be found using equation 224. These equations also conclude that if the current that flows into the surface electrode and the voltage in the electrode are measured, the motion of this structure could be predicted. Furthermore, by increasing / decreasing the charges, vibration of the shells could be controlled. This type of behavior can be used in the active tip-clearance control of engine blades.

### Computational Models

A prototype discrete-layer shell element program has been completed and is included as part of this report.

## 6. EXACT SOLUTIONS

Exact solutions are developed for predicting the coupled electromechanical vibration characteristics of simply-supported laminated piezoelectric plates. The three-dimensional equations of stress and electric displacement equilibrium are solved using the assumptions of the linear theory of piezoelectricity. The through-thickness distributions for the displacements and electrostatic potential are functions of eight constants for each layer of the laminate. Enforcing the continuity and surface conditions results in a linear system of equations representing the behavior of the complete laminate. The determinant of this system must be zero at a resonant frequency. The natural frequencies are found numerically by first incrementally stepping through the frequency spectrum and refining the final frequencies using bisection. Representative frequencies and mode shapes are presented for a variety of lamination schemes and aspect ratios.

This chapter is included because it represents the results of a tangential study undertaken as part of this research that was effectly a matter of necessity. Few solutions exist for laminated piezoelectric plates, and this phase of the study was crucial in determining the effectiveness of the discrete-layer approximations described as the main part of this research.

### Introduction

The behavior of linear elastic laminated plates composed of dissimilar orthotropic materials have been studied for a number of geometrical configurations, lamination schemes, and boundary conditions. The exact solutions of the equations of motion for these solids have only been obtained for the limited case of simple support. Static solutions have been comprehensively studied by Pagano [10, 11]. For the dynamic case, the two-dimensional case of cylindrical bending has been considered by Jones [76, 77] for two-layer cross-ply and angle-ply laminates, with the exact natural frequencies and mode shapes being obtained for a number of aspect ratios. The three-dimensional laminated plate geometry has been studied by Srinivas and coworkers [78, 79] using an exact solution for a rectangular plate with simple support.

Studies of the linear vibrations of finite laminated piezoelectric plates are limited. The monograph of Tiersten [80] provides a comprehensive study of the governing equations, fundamental behavior, and exact and approximate solution methodologies for single-ply piezoelectric plates. Studies involving piezoelectric laminates have for the most part been

confined either to infinite plates or approximate theories and solution techniques. These include the studies of Pauley [81], Ricketts [82, 83], Lee [84], and Yong and coworkers [85].

The objective of the present study is to develop exact solutions for the static response and natural frequencies of free vibration for simply-supported, laminated, rectangular plates composed in part of orthotropic piezoelectric layers. The simply-supported plate is one of the few geometries for which the in-plane functions can be selected to exactly satisfy the governing equations and boundary conditions. The through-thickness distributions are evaluated and found to be a function of eight unknown constants that are frequency dependent. Imposition of the interface and surface conditions for the complete laminate results in a linear system of equations that must be iteratively solved for each frequency. This study builds on the work of Pagano [11], who developed exact solutions for static behavior of elastic laminates.

The developed solution and results presented here should provide a good basis for comparison for approximate plate theories. The results could be especially important for thick plates, in which case many theories provide poor approximations, and will help establish the limitations and ranges of applicability of other approximate methods.

## Exact solution

### *Governing Equations*

The geometrical configuration of the laminate is such that the thickness dimension of the laminate coincides with the z-direction, with the lengths of the plate in the x and y directions denoted as  $L_x$  and  $L_y$ , respectively. Each layer of the laminate can have elastic, piezoelectric, or conducting material properties. The general problem considered in this study is to determine the behavior of the elastic and electric field components throughout the laminate under periodic vibration with arbitrary surface conditions.

The constitutive equations for each layer in the laminate are assumed to be those of a piezoelectric material. These equations can also be used to represent purely elastic or conducting layers, and are given by [80]

$$\sigma_i = C_{ij}S_j - e_{ji}E_j \quad (242)$$

$$D_i = e_{ij}S_j + \epsilon_{ij}E_j$$

Here  $\sigma_i$  are the components of the stress tensor,  $C_{ij}$  are the elastic stiffness components,  $S_j$  are the components of infinitesimal strain,  $e_{ji}$  are the piezoelectric coefficients,  $E_i$  are the components of the electric field,  $D_i$  are the components of the electric displacement, and  $\epsilon_{ij}$  are the dielectric constants. The standard contracted notation has been used here. In this study, the poling direction is coincident with the  $x_3$  or  $z$  axis.

The displacement components  $u_i$ , where  $u_1 = u$ ,  $u_2 = v$ , and  $u_3 = w$ , are related to the strain components through the relations

$$S_{ij} = \frac{1}{2} \left( \frac{\partial u_i}{\partial x_j} + \frac{\partial u_j}{\partial x_i} \right) \quad (243)$$

To be consistent with Equation 242, the conventional notation for the strain indices has been used, i.e.  $S_{11} = S_1$ ,  $S_{23} = S_4$ , etc. The electric field components can be related to the electrostatic potential  $\phi$  using the relation

$$E_i = -\frac{\partial \phi}{\partial x_i} \quad (244)$$

For the materials used in this study, it is assumed that the non-zero components of the rotated piezoelectric tensor  $e_{ij}$  are  $e_{31}$ ,  $e_{32}$ ,  $e_{33}$ ,  $e_{24}$ , and  $e_{15}$ . The elastic stiffnesses  $C_{ij}$  are those of an orthotropic material, and the dielectric constants are given by  $\epsilon_{11}$ ,  $\epsilon_{22}$ , and  $\epsilon_{33}$ .

The stress equations of motion are given by

$$\sigma_{ij,j} = \rho \ddot{u}_i \quad (245)$$

and the charge equation of electrostatics is given as

$$D_{i,i} = 0 \quad (246)$$

Substituting the constitutive relations, the stress-strain relations, and the field-potential relations into Eqs. 245 and 246 gives the governing equations of the laminae in terms of the displacement components  $u$ ,  $v$  and  $w$  and the electrostatic potential  $\phi$  as

$$C_{11} \frac{\partial^2 u}{\partial x^2} + C_{12} \frac{\partial^2 v}{\partial x \partial y} + C_{13} \frac{\partial^2 w}{\partial x \partial z} + e_{31} \frac{\partial^2 \phi}{\partial x \partial z} + C_{66} \left( \frac{\partial^2 u}{\partial y^2} + \frac{\partial^2 v}{\partial x \partial y} \right) + \quad (247)$$

$$C_{55} \left( \frac{\partial^2 u}{\partial z^2} + \frac{\partial^2 w}{\partial x \partial z} \right) + e_{15} \frac{\partial^2 \phi}{\partial x \partial z} = \rho \frac{\partial^2 u}{\partial t^2}$$

$$C_{12} \frac{\partial^2 u}{\partial x \partial y} + C_{22} \frac{\partial^2 v}{\partial y^2} + C_{23} \frac{\partial^2 w}{\partial y \partial z} + e_{32} \frac{\partial^2 \phi}{\partial y \partial z} + C_{44} \left( \frac{\partial^2 v}{\partial z^2} + \frac{\partial^2 w}{\partial y \partial z} \right) + \quad (248)$$

$$C_{66} \left( \frac{\partial^2 u}{\partial x \partial y} + \frac{\partial^2 v}{\partial x^2} \right) + e_{24} \frac{\partial^2 \phi}{\partial y \partial z} = \rho \frac{\partial^2 v}{\partial t^2}$$

$$C_{13} \frac{\partial^2 u}{\partial x \partial z} + C_{23} \frac{\partial^2 v}{\partial y \partial z} + C_{33} \frac{\partial^2 w}{\partial z^2} + C_{23} \frac{\partial^2 v}{\partial y \partial z} + e_{24} \frac{\partial^2 \phi}{\partial y^2} + \quad (249)$$

$$C_{44} \left( \frac{\partial^2 w}{\partial y^2} + \frac{\partial^2 v}{\partial y \partial z} \right) + C_{55} \left( \frac{\partial^2 u}{\partial x \partial z} + \frac{\partial^2 w}{\partial x^2} \right) + e_{33} \frac{\partial^2 \phi}{\partial z^2} = \rho \frac{\partial^2 w}{\partial t^2}$$

$$-e_{11} \frac{\partial^2 \phi}{\partial x^2} + e_{31} \frac{\partial^2 u}{\partial x \partial z} + e_{32} \frac{\partial^2 v}{\partial y \partial z} + e_{33} \frac{\partial^2 w}{\partial z^2} + e_{32} \frac{\partial^2 v}{\partial y \partial z} - e_{22} \frac{\partial^2 \phi}{\partial y^2} + \quad (250)$$

$$e_{24} \left( \frac{\partial^2 w}{\partial y^2} + \frac{\partial^2 v}{\partial y \partial z} \right) + e_{15} \left( \frac{\partial^2 u}{\partial x \partial z} + \frac{\partial^2 w}{\partial x^2} \right) - e_{33} \frac{\partial^2 \phi}{\partial z^2} = 0$$

These represent the coupled governing equations for a single layer within the laminate.

For the problems considered in this study, an arbitrary number of laminae are assumed to be perfectly bonded together. At the top and bottom surfaces of the laminate, a given load, displacement, potential, or charge can be specified. A number of surface conditions could be treated using this methodology, but the cases of primary interest are those in which both upper and lower surfaces are traction-free. It is also of interest to consider the influence of electric surface conditions, and the cases of specified homogeneous potential and transverse electric displacement are treated here. The laminate is assumed to be simply supported, and the vertical edges of the laminate are assumed to be fixed at zero (grounded) potential. Hence along a plate edge, the normal stress, tangential displacement, transverse displacement, and electrostatic potential are specified to be zero regardless of the remaining conditions on the remaining laminate surfaces.

At each interface between layers, continuity conditions of displacement, traction, potential, and electric displacement must be enforced. Using an indexing scheme, the conditions for the  $i$ -th layer can be expressed as, for example,

$$u^i \left( x, y, \frac{-h_i}{2} \right) = u^{i+1} \left( x, y, \frac{h_{i+1}}{2} \right) \quad (251)$$

Here  $i$  represents the layer number, with  $i=1$  the top layer, each layer has an individual coordinate system with the origin at the left end in the center of the layer, and  $h_i$  is the thickness of the  $i$ -th layer. Similar interface conditions exist for  $v$ ,  $w$ ,  $\phi$ ,  $\sigma_z$ ,  $\tau_{xz}$ ,  $\tau_{yz}$ , and  $D_z$ . At a single interface of a laminate with  $n$  plies, there are six conditions related to the elastic variables and two conditions related to the electrostatic variables for a total of  $8(n-1)$  interface conditions for the complete laminate. At both the top and bottom surfaces, there are three elastic boundary conditions and one electric condition for a total of 8 conditions. The surface conditions require specification of one variable from each of the pairs  $(u, \tau_{xz})$ ,  $(v, \tau_{yz})$ ,  $(w, \sigma_z)$ , and  $(\phi, D_z)$ . Enforcing all conditions leads to  $8n$  equations relating the variables within all layers of the laminate.

#### Method of Solution

Solutions for the displacement components and the electrostatic potential are sought in the form

$$\begin{aligned} u(x, y, z, t) &= U(z) \exp(j\omega t) \cos px \sin qy = \bar{U} \exp(j\omega t) \exp(sz) \cos px \sin qy \quad (252) \\ v(x, y, z, t) &= V(z, \exp(j\omega t)t) \sin px \cos qy = \bar{V} \exp(j\omega t) \exp(sz) \sin px \cos qy \\ w(x, y, z, t) &= W(z, t) \exp(j\omega t) \sin px \sin qy = \bar{W} \exp(j\omega t) \exp(sz) \sin px \sin qy \\ \phi(x, y, z, t) &= \Phi(z, t) \exp(j\omega t) \sin px \sin qy = \bar{\Phi} \exp(j\omega t) \exp(sz) \sin px \sin qy \end{aligned}$$

Here the overbarred terms are constants,  $s$  is an unknown number,  $p = m \pi/L_x$ ,  $q = n \pi/L_y$ , and  $z$  is the local layer coordinate whose origin is at the center of each laminae. Substitution of these expressions into the equations of motion and the charge equation yields the system of equations

$$\begin{bmatrix} A_{11} - C_{55}s^2 & A_{12} & A_{13}s & A_{14}s \\ A_{12} & A_{22} - C_{44}s^2 & A_{23}s & A_{24}s \\ -A_{13}s & -A_{23}s & A_{33} - C_{33}s^2 & A_{34} - e_{33}s^2 \\ -A_{14}s & -A_{24}s & A_{34} - e_{33}s^2 & A_{44} + \epsilon_{33}s^2 \end{bmatrix} \begin{Bmatrix} \bar{U} \\ \bar{V} \\ \bar{W} \\ \bar{\Phi} \end{Bmatrix} = \begin{Bmatrix} 0 \\ 0 \\ 0 \\ 0 \end{Bmatrix} \quad (253)$$

The  $A_{ij}$  elements of this matrix are

$$A_{11} = C_{11}p^2 + C_{66}q^2 - \rho\omega^2 \quad A_{12} = pq(C_{12} + C_{66}) \quad A_{13} = -p(C_{13} + C_{55}) \quad A_{14} = -(e_{31} + e_{15})p$$

$$A_{22} = C_{66}p^2 + C_{22}q^2 - \rho\omega^2 \quad A_{23} = -q(C_{23} + C_{44}) \quad A_{24} = -q(e_{32} + e_{24}) \quad (254)$$

$$A_{33} = C_{55}p^2 + C_{44}q^2 - \rho\omega^2 \quad A_{34} = e_{15}p^2 + e_{24}q^2 \quad A_{44} = -\epsilon_{11}p^2 - \epsilon_{22}q^2$$

A non-trivial solution to this system requires a zero determinant. The resulting characteristic equation is

$$As^8 + Bs^6 + Cs^4 + Ds^2 + E = 0 \quad (255)$$

Expressions for the coefficients of this polynomial are given in the Appendix. This equation can be written as the fourth-order equation

$$r^4 + cr^3 + dr^2 + er + f = 0 \quad (256)$$

where

$$r = s^2 \quad a = \frac{B}{A} \quad b = \frac{C}{A} \quad (257)$$

$$c = \frac{D}{A} \quad d = \frac{E}{A} \quad (258)$$

The roots of this equation are a function of the material properties, the laminae geometry, and the frequency  $\omega$ . The roots can be real, imaginary, or complex, which results in different forms for the solutions for each variable. Regardless of the nature of the roots, the solutions for a given value of  $s$  are based on the original form for the solution for  $U(z)$ . The remaining components can then be computed using Eq. 253, which is rearranged in terms of the unknown constants as

$$\begin{bmatrix} A_{22} - C_{44}s^2 & A_{23}s & A_{24}s \\ -A_{23}s & A_{33} - C_{33}s^2 & A_{34} - e_{33}s^2 \\ -A_{24}s & A_{34} - e_{33}s^2 & A_{44} + \epsilon_{33}s^2 \end{bmatrix} \begin{Bmatrix} \bar{V} \\ \bar{W} \\ \bar{\Phi} \end{Bmatrix} = \bar{U} \begin{Bmatrix} -A_{12} \\ A_{13}s \\ A_{14}s \end{Bmatrix} \quad (259)$$

General expressions that can be used to evaluate the constants  $\bar{V}$ ,  $\bar{W}$ , and  $\bar{\Phi}$  are constructed as a function of the real, imaginary, or complex roots. These are

$$\tilde{V}(s) = \frac{f_{11}s^4 + f_{12}s^2 + f_{13}}{\bar{D}(s)} \bar{U} \quad (260)$$



$$\tilde{W}(s) = \frac{s(f_{21}s^4 + f_{22}s^2 + f_{23})\bar{U}}{\tilde{D}(s)} \quad (261)$$

$$\tilde{\phi}(s) = \frac{s(f_{31}s^4 + f_{32}s^2 + f_{33})\bar{U}}{\tilde{D}(s)} \quad (262)$$

$$\tilde{D}(s) = d_1s^6 + d_2s^4 + d_3s^2 + d_4 \quad (263)$$

The constants  $d_i$  and  $f_{ij}$  are defined in the Appendix, and will change in nature depending on the type of root. These values and the corresponding solutions for the elastic and electric field components corresponding to each type of root are developed separately below.

*Case 1: Real roots for r*

Given  $n$  real roots for  $r$ , the  $2n$  roots for  $s$  can be obtained using equation 256. These roots are either real or imaginary depending on the sign of  $r$ . Following the nomenclature used in Pagano [10] and Heyliger and Brooks [87], the solution for the displacement components and electrostatic potential corresponding to these roots can be written in either case as

$$U(z) = \sum_{j=1}^n U_j(z) \quad V(z) = \sum_{j=1}^n L_j U_j(z) \quad W(z) = \sum_{j=1}^n M_j W_j(z) \quad \phi(z) = \sum_{j=1}^n N_j W_j(z) \quad (260)$$

where

$$U_j = F_j C_j(z) + G_j S_j(z) \quad (265)$$

$$W_j = G_j C_j(z) + \alpha_j F_j S_j(z)$$

Here  $F_j$  and  $G_j$  are real constants, there is no summation on  $j$ , and the functions  $C$  and  $S$  and the values  $m_j$  and  $\alpha_j$  are defined as

$$C_j(z) = \cosh(m_j z) \quad S_j(z) = \sinh(m_j z) \quad \alpha_j = 1 \quad (r > 0) \quad (266)$$

$$C_j(z) = \cos(m_j z) \quad S_j(z) = \sin(m_j z) \quad \alpha_j = -1 \quad (r < 0) \quad (267)$$

$$m_j = |s_j| \quad (268)$$

The coefficients  $L_j$ ,  $M_j$ , and  $N_j$  are more specific representations of the parameters given in Eqs. 269-271, and are given in this case as

$$L_j = \frac{1}{D_j} (f_{11}m_j^4 + f_{12}\alpha_j m_j^2 + f_{13}) \quad (269)$$

$$M_j = \frac{m_j}{D_j} (f_{21}m_j^4 + f_{22}\alpha_j m_j^2 + f_{23}) \quad (270)$$

$$N_j = \frac{m_j}{D_j} (f_{31}m_j^4 + f_{32}\alpha_j m_j^2 + f_{33}) \quad (271)$$

where the determinant  $D_j$  is given by

$$D_j = d_1\alpha_j m_j^6 + d_2m_j^4 + d_3\alpha_j m_j^2 + d_4 \quad (272)$$

Using the constitutive equations in (242), the corresponding expressions for the stress and electric displacement can be computed as

$$\sigma_i = \sin px \sin qy \sum_{j=1}^n [-pC_{i1} - qC_{i2}L_j + C_{i3}\alpha_j \frac{m_j^2}{D_j} (f_{21}m_j^4 + f_{22}m_j^2\alpha_j + f_{23}) + e_{3i}\alpha_j \frac{m_j^2}{D_j} (f_{31}m_j^4 + f_{32}m_j^2\alpha_j + f_{33})] U_j(z) \quad (273)$$

$$\tau_{yz} = \sin px \cos qy \sum_{j=1}^n [C_{44}(L_j m_j + qM_j) + e_{24}N_j q] W_j(z) \quad (274)$$

$$\tau_{xz} = \cos px \sin qy \sum_{j=1}^n [C_{55}(m_j + pM_j) + e_{24}N_j q] W_j(z) \quad (275)$$

$$\tau_{xy} = \cos px \cos qy \sum_{j=1}^n C_{66}(q + pL_j) U_j \quad (276)$$

$$D_i = \sin px \sin qy \sum_{j=1}^n [-e_{31}p - e_{32}qL_j + \quad (277)$$

$$e_{33}\alpha_j \frac{m_j^2}{D_j} (f_{21}m_j^4 + f_{22}m_j^2\alpha_j + f_{23}) + e_{33}\alpha_j \frac{m_j^2}{D_j} (f_{31}m_j^4 + f_{32}m_j^2\alpha_j + f_{33})] W_j(z)$$

Here  $i=1,2,3$  corresponds to  $x,y$ , and  $z$  for the stress and electric displacement components.

A special case in which there are real roots for  $r$  is the non-piezoelectric elastic layer. The  $e_{ij}=0$  in this case and the elastic and electric fields uncouple. The elastic solution has been given by Pagano [10], and the results are not repeated here except to note that the elastic field behavior is represented by six roots and six unknown constants within the layer. This corresponds to the 6 interface/boundary conditions (three displacements and the  $\sigma_{iz}$  stress components) for a single layer. The electrostatic behavior in this case is represented using the two roots

$$n_{1,2} = \sqrt{\frac{\epsilon_{11}p^2 + \epsilon_{22}q^2}{\epsilon_{33}}} \quad (278)$$

The potential and transverse electric displacement components in this case are given by

$$\phi(x, y, z) = \sin px \sin qy \sum_{j=1}^2 B_j \exp(n_j z) \quad (279)$$

$$D_z = -\epsilon_{33} \sin px \sin qy \sum_{j=1}^2 B_j n_j \exp(n_j z) \quad (280)$$

### Case 2: Complex roots for $r$

The elastic, electric, and geometric properties for some laminae yield complex roots. These appear in conjugate pairs, which result in the final roots for  $s$  in the form  $\pm(a \pm ib)$ , where  $i = \sqrt{-1}$  and  $a$  and  $b$  are positive constants. The solution for  $U(z)$  corresponding to these roots can be expressed as

$$U(z) = c_1 e^{az} \cos bz + c_2 e^{az} \sin bz + c_3 e^{-az} \cos bz + c_4 e^{-az} \sin bz \quad (281)$$

where  $c_1, \dots, c_4$  are real constants. Following some algebraic manipulations and using Eqs. (260-262), the solution for  $V(z)$  can be expressed as

$$V(z) = c_1 e^{az} (\Gamma_1 \cos bz - \Omega_1 \sin bz) + c_2 e^{az} (\Omega_1 \cos bz + \Gamma_1 \sin bz) + \quad (282)$$

$$c_3 e^{-az} (\Gamma_1 \cos bz + \Omega_1 \sin bz) + c_4 e^{-az} (-\Omega_1 \cos bz + \Gamma_1 \sin bz)$$

Here  $\Gamma_1 = \Re[\tilde{V}(a + ib)]$  and  $\Omega_1 = \Im[\tilde{V}(a + ib)]$ . Similarly, the final expression for  $W(z)$  can be expressed as

$$W(z) = c_1 e^{az} [(a\Gamma_2 - b\Omega_2) \cos bz + (-b\Gamma_2 - a\Omega_2) \sin bz] + \quad (283)$$

$$c_2 e^{az} [(b\Gamma_2 + a\Omega_2) \cos bz + (a\Gamma_2 - b\Omega_2) \sin bz] +$$

$$c_3 e^{-az} [(b\Omega_2 - a\Gamma_2) \cos bz + (-b\Gamma_2 - a\Omega_2) \sin bz] +$$

$$c_4 e^{-az} [(b\Gamma_2 + a\Omega_2) \cos bz + (-a\Gamma_2 + b\Omega_2) \sin bz]$$

where  $\Gamma_2 = \Re[\tilde{W}(a + ib)]$  and  $\Omega_2 = \Im[\tilde{W}(a + ib)]$ . The final expression for  $\phi$  can be obtained in similar fashion to yield

$$\phi(z) = c_1 e^{az} [(a\Gamma_3 - b\Omega_3) \cos bz + (-b\Gamma_3 - a\Omega_3) \sin bz] + \quad (284)$$

$$c_2 e^{az} [(b\Gamma_3 + a\Omega_3) \cos bz + (a\Gamma_3 - b\Omega_3) \sin bz] +$$

$$c_3 e^{-az} [(b\Omega_3 - a\Gamma_3) \cos bz + (-b\Gamma_3 - a\Omega_3) \sin bz] +$$

$$c_4 e^{-az} [(b\Gamma_3 + a\Omega_3) \cos bz + (-a\Gamma_3 + b\Omega_3) \sin bz]$$

where  $\Gamma_3 = \Re[\tilde{\phi}(a + ib)]$  and  $\Omega_3 = \Im[\tilde{\phi}(a + ib)]$ .

The functions for displacement and potential in each case must be combined with the solutions corresponding to the remaining roots to construct the complete solution for a given layer. The expressions for the stress and electric displacement components can be obtained by the appropriate differentiation and combination with the constitutive equations as given in Eq. 242. Because of their length and relative ease of calculation, these are not given here.

### *Solution for the Laminate*

The elastic and electric field components within each layer are expressed in terms of 8 unknown constants. These are determined using the interface and continuity conditions at the upper and lower surfaces of each lamina. For an elastic/dielectric layer, there

are 6 constants corresponding to the elastic part of the solution and 2 constants for the electrostatic solution. For most common piezoelectric materials, however, the roots fall into one of two categories. For some piezoelectric materials, the four roots for  $r$  are real. Correspondingly, there are 8 constants ( $F_1, \dots, F_4$  and  $G_1, \dots, G_4$  in Eq. 265) that uniquely define the fields within the layer. For other piezoelectric materials, there are 2 real or imaginary roots and 2 complex conjugate roots for  $r$ . Hence the eight constants are  $F_1, F_2, G_1,$  and  $G_2$  from Eq. 265 and  $c_1, \dots, c_4$  from Eqs. (281-284). Following the solution of the total system of equations for the constants, the solution for any component can be computed at any location within the laminate.

For static solutions, the coefficient matrices are all known as are the right-hand side elements. The solution for the unknown coefficients reduces to solving a linear system of equations.

A resonant frequency  $\omega$  is unknown *a priori*, yet the roots and through-thickness field distributions are a function of this value. An iterative scheme was used to evaluate these parameters. For the vibration problem, a necessary and sufficient condition for a non-trivial solution to exist is that the determinant  $\beta$  of the coefficient matrix  $[A]$  multiplying the unknown constants is zero. The  $[A]$  matrix contains the final coefficients multiplying the unknown constants following imposition of all interface and surface conditions and is written as

$$[A] \{\Delta\} = \{0\} \quad (285)$$

where  $\Delta$  is the column vector of coefficients. The zero determinant requirement establishes the necessary relationships for the calculation of the natural frequencies and the modal shapes for the plate.

To evaluate the roots of the characteristic equation, the following procedure was used. First, the frequency was stepped through a sequence of frequencies that are an increment of the lowest expected frequency. This can either be estimated or approximated from other plate theories. The sign of the determinant is then computed for each value and recorded. Once a sufficient number of sign changes have been noted, bisection was used to refine the values of the true frequencies using the sign-change values as the bounding initial guesses.

It can be a difficult numerical problem to evaluate the determinant of the matrix as

it becomes singular, especially if computed on a limited-precision machine. In this study, the determinant  $\beta$  was computed using

$$\beta = \prod_{j=1}^m \lambda_j \quad (286)$$

where  $\lambda_i$  is the  $i$ -th eigenvalue of the coefficient matrix  $[A]$ . This matrix is square and of order  $m$ , where  $m=8n$  and  $n$  is the number of layers within the laminate. The eigenvalues were computed using the QR algorithm in extended precision. Attempts to compute the eigenvalues using the diagonals from an LDU decomposition and QR with double precision failed.

Following computation of the frequencies  $\omega$ , the constants corresponding to these frequencies that define the modal displacements and potential are readily computed by solving the system of equations with the first constant in  $\Delta$  arbitrarily set to one. The reduced  $[A]$  matrix is no longer singular after this step, and the relative values for the remaining constants can be found. The through-thickness mode shapes can then be calculated using these constants.

Clearly, a different characteristic equation can be generated in determinant form for each combination of  $p$  and  $q$  in Eq. 259. These describe the in-plane modal characteristics of the elastic and electric fields. For each of these equations, there are an infinite number of eigenvalues corresponding to the through-thickness modes. The cases of interest in this study were the thickness modes corresponding to the fundamental in-plane mode with  $m=n=1$  in Eq. 252. Of particular interest is the relationship between the displacement components and the electrostatic potential, as this information could be used to electrically excite or sense the various modes of vibration.

## 7. NUMERICAL EXAMPLES AND RESULTS

This section contains results of applications of the computational and analytic models developed as part of this study. This includes

- Results from laminated piezoelectric plate element.
- Semi-analytic solutions for plates.
- Results of exact solutions for simply-supported plates.

The shell elements were in the process of being tested at the time of writing this report. Several simple test cases were being studied (simple electric field, uniform strain application, etc.). One of the difficulties of benchmarking these elements is the lack of solutions available for laminated piezoelectric shells. Although a proposed area for future study is development of an exact solution for this class of problem, no such solutions are currently available. Because of the preliminary status of the results for the shell, they were not included in this report.

### The Plate Element

In this section, several examples are investigated in order to test the accuracy, validity, and range of applicability of the theories presented in section 4. Initial examples are for the purely elastic plate, with later examples to include piezoelectric layers.

#### *Simply Supported Cross-Ply Plate Under Sinusoidal loading*

A simply supported symmetric cross-ply (0/90/0) laminated rectangular plate under a sinusoidal transverse distributed load on the upper surface is considered. This example is chosen because it has an elasticity solution developed by Pagano [10] and therefore, provides an excellent tool to check the level of accuracy of the two theories presented herein for purely elastic laminates.

Each of the three layers has equal thickness and is idealized as a homogeneous orthotropic material with the following properties:

$$\begin{aligned} E_1 &= 25 * 10^6 \text{ psi} & E_2 = E_3 &= 1.0 * 10^6 \text{ psi} \\ G_{23} &= 0.2 * 10^6 \text{ psi} & G_{12} = G_{13} &= 0.5 * 10^6 \text{ psi} \end{aligned}$$

$$\nu_{12} = \nu_{23} = \nu_{13} = 0.25$$

The domain of the rectangular plate is  $0 < x < a$ ,  $0 < y < b$ , and  $0 < z < H$  with  $b = 3a$ . The transverse sinusoidal distributed load is given by:

$$q(x, y) = q_0 \sin\left(\frac{\pi x}{a}\right) \sin\left(\frac{\pi y}{b}\right) \quad (287)$$

Because of the symmetry of the problem, only a quarter of the plate is modeled ( $0 < x < \frac{a}{2}$ ,  $0 < y < \frac{b}{2}$ ) and the corresponding boundary conditions are given by:

$$\begin{aligned} u(x, 0, z) &= 0 \\ u(a/2, y, z) &= 0 \\ v(0, y, z) &= 0 \\ v(x, b/2, z) &= 0 \\ w(0, y, z) &= 0 \\ w(x, 0, z) &= 0 \end{aligned} \quad (288)$$

The deflections and stresses are computed by using two theories. one considering  $w$  varying linearly through the thickness of the plate and the other one, with  $w$  constant through the thickness. The stresses are determined using the computed displacements and the constitutive relations 38 and 39, and they are evaluated at the closest gauss point to the the following locations:

$$\begin{aligned} \sigma_x(a/2, b/2, H) \\ \sigma_y(a/2, b/2, H/3) \\ \tau_{xy}(0, 0, H) \\ \tau_{xz}(0, b/2, 0) \\ \tau_{yz}(a/2, 0, 0) \end{aligned} \quad (289)$$

Regarding the transverse displacement  $w$ , it is evaluated at the center of the rectangular plate.

The fortran programs written to compute the deflections and stresses according to the two theories presented herein were run for four different meshes : a 6x6 linear element mesh with 6 and 12 layers in the  $z$ -direction and denoted by L6x6-6 and L6x6-12 respectively, and a 3x3 quadratic element mesh with 6 and 12 layers in the  $z$ -direction and denoted



Mesh	a/h=2	a/h=4	a/h=10	a/h=20	a/h=50	a/h=100
	$10^{-6}$	$10^{-5}$	$10^{-5}$	$10^{-4}$	$10^{-3}$	$10^{-2}$
L6x6-12 (F)	0.64710	0.17956	0.90463	0.46290	0.49566	0.22721
L6x6-12 (FR)	0.65119	0.18103	0.91918	0.48600	0.64715	0.50479
L6x6-12 (R)	0.65163	0.18128	0.92210	0.48831	0.65075	0.50767
L6x6-6 (F)	0.62983	0.17752	0.90058	0.46212	0.49571	0.22719
L6x6-6 (FR)	0.6	0.17894	0.91494	0.48513	0.64688	0.50470
L6x6-6 (R)	0.63405	0.179192	0.91786	0.48743	0.65048	0.50759
Q3x3-12 (F)	0.64553	0.17968	0.91673	0.48660	0.64773	0.50256
Q3x3-12 (R)	0.64570	0.179699	0.91695	0.48711	0.65024	0.50742
Q3x3-6 (F)	0.62823	0.17762	0.91255	0.48573	0.64744	0.50245
Q3x3-6 (R)	0.62841	0.17765	0.91278	0.48625	0.64998	0.50733
EXACT	0.65327	0.18055	0.91891	0.48763	0.65060	0.50766

Table 1: Transverse Displacements at the Center of Plate.  $w$  Varying Linearly Through the Thickness

by Q3x3-6 and Q3x3-12 respectively. The results are obtained using the full integration (denoted by F), the reduced integration (denoted by R), and the full integration for the bending terms and the reduced integration for the shear terms (denoted by FR). Tables 1 and 2 shows the non-dimensionalized transverse displacements at the center of the plate for both theories and for a wide range of thickness/lenght ratio.

The results for the case where  $a/h=4$  are represented in figures 19 through 26

#### *Single Layer of PVDF Under Sinusoidal Load and Sinusoidal Potential*

A single square layer of PVDF is considered under two types of loads in using the two theories used in the previous section. First, a transverse sinusoidal load,  $q(x, y) = q_0 \sin(\frac{\pi x}{a}) \sin(\frac{\pi y}{b})$  where  $q_0 = 1$ , is applied on the upper surface. Because of the symmetry of the problem, only one quarter or the plate is modelled and the boudary conditions used are as follows (see figure 17):

$$u(x, 0, z) = 0 \quad ; \quad u(a/2, y, z) = 0$$

$$v(0, y, z) = 0 \quad ; \quad v(x, b/2, z) = 0$$

$$w(0, y, z) = 0 \quad ; \quad w(x, 0, z) = 0$$

$$\varphi(x, 0, z) = 0 \quad ; \quad \varphi(0, y, z) = 0$$

$$\varphi(x, y, 0) = 0 \quad ; \quad \varphi(x, y, h) = 0$$

The results for the case where  $a/h = 10$  are represented in figures 27 through 37.

Mesh	a/h=2	a/h=4	a/h=10	a/h=20	a/h=50	a/h=100
	$10^{-6}$	$10^{-5}$	$10^{-5}$	$10^{-4}$	$10^{-3}$	$10^{-2}$
L6x6-12 (F)	0.66942	0.18084	0.90358	0.46131	0.49409	0.22671
L6x6-12 (FR)	0.67351	0.18232	0.91807	0.48423	0.64409	0.50232
L6x6-12 (R)	0.67421	0.18226	0.92098	0.48652	0.64766	0.50518
L6x6-6 (F)	0.65305	0.17883	0.89952	0.46055	0.49397	0.22670
L6x6-6 (FR)	0.65682	0.18026	0.91383	0.48338	0.64388	0.50228
L6x6-6 (R)	0.65755	0.18053	0.91674	0.48566	0.64745	0.50513
Q3x3-12 (F)	0.66766	0.18096	0.91557	0.48480	0.64466	0.50013
Q3x3-12 (R)	0.66714	0.18087	0.91571	0.48539	0.64716	0.50492
Q3x3-6 (F)	0.65126	0.17893	0.91139	0.48396	0.64443	0.50004
Q3x3-6 (R)	0.65072	0.17884	0.91153	0.48447	0.64695	0.50488
EXACT	0.65327	0.18055	0.91891	0.48763	0.65060	0.5766

Table 2: Transverse Displacements at the Center of Plate.  $w$  Constant Through the Thickness

In the second case when the sinusoidal potential,  $\varphi(x, y) = q_0 \sin(\frac{\pi x}{a}) \sin(\frac{\pi y}{b})$  where  $\varphi_0 = 1$ , is applied to the single layer of PVDF, the boundary condition are as follows:

$$\begin{aligned}
 u(x, 0, z) &= 0 ; u(a/2, y, z) = 0 \\
 v(0, y, z) &= 0 ; v(x, b/2, z) = 0 \\
 w(0, y, z) &= 0 ; w(x, 0, z) = 0 \\
 \varphi(x, 0, z) &= 0 ; \varphi(0, y, z) = 0 \\
 \varphi(x, y, 0) &= 0
 \end{aligned}$$

The results for this case with aspect ratio equal to 10,  $a/h = 10$ , are presented in in figures 38 through 48.

#### *Single Layer of PZT4 Under Sinusoidal Load and Sinusoidal Potential*

A single layer of PZT4 is considered under the same types of loads as those examined with the single layer of PVDF. The geometry is shown in figure 17 wich is the same used for the example on section .The boundary conditions for the two cases, sinusoidal load and sinusoidal potential ,are the same as those in section respectively.

The results for both cases, sinusoidal load load and sinusoidal potential, are shown in figures 49 through 56 and in figures 57 through 64.

#### *Four Layer PVDF/Graphite/Epoxy/PVDF laminate*

A simple supported square laminate composed of 4 layers, is considered in this section.

a/h	Mesh	$\bar{\sigma}_x$		$\bar{\sigma}_y$		$\bar{\tau}_{xy}$		$\bar{\tau}_{xz}$	$\bar{\tau}_{yz}$
2	L6x6-12(F)	8.0302	-6.0920	0.8767	-1.0261	-0.2166	0.2112	0.5160	0.1229
	L6x6-12(FR)	8.0747	-6.1332	0.8849	-0.10341	-0.2183	0.2129	0.5066	0.1233
	L6x6-12(R)	8.1171	-6.1494	0.8866	-1.0373	-0.2191	0.2134	0.5072	0.1230
	L6x6-6(F)	7.1797	-5.4417	0.8313	-0.9899	-0.2054	0.2021	0.4940	0.1063
	L6x6-6(FR)								
	L6x6-6(R)	7.2519	-5.4885	0.8403	-1.0003	-0.2075	0.2041	0.4979	0.1061
	Q3x3-12(F)	8.0676	-6.1373	0.8801	-1.0324	-0.2179	0.2126	0.5049	0.1238
	Q3x3-12(R)	8.0693	-6.1397	0.8811	-1.0334	-0.2180	0.2126	0.5050	0.1238
	Q3x3-6(F)	7.2169	-5.4850	0.8350	-0.9964	-0.2065	0.2034	0.4956	0.1072
	Q3x3-6(R)	7.2180	-5.48645	0.8354	-0.9970	-0.2066	0.2034	0.4957	0.1072
EXACT	8.5323	-6.4962	0.9181	-1.0709	-0.2255	0.2193	0.5182	0.1272	
4	L6x6-12(F)	17.7195	-17.0093	1.6819	-1.8451	-0.4182	0.4371	1.3785	0.1224
	L6x6-12(FR)	17.8784	-17.1650	1.7038	-1.8670	-0.4233	0.4421	1.3927	0.1199
	L6x6-12(R)	17.9508	-17.2284	1.7070	-1.8719	-0.4242	0.4432	1.3941	0.1196
	L6x6-6(R)	17.1557	-16.4718	1.6430	-1.8087	-0.4107	0.4298	1.3756	0.1088
	L6x6-6(FR)	17.3022	-16.6154	1.6642	-1.8299	-0.4155	0.4347	1.3895	0.1060
	L6x6-6(R)	17.3748	-16.6793	1.6672	-1.8346	-0.4165	0.4358	1.3910	0.1058
	Q3x3-12(F)	17.8687	-17.1653	1.6911	-1.8574	-0.4218	0.4407	1.3865	0.1263
	Q3x3-12(R)	17.8790	-17.1780	1.6948	-1.8611	-0.4220	0.4407	1.3867	0.1263
	Q3x3-6(F)		-16.6279	1.6529	-1.8218	-0.4141	0.4333	1.3833	0.1126
	Q3x3-6(R)		-16.6356	1.6559	-1.8244	-0.4143	0.4334	1.3835	0.1126
EXACT	18.3088	-17.5873	1.7405	-1.9086	-0.4301	0.4490	1.4076	0.1291	
10	L6x6-12(F)	70.0011	-69.9408	4.0293	-4.1974	-1.1556	1.1846	4.0714	0.1246
	L6x6-12(FR)	71.2801	-71.2188	4.1162	-4.2843	-1.1794	1.2084	4.1527	0.1014
	L6x6-12(R)	71.6333	-71.5713	4.1301	-4.3000	-1.1839	1.2133	4.1535	0.1013
	L6x6-6(F)	69.5283	-69.4711	4.0047	-4.1732	-1.1491	1.1781	4.0688	0.1126
	L6x6-6(FR)	70.7863	-70.7283	4.0906	-4.2591	-1.1725	1.2016	4.1498	0.0892
	L6x6-6(R)	71.1398	-71.0810	4.1044	-4.2748	-1.1771	1.2064	4.1506	0.0891
	Q3x3-12(F)	71.4377	-71.3816	4.0872	-4.2585	-1.1802	1.2093	4.1476	0.1466
	Q3x3-12(R)	71.5426	-71.4925	4.1117	-4.2821	-1.1806	1.2095	4.1486	0.1471
	Q3x3-6(F)	70.9790	-70.9259	4.0635	-4.2351	-1.1734	1.2025	4.1443	0.1341
	Q3x3-6(R)	71.0574	-71.0074	4.0880	-4.2585	-1.1737	1.2027	4.1454	0.1347
EXACT	72.5977	-72.5396	4.1757	-4.3490	-1.1977	1.2271	4.2018	0.1490	

Table 3: Stresses on Cross-Ply.  $w$  varying through thickness

a/h	Mesh	$\bar{\sigma}_x$		$\bar{\sigma}_y$		$\bar{\tau}_{xy}$		$\bar{\tau}_{xz}$	$\bar{\tau}_{yz}$
20	L6x6-12(F)	0.2421	-0.2422	0.1102	-0.1119	-0.3442	0.3472	0.8049	0.1187
	L6x6-12(FR)	0.2553	-0.2553	0.1164	-0.1181	-0.3632	0.3662	0.8407	0.0165
	L6x6-12(R)	0.2567	-0.2567	0.1169	-0.1186	-0.3651	0.3682	0.8406	0.0173
	L6x6-6(F)	0.2418	-0.2418	0.1105	-0.1122	-0.3435	0.3466	0.8040	0.1029
	L6x6-6(FR)	0.2548	-0.2549	0.1167	-0.1184	-0.3625	0.3656	0.8397	0.0332
	L6x6-6(R)	0.2563	-0.2563	0.1173	-0.1190	-0.3644	0.3675	0.8396	0.0340
	Q3x3-12(F)	0.2559	-0.2560	0.1155	-0.1172	-0.3646	0.3676	0.8575	0.2314
	Q3x3-12(R)	0.2567	-0.2567	0.1167	-0.1184	-0.3648	0.3678	0.8577	0.2331
	Q3x3-6(F)	0.2556	-0.2556	0.1157	-0.1175	-0.3639	0.3669	0.8565	0.2135
	Q3x3-6(R)	0.2562	-0.2563	0.1171	-0.1188	-0.3641	0.3671	0.8566	0.2158
EXACT	0.2600	-0.2601	0.1178	-0.1195	-0.3696	0.3727	0.8686	0.2344	
50	L6x6-12(F)	1.1741	-1.1740	0.4864	-0.4881	-0.1577	0.1580	1.5278	.
	L6x6-12(FR)	1.5405	-1.5406	0.6387	-0.6404	-0.2070	0.2073	1.7991	.
	L6x6-12(R)	1.5493	-1.5493	0.6421	-0.6439	-0.2082	0.2085	1.7969	.
	L6x6-6(F)	1.1740	-1.1741	0.4998	-0.4915	-0.1577	0.1580	1.5257	.
	L6x6-6(FR)	1.5440	-1.5405	0.6431	-0.6448	-0.2069	0.2073	1.7962	.
	L6x6-6(R)	1.5492	-1.5493	0.6466	-0.6483	-0.2081	0.2084	1.7939	.
	Q3x3-12(F)	1.5373	-1.5374	0.6314	-0.6331	-0.2076	0.2079	2.1727	0.5277
	Q3x3-12(R)	1.5497	-1.5498	0.6417	-0.6434	-0.2082	0.2085	2.1654	0.5395
	Q3x3-6(F)	1.5374	-1.5375	0.6358	-0.6375	-0.2075	0.2078	2.1696	0.4888
	Q3x3-6(R)	1.5496	-1.5497	0.6461	-0.6479	-0.2081	0.2085	2.1624	0.5014
EXACT	1.5690	-1.5691	0.6457	-0.6475	-0.2109	0.2112	2.1927	0.5393	
100	L6x6-12(F)	2.7435	-2.7436	1.1199	-1.1216	-0.3653	0.3657	1.2475	.
	L6x6-12(FR)	6.1300	-6.1301	2.5033	-2.5050	-0.8166	0.8168	1.2881	.
	L6x6-12(R)	6.1651	-6.1652	2.5173	-2.5100	-0.8212	0.8215	1.2702	.
	L6x6-6(F)	2.7446	-2.7446	1.1285	-1.1302	-0.3653	0.3656	1.3565	.
	L6x6-6(FR)	6.1312	-6.1313	2.5223	-2.5240	-0.8164	0.8167	1.2825	.
	L6x6-6(R)	6.1664	-6.1665	2.5365	-2.5382	-0.8211	0.8214	1.2646	.
	Q3x3-12(F)	6.0621	-6.0622	2.4590	-2.4607	-0.8146	0.8149	4.3995	1.0025
	Q3x3-12(R)	6.1668	-6.1669	2.5175	-2.5192	-0.8214	0.8217	4.3383	1.0709
	Q3x3-6(F)	6.0634	-6.0635	2.4778	-2.4795	-0.8144	0.8147	4.3936	0.9265
	Q3x3-6(R)	6.1681	-6.1682	2.5366	-2.5383	-0.8213	0.8216	4.3320	0.9975
EXACT	6.2435	-6.2436	2.5308	-2.5326	-0.8319	0.8322	4.3916	1.0652	

Table 4: Stresses on Cross-Ply.  $w$  varying through thickness

a/h	Mesh	$\bar{\sigma}_x$		$\bar{\sigma}_y$		$\bar{\tau}_{xy}$		$\bar{\tau}_{xz}$	$\bar{\tau}_{yz}$
2	L6x6-12(F)	6.8657	-6.8657	0.9860	-0.9860	-0.2220	0.2220	0.5082	0.1205
	L6x6-12(FR)	6.9080	-6.9080	0.9945	-0.9945	-0.2238	0.2238	0.5115	0.1209
	L6x6-12(R)	6.9345	-6.9345	0.9972	-0.9972	-0.2244	0.2244	0.5122	0.1205
	L6x6-6(F)	6.1660	-6.1660	0.9588	-0.9588	-0.2120	0.2120	0.4957	0.1071
	L6x6-6(FR)	6.1960	-6.1960	0.9667	-0.9667	-0.2136	0.2136	0.4987	0.1072
	L6x6-6(R)	6.2231	-6.2231	0.9694	-0.9694	-0.2142	0.2142	0.4995	0.1069
	Q3x3-12(F)	6.9088	-6.9088	0.9909	-0.9909	-0.2233	0.2233	0.5099	0.1215
	Q3x3-12(R)	6.9116	-6.9116	0.9917	-0.9917	-0.2233	0.2233	0.5099	0.1217
	Q3x3-6(F)	6.2077	-6.2077	0.9638	-0.9638	-0.2132	0.2132	0.4974	0.1081
	Q3x3-6(R)	6.2092	-6.2092	0.9643	-0.9643	-0.2132	0.2132	0.4974	0.1083
	EXACT	1.62	2.13	0.268	0.230	0.0548	0.0561	0.257	0.0668
4	L6x6-12(F)	17.3295	-17.3295	1.7392	-1.7392	-0.4307	0.4307	1.3764	0.1186
	L6x6-12(FR)	17.4866	17.4866	1.7610	-1.7610	-0.4357	0.4357	1.3905	0.1160
	L6x6-12(R)	17.5540	-17.5540	1.7647	-1.7647	-0.4368	0.4368	1.3919	0.1156
	L6x6-6(R)	16.7843	-16.7843	1.7173	-1.7173	-0.4233	0.4233	1.3711	0.1070
	L6x6-6(FR)	16.9292	-16.9292	1.7385	-1.7385	-0.4282	0.4282	1.3849	0.1041
	L6x6-6(R)	16.9970	-16.9970	1.7422	-1.7422	-0.4292	0.4292	1.3863	0.1038
	Q3x3-12(F)	17.4836	-17.4836	1.7499	-1.7499	-0.4342	0.4342	1.3844	0.1225
	Q3x3-12(R)	17.4963	-17.4963	1.7528	-1.7528	-0.4343	0.4343	1.3846	0.1229
	Q3x3-6(F)	16.9386	-16.9386	1.7287	-1.7287	-0.4268	0.4268	1.3789	0.1109
	Q3x3-6(R)	16.9462	-16.9462	1.7310	-1.7310	-0.4268	0.4268	1.3791	0.1113
	EXACT	1.10	1.14	0.119	0.109	0.0281	0.0269	0.351	0.0334
10	L6x6-12(F)	70.0028	-70.0028	4.0930	-4.0930	-1.1682	1.1682	4.0684	0.1266
	L6x6-12(FR)	71.2805	-71.2805	4.1794	-4.1794	-1.1919	1.1919	4.1496	0.1036
	L6x6-12(F)	71.6336	-71.6336	4.1940	-4.1940	-1.1966	1.1966	4.1504	0.1034
	L6x6-6(F)	69.5053	-69.5053	4.0728	-4.0728	-1.1617	1.1617	4.0647	0.1154
	L6x6-6(FR)	70.7613	-70.7613	4.1582	-4.1582	-1.1851	1.1851	4.1456	0.0920
	L6x6-6(R)	71.1144	-71.1144	4.1729	-4.1729	-1.1898	1.1898	4.1464	0.0920
	Q3x3-12(F)	71.4394	-71.4394	4.1527	-4.1527	-1.1927	1.1927	4.1446	0.1487
	Q3x3-12(R)	71.5489	-71.5489	4.1751	-4.1751	-1.1930	1.1930	4.1456	0.1496
	Q3x3-6(F)	70.9549	-70.9549	4.1331	-4.1331	-1.1859	1.1859	4.1402	0.1370
	Q3x3-6(R)	71.0357	-71.0357	4.1557	-4.1557	-1.1862	1.1862	4.1413	0.1379
	EXACT	0.725	0.726	0.0435	0.0418	0.0123	0.0120	0.420	0.0152

Table 5: Stresses on Cross-Ply.  $w$  constant

a/h	Mesh	$\bar{\sigma}_x$		$\bar{\sigma}_y$		$\bar{\tau}_{xy}$		$\bar{\tau}_{xz}$	$\bar{\tau}_{yz}$
20	L6x6-12(F)	0.2421	-0.2421	0.1121	-0.1121	-0.3444	0.3444	0.8048	0.1276
	L6x6-12(FR)	0.2552	-0.2552	0.1183	-0.1183	-0.3633	0.3633	0.8406	0.0066
	L6x6-12(R)	0.2566	-0.2566	0.1189	-0.1189	-0.3652	0.3652	0.8382	0.0073
	L6x6-6(F)	0.2417	-0.2417	0.1120	-0.1120	-0.3438	0.3438	0.8039	0.1117
	L6x6-6(FR)	0.2547	-0.2547	0.1181	-0.1181	-0.3626	0.3626	0.8395	0.0232
	L6x6-6(R)	0.2561	-0.2561	0.1187	-0.1187	-0.3645	0.3645	0.8394	0.0239
	Q3x3-12(F)	0.2558	-0.2558	0.1175	-0.1175	-0.3637	0.3647	0.8573	0.2403
	Q3x3-12(R)	0.2566	-0.2566	0.1187	-0.1187	-0.3649	0.3649	0.8574	0.2422
	Q3x3-6(F)	0.2554	-0.2554	0.1173	-0.1173	-0.3640	0.3640	0.8562	0.2228
	Q3x3-6(R)	0.2561	-0.2561	0.1185	-0.1185	-0.3642	0.3642	0.8563	0.2250
EXACT	0.2600	-0.2601	0.1178	-0.1195	-0.3696	0.3727	0.8686	0.2344	
50	L6x6-12(F)	1.1745	-1.1745	0.4961	-0.4961	-0.1573	0.1573	1.5298	.
	L6x6-12(FR)	1.5394	-1.5394	0.6504	-0.6504	-0.2062	0.2062	1.8006	.
	L6x6-12(R)	1.5482	-1.5482	0.6540	-0.6540	-0.2074	0.2074	1.7984	.
	L6x6-6(F)	1.1742	-1.1742	0.4960	-0.4960	-0.1573	0.1573	1.5276	.
	L6x6-6(FR)	1.5389	-1.5389	0.6502	-0.6502	-0.2061	0.2061	1.7975	.
	L6x6-6(R)	1.5477	-1.5477	0.6538	-0.6538	-0.2073	0.2073	1.7953	.
	Q3x3-12(F)	1.5363	-1.5363	0.6432	-0.6432	-0.2068	0.2068	2.1724	0.5536
	Q3x3-12(R)	1.5485	-1.5485	0.6534	-0.6534	-0.2074	0.2074	2.1650	0.5655
	Q3x3-6(F)	1.5359	-1.5359	0.6429	-0.6429	-0.2067	0.2067	2.1697	0.5139
	Q3x3-6(R)	1.5480	-1.5480	0.6533	-0.6533	-0.2073	0.2073	2.1619	0.5265
EXACT	1.5690	-1.5691	0.6458	-0.6475	-0.2109	0.2112	2.1927	0.5393	
100	L6x6-12(F)	2.7489	-2.7489	1.1443	-1.1443	-0.3647	0.3647	1.3652	.
	L6x6-12(FR)	6.1254	-6.1254	2.5499	-2.5499	-0.8127	0.8127	1.3026	.
	L6x6-12(R)	6.1604	-6.1604	2.5644	-2.5644	-0.8173	0.8173	1.2849	.
	L6x6-6(F)	2.7489	-2.7489	1.1442	-1.1442	-0.3647	0.3647	1.3625	.
	L6x6-6(FR)	6.1249	-6.1249	2.5497	-2.5497	-0.8126	0.8126	1.2966	.
	L6x6-6(R)	6.1599	-6.1599	2.5642	-2.5642	-0.8173	0.8173	1.2789	.
	Q3x3-12(F)	6.0577	-6.0577	2.5056	-2.5056	-0.8107	0.8107	4.3986	1.0551
	Q3x3-12(R)	6.1619	-6.1619	2.5642	-2.5642	-0.8175	0.8175	4.3376	1.1238
	Q3x3-6(F)	6.0573	-6.0573	2.5052	-2.5053	-0.8107	0.8106	4.3925	0.9772
	Q3x3-6(R)	6.1617	-6.1614	2.5639	-2.5640	-0.8174	0.8174	4.3311	1.0485
EXACT	6.2435	-6.2436	2.5308	-2.5326	-0.8319	0.8322	4.3917	1.0652	

Table 6: Stresses on Cross-Ply.  $w$  constant

z	$u * 10^{-10}$			$\phi$		
	Exact	Variable W	Constant W	Exact	Variable W	Constant W
1.0000	-0.530075	-0.524338	-0.537309	0.000000	0.000000	0.000000
0.9667	-0.441401	-0.436096	-0.454397	0.009646	0.009699	0.002594
0.9333	-0.371682	-0.366761	-0.390129	0.018931	0.019036	0.004859
0.9000	-0.318131	-0.313540	-0.341897	0.027862	0.028021	0.006856
0.9000	-0.318131	-0.313540	-0.341897	0.027862	0.028021	0.006856
0.7667	-0.202195	-0.198911	-0.240958	0.023203	0.023310	0.006476
0.6333	-0.124831	-0.122843	-0.163878	0.019096	0.19158	0.006252
0.6333	-0.124831	-0.122843	-0.163878	0.019096	0.19158	0.006252
0.5000	0.036839	0.037103	0.000000	0.015443	0.015466	0.006177
0.3667	0.199435	0.198031	0.163878	0.012160	0.012145	0.006252
0.3667	0.199435	0.198031	0.163878	0.012160	0.012145	0.006252
0.2333	0.273535	0.270900	0.240958	0.009165	0.009115	0.006476
0.1000	0.361385	0.357215	0.341897	0.006388	0.006304	0.006856
0.1000	0.361385	0.357215	0.341897	0.006388	0.006304	0.006856
0.0667	0.405321	0.400719	0.390129	0.004599	0.004543	0.004859
0.0333	0.465517	0.460434	0.454397	0.002469	0.002440	0.002594
0.0000	0.544384	0.538772	0.537309	0.000000	0.000000	0.000000

Table 7: Inplane displacement and electrostatic potential

The laminate is constructed with the upper and lower layers composed of polyvinylidene fluoride, PVDF, oriented at 0 degrees, and with the internal two layers composed of a cross-ply of graphite-epoxy oriented at 0, and 90 degrees, respectively [0/90]. The geometry of the laminate is shown in figure 18. In this example, two loading cases are considered. In the first case, the sinusoidal load is applied to the top surface with the top and bottom surfaces and the vertical edges of the laminate grounded. In the second case, the sinusoidal potential is applied to the top surface of the laminate with the bottom surface grounded.

The results for the case  $l/h = 4$  are presented on tables 7 through 9 for the case in which the sinusoidal load is applied, and on tables 10 through 12 for the case when the sinusoidal potential is applied.

### Semi-Analytic Solutions

Of primary interest in this section is the basic behavior of the displacement, stress, electrostatic potential, and electric displacement of a laminate with embedded piezoelectric layers. Both the variable-w and constant-w cases are examined below for the static behavior, with the added theory of the independent-w approximation studied for the dynamic case.

$z$	$\sigma_x$			$\tau_{xy}$		
	Exact	Variable W	Constant W	Exact	Variable W	Constant W
1.0000	10.33504	10.04129	10.10107	-0.659511	-0.639464	-0.650112
0.9667	8.652445	8.395070	8.552297	-0.567147	-0.549237	-0.564983
0.9333	7.324507	7.098908	7.347798	-0.489060	-0.472978	-0.493142
0.9000	6.299222	6.099411	6.440052	-0.423323	-0.408792	-0.432799
0.9000	0.855399	0.854236	0.589416	-0.372215	-0.359438	-0.380547
0.7667	0.638399	0.616228	0.368611	-0.193170	-0.185308	-0.216892
0.6333	0.449534	0.453350	0.205646	-0.067341	-0.063584	-0.098115
0.6333	1.553872	1.492791	1.727943	-0.067341	-0.063584	-0.098115
0.5000	-0.213979	-0.210662	0.000000	0.034551	0.034255	0.000000
0.3667	-1.988776	-1.919539	-1.727943	0.131542	0.127279	0.098115
0.3667	-0.030955	-0.037756	-0.205646	0.131542	0.127279	0.098115
0.2333	-0.212196	-0.193350	-0.368611	0.247282	0.239053	0.216892
0.1000	-0.400353	-0.394469	-0.589416	0.403180	0.390294	0.389547
0.1000	-6.892361	-6.686350	-6.44052	0.458540	0.443884	0.432799
0.0667	-7.736448	-7.505797	-7.347798	0.516071	0.499933	0.493142
0.0333	-8.884439	-8.623567	-8.552297	0.585343	0.567453	0.564983
0.0000	-10.38138	-10.08549	-10.10107	0.668041	0.648098	0.650112

Table 8: Inplane stress distribution

$z$	$\tau_{yz}$			$D_z * 10^{-11}$		
	Exact	Variable W	Constant W	Exact	Variable W	Constant W
0.9833	0.030842	0.027313	0.025778	-0.126731	-0.120614	-0.019162
0.9500	0.086931	0.082322	0.077648	-0.120156	-0.114803	-0.016218
0.9167	0.136315	0.130711	0.123182	-0.107478	-0.102818	-0.010268
0.8333	0.435957	0.410734	0.405381	-0.092683	-0.092463	-0.007448
0.7000	0.750776	0.726830	0.736019	-0.081694	-0.081487	-0.004399
0.5667	0.831595	0.817600	0.827206	-0.072650	-0.072465	-0.001452
0.4333	0.849577	0.835698	0.827206	-0.065336	-0.065183	0.001452
0.3000	0.766156	0.743298	0.736019	-0.059577	-0.059464	0.004399
0.1667	0.426790	0.403100	0.405381	-0.055236	-0.055172	0.007448
0.0833	0.126715	0.121428	0.123182	-0.049454	-0.053851	0.010268
0.0500	0.080648	0.076351	0.077648	-0.043180	-0.048213	0.016218
0.0167	0.028558	0.025335	0.025778	-0.039831	-0.045558	0.019162

Table 9: Transverse shear stress and electric displacement



$z$	$\tau_{yz}$			$D_z * 10^{-11}$		
	Exact	Variable W	Constant W	Exact	Variable W	Constant W
1.0000	-0.464016	-0.454333	-0.274944	1.000000	1.000000	1.000000
0.9667	-0.750174	-0.740068	-0.776016	0.985118	0.985081	0.984102
0.9333	-1.093318	-1.082760	-1.229627	0.971528	0.971463	0.969594
0.9000	-1.505134	-1.494176	-1.661744	0.959215	0.959128	0.956455
0.9000	-1.505134	-1.494176	-1.661744	0.959215	0.959128	0.956455
0.7667	-1.016508	-1.006818	-1.105801	0.770200	0.769887	0.767967
0.6333	-0.609389	-0.600110	-0.660315	0.599521	0.599117	0.597904
0.6333	-0.609389	-0.600110	-0.660315	0.599521	0.599117	0.597904
0.5000	-0.364444	-0.356267	-0.399691	0.443115	0.442720	0.442186
0.3667	-0.234489	-0.228002	-0.268975	0.297258	0.296946	0.297076
0.3667	-0.234489	-0.228002	-0.268975	0.297258	0.296946	0.297076
0.2333	-0.244599	-0.239503	-0.298538	0.158478	0.158295	0.159094
0.1000	-0.283474	-0.279194	-0.363899	0.023471	0.023443	0.024929
0.1000	-0.283474	-0.279194	-0.363899	0.023471	0.023443	0.024929
0.0677	-0.311356	-0.307364	-0.371325	0.015630	0.015611	0.016599
0.0333	-0.367545	-0.363802	-0.351645	0.007809	0.007800	0.008294
0.0000	-0.454328	-0.450824	-0.304332	0.000000	0.000000	0.000000

Table 10: Inplane displacement and electrostatic potential

$z$	$\sigma_x * 10^{-1}$			$\tau_{xy} * 10^{-3}$		
	Exact	Variable W	Constant W	Exact	Variable W	Constant W
1.0000	-0.252476	-0.238020	-0.307042	0.061703	0.078828	-0.197721
0.9667	-0.168379	-0.169224	-0.196349	-0.508764	-0.480931	-0.572105
0.9333	-0.074172	-0.076568	-0.079646	-1.072601	-1.033926	-1.223532
0.9000	0.032380	0.014740	-0.017074	-1.643345	-1.593534	-1.783186
0.9000	0.017152	0.018635	0.026079	-1.444943	-1.401145	-1.567900
0.7667	0.012998	0.012217	0.017026	-0.941803	-0.908786	-1.007435
0.6333	0.009345	0.007959	0.010671	-0.616103	-0.590772	-0.656807
0.6333	0.067112	0.065187	0.072009	-0.616103	-0.590772	-0.656807
0.5000	0.041152	0.039400	0.044246	-0.436790	-0.416920	-0.469842
0.3667	0.027072	0.025825	0.030211	-0.330848	-0.314971	-0.363867
0.3667	0.005157	0.004695	0.005225	-0.330848	-0.314971	-0.363867
0.2333	0.004410	0.004098	0.005279	-0.303844	-0.289910	-0.346856
0.1000	0.003844	0.004317	0.006324	-0.346085	-0.332338	-0.410615
0.1000	-0.116128	-0.115099	-0.117675	-0.393606	-0.377970	-0.466996
0.0667	-0.109948	-0.109214	-0.115478	-0.500968	-0.483674	-0.562701
0.0333	-0.098760	-0.098185	-0.118428	-0.605557	-0.586605	-0.595639
0.0000	-0.082135	-0.081793	-0.127015	-0.709345	-0.688722	-0.566045

Table 11: Inplane stress distribution

z	$\tau_{yz} * 10^{-3}$			$D_z * 10^{-10}$		
	Exact	Variable W	Constant W	Exact	Variable W	Constant W
0.9833	-0.540721	-0.497105	-0.568975	-0.506163	-0.500145	-0.498431
0.9500	-1.510913	-1.455750	-1.668638	-0.462265	-0.456622	-0.454952
0.9167	-2.336173	-2.270831	-2.602503	-0.418973	-0.413703	-0.412115
0.8333	-1.757666	-1.768708	-2.025278	-0.376004	-0.371419	-0.369941
0.7000	-0.398307	-0.407344	-0.474639	-0.339528	-0.335167	-0.333779
0.5667	0.194760	0.192967	0.205508	-0.311136	-0.306955	-0.305625
0.4333	0.330157	0.324822	0.354593	-0.290150	-0.286109	-0.284803
0.3000	0.677038	0.660715	0.739205	-0.276072	-0.272126	-0.270814
0.1667	1.211837	1.192111	1.364158	-0.268567	-0.264672	-0.263323
0.0833	1.236155	1.218844	1.410369	-0.266737	-0.262607	-0.261199
0.0500	0.733438	0.724337	0.841775	-0.266039	-0.261917	-0.260464
0.0167	0.242057	0.241098	0.279375	-0.265690	-0.261570	-0.260096

Table 12: Transverse shear stress and electric displacement

### Quasi-static response

In this section, the static response of piezoelectric laminates is studied and compared with the exact three-dimensional solution. Two different types of loading are considered. The first is an applied sinusoidal transverse load of the form

$$F(x, y) = f_o \sin \frac{\pi x}{L_x} \sin \frac{\pi y}{L_y} \quad (290)$$

where  $f_o$  is the peak intensity of the load at the center of the plate. This could simulate the sensory characteristics of a laminate by determining the behavior of the electric field as a function of loading. The second type of loading simulates the active response of a laminate under a sinusoidal surface potential similar in nature to that described in Equation 287 except that now  $f_o$  is the peak potential at the plate center. Both of these cases have exact solutions [87] and demonstrate not only the fundamental behavior of the laminate but also the accuracy of the discrete-layer approach as a function of the number of layers used within the laminate.

Two geometries are used in this example: a single layer of PZT-4 and a 5-ply hybrid laminate. The 5-ply laminate geometry consists of a symmetric [0/90/0] cross-ply of an elastic, orthotropic plate with the material properties  $C_{11} = 134.9$  (all in GPa),  $C_{22} = 14.35$ ,  $C_{33} = 14.35$ ,  $C_{12} = 5.156$ ,  $C_{13} = 5.156$ ,  $C_{23} = 7.133$ ,  $C_{44} = 3.606$ ,  $C_{55} = 5.654$ ,  $C_{66} = 5.654$ ,  $\epsilon_{11}/\epsilon_o = 3.5$ ,  $\epsilon_{22}/\epsilon_o = \epsilon_{33}/\epsilon_o = 3.0$ . These three layers are all of equal thickness. Two layers of the piezoceramic material PZT-4 of equal thickness are bonded to the upper

and lower surfaces of the laminate. The total laminate thickness is defined as  $h$ , with the thickness of each of the piezoelectric layers taken as  $0.1h$ . The plate is square, with the length/thickness ratio of the plate specified as 4.

The boundary conditions along the vertical edges are those consistent with the functions described in Equation 25. Hence along an edge the transverse and tangential displacements are zero as are the normal stress and electrostatic potential. The top and bottom surfaces of the laminate are grounded for the transverse load case, with the bottom of the laminate stress-free. For the sinusoidal unit potential, the bottom surface of the laminate is grounded with the upper and lower surfaces of the laminate stress-free.

Three different discretizations are used in the thickness direction of the laminate. Each of the laminae are divided into 1, 2, and 4 layers with linear interpolations used within each layer. Hence the total laminate is divided into 5, 10, and 20 layers. The in-plane functions are selected to coincide exactly with the distributions given in Equation 25, which also match the forms for the exact solutions.

The through-thickness distributions of  $u$ ,  $w$ ,  $\phi$ ,  $\sigma_y$ ,  $\sigma_z$ ,  $\tau_{yz}$ , and  $D_z$  are shown in Figures 65-80 for the single layer of PZT-4 using a 12 layer discretization. This example clearly demonstrates the poor behavior of the constant- $w$  theory and the excellent agreement with the variable- $w$  theory.

The results for the 5-ply laminate in Figures 81-102. The in-plane displacements for both applied load and potential contain distinct breaks in slope at the interface locations. This is especially true for the applied potential, for which the displacement gradient in the PZT layer is very high compared to the other layers. The transverse displacement  $w$  also has a highly non-uniform behavior over the thickness of the laminate. These distributions indicate that even for a relatively simple lamination scheme, the assumption of linear global behavior for the displacements or potential would be highly detrimental for a plate of this thickness. Also of note are the excellent results obtained using the minimal number of discrete-layers through the thickness. Even the 5-layer approximation (one layer per laminae) provides excellent results for all field distributions. The stress variables in this case are computed at the sub-layer centroids using the constitutive laws for the material. The worst agreement for the 5-layer case is the transverse displacement for the applied potential loading, for which the values differ from the exact solution by about seven percent. This also influences the  $\sigma_z$  and  $\tau_{yz}$  stress distributions. All other values are in very good agreement for both load cases.

The distribution of the normal component of electric displacement is fairly uniform through the thickness of the cross-ply by changes dramatically within the piezoelectric layers because of the electromagnetic coupling. Assuming linear material behavior, this behavior could be used to model the laminate response in a sensory fashion for the case of the applied loading.

### *Dynamic Analysis*

Exact solutions for the free-vibration of simply-supported piezoelectric plates are available [89], and provide a good benchmark for comparative purposes. The primary quantities of interest are the resonant frequencies and the through-thickness modal distributions corresponding to these frequencies. Two sets of boundary conditions are considered in this analysis. In the first, the top and bottom surfaces are grounded during the vibration. In the second, the electric displacement on these surfaces are zero. These cases are termed closed-circuit and open-circuit, respectively. The fundamental in-plane mode with  $m=n=1$  is the focus of this example.

A square plate composed of a single layer of the piezoceramic PZT-4 is considered first. The length of each side is taken as  $L_x = L_y = a$ . The height is taken as  $h$ , and three  $a/h$  ratios are studied: 4, 10, and 50. The fundamental through-thickness frequency is of most interest, and is given as a function of the number of layers used to describe the piezoelectric layer. The results are shown in Table 13. The frequencies are represented in the tables in terms of the parameter  $\omega h/\rho$ .

A second plate is composed of two dissimilar piezoelectric materials modeled after PZT-4 [68] and PVDF [16]. The densities of the two materials are taken to be the same. A three-ply laminate is constructed with the configuration [PZT/PVDF/PZT], with the PVDF layer oriented at 0 degrees. The thickness of each PZT layer is  $0.25h$ . Both open and closed circuit conditions are considered, with the length/thickness ratios of 4 and 50 studied. The convergence of the first six modes as a function of a number of sub-layers is shown and compared with the exact frequencies in Table 14. For both of these examples, it is clear that even a small number of layers yields frequencies accurate well within several percent.

A final example is a 5-ply laminate identical to that considered in the static analysis in the previous sub-section. The first six thickness mode frequencies are listed in Table 15, and are again very accurate with respect to the exact solution. The mode shapes can

also be easily calculated, and exhibit trends similar to the static example in terms of the convergence. The through-thickness distributions of the displacements and potential for the closed-circuit boundary conditions can be easily computed for  $a/l_1=4$  and  $a/h=50$ . The plots are indistinguishable from those generated using the exact solution, and are given in the next section.

### Exact Solution

Although both the static and dynamic cases have been investigated, the dynamic case is of most interest and can be obtained as a special case of the static solution with  $\omega = 0$ . The focus of the results in this report is for the dynamic case.

In all cases studied, the plates are square with simply supported edges and  $L_x = L_y = a$ . The plate surfaces are assumed to be traction-free unless otherwise noted. Although other surface conditions can easily be considered along with rectangular plate geometries, these were selected for simplicity. Two sets of electric boundary conditions are typically applied: homogeneous potential or homogeneous electric displacement. The frequencies for these examples are expressed in terms of the frequency parameter  $\gamma = \omega h / \sqrt{\rho}$ , where  $\omega$  is the initial frequency in radians per second.

The frequencies were determined using bisection with the bounding guesses determined two different ways. In the first, the frequency was stepped in increments of one percent of the elastic plate frequency neglecting the electromechanical coupling and using classical lamination theory [88]. At locations where the determinant changed sign, bisection was used to refine the roots to the required accuracy. A second method used as a check was the discrete-layer theory developed by the authors [89], which is extremely accurate and gave excellent estimates for the exact values of the frequencies. For the most part, these two different sets were in very good agreement. The only exceptions existed in the stepping method where there could be sign change in determinant and convergence obtained for a frequency, but there was no analogous root predicted by the discrete-layer theory. In these cases, the resulting exact eigenfunctions did not satisfy the appropriate interface and boundary conditions. The source of this anomaly is unknown. Such modes and their frequencies are not included in the results that follow.

#### *The Piezoelectric Single Layer*

A single homogeneous layer of a piezoceramic is considered first. This problem is useful to demonstrate the nature of the thickness modes and to partially demonstrate the influ-

ence of aspect ratio and the electric boundary conditions. The material properties used here, selected to model PZT-4, are shown in the Table A1 in the Appendix along with the properties for all materials used in this study. The material used here is material 2. Four thickness ( $a/h$ ) ratios were considered: 1, 4, 10, and 50. The frequencies corresponding to the first six thickness modes are shown in Table 16 for both  $\phi=0$  and  $D_z=0$  conditions, which are referred to as cases I and II, respectively. It is clear from these results that as the aspect ratio decreases (thick plates), the influence of the electric boundary conditions becomes more pronounced, with the homogeneous electric displacement providing higher frequencies for all cases.

The mode shapes corresponding to the frequencies of vibration are also of significant interest, as these describe the nature of the motion and the extent of electromechanical coupling. The three displacement components are normalized with respect to the largest value of  $u$ ,  $v$ , or  $w$  through the thickness for a particular mode. The potential was also normalized with respect to its largest value as well for plotting purposes. A scaling factor  $\alpha$  was used to denote the relationship between the potential and the displacements. This value is the magnitude of the potential at the middle surface of the plate ( $z=0$ ) divided by the  $u$  displacement component at the top of the plate ( $z=h/2$ ). If the potential is zero at the mid-surface, the location used for the computed scale factor is at  $z=0.25h$ . This is noted in the table by placing parentheses around the value.

The first mode for this laminate is the so-called flexural mode. It is distinguished by the symmetric distributions for the transverse displacement and potential and the antisymmetric distribution of in-plane displacement. As the thickness ratio increases, the in-plane displacements become more linear and the transverse displacement becomes more uniform. The second mode is a purely extensional mode with the eigenfunctions described by  $u(z) = -v(z) = 1$ ,  $w(z) = \phi(z) = 0$ . There is no electromechanical coupling in this mode, and the same frequency is obtained for both case I and case II surface conditions. The third mode yields displacement functions that tend toward  $u(z) = v(z) = 1$  and  $w(z) = 0$  as the plate becomes thin. The in-plane functions are symmetric and the transverse displacement is antisymmetric. The potential distribution changes little relative to the aspect ratio. The fourth mode is also purely elastic with no coupling and is the first thickness shear mode. This is distinguished by in-plane displacement functions given by  $u(z) = -v(z) = \sin \pi z/h$  and zero transverse displacement and potential. These modes demonstrate the deviations in the displacement and electrostatic potential from

the kinematic assumptions of some simplified laminate theories (linear  $u$ ,  $v$ , and  $\phi$  and constant  $w$ ) as the plate  $a/h$  ratio decreases.

In general, the modes for the two types of electric boundary condition have similar features. The features can change depending on the electric boundary conditions. For example, for  $a/h=1$  the second thickness shear mode corresponds to mode 6 (case I) and mode 5 (case 2). This mode has features similar to the first thickness-shear mode except  $u(z) = -v(z) = \sin 3\pi z/h$ .

#### *Three-ply Symmetric Laminate*

A second example is a laminate composed of two dissimilar materials with a mismatch in both elastic and electric properties. The materials, denoted as 1 and 2, are adapted from the properties of the transversely isotropic PZT-4 and the orthotropic PVDF. Two aspect ratios of 4 and 50 are considered, with both types of electric boundary conditions, I and II, considered. Two lamination schemes are studied. The first has the layup of  $[1/2/2/1]$ , and the second  $[2/1/1/2]$ , where the numbers indicate the piezoelectric material. Each layer has equal thickness of  $0.25h$ . The frequency parameters are shown in Table 17. In this case, there are no cases for which the elastic and electric fields uncouple. It is also not possible to classify these modes as pure shear or extension because of the dissimilar materials.

Plots of the first six through-thickness modes for  $[1/2/2/1]$  are shown in Figures 103-114 for the two aspect ratios. It is clear from these plots that the influence of the dissimilar properties on the displacements and the potential decreases as the aspect ratio increases. It is also clear that even for thin laminates the modal potential cannot be accurately represented by a simple linear function through the laminate thickness. This requires specific attention in constructing approximate solutions to this class of problem.

#### *Hybrid Composite Laminate*

In many structural applications, several layers of piezoelectric material are bonded to a substructure of elastic composite plies. This type of configuration is considered here, with single layers of piezoceramic material PZT (material 2) bonded to the upper and lower faces of an elastic, symmetric cross-ply. The 5-ply laminate  $[PZT/0/90/0/PZT]$  is considered, with the cross-ply formed by a composite material and denoted as material 3 in Table A1.

The natural frequencies for case I and II electric boundary conditions are shown in

Table 18. The through-thickness displacement and potential functions are presented for the first (flexural) mode in Figures 115-116 for  $a/h=4$  and  $a/h=50$ . The line definitions are given by  $u$  (solid),  $v$  (dash-dot),  $w$  (dash), and the potential (dot). In addition, representative plots of the intralaminar ( $\sigma_1, \sigma_2, \sigma_6$ ) and interlaminar ( $\sigma_3, \sigma_4, \sigma_5$ ) stress components and transverse electric displacement ( $D_z$ ) are also given for the same mode in Figures 117-120, respectively. Here the lines are  $\sigma_x$  (solid),  $\sigma_y$  (dash),  $\sigma_{xy}$  (dot) in Figures 117-118 and  $\sigma_z$  (solid),  $\tau_{xz}$  (dash),  $\tau_{yz}$  (dot) and  $D_z$  (dash-dot) in Figures 119-120 for both two thickness ratios. As the plate becomes thin, the in-plane displacements tend to the same distribution, with the transverse displacement tending to a constant through-thickness value. Also, the in-plane stresses tend to become more linear, with the transverse normal stress decreasing in relative magnitude as expected.

#### *Single-layer PZT-4: Independent-w theory*

The final example of this report contains perhaps the most important example of this study, and provides an example of the theory constructed to combat the poor performance of the constant-w theory described in earlier sections. By allowing a transverse normal strain that is still less computationally intensive than the total variable-w theory, the actuation strain can be captured to yield results that are much closer to reality than the constant-w case.

As a simple demonstration, the closed-circuit free-vibration behavior of a single layer of PZT-4 is examined using 1) variable-w theory with two layers, 2)  $u-v-\phi$  approximations using two layers and  $w$ -approximation using a single layer, and 3) the exact solution. The results of the first 6 frequencies are shown in Table 19. Clearly, the independent-w theory yields a higher fundamental mode, but is indicative of the relatively good accuracy with a small number of  $w$ -layers. Many of the higher modes (pure extension and those with no coupling) exactly capture the frequency of the plate.

This theory was just completed and debugged code produced at the end of this study. The full power and versatility of this theory and element await full exploration.



a/h	4		10		50	
N	Open	Closed	Open	Closed	Open	Closed
1	110,189	104,105	20,485.7	20,217.4	848.586	848.094
2	102,599	100,294	18,761.5	18,656.2	773.651	773.458
4	99,454	97,915	18,255.4	18,180.8	753.622	753.525
8	98,456	97,186	18,122.4	18,055.7	748.576	748.452
16	98,311	96,994	18,088.9	18,024.0	747.299	747.177
32	98,251	96,946	18,080.6	18,016.0	746.979	746.859
64	98,236	96,934	18,078.4	18,014.0	746.898	746.779
Exact	98,232	96,930	18,077.8	18,013.4	746.873	746.752

Table 13 Convergence of fundamental frequency for single-layer of PZT-4.

a/h=4: C	Mode					
	1	2	3	4	5	6
N=4	74.7732	197.353	329.301	342.387	447.653	549.479
N=8	72.8253	195.402	311.843	338.628	432.976	534.030
N=16	72.3376	194.920	307.606	337.504	426.810	530.343
N=32	72.2152	194.800	306.558	337.207	425.160	529.432
N=64	72.1846	194.770	306.296	337.132	424.742	529.205
Exact	72.1744	194.760	306.209	337.107	424.602	529.129
a/h=4: O	1	2	3	4	5	6
N=4	74.8023	197.483	329.691	342.481	447.733	550.079
N=8	72.8451	195.525	312.190	338.718	433.049	534.493
N=16	72.3554	195.042	307.940	337.593	426.875	530.769
N=32	72.2325	194.921	306.888	337.296	425.223	529.849
N=64	72.2017	194.891	306.626	337.221	424.804	529.620
Exact	72.1915	194.881	306.539	337.196	424.664	529.543
a/h=50: C	1	2	3	4	5	6
N=4	0.637707	16.4328	28.5365	292.035	379.322	400.300
N=8	0.634494	16.4315	28.5356	273.945	359.391	379.362
N=16	0.633687	16.4312	28.5353	269.563	354.642	371.982
N=32	0.633485	16.4311	28.5353	268.479	353.469	370.048
N=64	0.633434	16.4311	28.5353	268.208	353.177	369.559
Exact	0.633417	16.4311	28.5352	268.118	353.079	369.396
a/h=50: O	1	2	3	4	5	6
N=4	0.637786	16.4426	28.5566	295.866	390.811	400.301
N=8	0.634566	16.4413	28.5556	277.248	369.149	379.363
N=16	0.633757	16.4410	28.5554	272.717	363.958	371.982
N=32	0.633555	16.4409	28.5554	271.595	362.674	370.048
N=64	0.633506	16.4409	28.5553	271.315	362.354	369.560
Exact	0.633487	16.4409	28.5553	271.222	362.248	369.396

Table 14 Convergence of frequencies for 3-ply piezoelectric laminate.

	Mode					
a/h=4: C	1	2	3	4	5	6
N=5	57.2531	194.840	255.648	282.168	368.461	389.525
N=10	57.1249	192.190	252.024	276.853	364.218	383.352
N=20	57.0875	191.524	251.085	275.425	362.939	381.629
N=32	57.0855	191.350	250.845	275.040	362.592	381.171
N=64	57.0773	191.313	250.786	274.969	362.516	381.072
Exact	57.0745	191.301	250.769	274.941	362.522	381.049
a/h=4: O	1	2	3	4	5	6
N=5	57.2707	194.843	255.648	282.168	368.505	389.534
N=10	57.1403	192.192	252.025	276.853	364.252	383.364
N=20	57.1023	191.526	251.086	275.425	362.971	381.641
N=32	57.1005	191.353	250.845	275.040	362.623	381.184
N=64	57.0921	191.316	250.786	274.969	362.548	381.084
Exact	57.0893	191.304	250.770	274.941	362.522	381.049
a/h=50: C	1	2	3	4	5	6
N=5	0.619025	15.6835	21.4947	212.811	214.690	384.953
N=10	0.618348	15.6820	21.4933	210.561	211.596	379.943
N=20	0.618175	15.6817	21.4929	209.925	210.791	378.575
N=32	0.618156	15.6816	21.4928	209.754	210.582	378.207
N=64	0.618127	15.6816	21.4928	209.718	210.538	378.132
Exact	0.618118	15.6816	21.4928	209.704	210.522	378.104
a/h=50: O	1	2	3	4	5	6
N=5	0.619038	15.6835	21.4949	212.827	214.736	384.953
N=10	0.618351	15.6821	21.4935	210.568	211.645	379.944
N=20	0.618179	15.6817	21.4931	209.929	210.841	378.575
N=32	0.618160	15.6816	21.4930	209.758	210.632	378.207
N=64	0.618141	15.6816	21.4930	209.721	210.589	378.133
Exact	0.618120	15.6816	21.4930	209.707	210.573	378.105

Table 15 Convergence of frequencies for 5-ply hybrid laminate.

	I		II	
a/h=1	$\gamma$	$\alpha$	$\gamma$	$\alpha$
1	713,061	-1.744e+9	724,602	-1.675e+9
2	777,021	0	777,021	0
3	889,902	(-1.515e+11)	912,912	(-1.498e+9)
4	925,431	0	925,431	0
5	1,243,819	-1.534e+9	1,270,594	0
6	1,270,594	0	1,293,504	(-2.57e+10)
a/h=4	$\gamma$	$\alpha$	$\gamma$	$\alpha$
1	96,929.9	-4.87e+8	98,231.7	-7.78e+8
2	194,255	0	194,255	0
3	327,663	(2.276e+7)	355,110	(4.57e+9)
4	538,885	0	538,885	0
5	609,186	-1.08e+8	690,767	2.55e+9
6	958,922	(-2.66e+8)	960,103	(-3.48e+8)
a/h=10	$\gamma$	$\alpha$	$\gamma$	$\alpha$
1	18,013.4	-1.78e+8	18,077.8	-3.40e+8
2	77,702.1	0	77,702.1	0
3	133,695	(1.27e+6)	145,221	(1.74e+8)
4	508,625	0	508,625	0
5	522,320	-4.87e+7	604,752	6.26e+9
6	988,021	(-1.76e+8)	990,953	(-2.88e+8)
a/h=50	$\gamma$	$\alpha$	$\gamma$	$\alpha$
1	746.752	-3.48e+7	746.873	-7.78e+8
2	15,540.4	0	15,540.4	0
3	26,828.0	(9.94e+3)	29,153.3	(3.48e+7)
4	502,895	0	502,895	0
5	503,469	-1.01e+7	586,240	3.10e+10
6	1,004,344	(-4.56e+7)	1,004,612	(-7.21e+7)

Table 16. Frequency parameters for single-ply piezoelectric layer for differing electric surface conditions.

Frequency parameter $\gamma$					
		a/h=4		a/h=50	
Mode	I	II	I	II	
1	72,174.4	72,191.5	633.417	633.487	
2	194,760	194,881	16,431.1	16,440.9	
3	216,505	216,505	17,320.4	17,320.4	
4	306,209	306,539	28,535.2	28,555.3	
5	337,107	337,196	268,118	271,222	
6	424,602	424,664	353,079	362,248	

17a. [1/2/2/1] lamination scheme.

Frequency parameter $\gamma$					
		a/h=4		a/h=50	
Mode	I	II	I	II	
1	58,248.7	58,354.0	725.219	725.241	
2	192,408	192,436	16,430.2	16,438.8	
3	271,757	271,758	28,535.7	28,555.1	
4	329,584	329,593	159,732	159,865	
5	363,048	364,072	226,218	226,643	
6	406,665	407,771	353,386	363,810	

17b. [2/1/1/2] lamination scheme.

Table 17. Frequency parameters for laminate with dissimilar piezoelectric layers.

Frequency parameter $\gamma$				
		a/h=4		a/h=50
Mode	I	II	I	II
1	57,074.5	57,089.3	618.118	618.120
2	191,301	191,304	15,681.6	15,681.6
3	250,769	250,770	21,492.8	21,493.0
4	274,941	274,941	209,704	209,707
5	362,492	362,522	210,522	210,573
6	381,036	381,049	378,104	378,105

Table 18. Frequency parameters for 5-ply elastic/piezoelectric laminate.

Frequency parameter $\gamma$			
Mode	Variable w	Linear w	Exact
1	100,293.4	104145.2	96,929.9
2	194,255	194,255	194,255
3	328,560	328,560	327,663
4	587,312	587,312	508,625
5	673,851	706,727	522,320
6	1,125,404	1,125,404	988,021

Table 19. Comparison of frequencies for variable w, linear w, and exact, single layer PZT-4.

## 8. SUMMARY AND FUTURE WORK

### Developed Algorithms

The following algorithms have been developed as part of this research to aid in the simulation of active tip clearance control using adaptive composites:

- Semi-analytic solutions using variable, constant, and independent approximations for out-of-plane transverse displacements for laminated piezoelectric plates.
- Finite element approximations using constant and variable variations. Implementation of independent-w theory is straightforward. Both static and dynamic problems can be modeled.
- Exact solutions of simply-supported laminated piezoelectric plates: static and dynamic behavior.
- Discrete-layer shell elements for arbitrary geometry.

Deliverables to NASA-Lewis are the source code for the plate and beam elements, and have been delivered to NASA via internet. All other source codes for the semi-analytic and exact solutions is also available.

### Summary of Results

Inspection of the results included here and as part of this study, the primary thrusts of the working algorithms are:

- Excellent accuracy for variable-w theory and promising results for the independent-w theory.
- As currently formulated, the constant-w theory is not suitable for coupled problems in electroelasticity because of the inability to model transverse normal strain. For elastic problems, however, this methodology yields very acceptable results.
- Exact solutions developed will provide extremely useful benchmarks for the enclosed theories and those developed by others.

- Flat-plate results for plate element are good and encouraging. The application to an assemblage of flat plates to approximate a curved surface has not been made, but can be with the inclusion of developed transformation matrices.
- Elements developed here can be incorporated into general purpose finite element code to simulate the control process for a wide array of problems.
- Results of shell element are promising, but this application has not been extensively tested because of lack of comparative solutions available in literature and elsewhere.

### Future Work

The potential applications of the elements developed here are numerous. Before this occurs, additional testing of both the plate and shell elements would be prudent and is necessary for the shell element. What follows are suggestions for future work by the present investigators or others:

- Complete implementation and testing of plate element with independent-w theory.
- Use of rotated plate elements as collection of flat plates to model curved shell.
- Development of exact solution for laminated piezoelectric cylindrical shell for purposes of benchmarking general shell element.
- Further testing of shell element and comparison of each discrete-layer theory.
- Application to active tip clearance control and other problems requiring adaptive composite laminates.

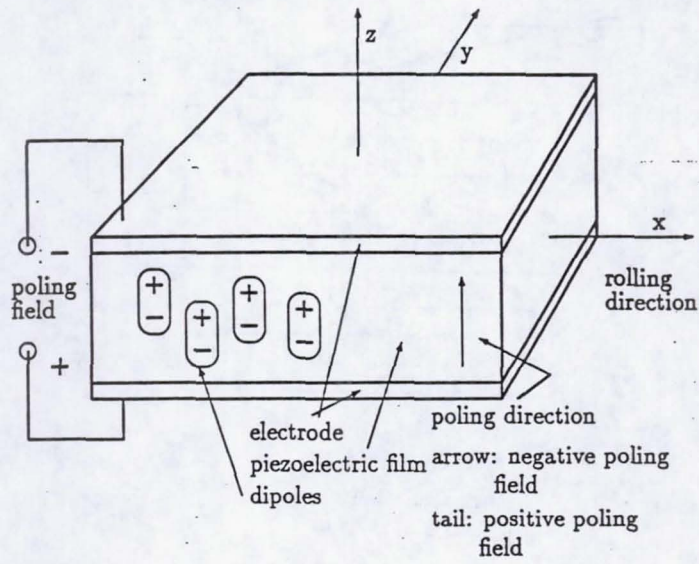


Figure 1: Coordinate axes for typical piezoelectric layer.

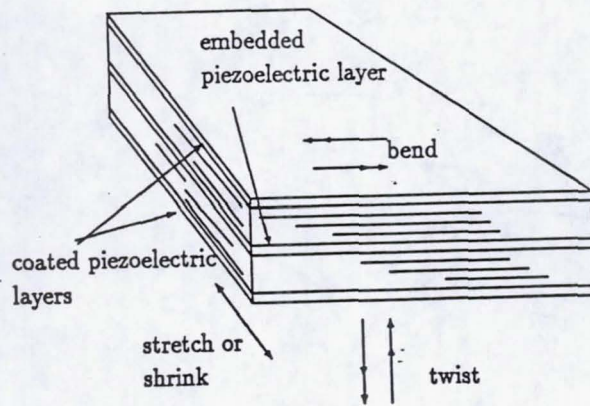


Figure 2: Laminated piezoelectric plate and possible deformation.



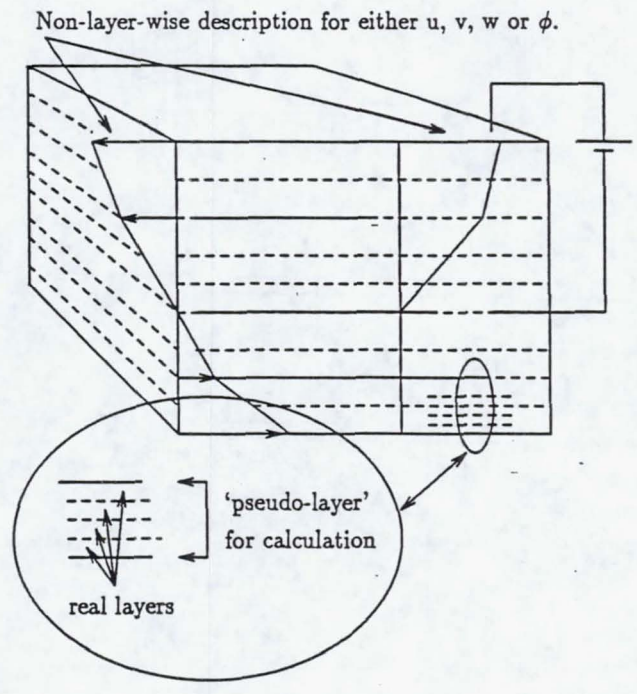


Figure 3: Description of pseudo-layer within laminate geometry.

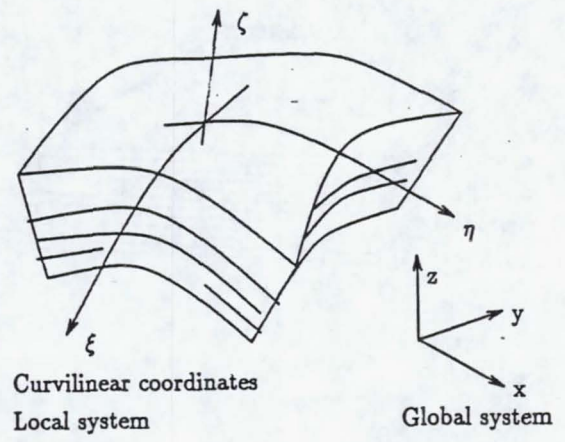


Figure 4: Curvilinear coordinates in a general shell.

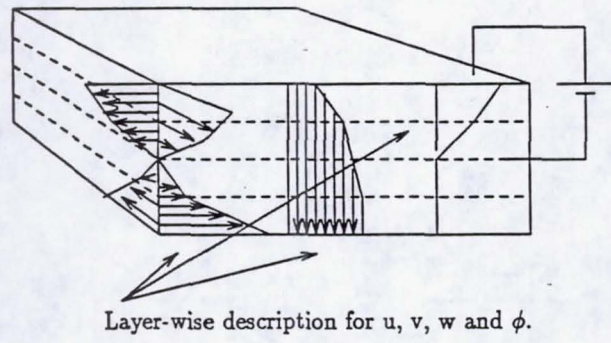
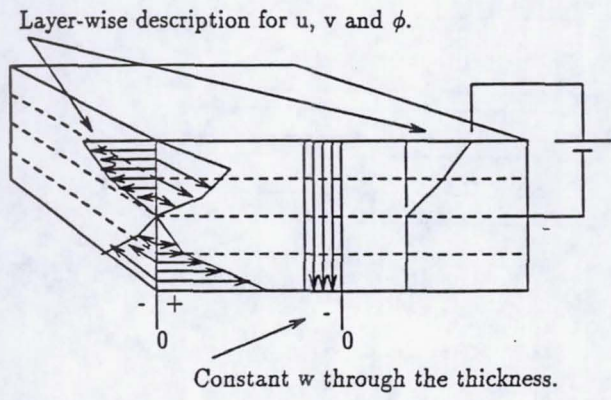


Figure 5: Through-thickness approximations for discrete-layer theories.

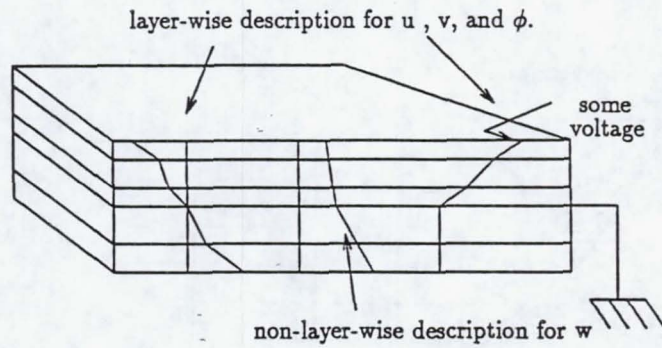


Figure 6: Assumed form for independent-w approximation.

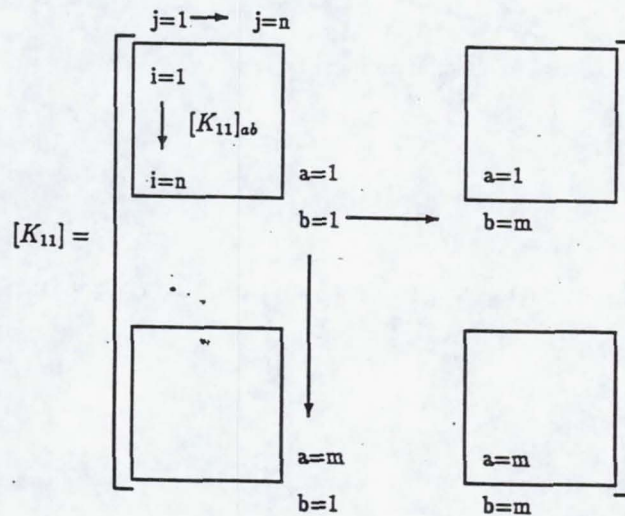


Figure 7: Structure of sub-matrices.

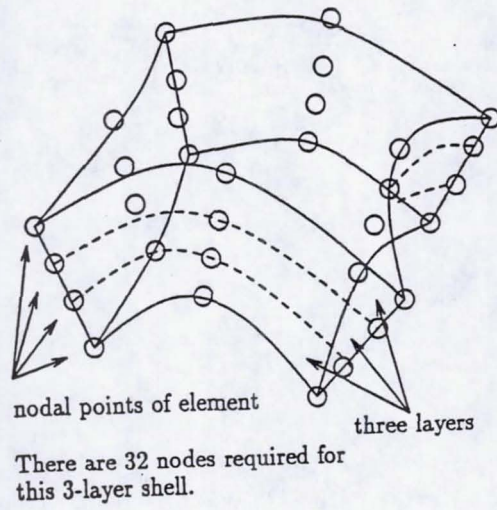


Figure 8: Discrete-layer element for general shells.

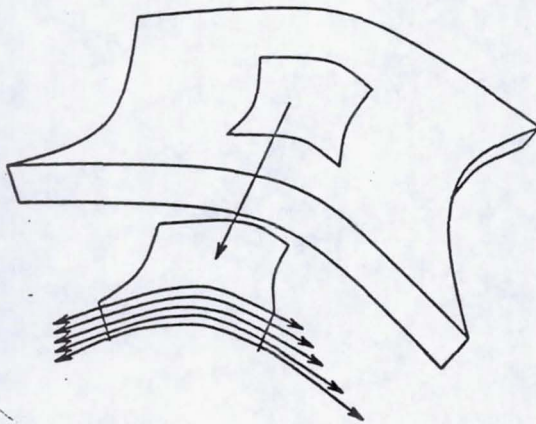


Figure 9: Continuity requirements at through-thickness locations.

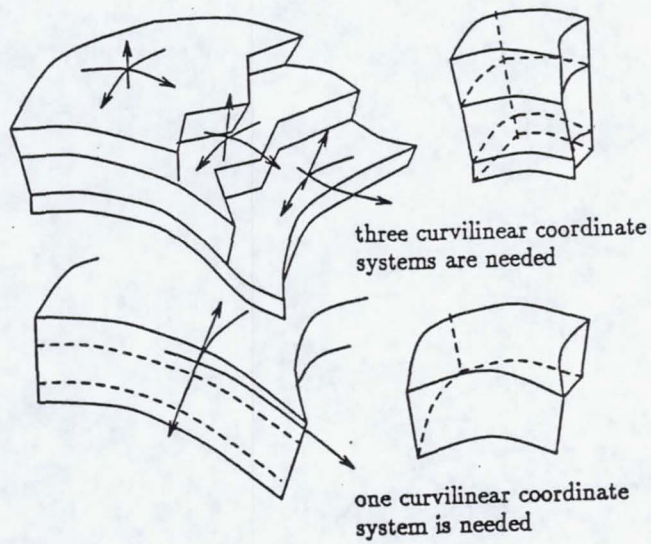


Figure 10: Shell element with different layers/coordinate systems.

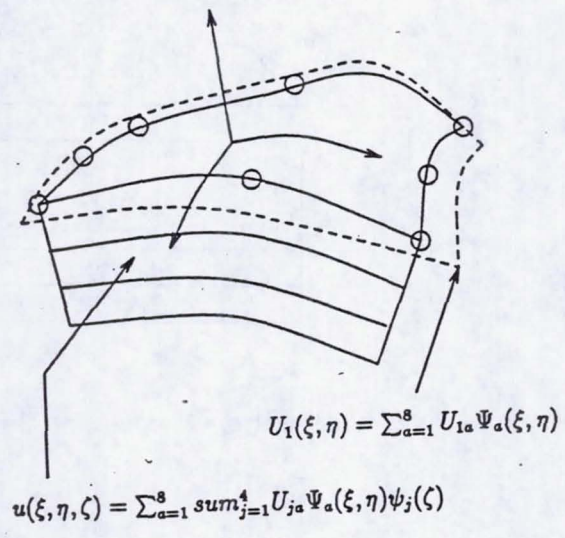
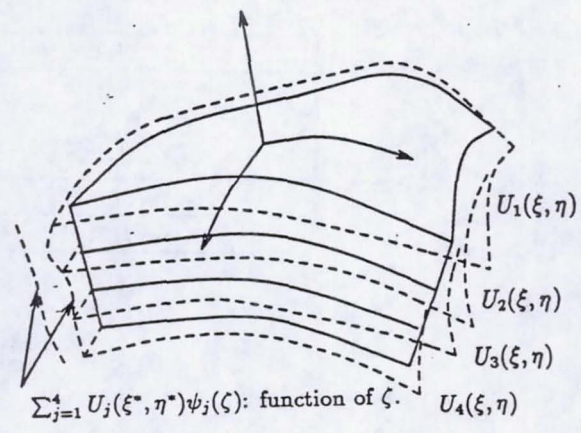


Figure 11: Form of approximations for general shell element.

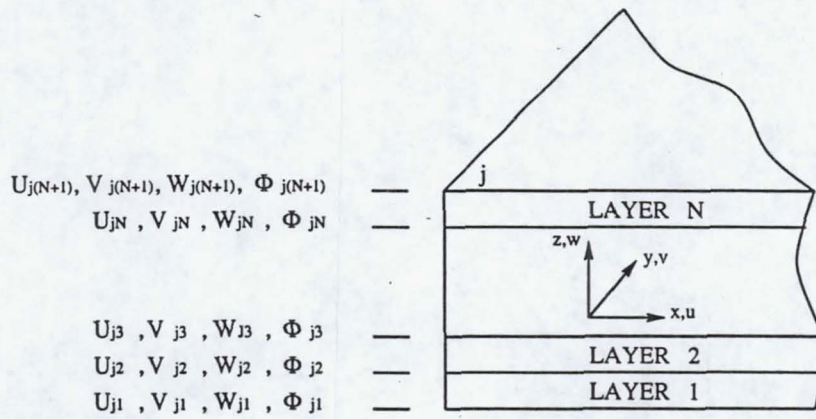


Figure 12: Geometry and layer numbering.  
 $W$  varying linearly through thickness

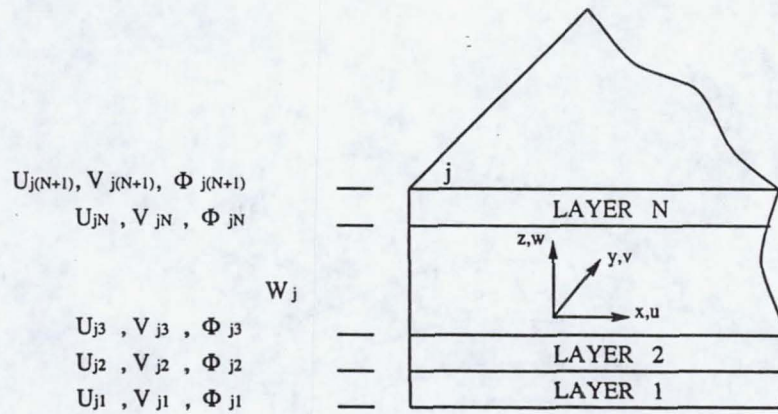


Figure 13: Geometry and layer numbering.  $W$  constant through thickness

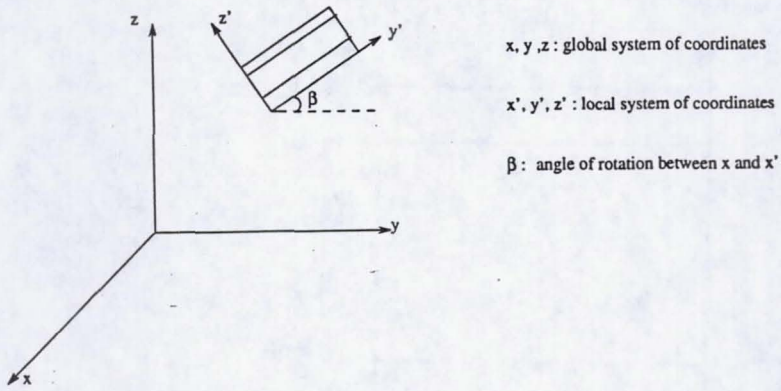


Figure 14: local and global coordinates.

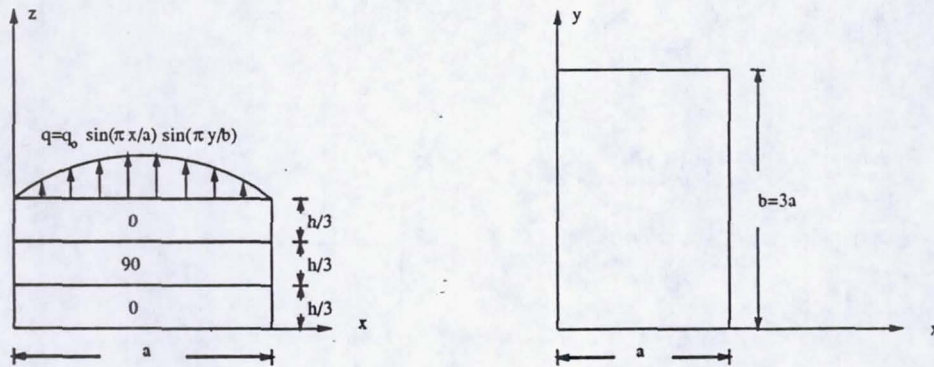


Figure 15: Geometry of Rectangular Plate



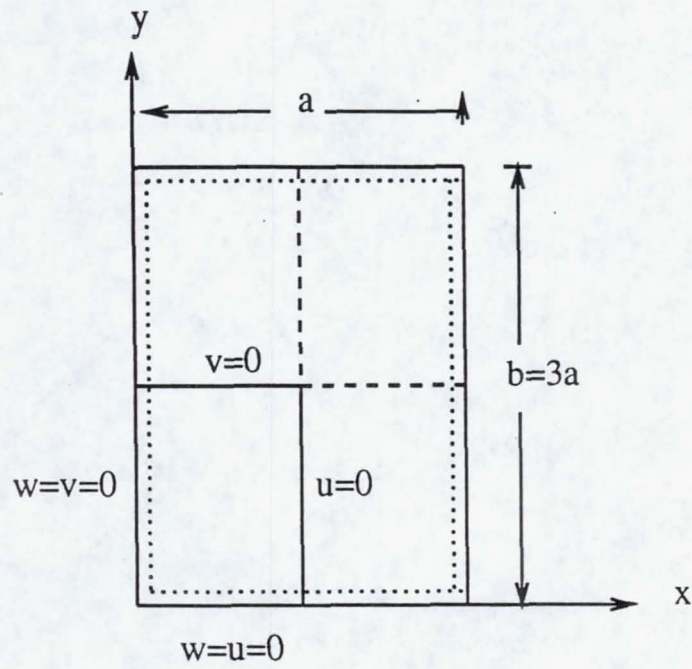


Figure 16: Boundary Conditions for the Quarter Plate

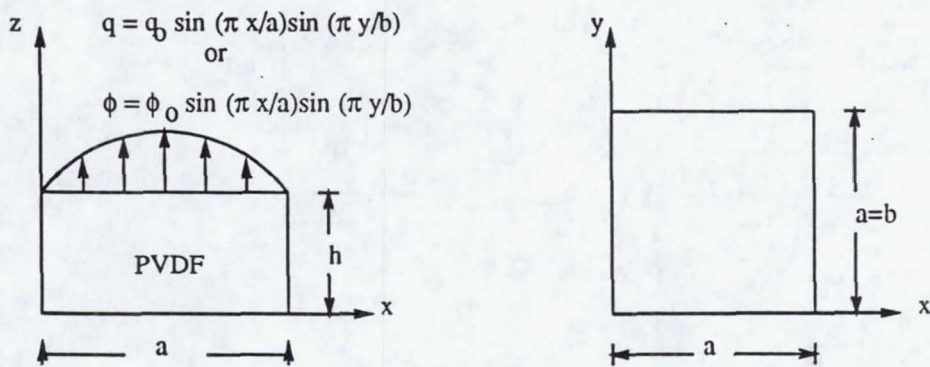


Figure 17: Geometry of PVDF Square Plate

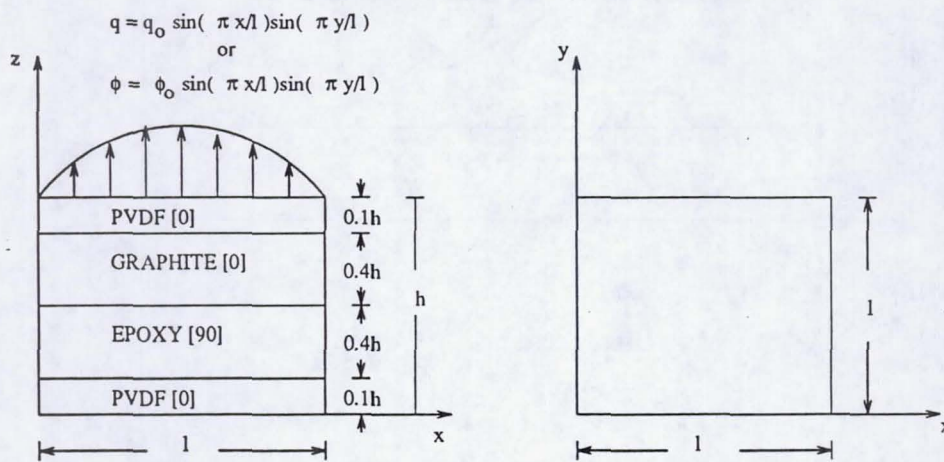


Figure 18: Geometry of PVDF/GRAPHITE/EPOXY/PVDF Square Plate

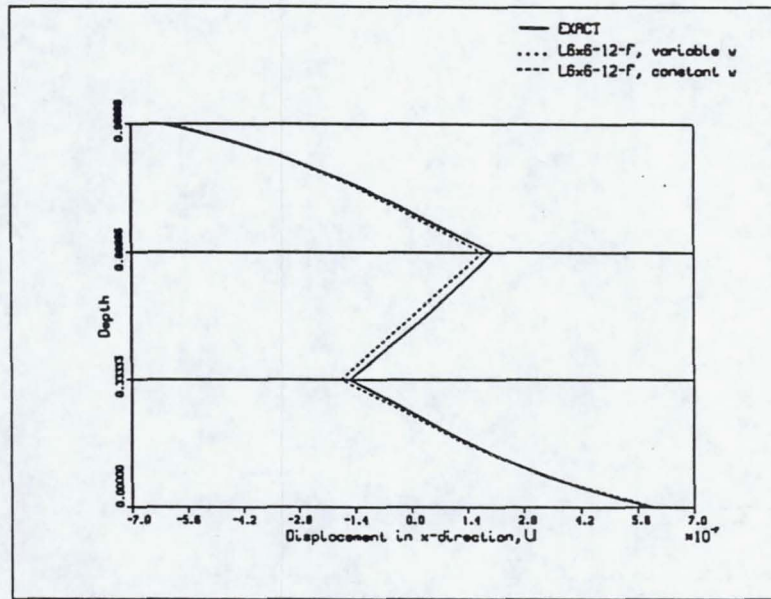


Figure 19: Displacement in x-direction

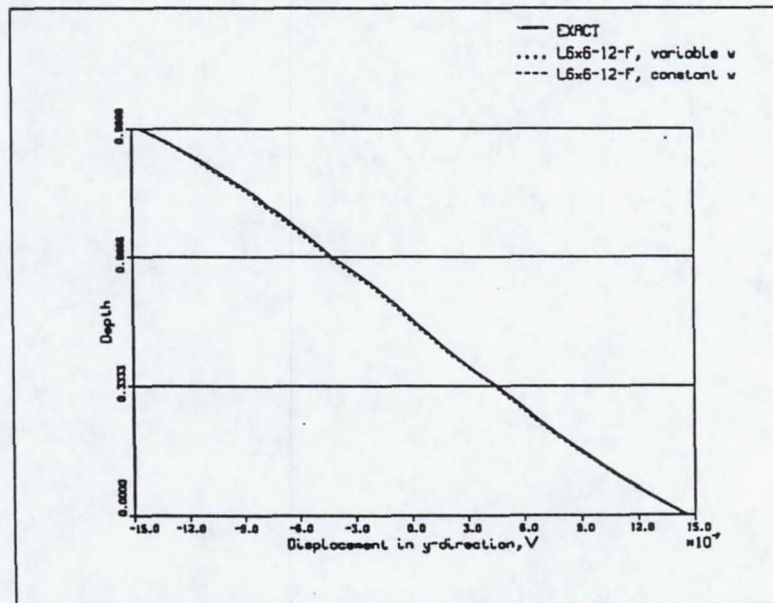


Figure 20: Displacement in y-direction

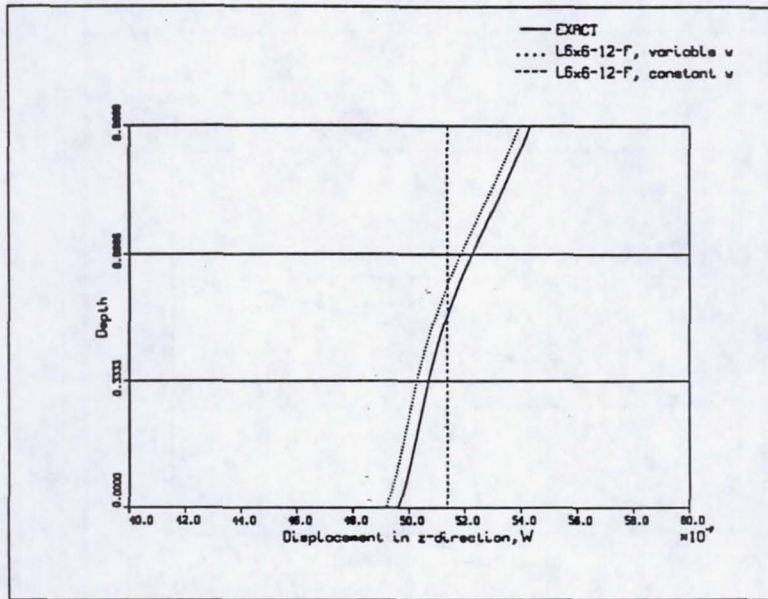


Figure 21: Displacement in z-direction

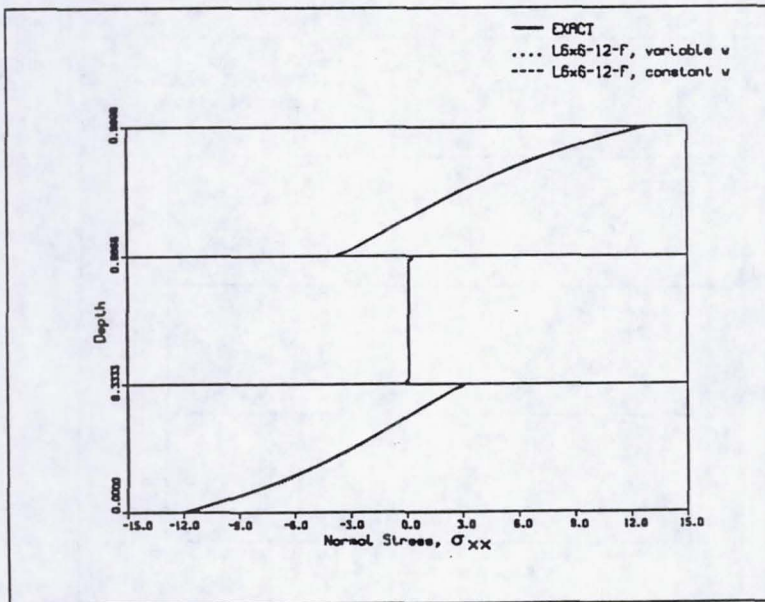


Figure 22: Normal Stress Distribution on x-direction

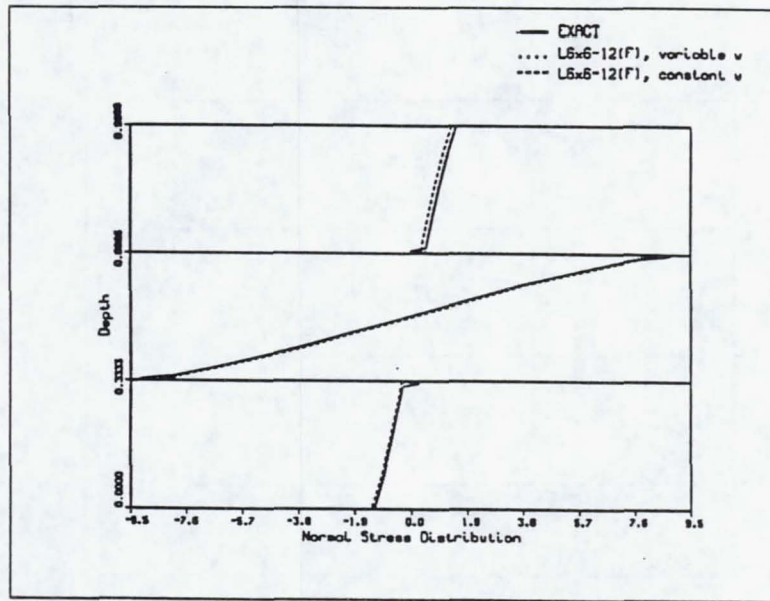


Figure 23: Normal Stress Distribution on y-direction

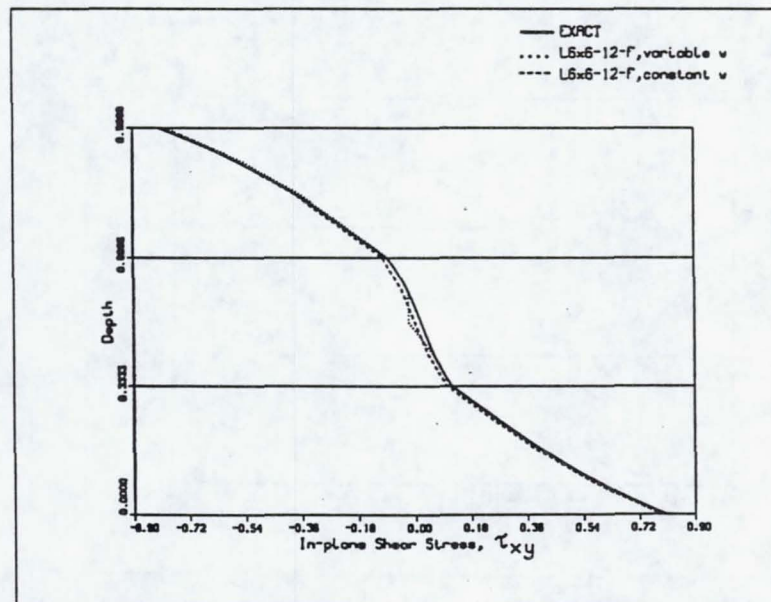


Figure 24: In-Plane Stress Distribution

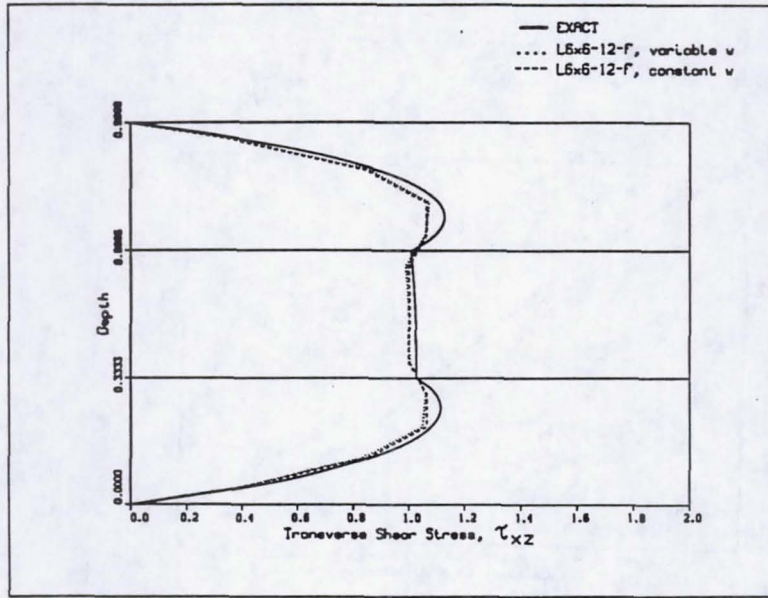


Figure 25: Out-plane Stress Distribution

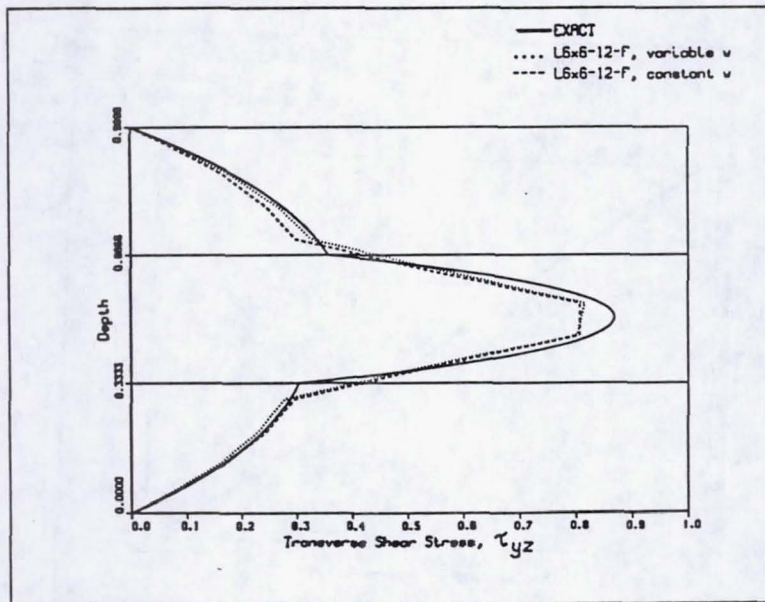


Figure 26: Out-plane Stress Distribution

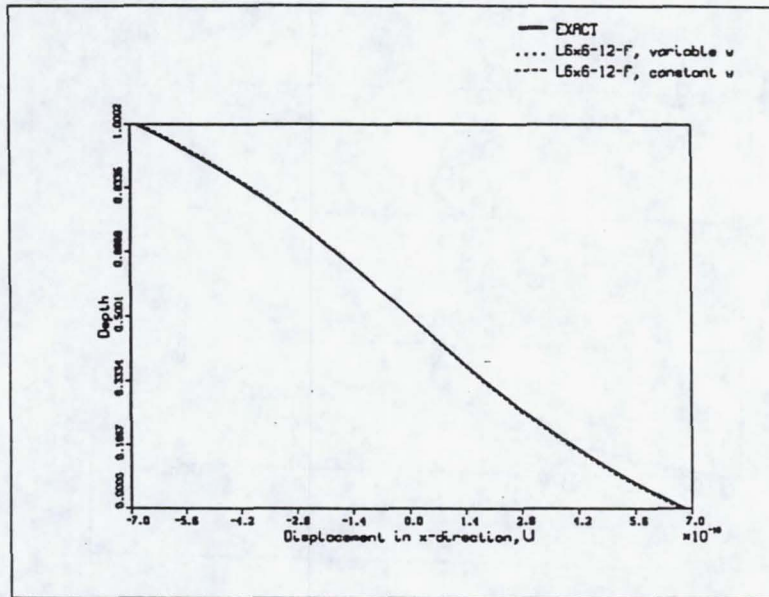


Figure 27: Displacement in x-direction, applied load,  $a/h = 10$ , PVDF

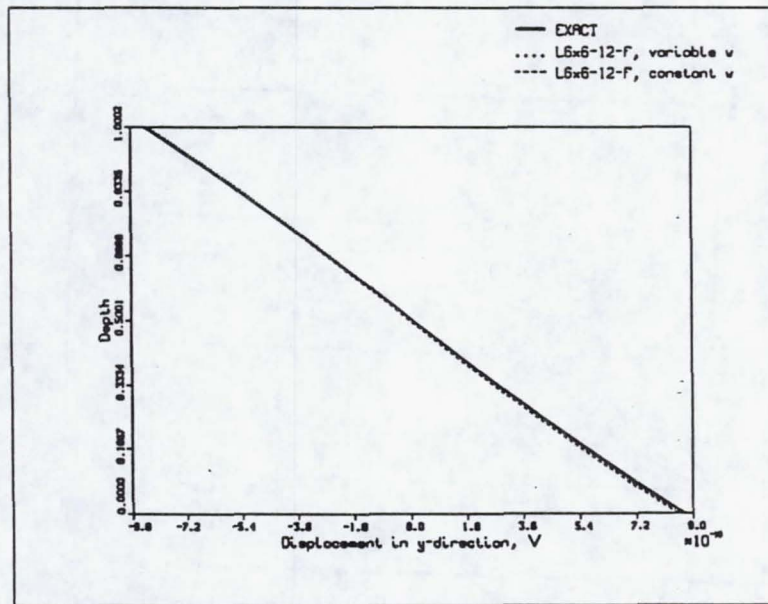


Figure 28: Displacement in y-direction with applied load,  $a/h = 10$ , PVDF

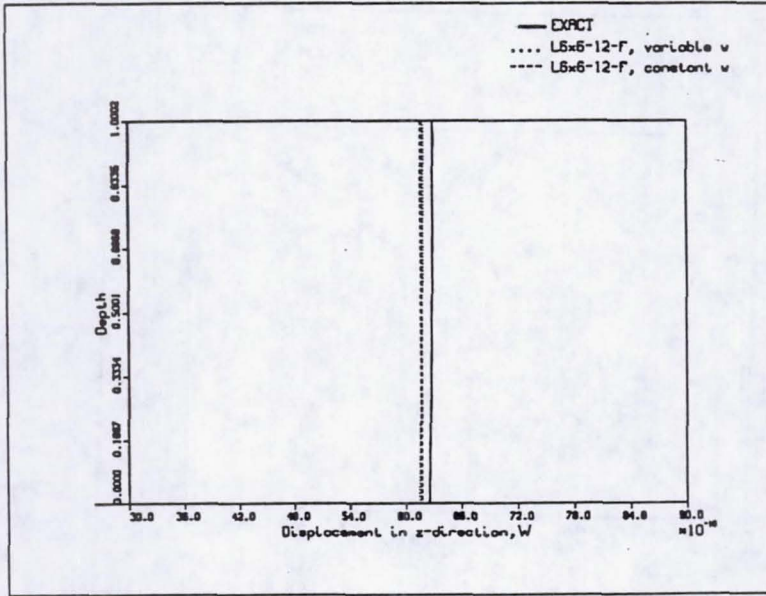


Figure 29: Displacement in z-direction, applied load,  $a/h = 10$ , PVDF

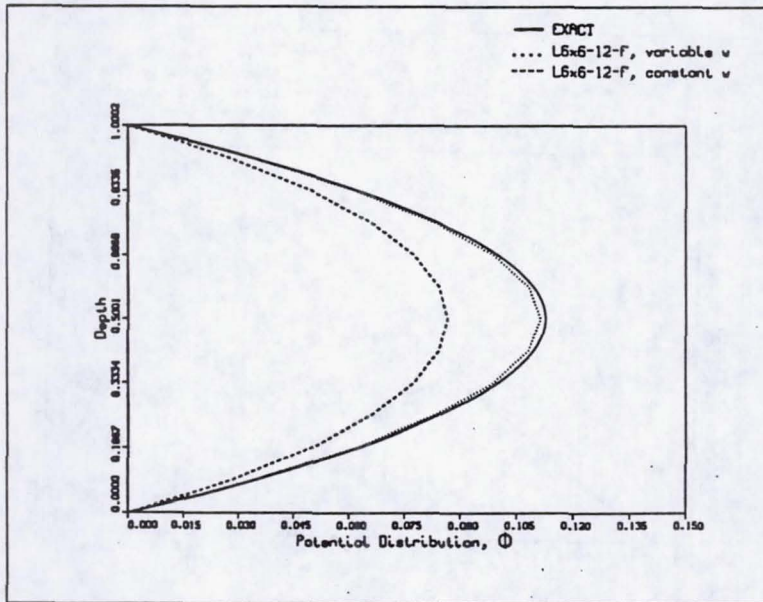


Figure 30: Potential Distribution, applied load,  $a/h = 10$ , PVDF



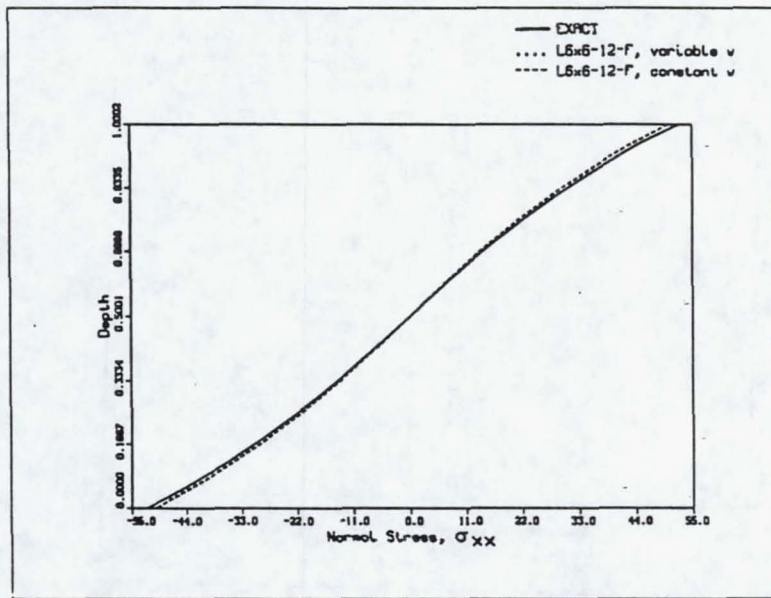


Figure 31: Normal stress distribution on x-direction, applied load  $a/h = 10$ , PVDF

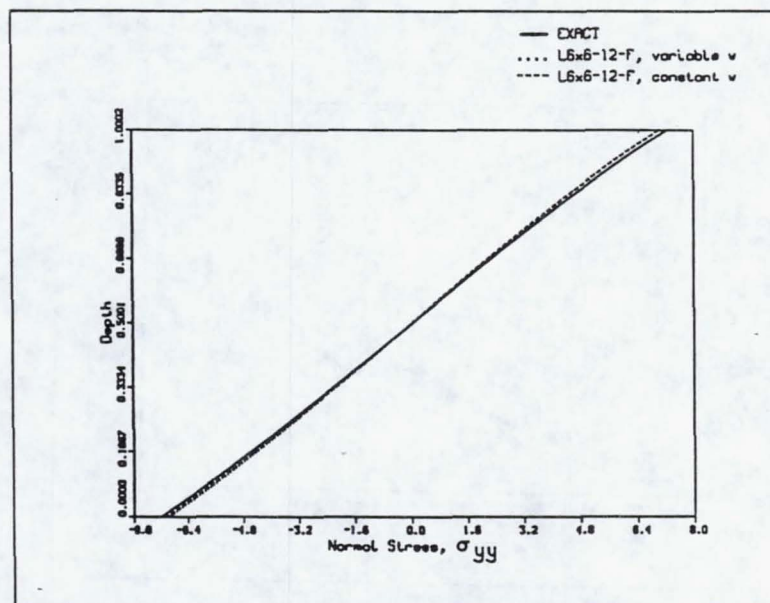


Figure 32: Normal stress distribution on y-direction, applied load  $a/h = 10$ , PVDF

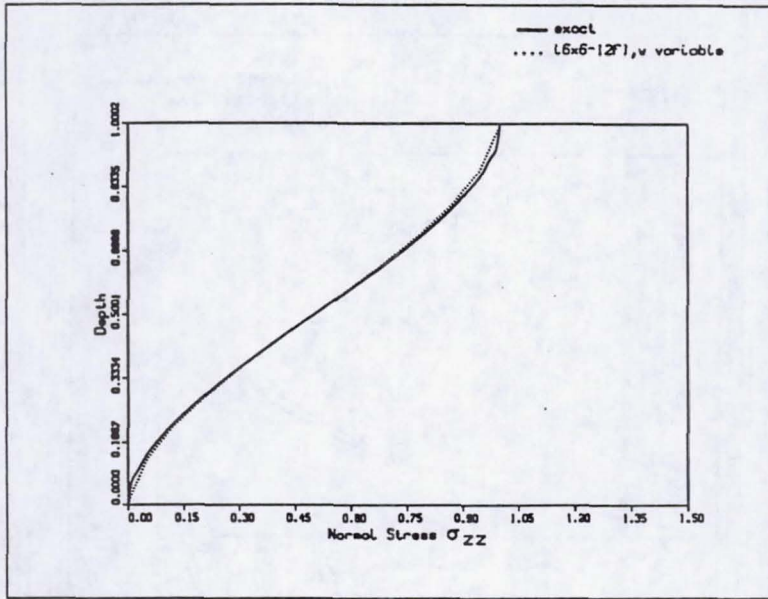


Figure 33: Normal stress distribution on z-direction, applied load,  $a/h = 10$ , PVDF

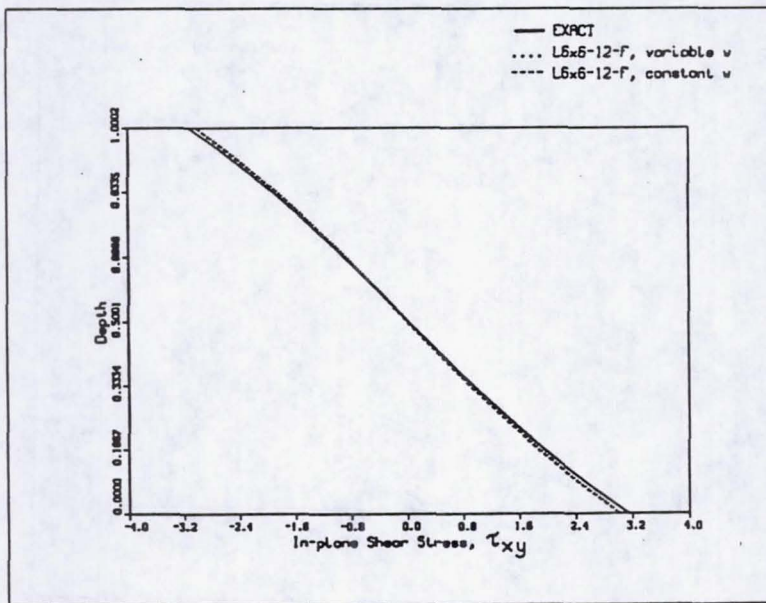


Figure 34: In-plane stress distribution, applied load,  $a/h = 10$ . PVDF

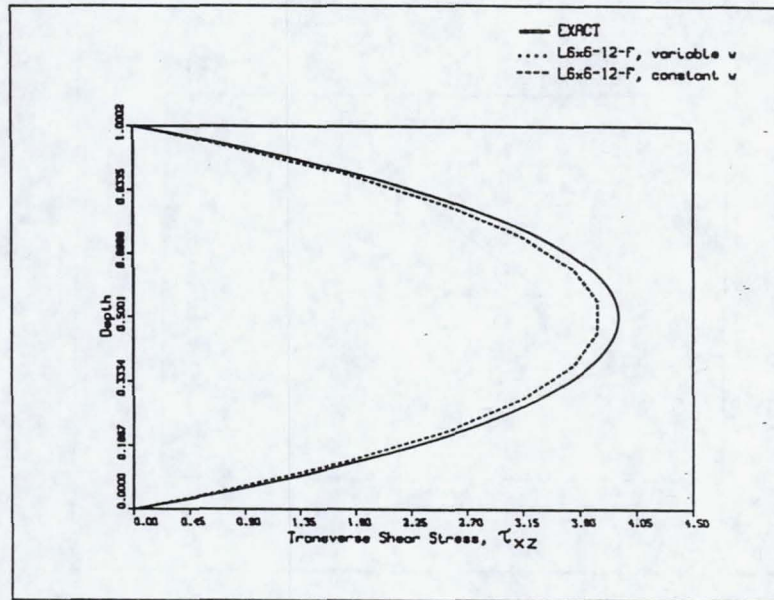


Figure 35: Out-plane stress distribution, applied load,  $a/h = 10$ , PVDF

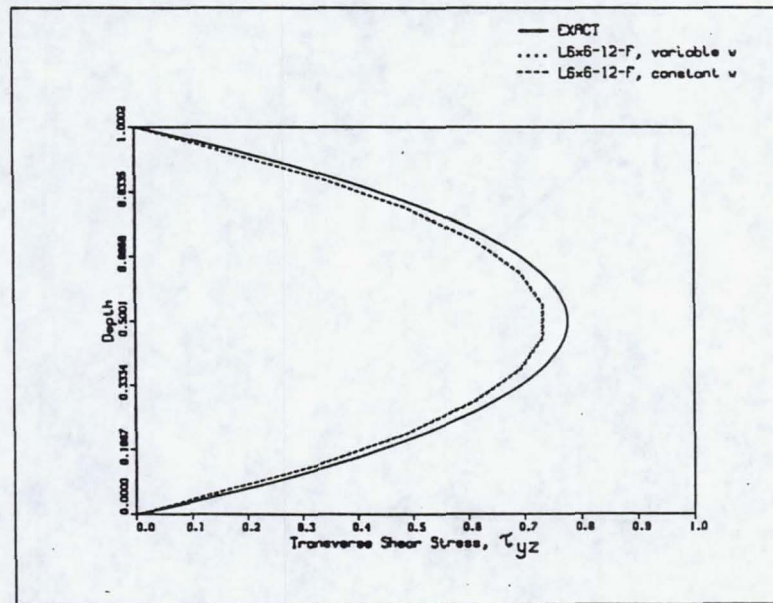


Figure 36: Out-plane stress distribution, applied load,  $a/h = 10$ , PVDF

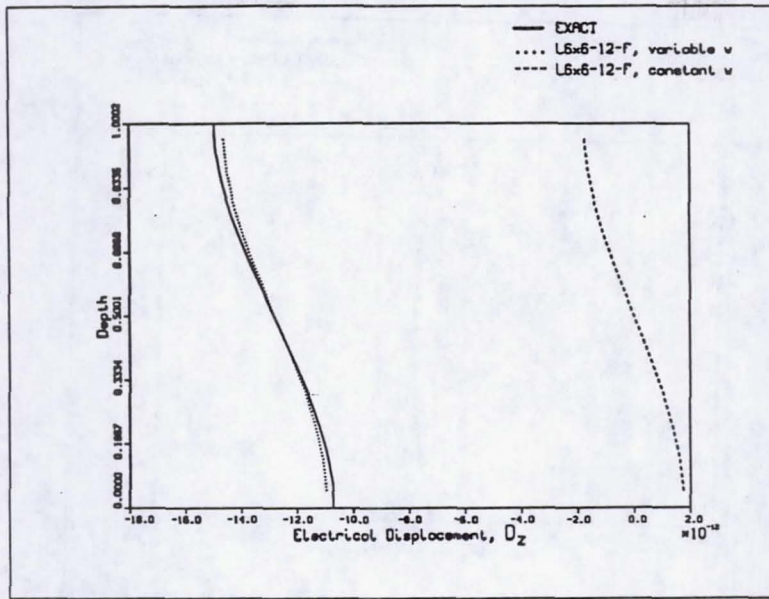


Figure 37: Electric displacement distribution, applied load,  $a/h = 10$ , PVDF

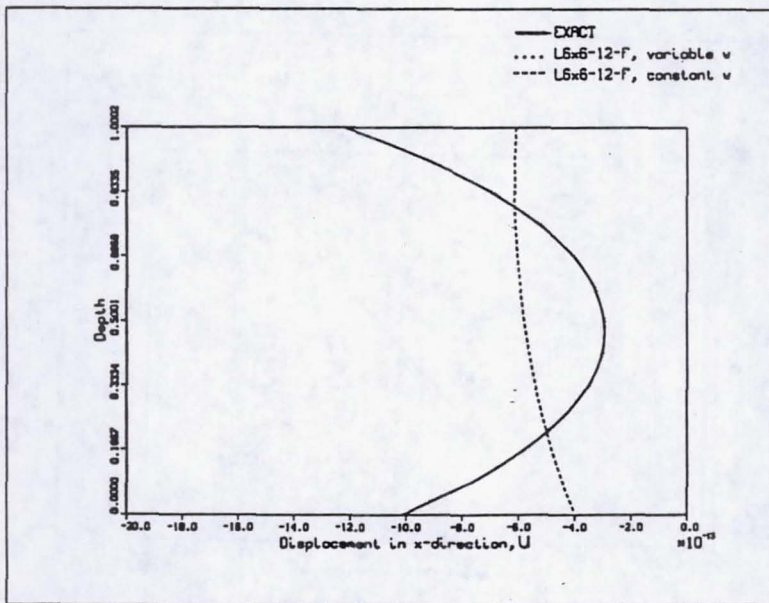


Figure 38: Displacement in x-direction, applied potential,  $a/h = 10$ , PVDF

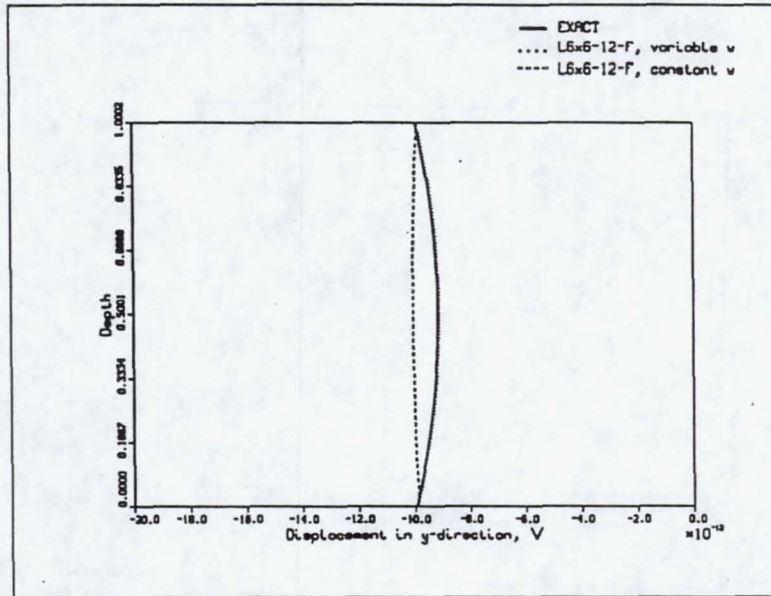


Figure 39: Displacement in y-direction, applied potential,  $a/h = 10$ , PVDF

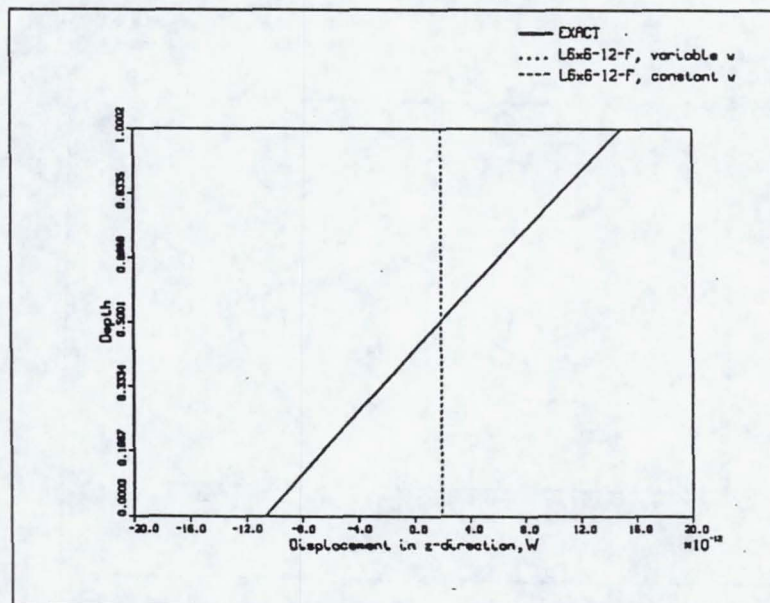


Figure 40: Displacement in z-direction, applied potential,  $a/h = 10$ , PVDF

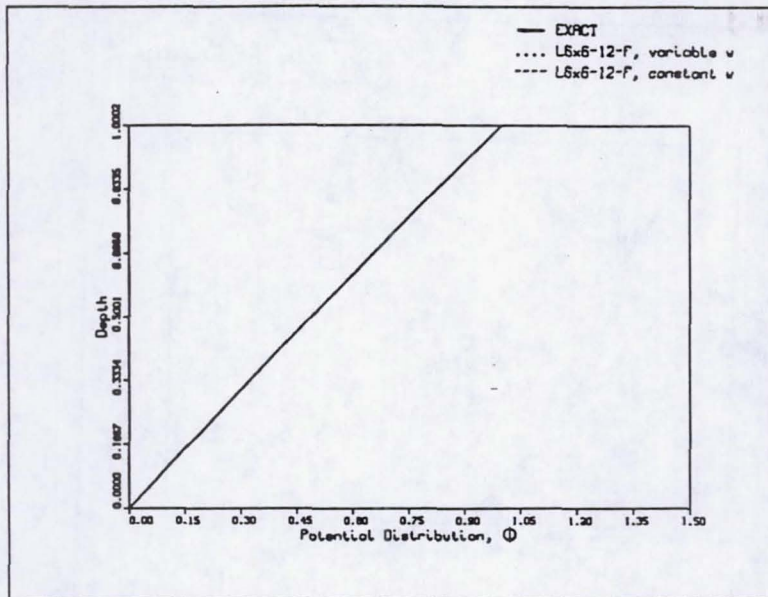


Figure 41: Potential distribution, applied potential,  $a/h = 10$ , PVDF

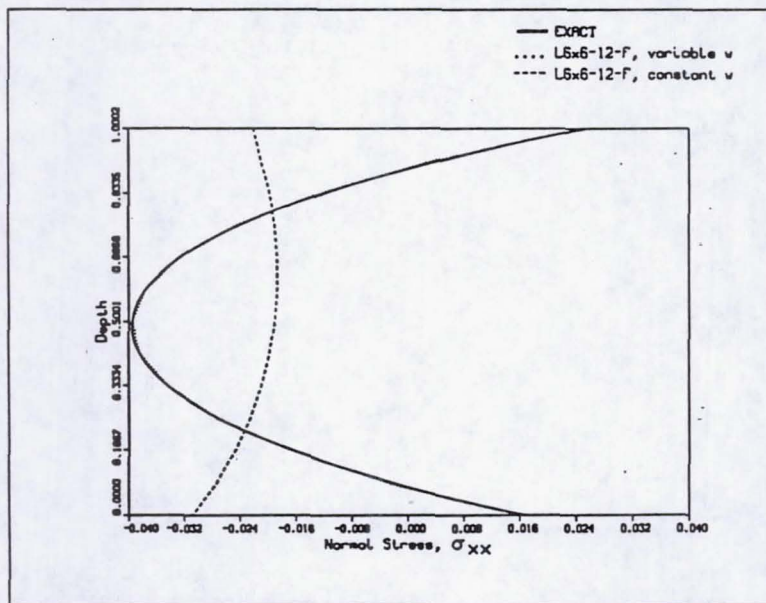


Figure 42: Normal stress distribution on x-direction, applied potential  $a/h = 10$ , PVDF

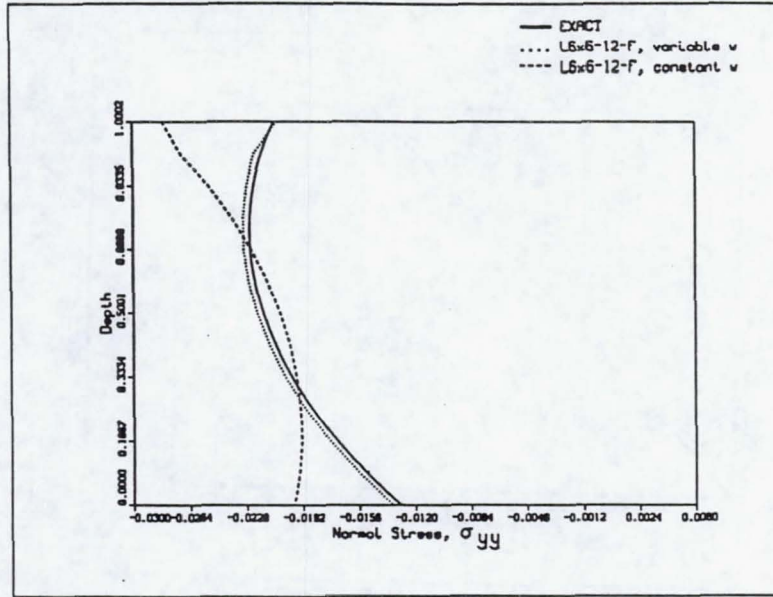


Figure 43: Normal stress distribution on y-direction, applied potential  $a/h = 10$ , PVDF

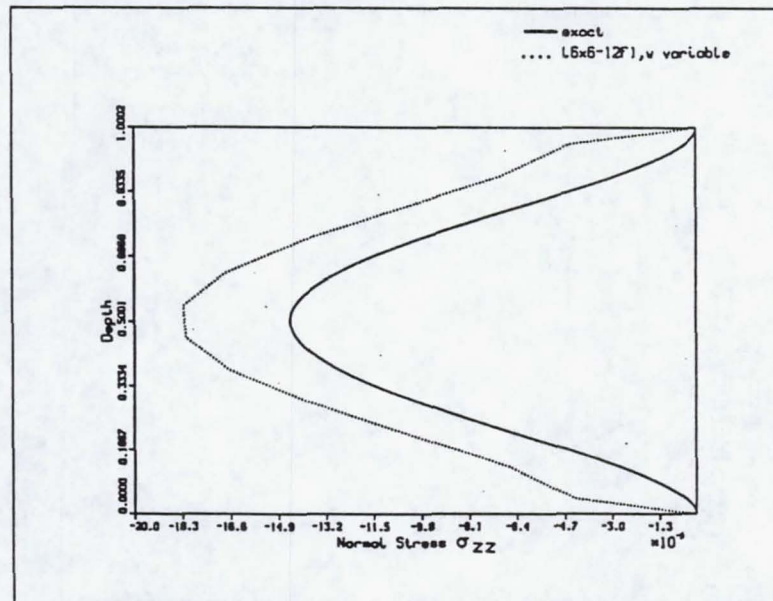


Figure 44: Normal stress distribution on z-direction, applied potential  $a/h = 10$ , PVDF

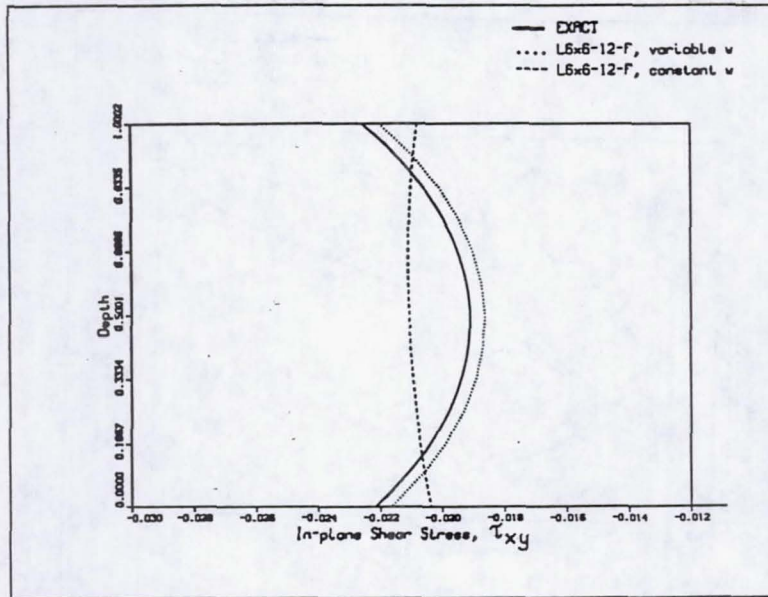


Figure 45: In-plane stress distribution, applied potential,  $a/h = 10$ , PVDF

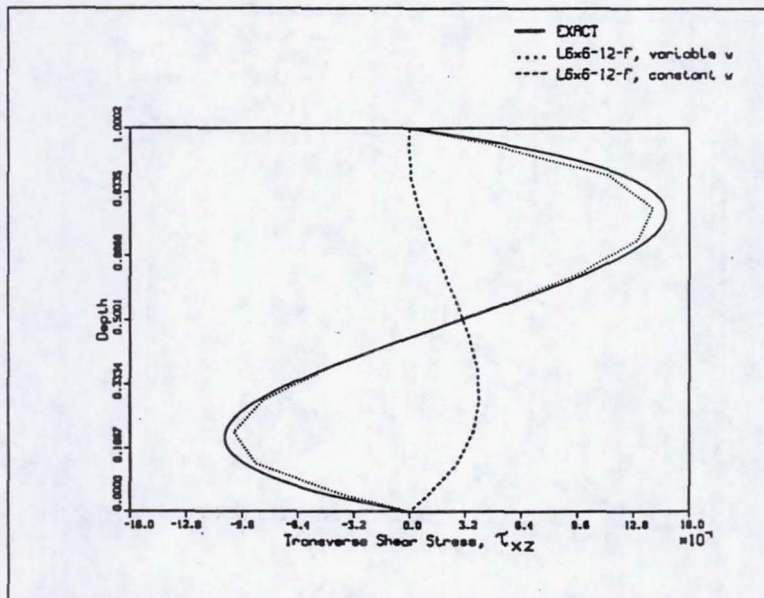


Figure 46: Out-plane stress distribution, applied potential,  $a/h = 10$ , PVDF



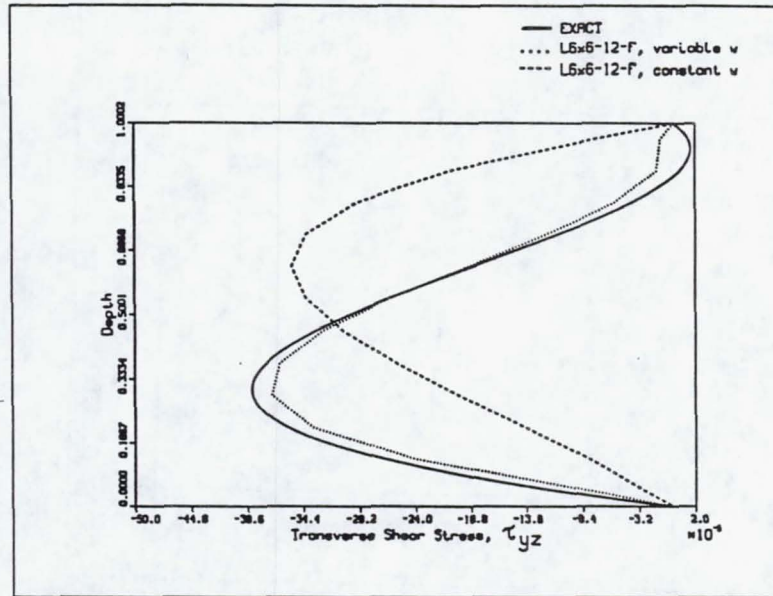


Figure 47: Out-plane stress distribution, applied potential,  $a/h = 10$ , PVDF

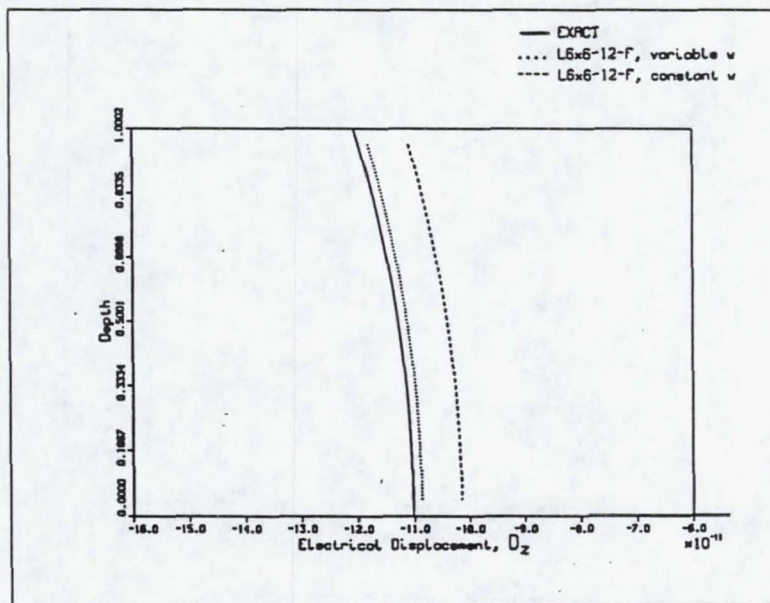


Figure 48: Electric displacement distribution, applied potential,  $a/h = 10$ , PVDF

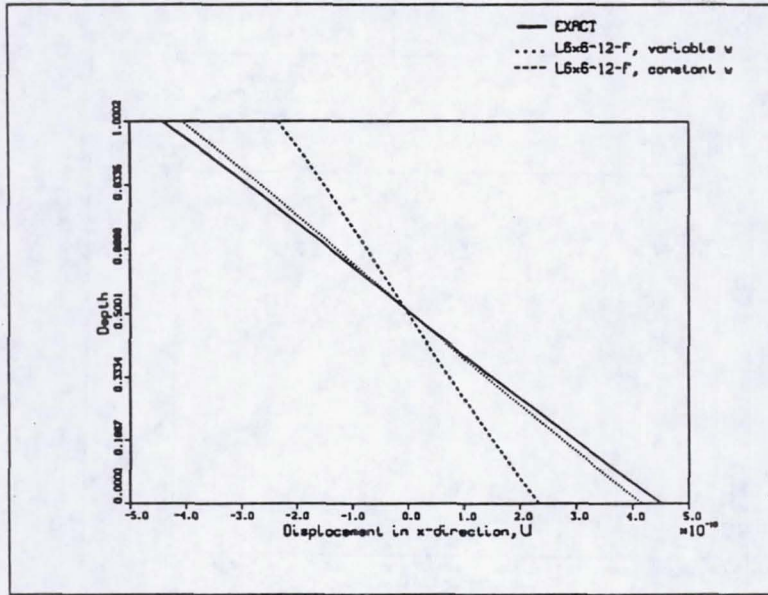


Figure 49: Displacement in x-direction, applied load,  $a/h = 10$ , PZT4

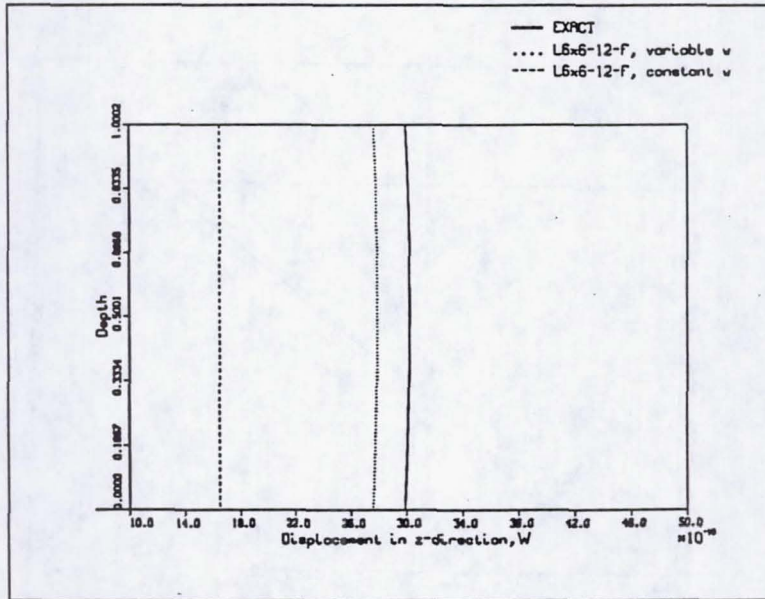


Figure 50: Displacement in z-direction, applied load,  $a/h = 10$ , PZT4

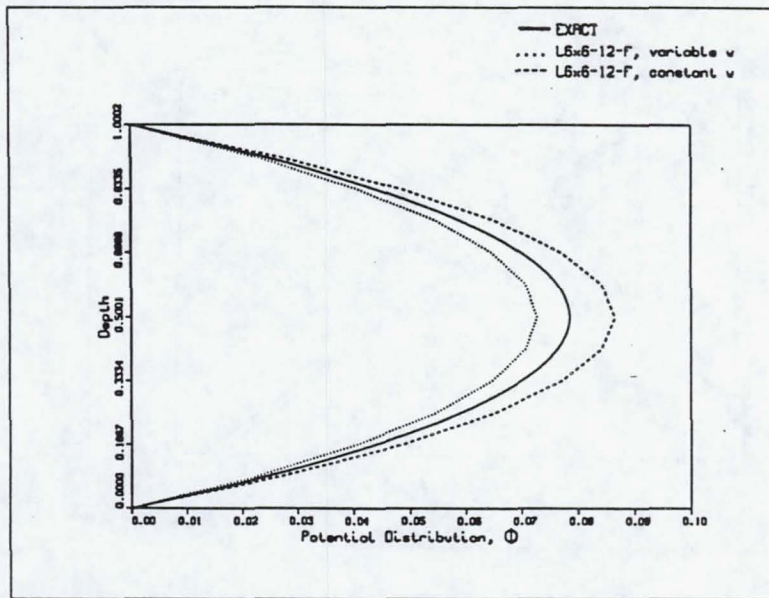


Figure 51: Potential distribution, applied load,  $a/h = 10, P/ZT^4$

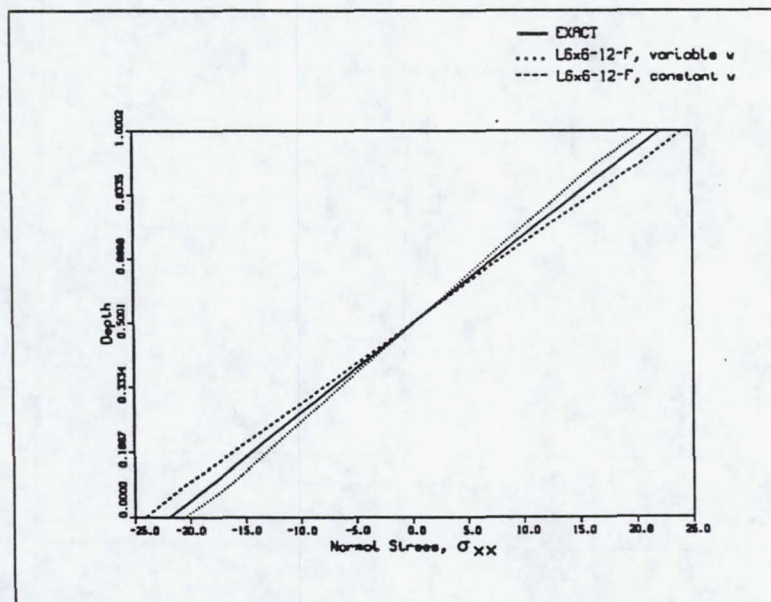


Figure 52: Normal stress distribution on x-direction, applied load,  $a/h = 10, P/ZT^4$

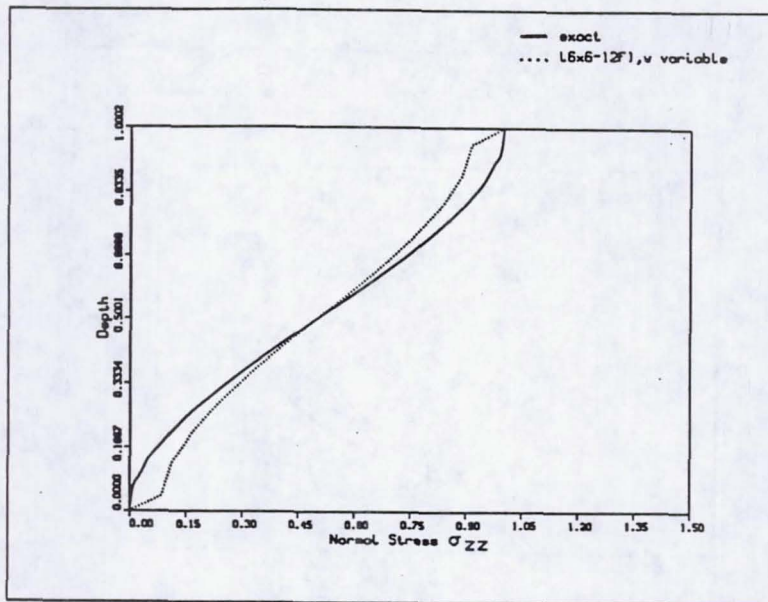


Figure 53: Normal stress distribution on z-direction, applied load  $a/h = 10$ , PZT4

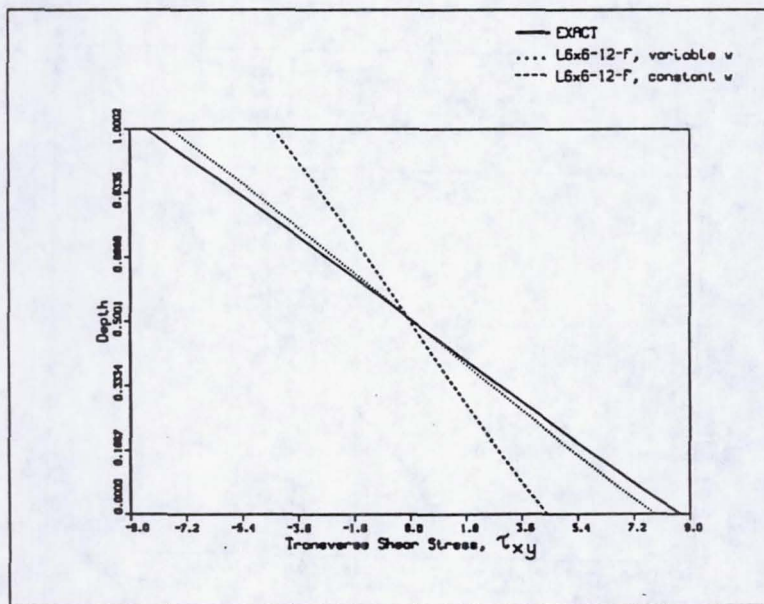


Figure 54: In-plane stress distribution, applied load  $a/h = 10$ , PZT4

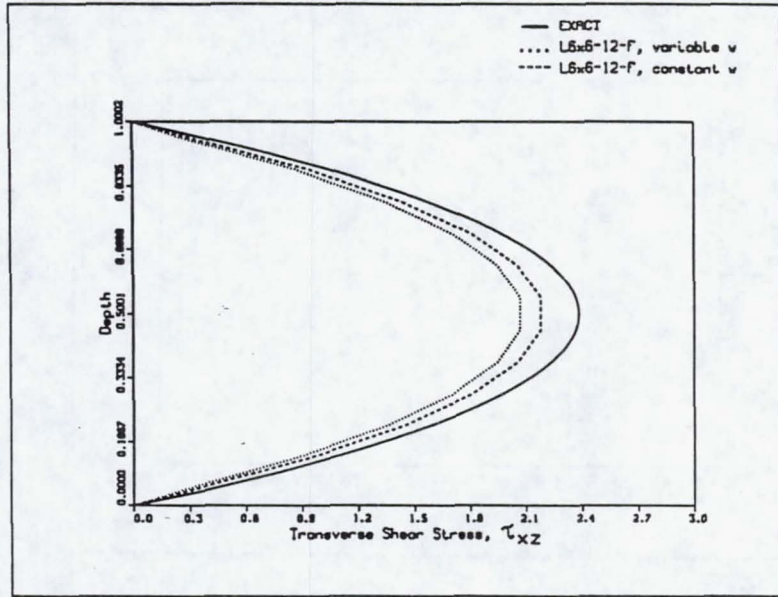


Figure 55: Out-plane stress distribution, applied load,  $a/h = 10$ , PZT4

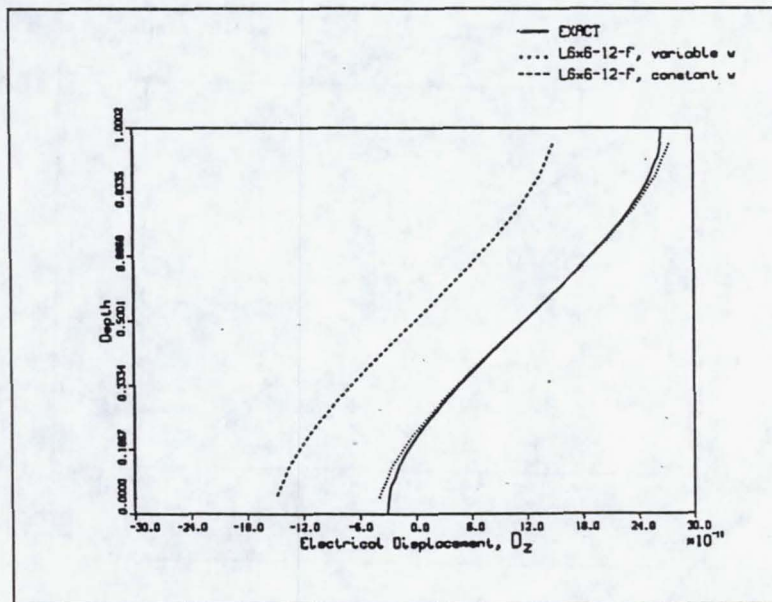


Figure 56: Electric displacement distribution, applied load,  $a/h = 10$ , PZT4

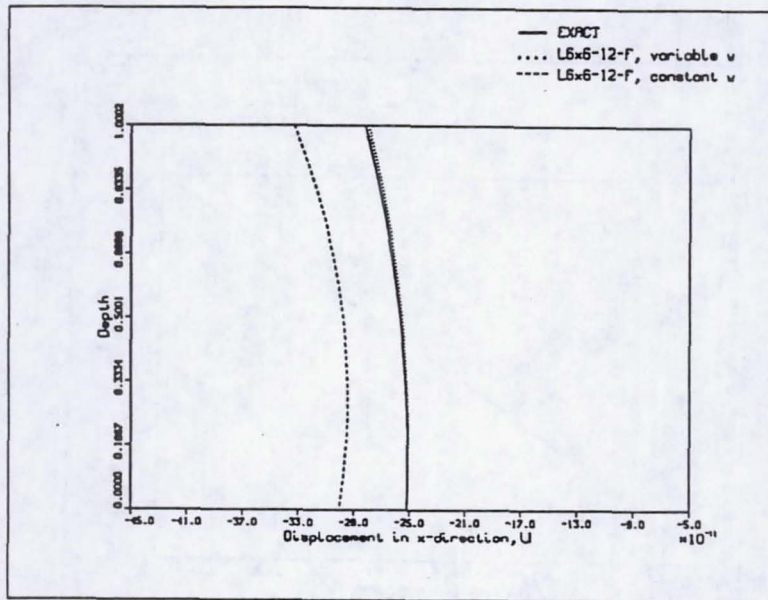


Figure 57: Displacement in x-direction, applied potential,  $a/h = 10$ , PZT4

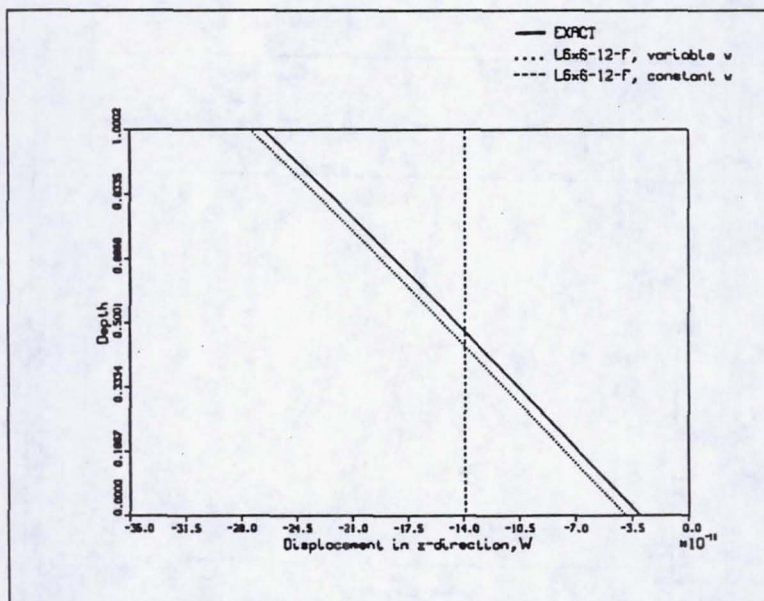


Figure 58: Displacement in z-direction, applied potential,  $a/h = 10$ , PZT4

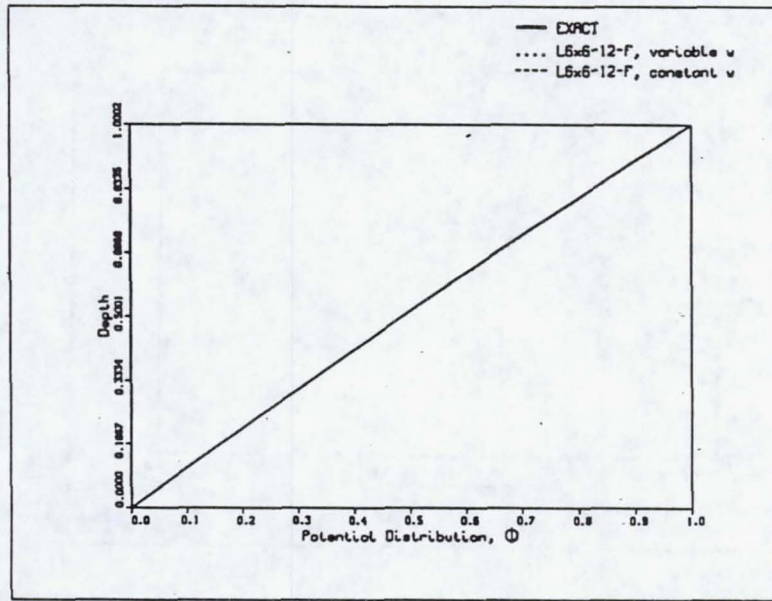


Figure 59: Potential distribution, applied potential,  $a/h = 10$ , PZT4

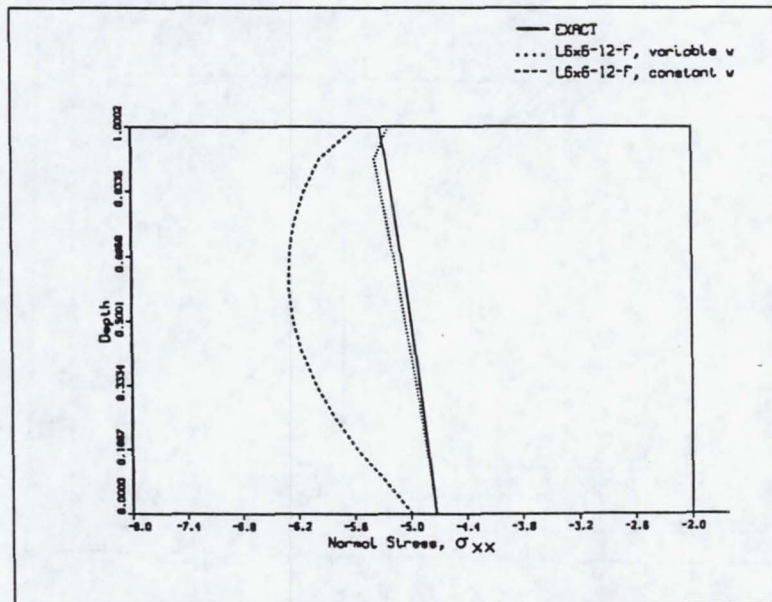


Figure 60: Normal stress distribution on x-direction, applied potential  $a/h = 10$ , PZT4

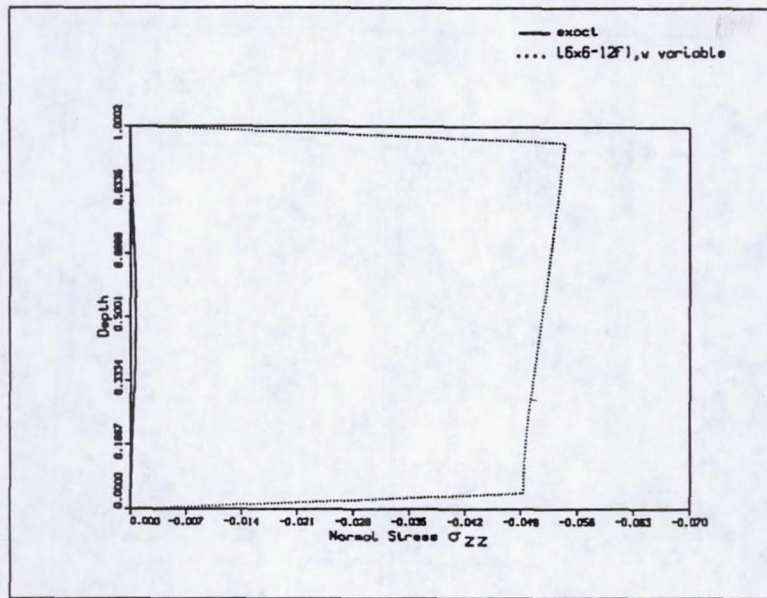


Figure 61: Normal stress distribution on z-direction, applied potential  $a/h = 10, PZT4$

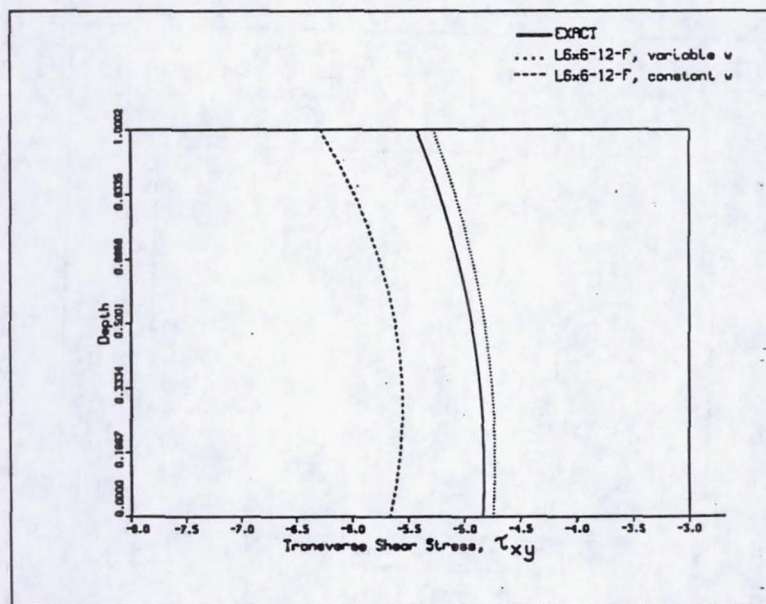


Figure 62: In-plane stress distribution, applied potential,  $a/h = 10, PZT4$



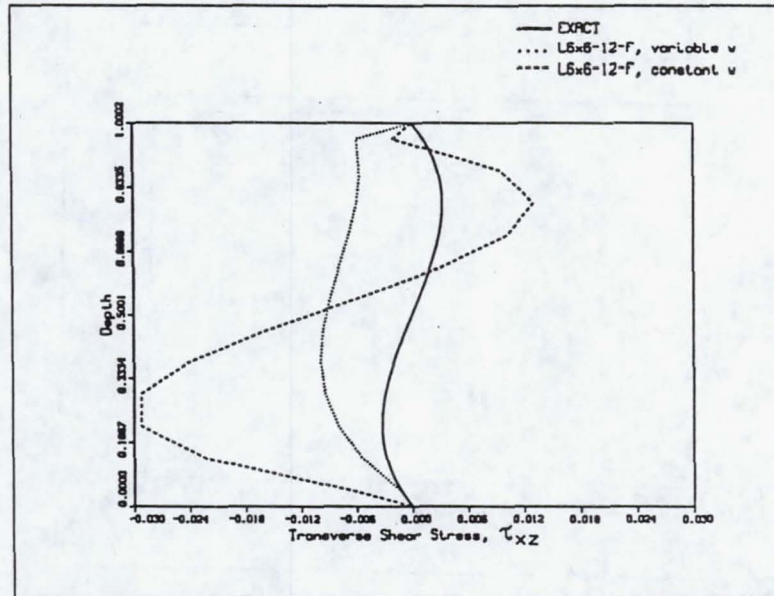


Figure 63: Out-plane stress distribution, applied potential,  $a/h = 10$ , PZT4

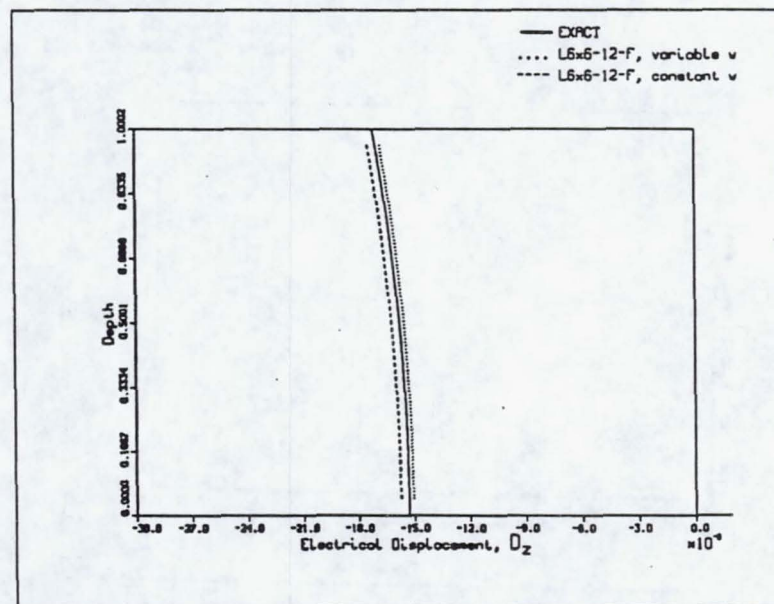


Figure 64: Electric displacement distribution, applied potential,  $a/h = 10$ , PZT4

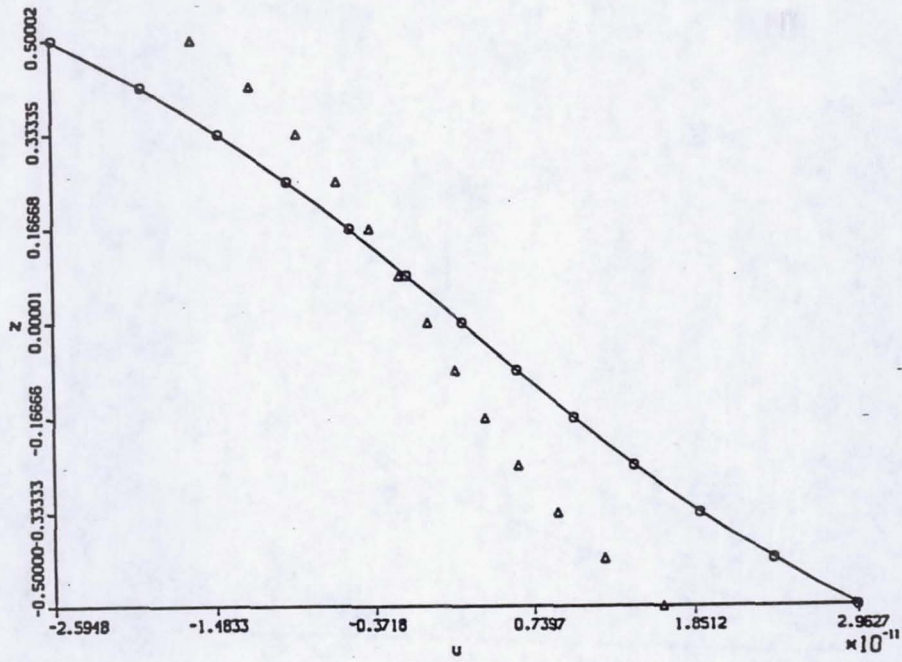


Figure 65: u-displacement for single layer PZT-4 (load).

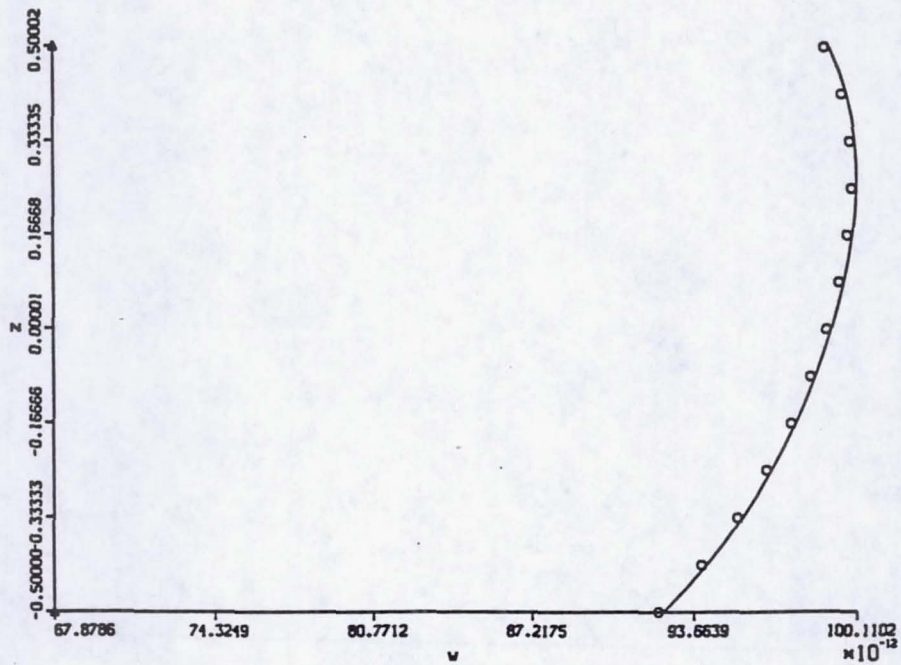


Figure 66: w-displacement for single layer PZT-4 (load).

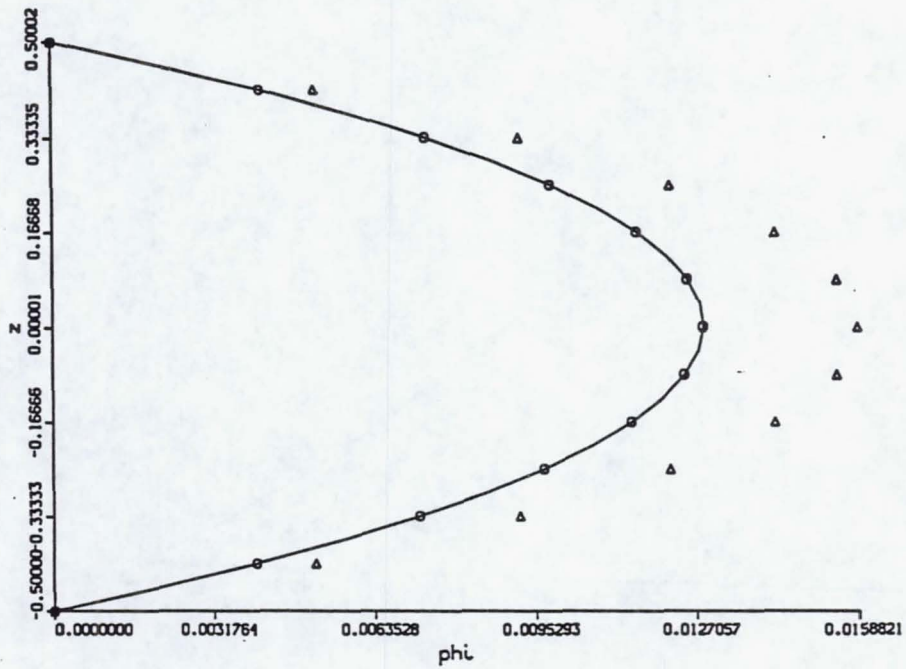


Figure 67: Potential for single layer PZT-4 (load).

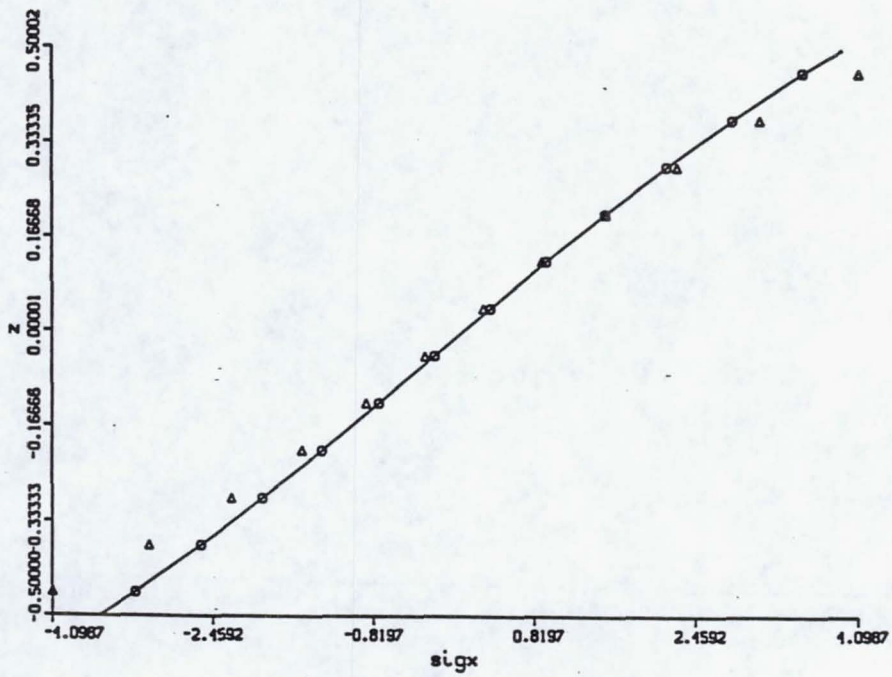


Figure 68: In-plane normal stress for single layer PZT-4 (load).

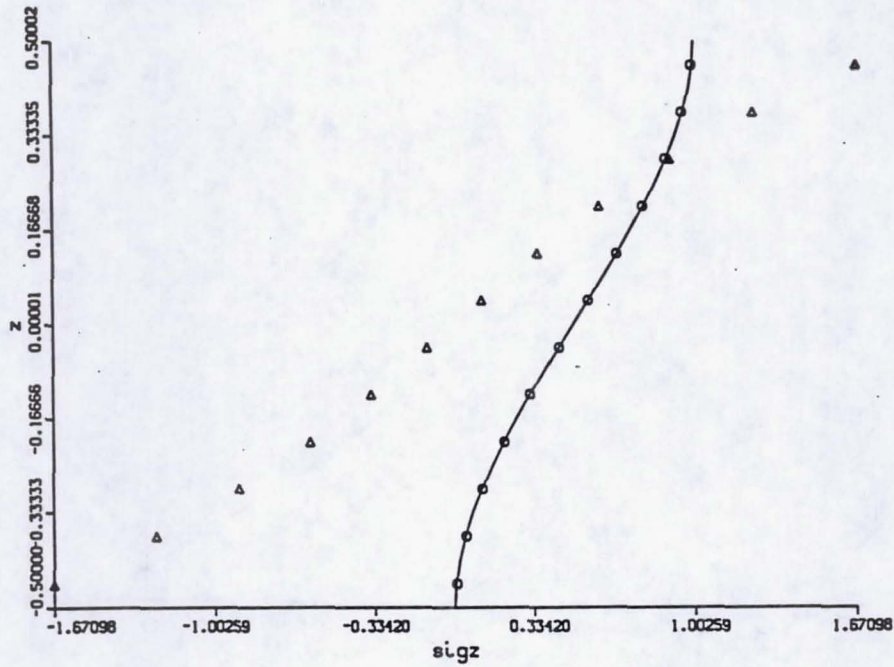


Figure 69: Out-of-plane normal stress for single layer PZT-4 (load).

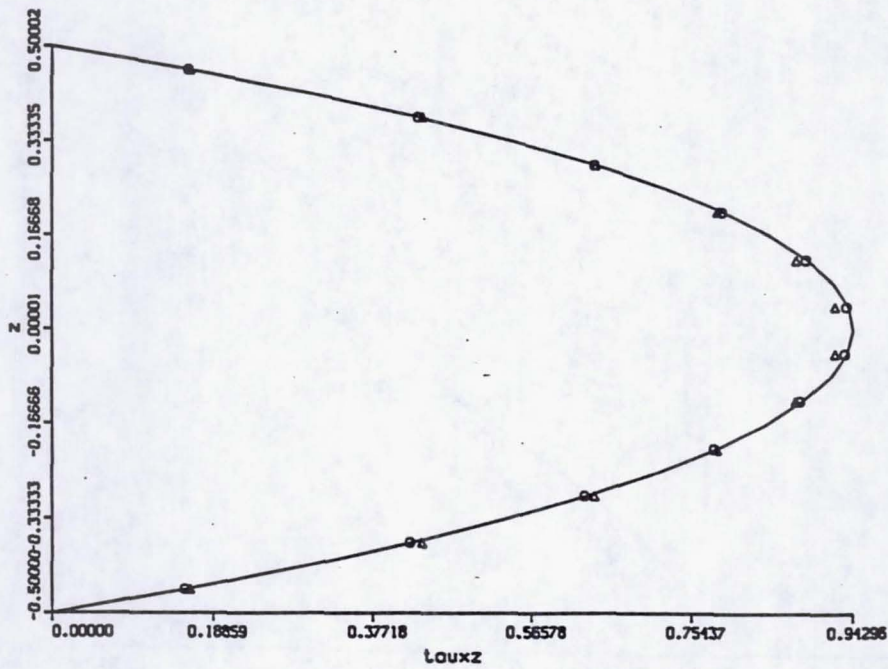


Figure 70: Out-of-plane shear stress for single layer PZT-4 (load).

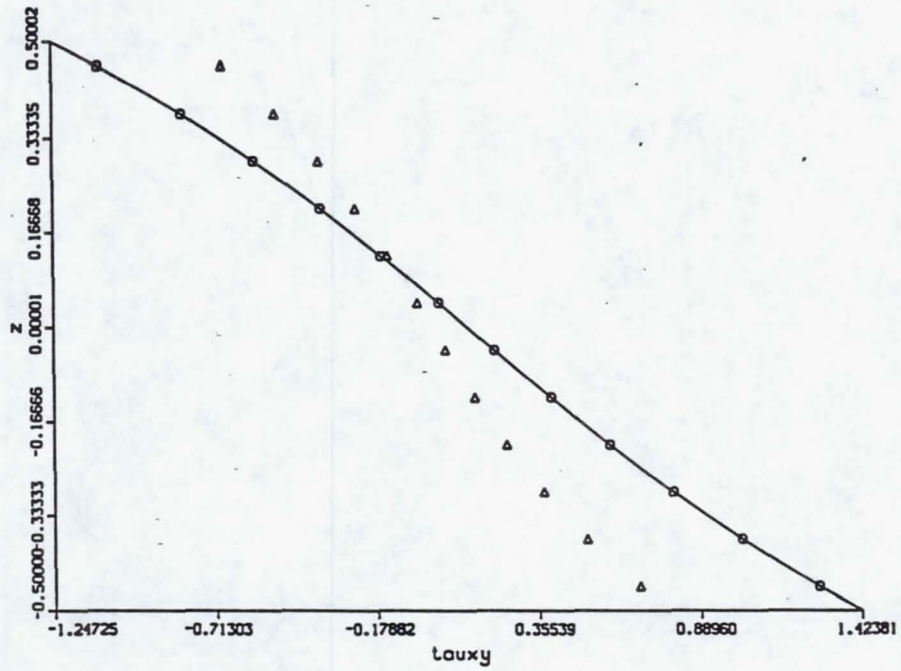


Figure 71: In-plane shear stress for single layer PZT-4 (load).

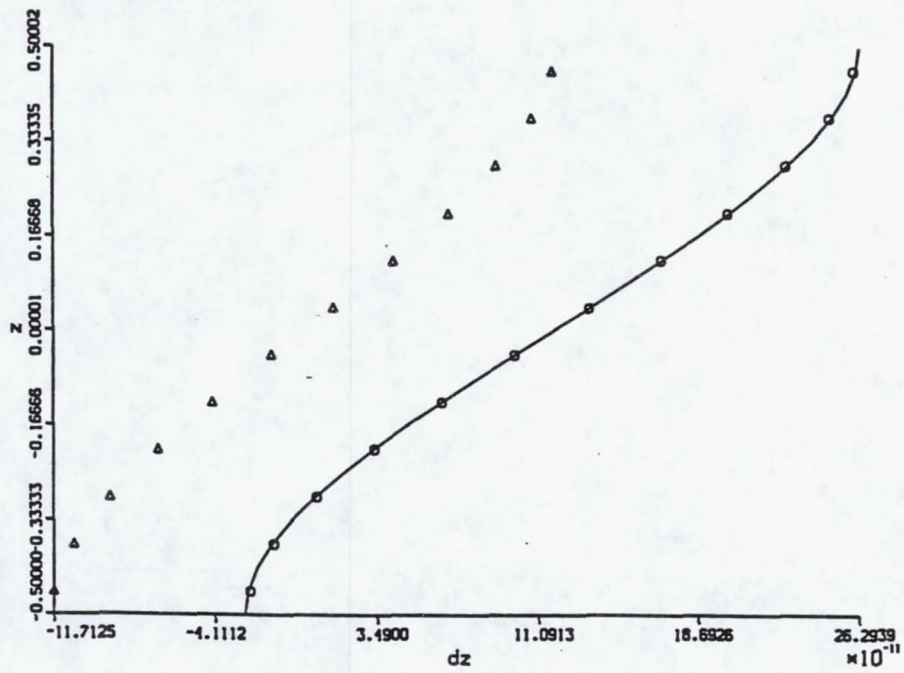


Figure 72: Normal electric displacement for single layer PZT-4 (load).

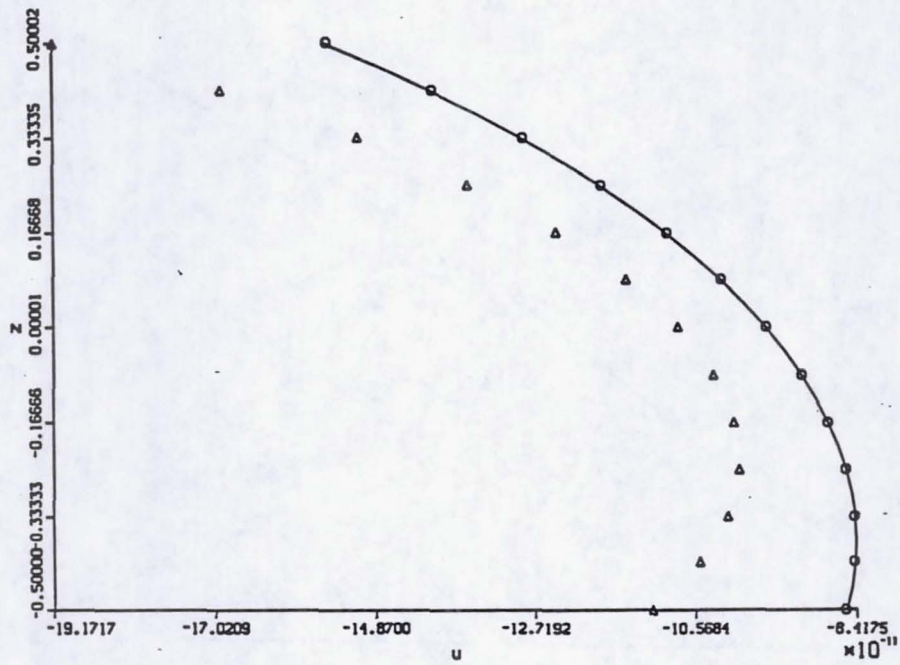


Figure 73: u-displacement for single layer PZT-4 (potential).

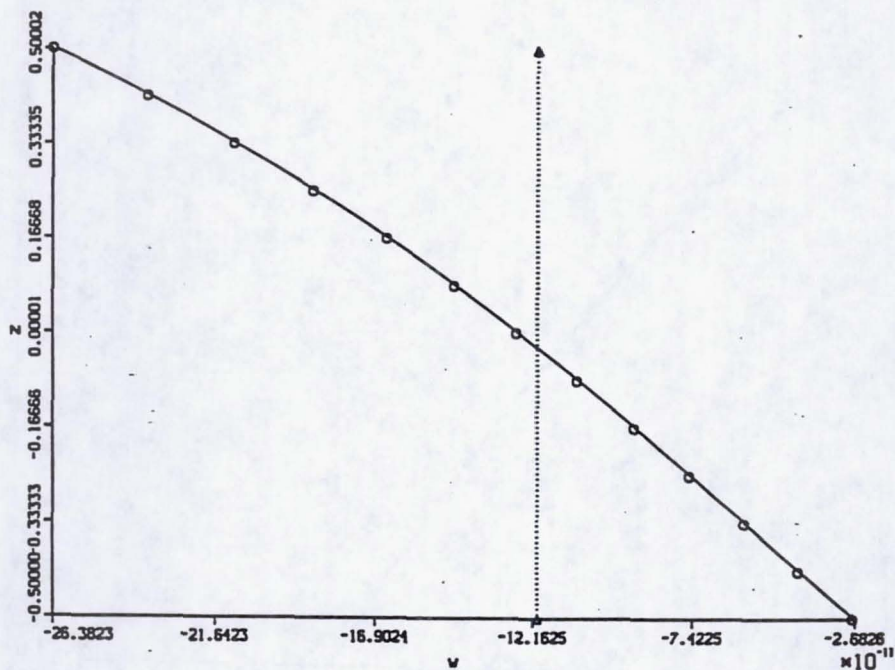


Figure 74: w-displacement for single layer PZT-4 (potential).

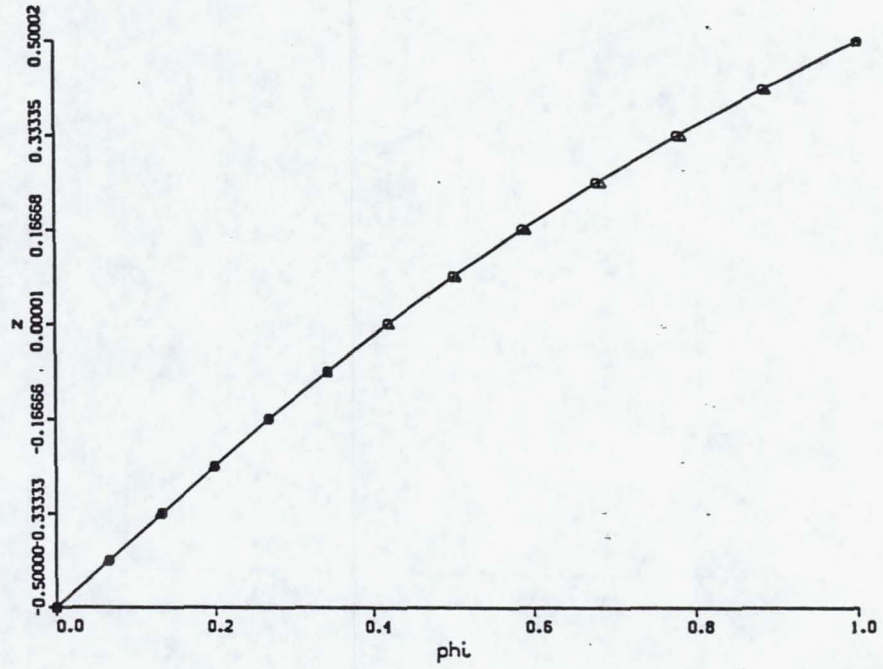


Figure 75: Potential for single layer PZT-4 (potential).

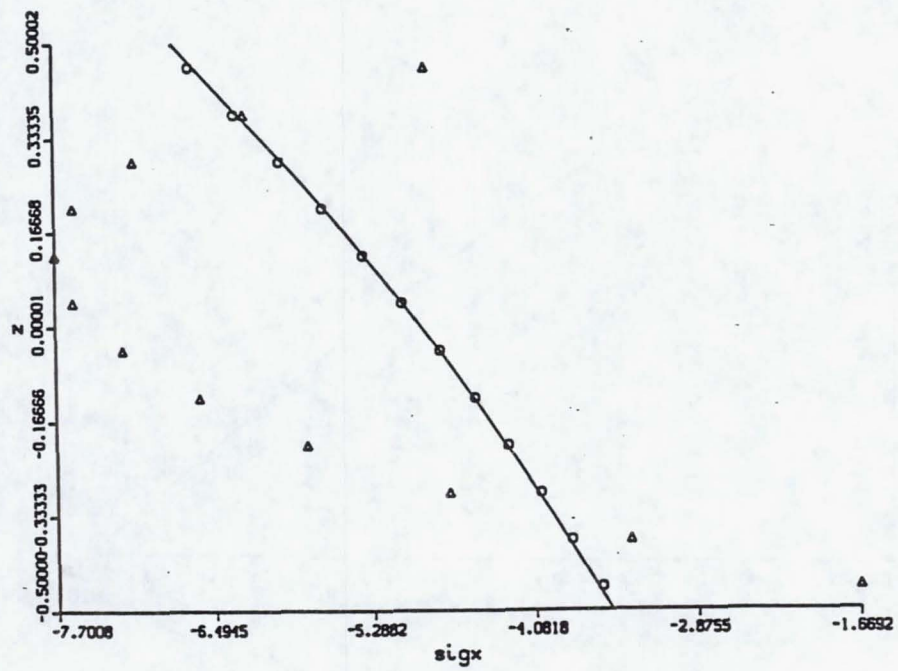


Figure 76: In-plane normal stress for single layer PZT-4 (potential).

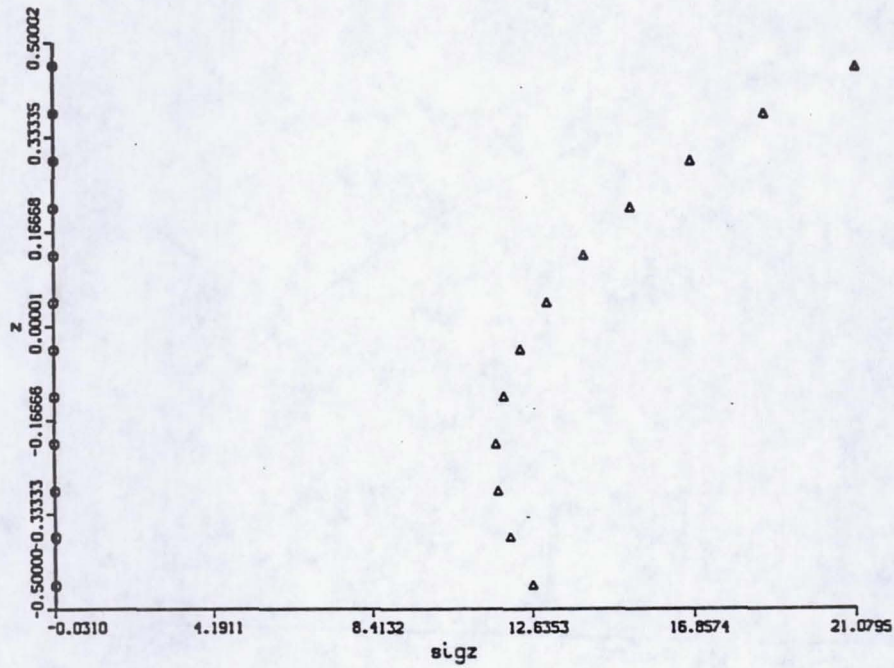


Figure 77: Out-of-plane normal stress for single layer PZT-4 (potential).

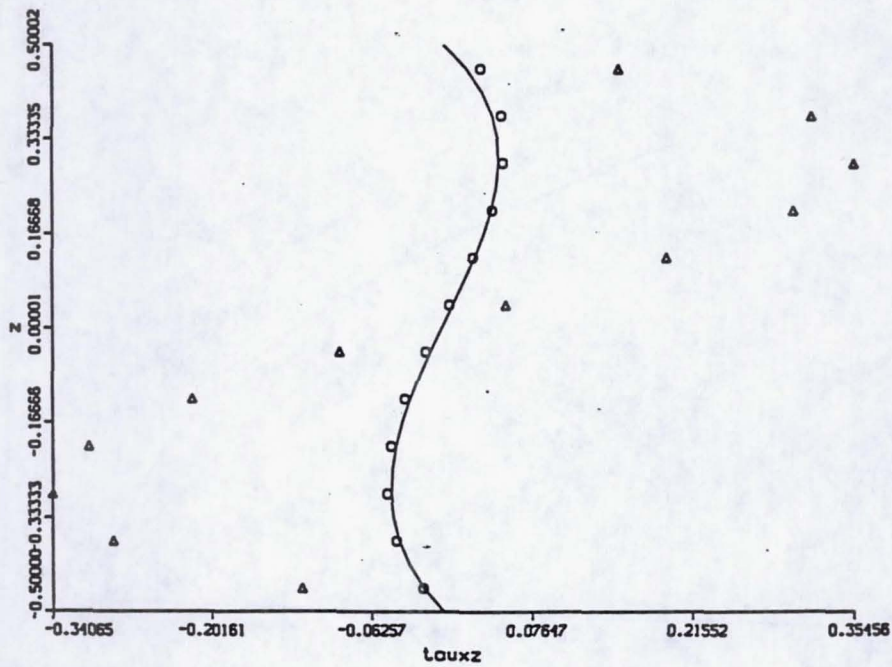


Figure 78: Out-of-plane shear stress for single layer PZT-4 (potential).



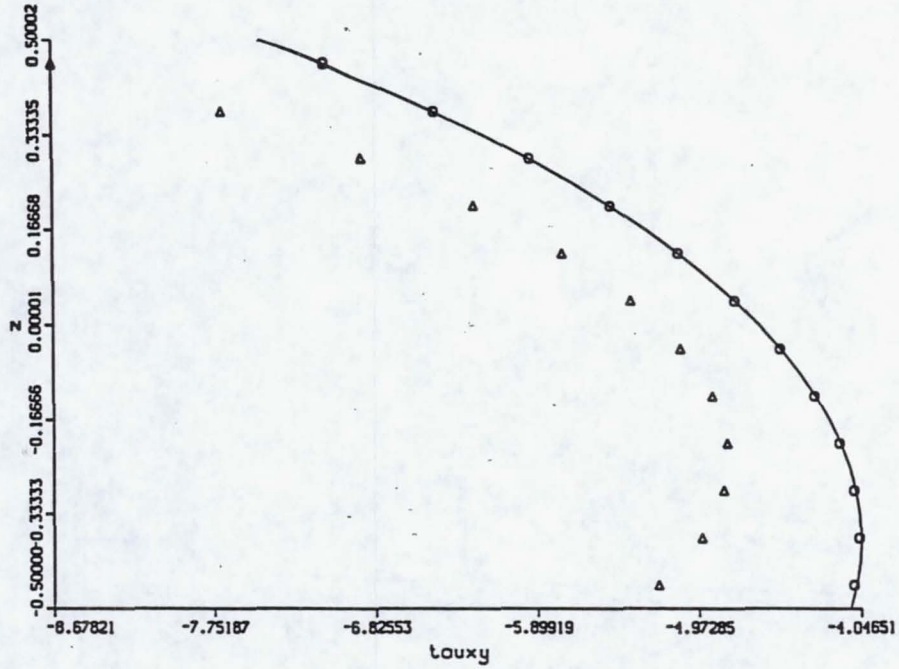


Figure 79: In-plane shear stress for single layer PZT-4 (potential).

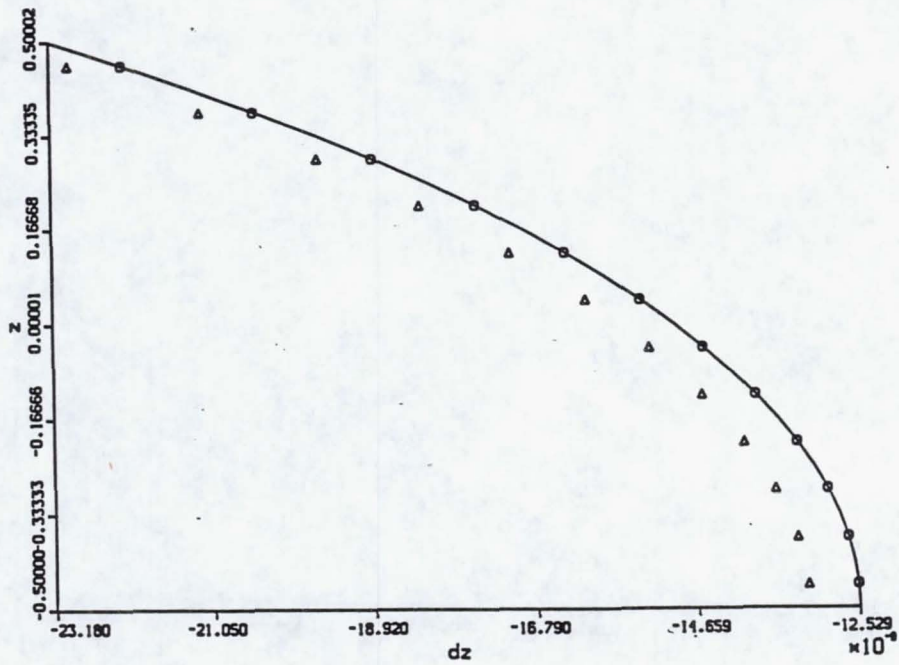


Figure 80: Normal electric displacement for single layer PZT-4 (potential).

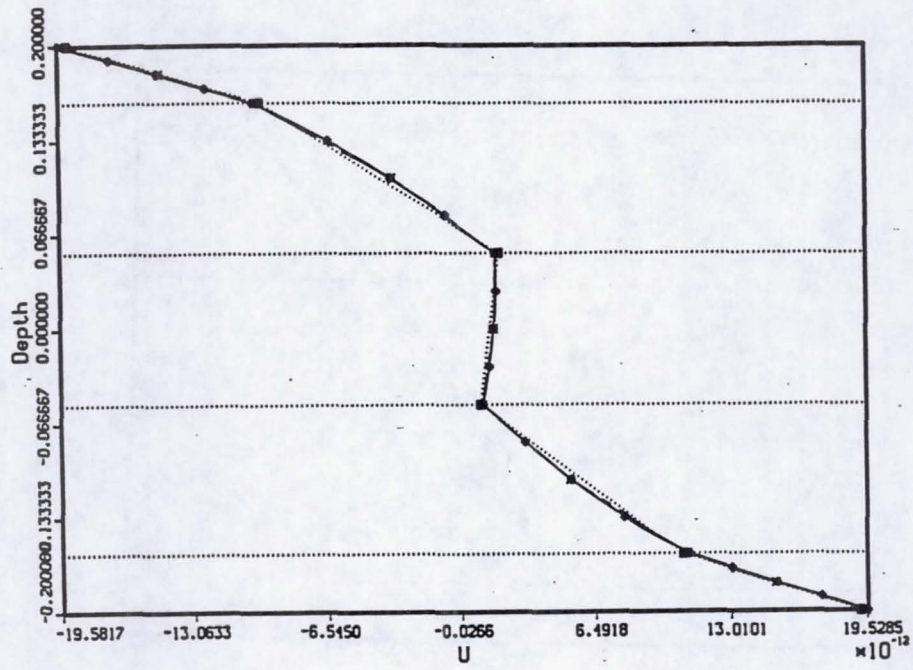


Figure 81: u-displacement for 5-ply, applied load.

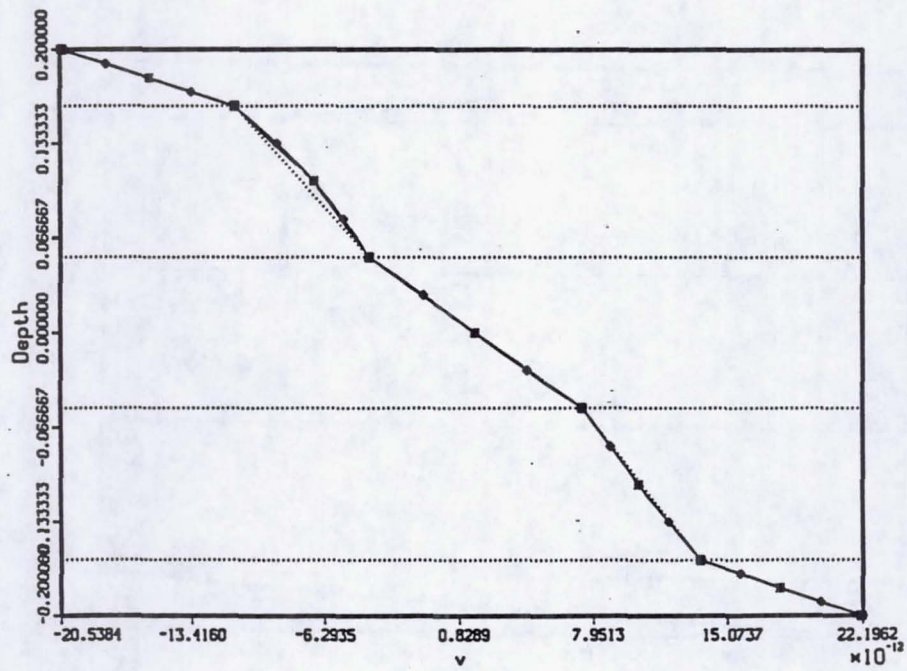


Figure 82: v-displacement for 5-ply, applied load.

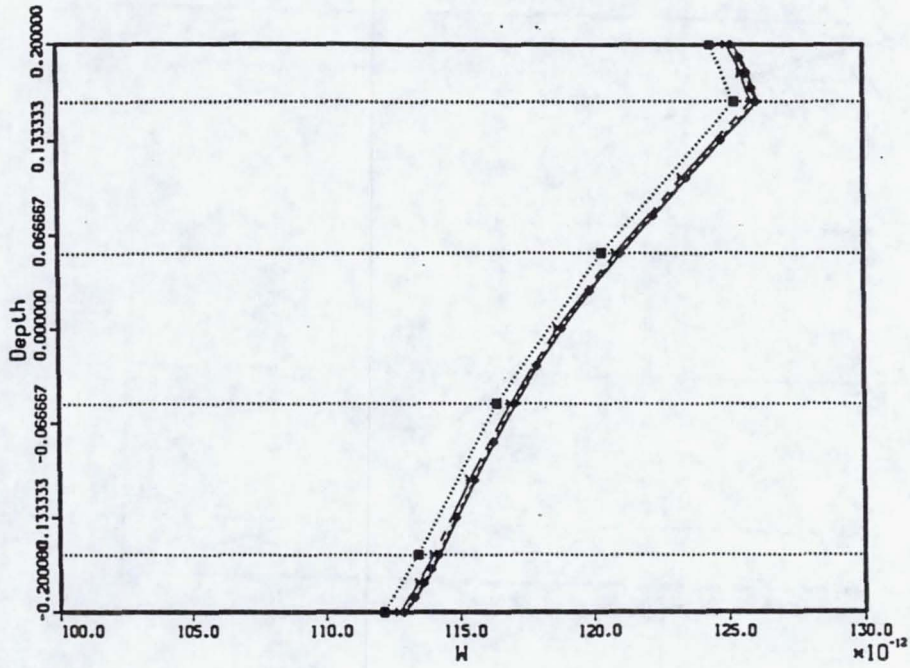


Figure 83: w-displacement for 5-ply, applied load.

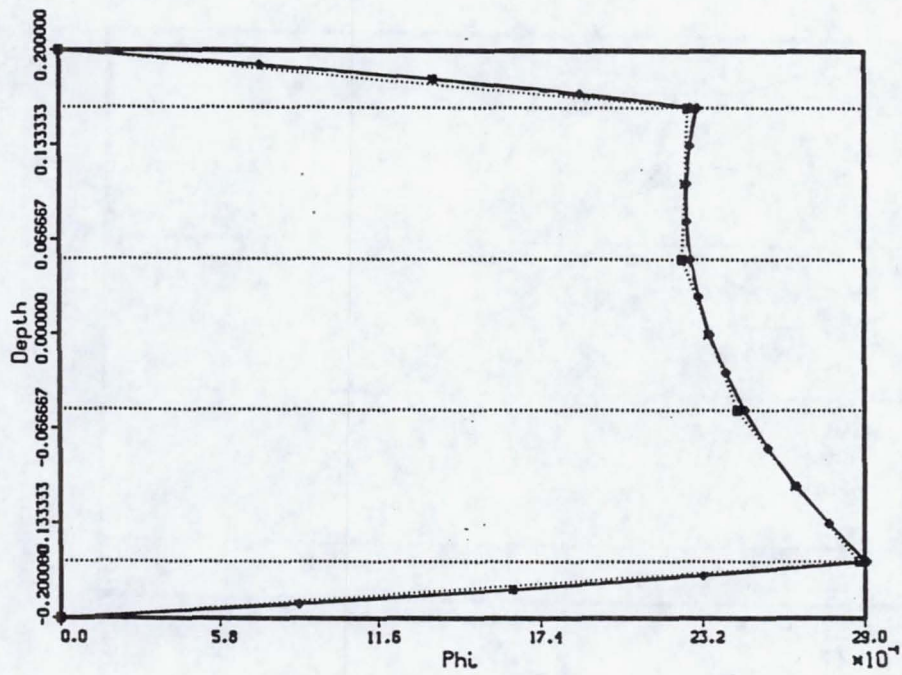


Figure 84: Potential for 5-ply, applied load.

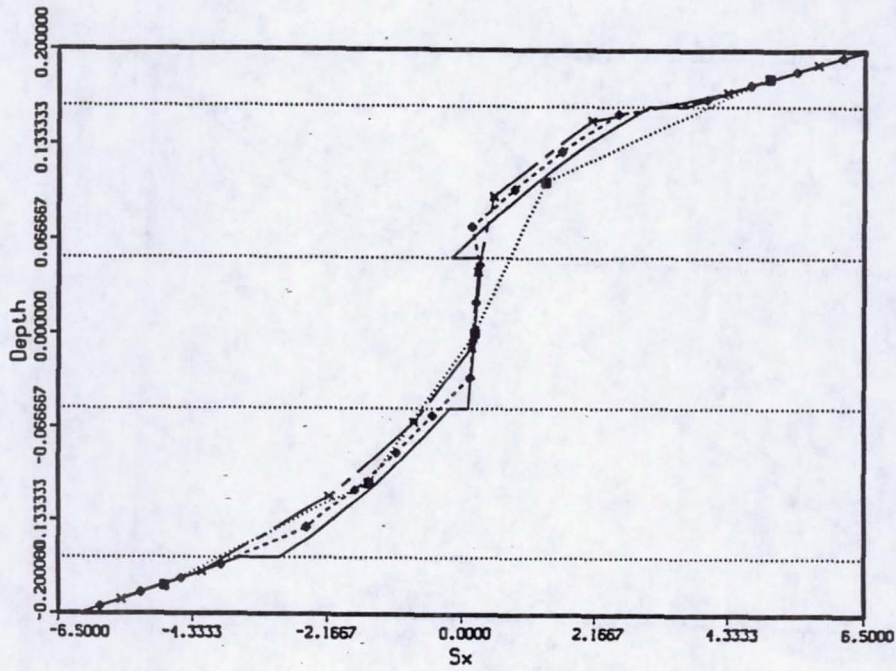


Figure 85: Normal (x) stress, 5-ply, applied load.

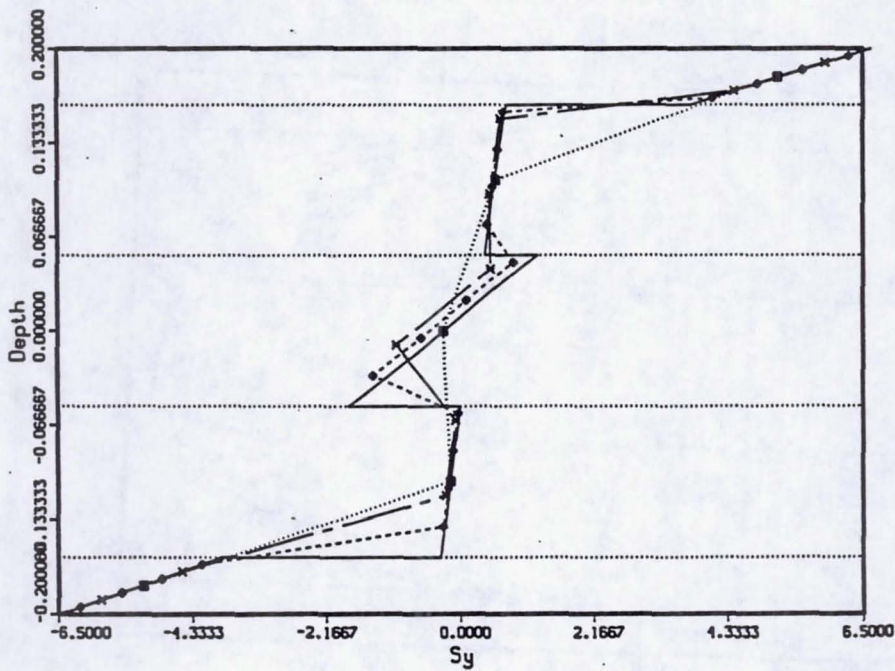


Figure 86: Normal (y) stress, 5-ply, applied load.

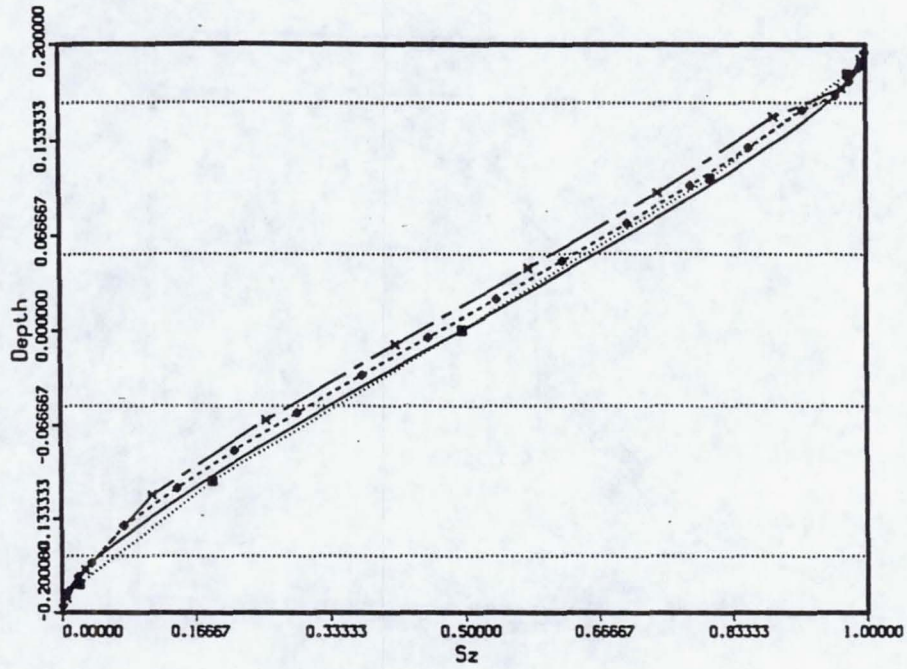


Figure 87: Normal (z) stress, 5-ply, applied load.

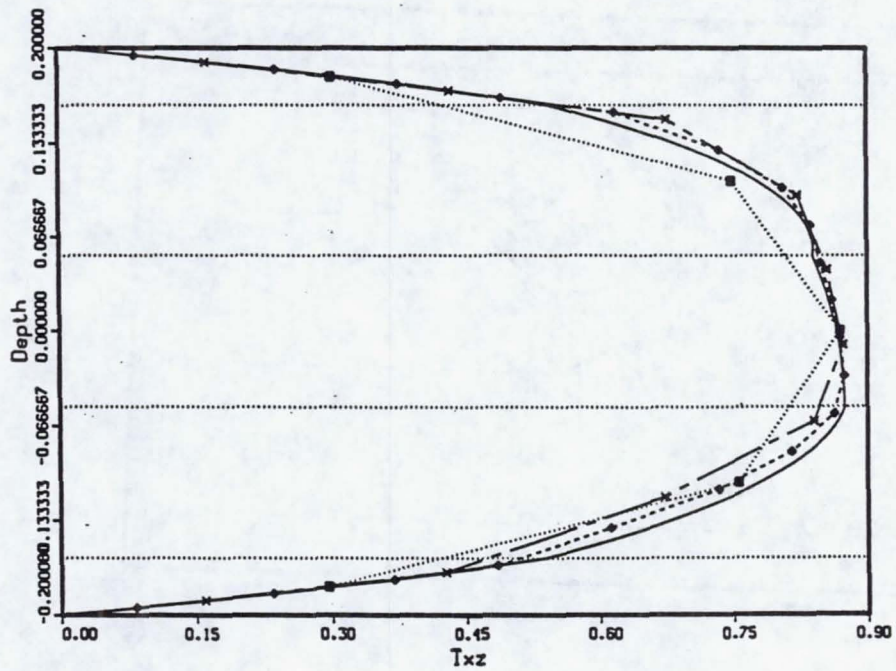


Figure 88: Shear (xz) stress, 5-ply, applied load.

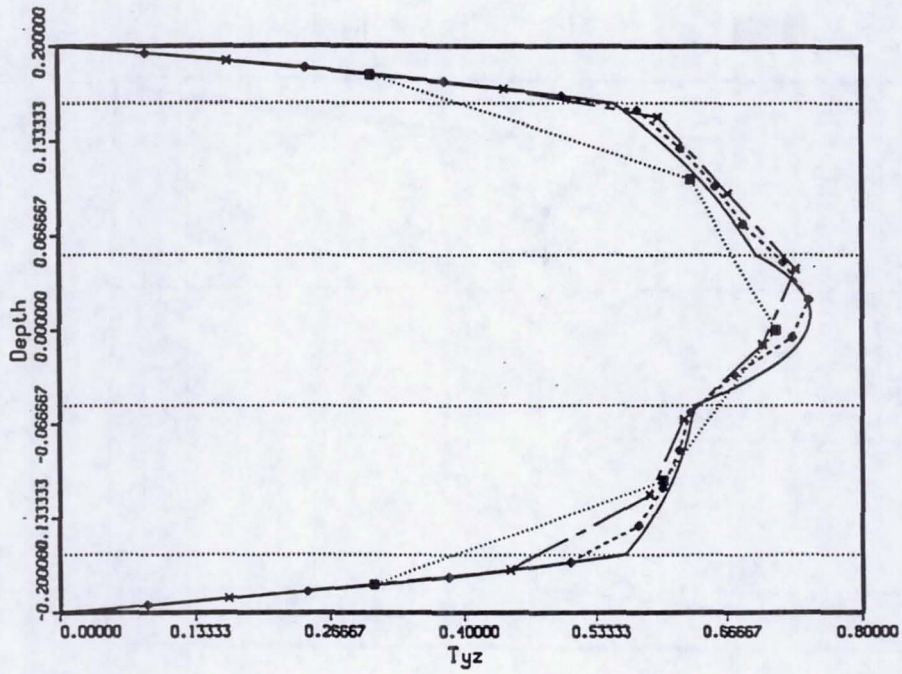


Figure 89: Shear (yz) stress, 5-ply, applied load.

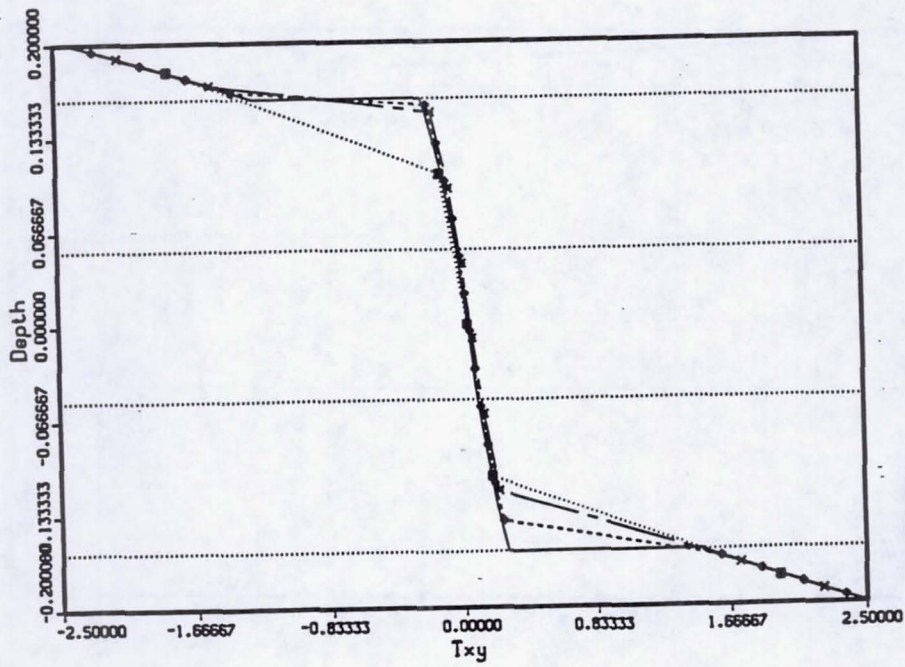


Figure 90: Shear (xy) stress, 5-ply, applied load.

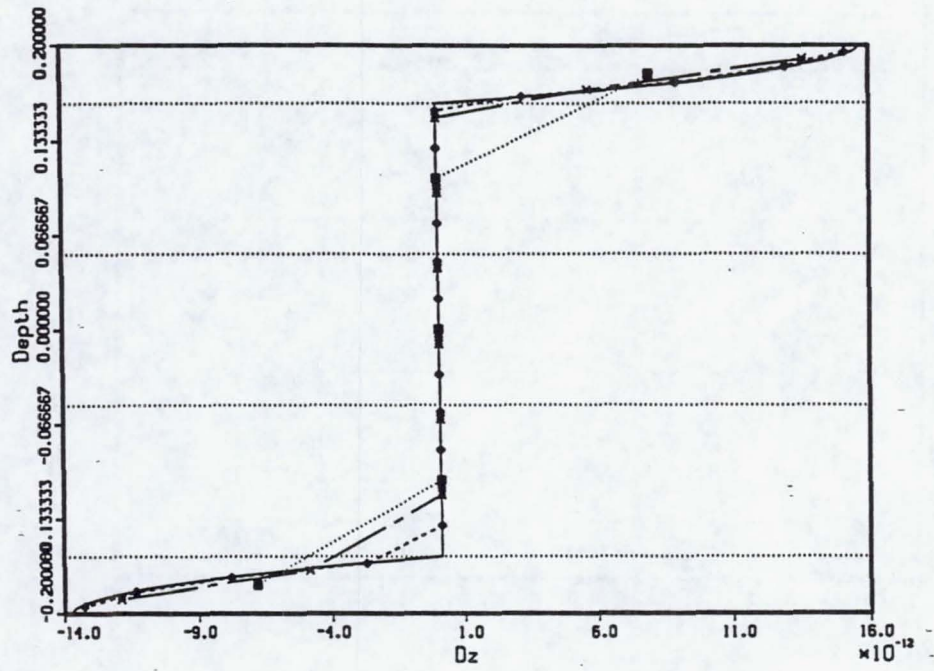


Figure 91: Normal electric displacement, 5-ply, applied load.

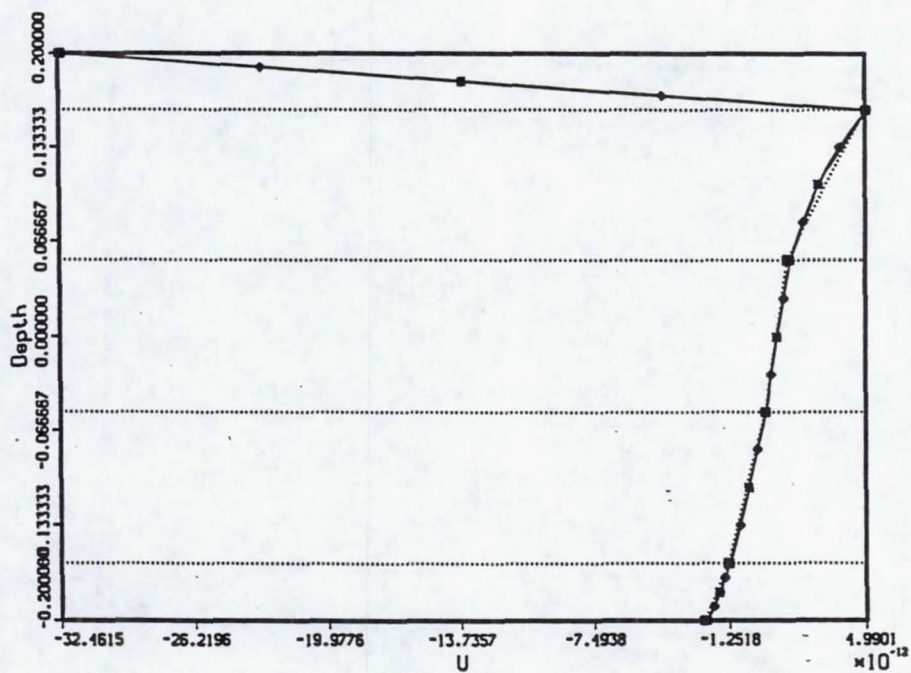


Figure 92: u-displacement for 5-ply, applied potential.

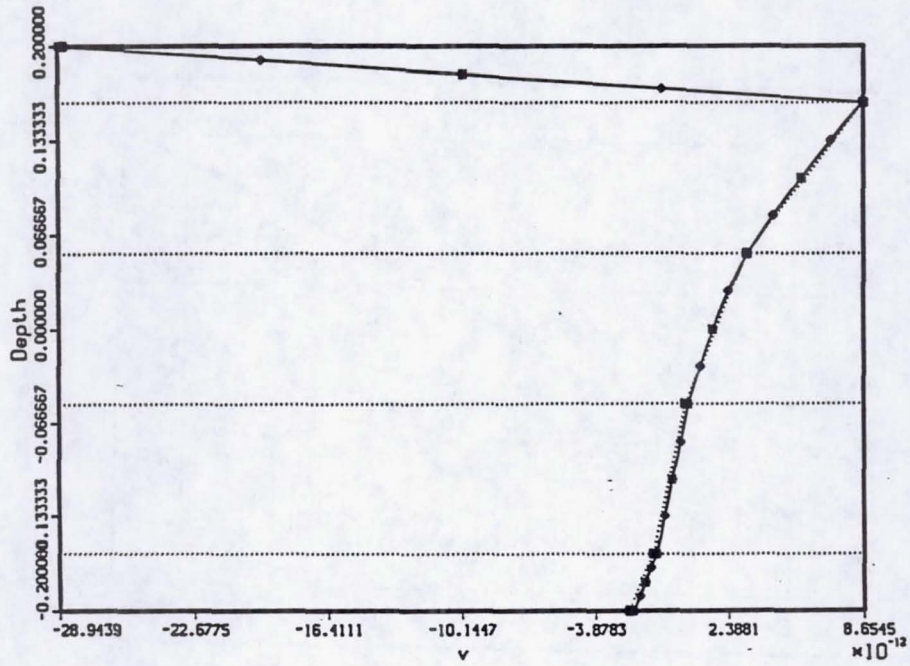


Figure 93: v-displacement for 5-ply, applied potential.

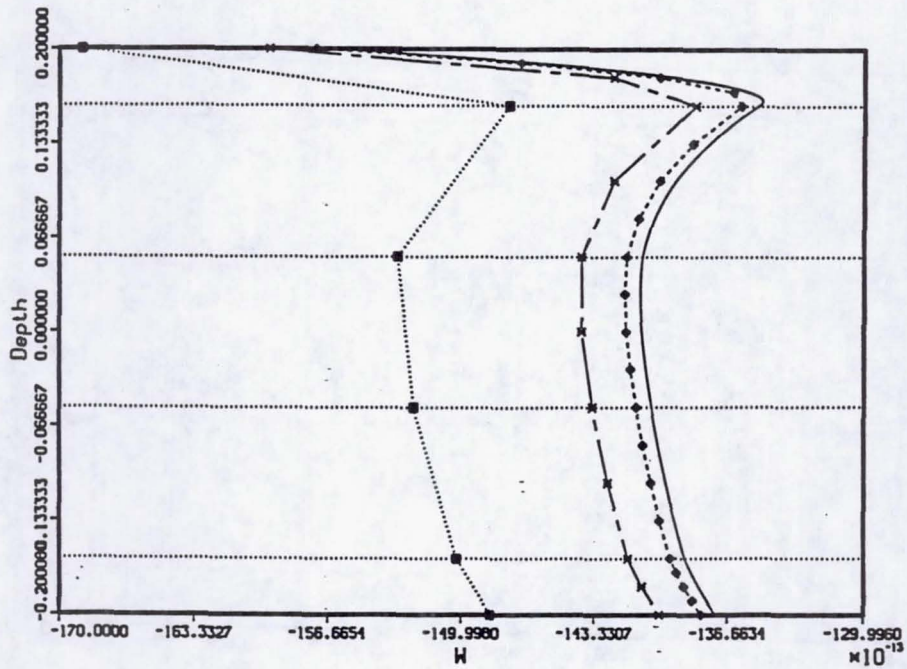


Figure 94: w-displacement for 5-ply, applied potential.



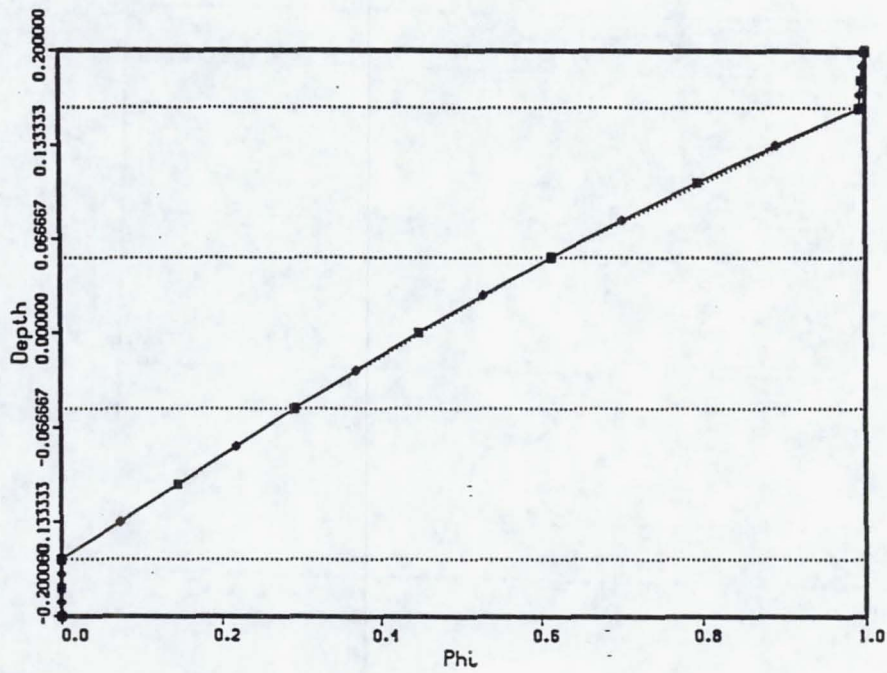


Figure 95: Potential for 5-ply, applied potential.

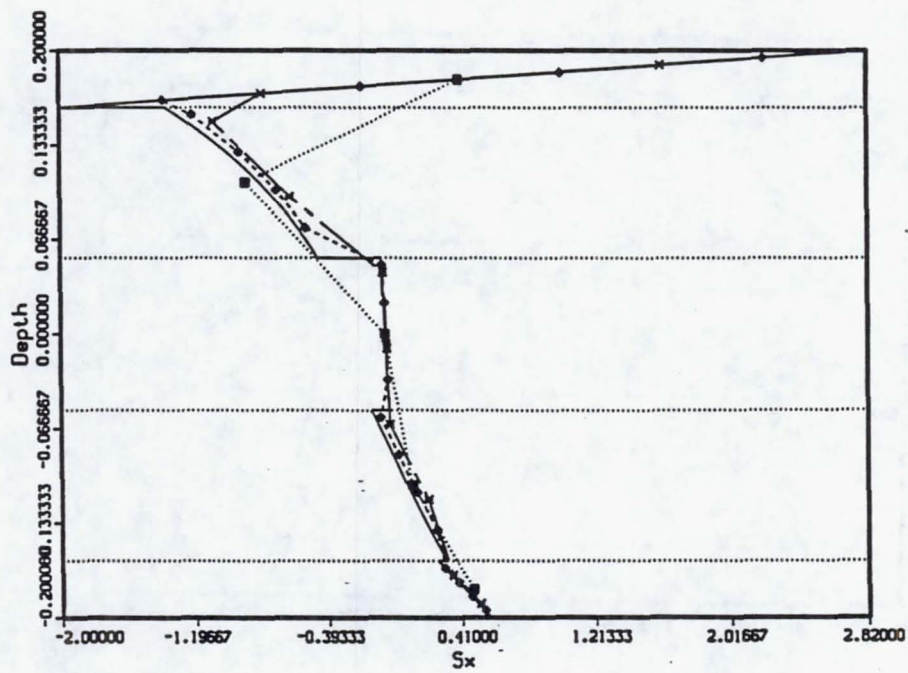


Figure 96: Normal (x) stress, 5-ply, applied potential.

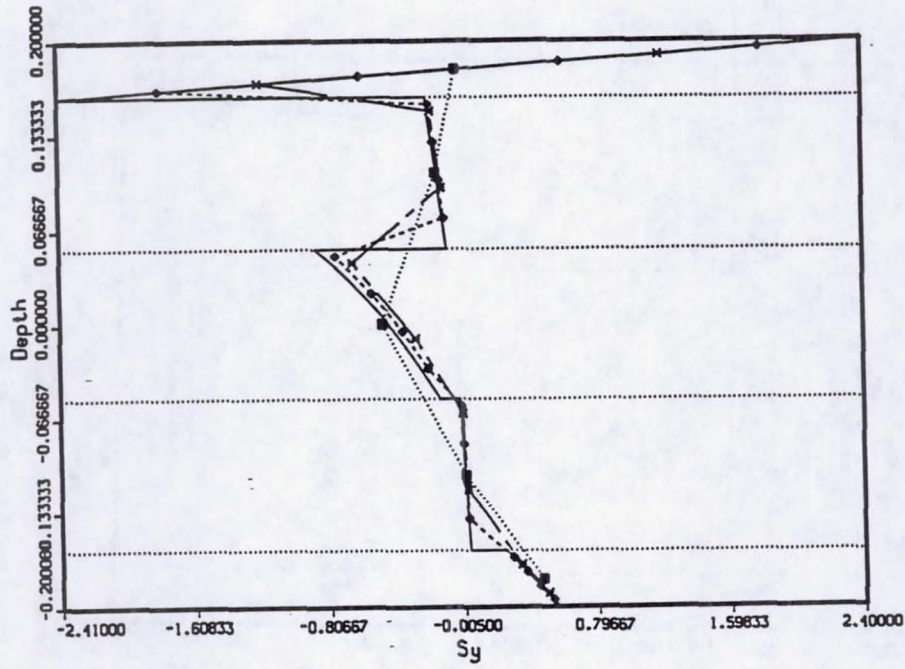


Figure 97: Normal (y) stress, 5-ply, applied potential.

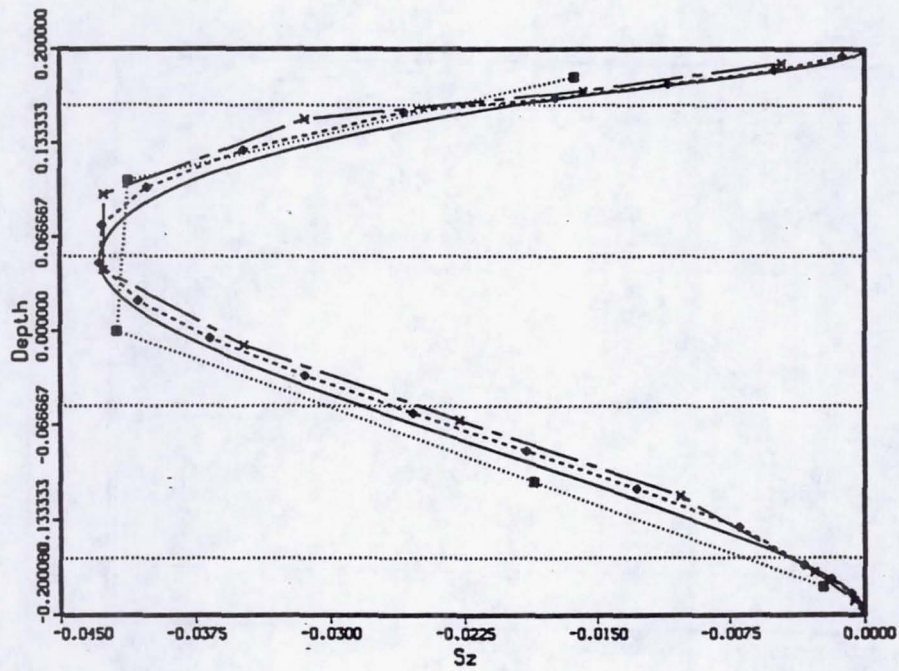


Figure 98: Normal (z) stress, 5-ply, applied potential.

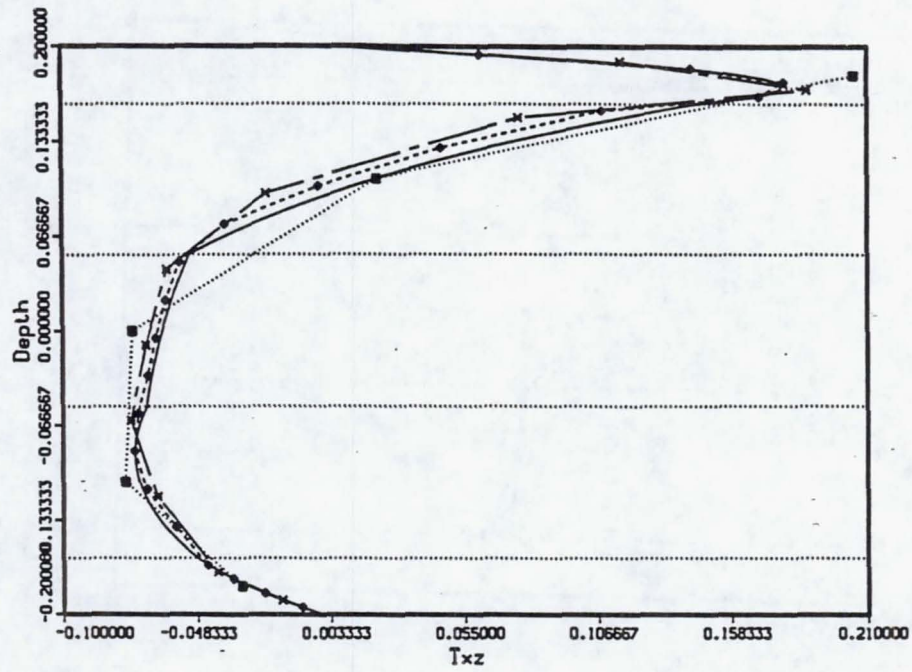


Figure 99: Shear (xz) stress, 5-ply, applied potential.

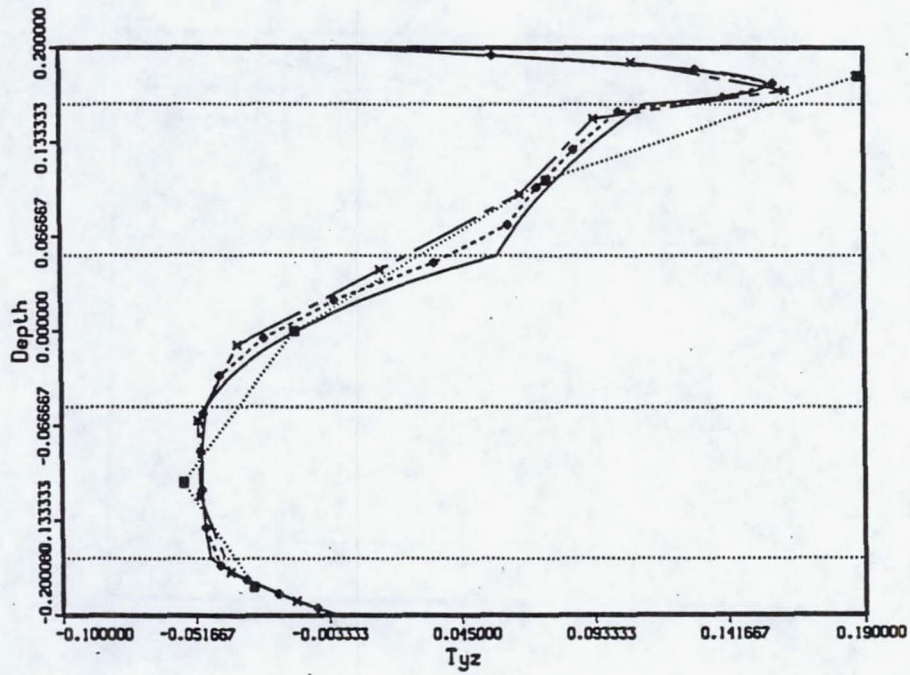


Figure 100: Shear (yz) stress, 5-ply, applied potential.

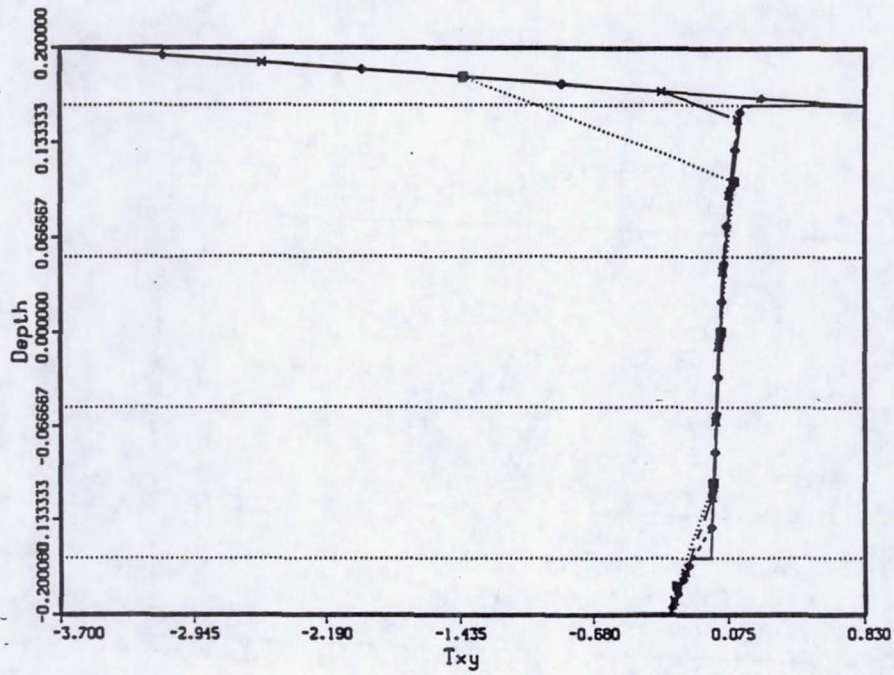


Figure 101: Shear (xy) stress, 5-ply, applied potential.

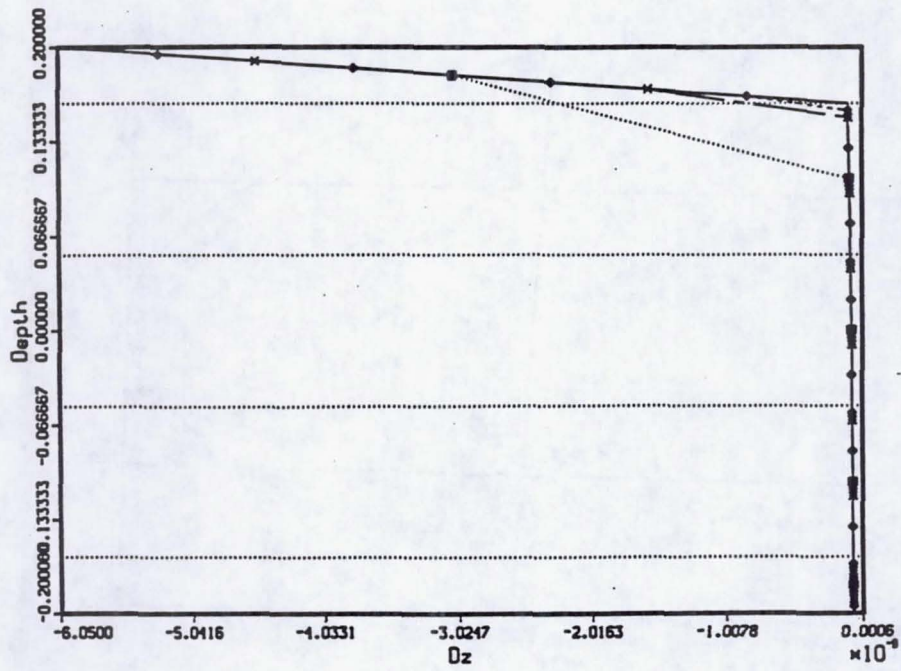


Figure 102: Normal electric displacement, 5-ply, applied potential.

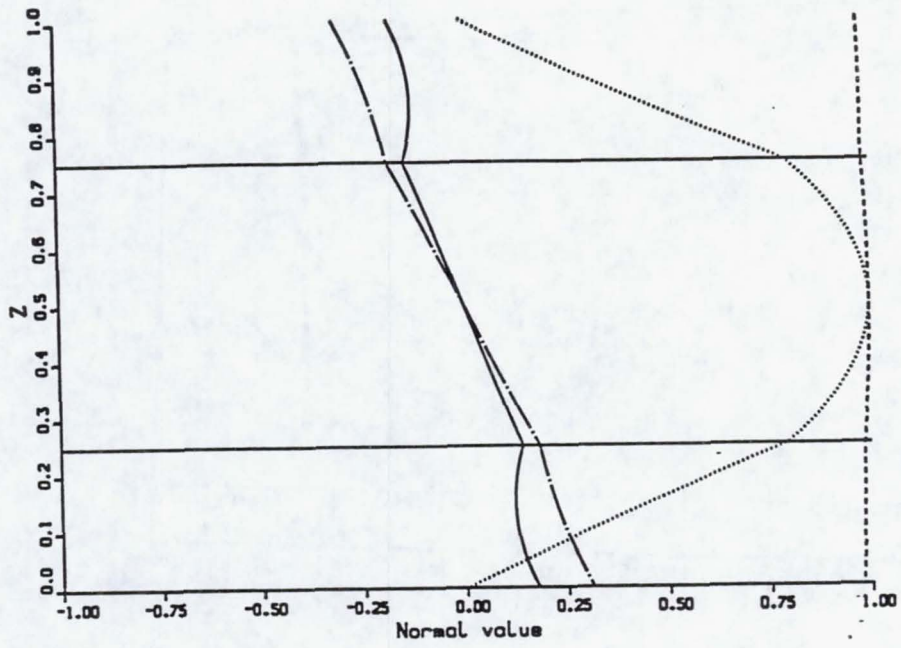


Figure 103: Mode 1, 3-ply,  $a/h=4$ .

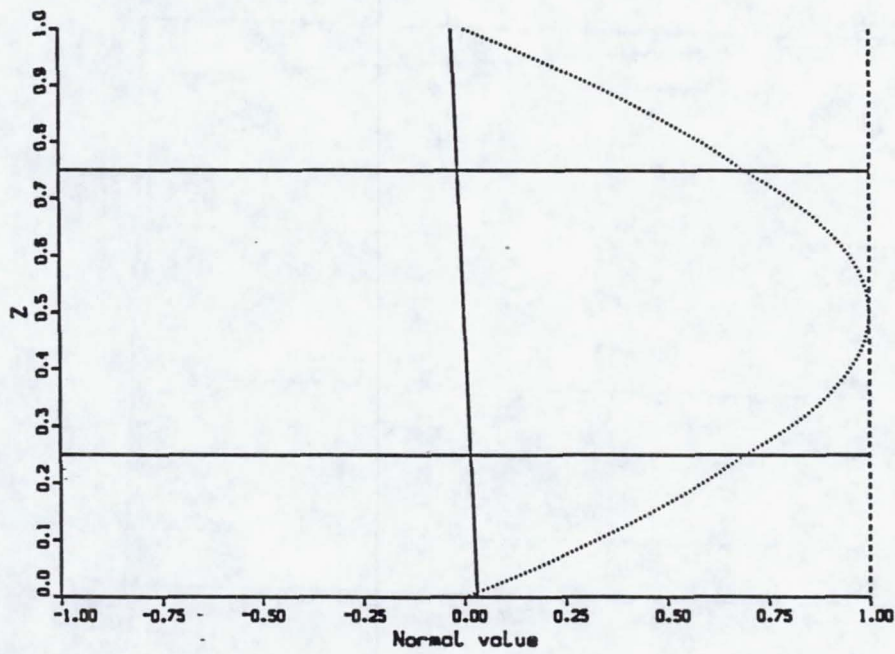


Figure 104: Mode 1, 3-ply,  $a/h=50$ .

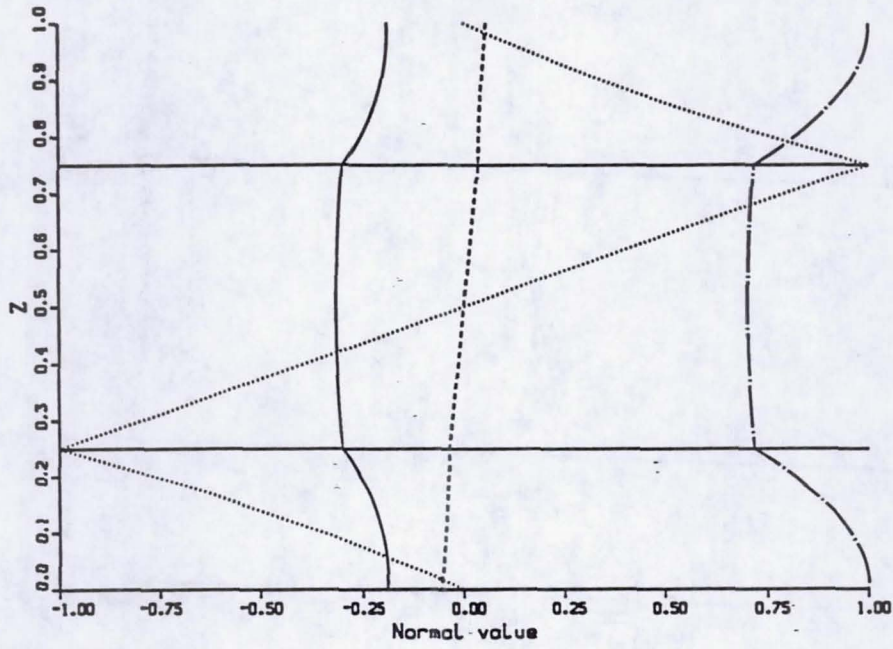


Figure 105: Mode 2, 3-ply,  $a/h=4$ .

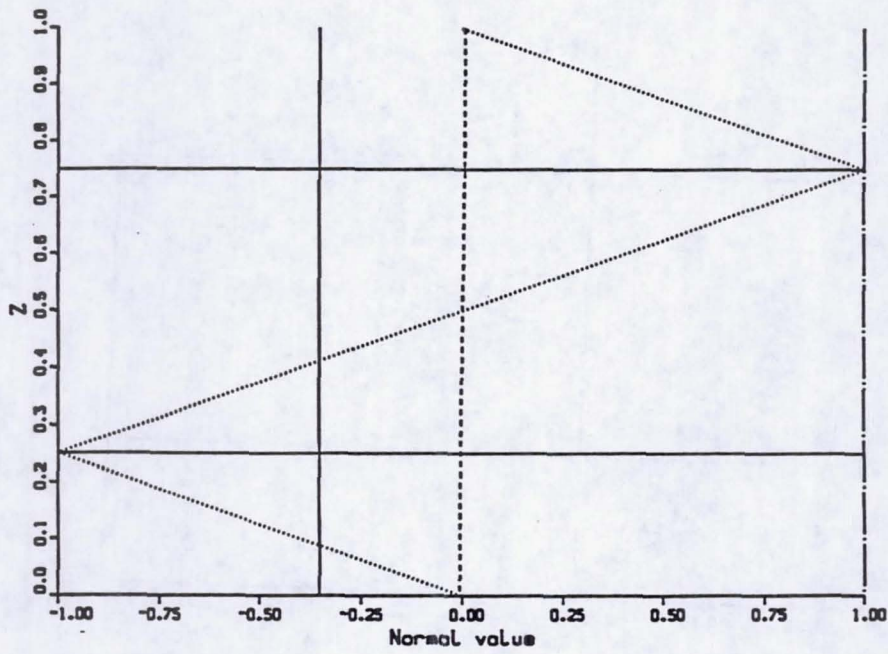


Figure 106: Mode 2, 3-ply,  $a/h=50$ .

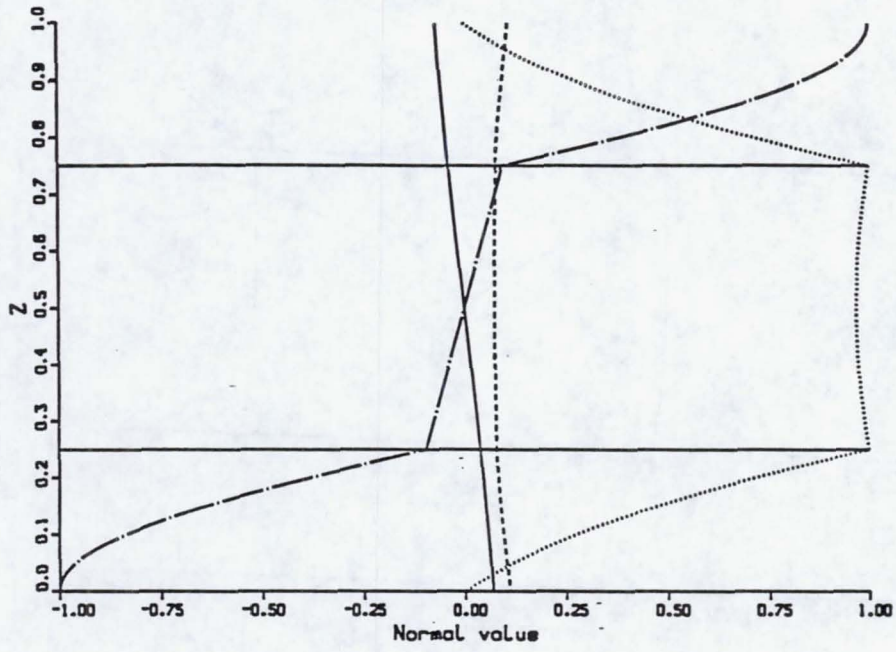


Figure 107: Mode 3, 3-ply,  $a/h=4$ .

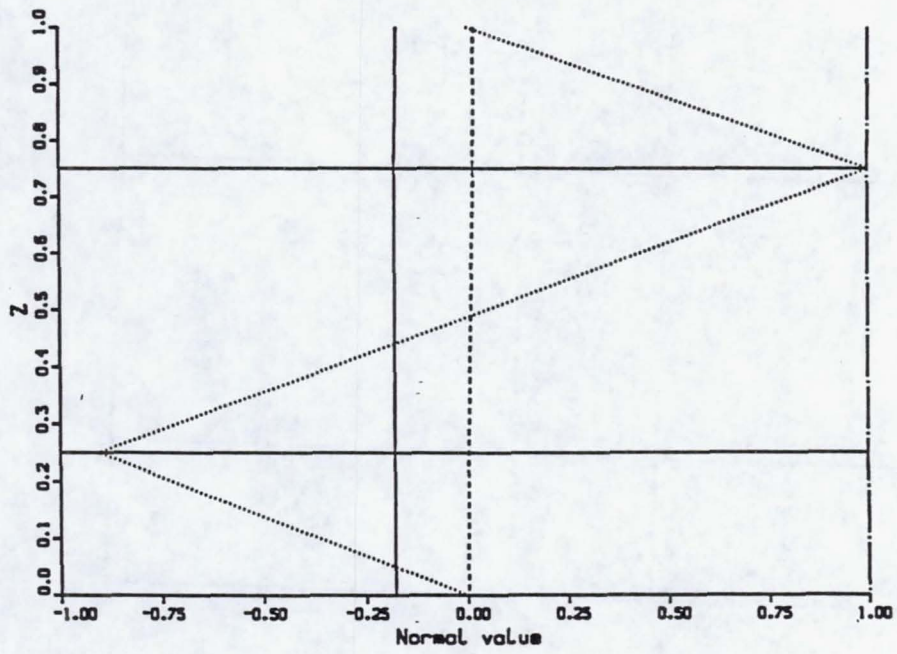


Figure 108: Mode 3, 3-ply,  $a/h=50$ .

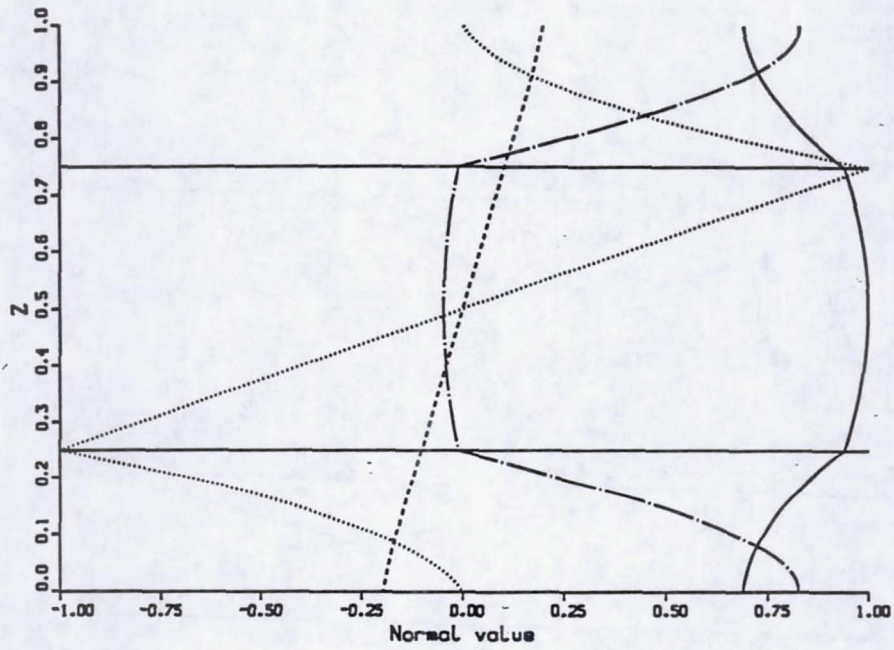


Figure 109: Mode 4, 3-ply,  $a/h=4$ .

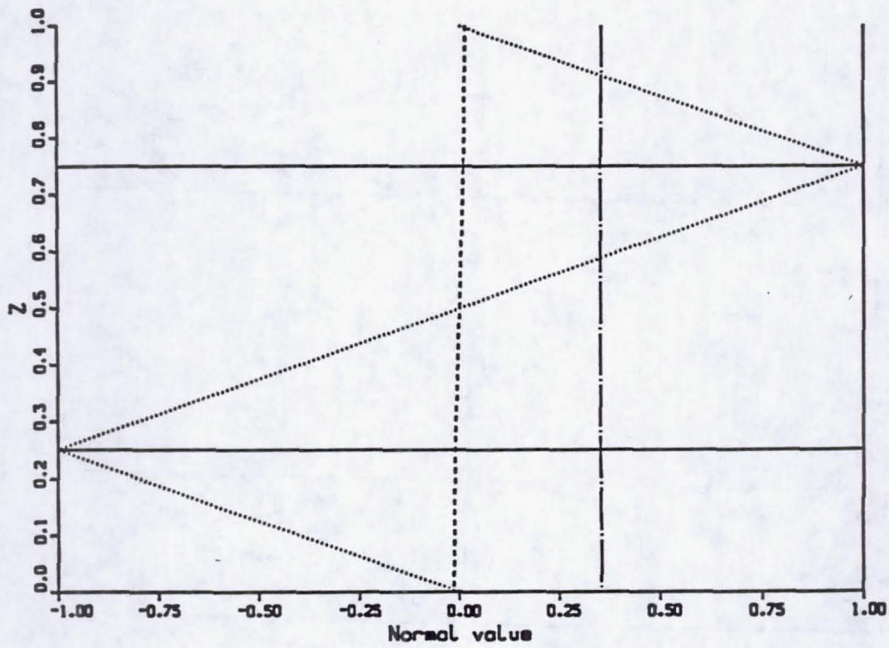


Figure 110: Mode 4, 3-ply,  $a/h=50$ .



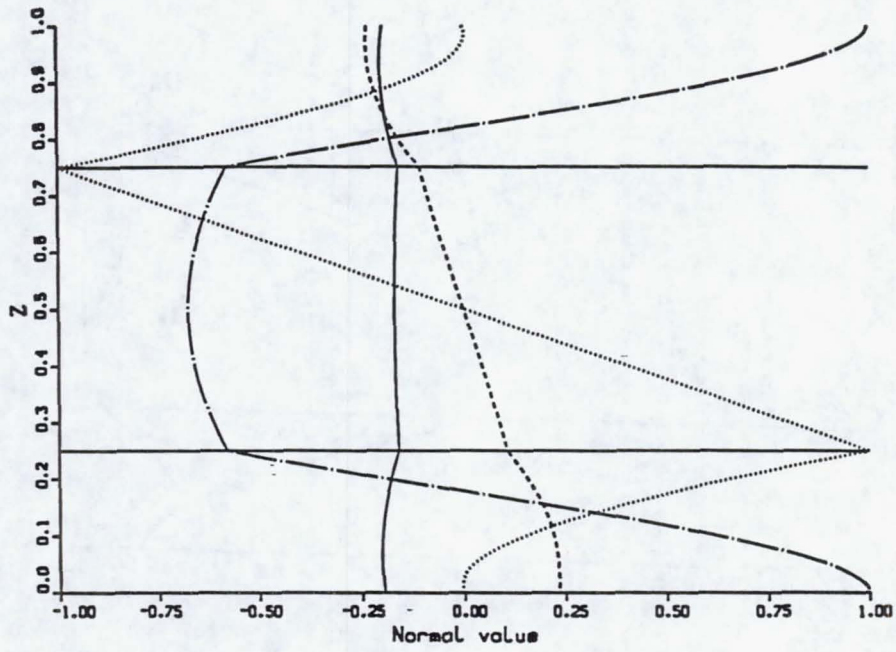


Figure 111: Mode 5, 3-ply,  $a/h=4$ .

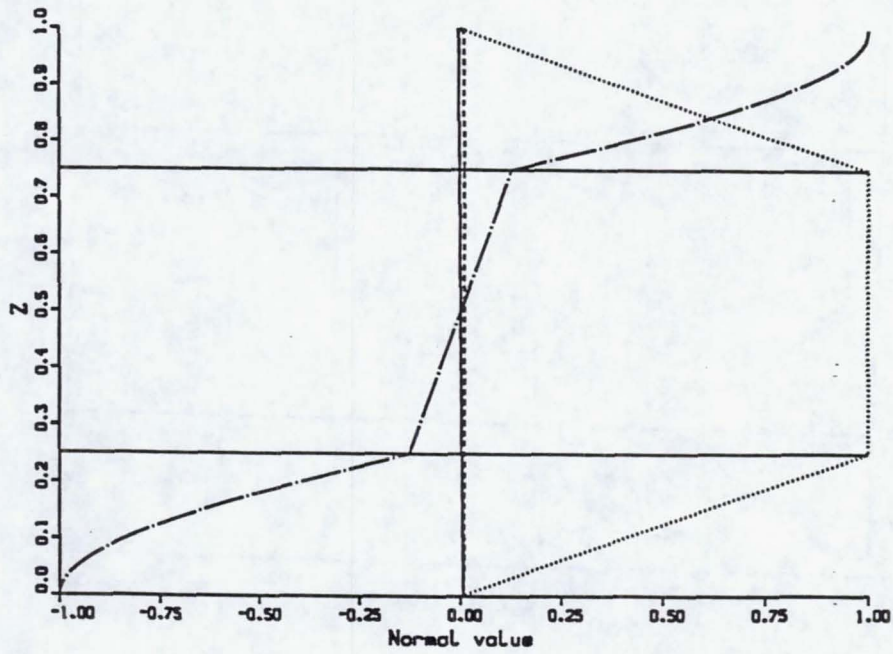


Figure 112: Mode 5, 3-ply,  $a/h=50$ .

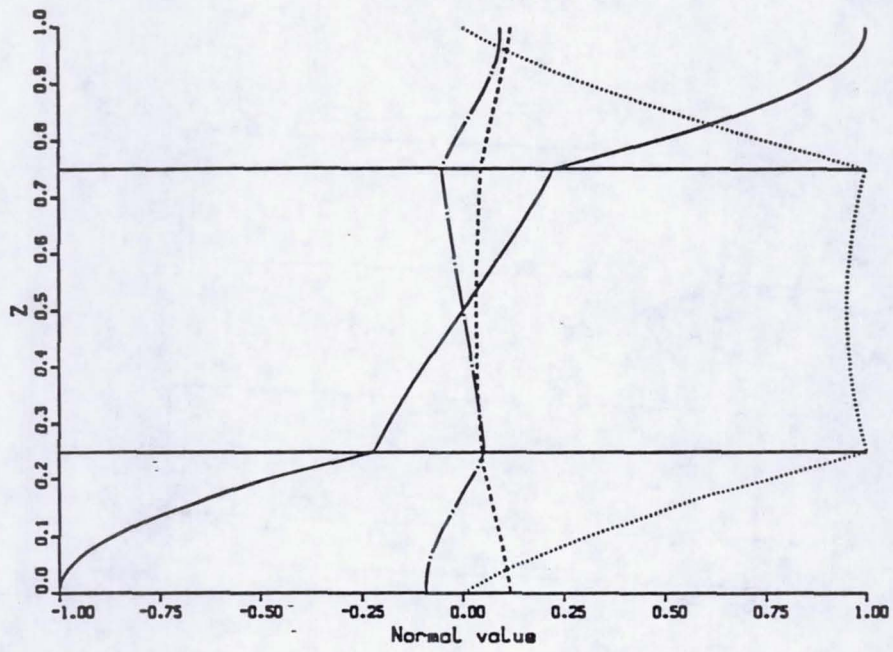


Figure 113: Mode 6, 3-ply,  $a/h=4$ .

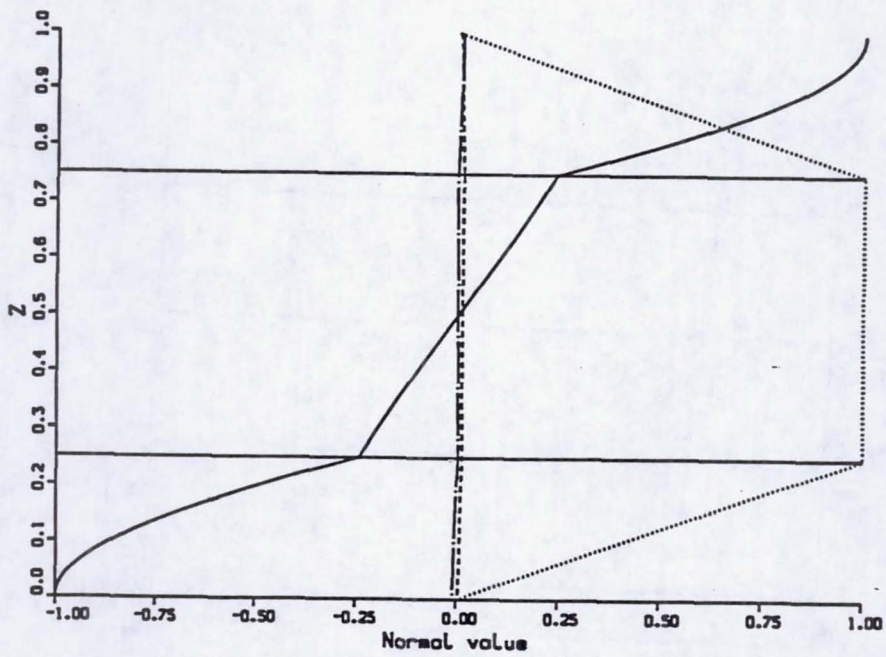


Figure 114: Mode 6, 3-ply,  $a/h=50$ .

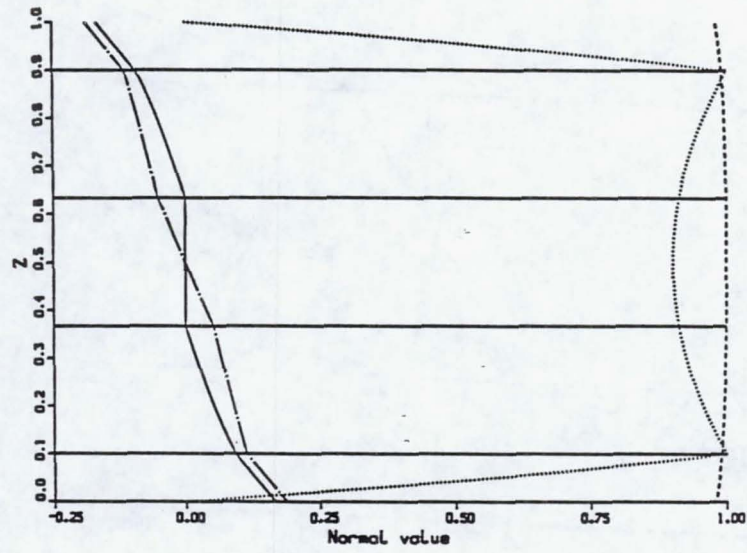


Figure 115: Displacement and potential, mode 1, 5-ply,  $a/h=4$ .

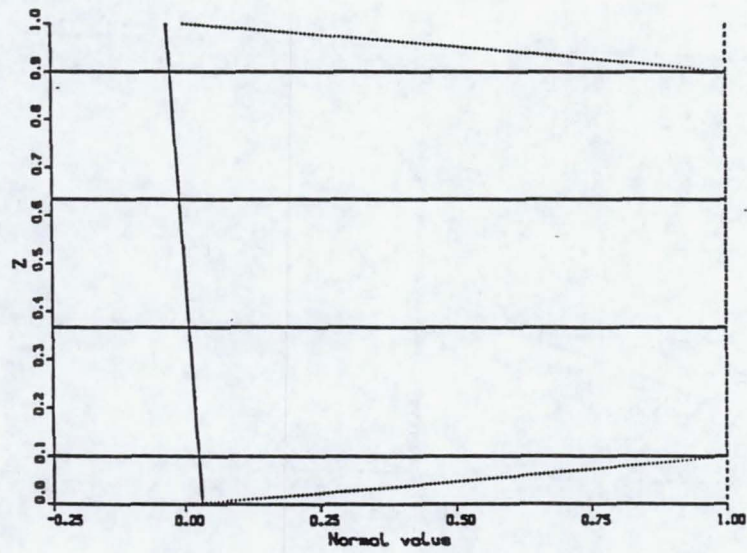


Figure 116: Displacement and potential, mode 1, 5-ply,  $a/h=50$ .

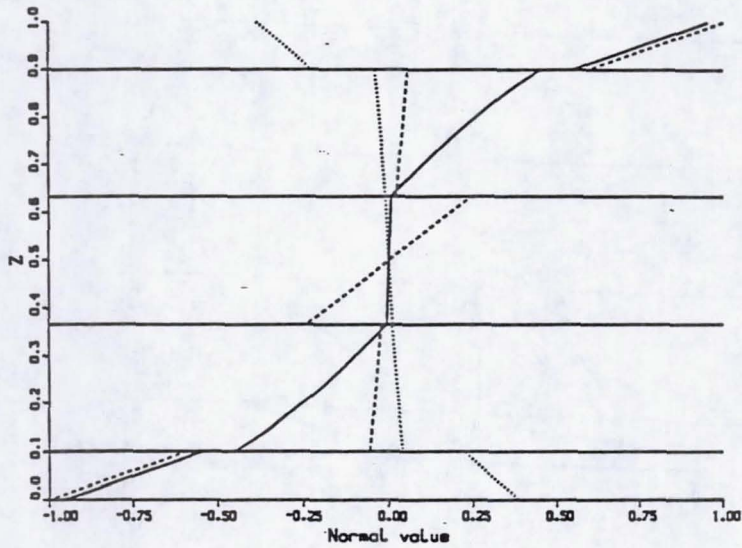


Figure 117: In-plane stresses, mode 1, 5-ply,  $a/h=1$ .

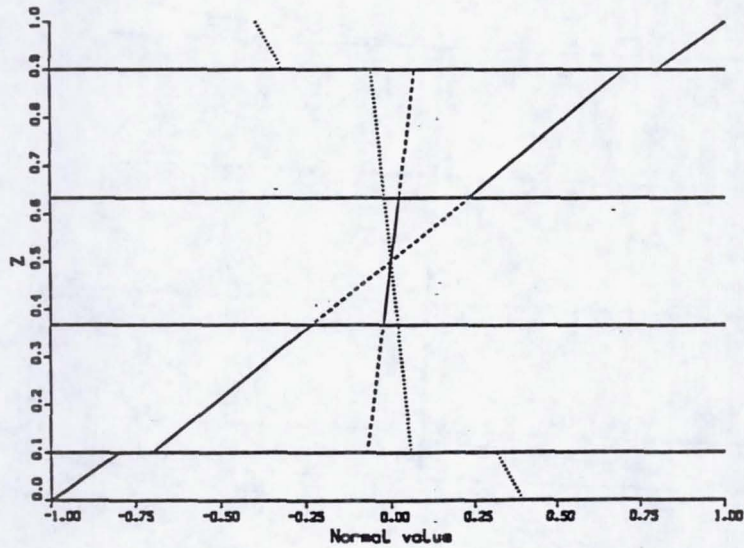


Figure 118: In-plane stresses, mode 1, 5-ply,  $a/h=50$ .

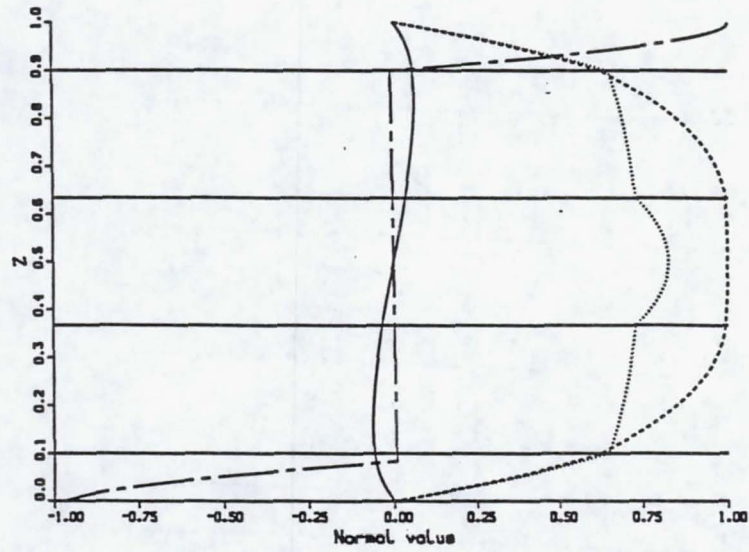


Figure 119: Out-of-plane stresses, mode 1, 5-ply,  $a/h=1$ .

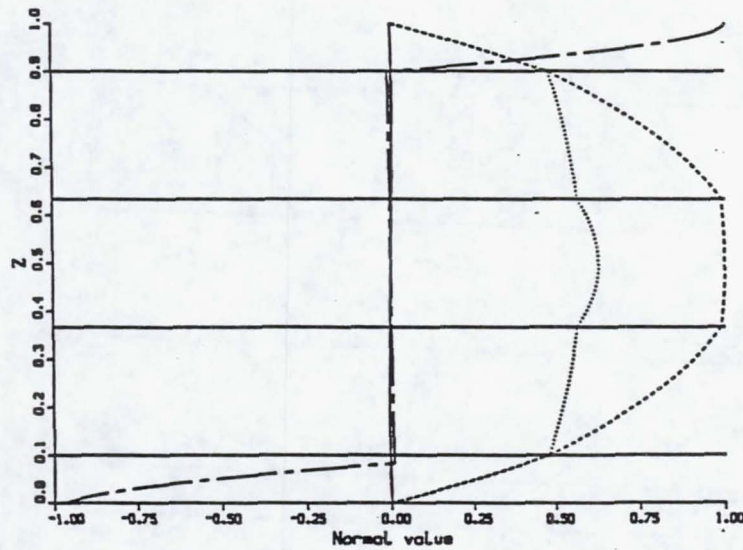


Figure 120: Out-of-plane stresses, mode 1, 5-ply,  $a/h=50$ .

## References

- [1] A. B. Basset, "On The Extension and Flexure of Cylindrical and Spherical Thin Elastic Shells", *Phil. Trans. Royal Soc. (Lond.), ser. A*, 181(6), 1890, pp. 433-480.
- [2] F. B. Hidebrand, E. Reissner and G. B. Thomas, "Notes on The Foundations of The Theory of Small Displacements of Orthotropic Shells", *NACA Tech. Note 1833*, Mar, 1949
- [3] R. D. Mindlin, "Influence of Rotatory Inertia and Shear on Flexural Motions of Isotropic, Elastic Plates", *Journal of Applied Mechanics*, Vol. 18, Mar, 1951, pp. 31-38.
- [4] P. C. Yang, C. H. Norris and Y. Stavsky, "Plastic Wave Propagation in Heterogeneous Plates", *International Journal of Solids Structures*, Vol. 2, 1966, pp. 665-684.
- [5] Errol P. Eer Nisse, "Resonances of One-dimensional Composite Piezoelectric and Elastic Structures", *IEEE Transactions on Sonic and Ultrasonics*. Vol. SU-14, Apr., 1967, pp. 59-67.
- [6] Errol P. Eer Nisse, "Variational Method for Electroelastic Vibration Analysis", *IEEE Transactions on Sonic and Ultrasonics*, Vol. SU-14, No. 4, Oct., 1967, pp. 153-160.
- [7] Richard Holland, "Resonant Properties of Piezoelectric Ceramic Rectangular Parallelepipeds", *Journal of the Acoustical Society of America*, Vol. 43, No. 5, 1968, pp. 988-997.
- [8] S. Srinivas, C. V. Joga Rao, and A. K. Rao, "Some Results From an Exact Analysis of Thick Laminates in Vibration And Buckling", *Journal of Applied Mechanics*, Vol. 37, Sep., 1970, pp. 868-870.
- [9] Henno Allik and Thomas J. R. Hughes, "Finite Element Method for Piezoelectric Vibration", *International Journal for Numerical Methods in Engineering*, Vol. 2, 1970, pp. 151-157.
- [10] M. J. Pagano, "Exact Solutions for Composite Laminates in Cylindrical Bending", *Journal of Composite Materials*, Vol. 3, July, 1969, pp. 398-411.

- [11] M. J. Pagano, "Exact Solutions for Rectangular Bidirectional Composites And Sandwich Plates", *Journal of Composite Materials*, Vol. 4, Jan., 1970, pp. 20-35.
- [12] J. M. Whitney and M. J. Pagano, "Shear Deformation in Heterogeneous Anisotropic Plates", *Journal of Applied Mechanics*, Vol. 37, Dec, 1970, pp. 1031-1036.
- [13] Kenneth E. Pauley, "Analysis of Plane Waves in Infinite Laminated, Piezoelectric Plates", University of California, Los Angeles, Ph.D, Engineering, Mechanics, 1974.
- [14] Yukio Kagawa and Tatsuo Yamabuchi, "Finite Element Approach for a Piezoelectric Circular Rod", *IEEE Transactions on Sonic and Ultrasonics*, Vol. SU-23, No. 6, Nov., 1976, pp. 379-385.
- [15] M. Cengiz Dökmeci, "Theory of Vibrations of Coated, Thermopiezoelectric Laminæ", *Journal of Mathematical Physics*, Vol. 19, Jan., 1978, pp. 109-126.
- [16] H. Kawai, "The Piezoelectricity of Poly(vinylidene Fluoride)", *Jpn. J. Appl. Phys.*, 1979, pp. 957-976.
- [17] J. N. Reddy, "A Penalty Plate-bending Element for The Analysis of Laminated Anisotropic Composite Plates", *International Journal for Numerical Methods in Engineering*, Vol. 15, 1980, pp. 1187-1206.
- [18] Didier Boucher, Michell Lagier, and C. Maerfeld, "Computation of the Vibration Modes for Piezoelectric Array Transducers Using a Mixed Finite Element-Perturbation Method", *IEEE Transactions on Sonic and Ultrasonics*, Vol. SU-28, No. 5, Sep., 1981, pp. 318-330.
- [19] J. N. Reddy, "Dynamic (Transient) Analysis of Layered Anisotropic Composite-Material Plates", *International Journal for Numerical Methods in Engineering*, Vol. 19, 1983, pp. 237-255.
- [20] M. Naillon, R. H. Coursant and F. Besnier, "Analysis of Piezoelectric Structures by a Finite Element Method", *Acta Electronica*, Vol. 25, 1983, pp.341-362
- [21] J. N. Reddy, "A Note on Symmetry Considerations in The Transient Response of Unsymmetrically Laminated Anisotropic Plates", *International Journal for Numerical Methods in Engineering*, Vol. 20, 1984, pp. 175-194.

- [22] J. N. Reddy, "A Simple Higher-order Theory for Laminated Composite Plates", *Journal of Applied Mechanics*, Vol. 51, 1984, pp. 745-752.
- [23] T. Bailey and J. E. Hubbard, "Distributed Piezoelectric Polymer Active Vibration Control of Cantilever Beam", *AIAA Journal of Guidance and Control*, Vol. 8, 1985, pp.606-610.
- [24] H. C. Huang and E. Hinton, "A New Nine Node Degenerated Shell Element with Enhanced Membrane and Shear Interpolation", *International Journal for Numerical Methods in Engineering*, Vol. 22, 1986, pp. 73-92.
- [25] D. F. Ostergaard and T. P. Pawlak, "Three-dimensional Finite Elements for Analyzing Piezoelectric Structures", in *Proceedings of 1986 IEEE Ultrasonics Symposium*, 1986, pp. 639-644.
- [26] G. Dhatt, L. Marcotte and Y. Matte, "A New Triangular Discrete Kirchhoff Plate/Shell Element", *International Journal for Numerical Methods in Engineering*, Vol. 23, 1986, pp. 453-470.
- [27] N. S. Putcha and J. N. Reddy, "Stability And Natural Vibration Analysis of Laminated Plates by Using a Mixed Element Based on a Refined Plate Theory", *Journal of Sound and Vibration*, Vol. 104, 1986, pp. 285-300.
- [28] J. L. Fanson and J. C. Chen, "Structural Control by The Use of Piezoelectric Active Members", *Proceeding of NASA/DOD Control-Structures Interaction Conference*, NASA CP-2447, Part II, 1986.
- [29] J. L. Fanson, "An Experimental Investigation of Vibration Suppression in Large Space Structures Using Positive Position Feedback", Ph.D. Thesis. California Institute of Technology, Pasadena, CA, 1987.
- [30] Edward F. Crawley and Javier de Luis, "Use of Piezoelectric Actuators as Elements of Intelligent Structures", *AIAA Journal*, Vol. 25, No. 10, 1987, pp. 1373-1385.
- [31] Paul Seide and R. A. Chaudhuri, "Triangular Finite Element for Analysis of Thick Laminated Shells", *International Journal for Numerical Methods in Engineering*, Vol. 24, 1987, pp. 1563-1579.



- [32] J. N. Reddy, "A Generalization of Two-dimensional Theories of Laminated Composite Plates", *Communication in Applied Numerical Methods*, Vol. 3, 1987, pp. 113-180.
- [33] Junho Jang and M. Pinsky, "An Assumed Covariant Strain Based 9-node Shell Element", *International Journal for Numerical Methods in Engineering*, Vol. 24, 1987, pp. 2389-2411.
- [34] C. L. Liao, J. N. Reddy and S. P. Engelstad, "A Solid-Shell Transition Element for Geometrically Non-Linear Analysis of Laminated Composite Structures", *International Journal for Numerical Methods in Engineering*, Vol. 26, 1988, pp. 1843-1854.
- [35] M. Cengiz Dökmeçi, "Certain Integral And Differential Type of Variational Principles in Nonlinear Piezoelectricity", *IEEE Transactions on Ultrasonics, Ferroelectrics, and Frequency Control*, Vol. 35, No. 6, Nov., 1988, pp. 775-787.
- [36] T. Belytschko B. L. Wong and H. Stolarski, "Assumed Strain Stabilization Procedure for the 9-node Lagrange Shell Element", *International Journal for Numerical Methods in Engineering*, Vol. 28, 1989, pp. 385-414.
- [37] C. H. Yeom and S. W. Lee, "An Assumed Strain Finite Element Model for Large Deflection Composite Shells", *International Journal for Numerical Methods in Engineering*, Vol. 28, 1989, pp. 1749-1768.
- [38] H. A. Kunkel, S. Locke, and B. Pikeroen, "Finite-Element Analysis of Vibrational Modes in Piezoelectric Ceramic Disks", *IEEE Transactions on Ultrasonics, Ferroelectrics, and Frequency Control*, Vol. 37, No. 4, July, 1990, pp. 316-328.
- [39] C. K. Lee and F. C. Moon, "Laminated Piezopolymer Plates for Torsion And Bending Sensors And Actuators", *Journal of the Acoustical Society of America*, Vol. 85, June, 1989, pp. 2432-2439.
- [40] A. A. Khdeir, "Free Vibration And Buckling of Unsymmetric Cross-Ply Laminated Plates Using a Refined Theory", *Journal of Sound and Vibration*, Vol. 128, 1989, pp. 377-395.
- [41] C. K. Lee, "Theory of Laminated Piezoelectric Plates for The Design of Distributed Sensors/Actuators. Part I : Governing Equations And Reciprocal Relationships", *Journal of the Acoustical Society of America*, Vol. 87, Mar., 1990, pp. 1144-1158.

- [42] H. S. Tzou and M. Gadre, "Theoretical Analysis of a Multi-Layered Thin Shell Coupled With Piezoelectric Shell Actuators for Distributed Vibration Controls", *Journal of Sound and Vibration*, Vol. 132, 1989, pp. 433-450.
- [43] J. N. Reddy, E. J. Barbero and J. L. Teply, "A Plate Bending Element Based on a Generalized Laminate Plate Theory", *International Journal for Numerical Methods in Engineering*, Vol. 28, 1989, pp. 2275-2292.
- [44] J. N. Reddy, E. J. Barbero and J. L. Teply, "An Accurate Determination of Stresses in Thick Laminates Using a Generalized Plate Theory", *International Journal for Numerical Methods in Engineering*, Vol. 29, 1990, pp. 1-14.
- [45] Stefanos Vlachoutsis, "Explicit Integration for Three-Dimensional Degenerated Shell Finite Elements", *International Journal for Numerical Methods in Engineering*, Vol. 29, 1990, pp. 861-880.
- [46] K. S. Surana and R. M. Sorem, "Curved Shell Elements Based on Hierarchical  $p$ -Approximation in the Thickness Direction for Linear Static Analysis of Laminated Composites", *International Journal for Numerical Methods in Engineering*, Vol. 29, 1990, pp. 1393-1420.
- [47] C. K. Lee and F. C. Moon, "Modal Sensors/Actuators", *Journal of Applied Mechanics*, Vol. 57, June, 1990, pp. 434-441.
- [48] M. Cengiz Dökmeci, "Shell Theory for Vibrations of Piezoceramics Under a Bias", *IEEE Transactions on Ultrasonics, Ferroelectrics, and Frequency Control*, Vol. 37, No. 5, Sep., 1990, pp. 369-385.
- [49] H. S. Tzou, "Distributed Sensing And Controls of Flexible Plates And Shells Using Distributed Piezoelectric Elements", *Int. Conference on Coating and Sensors, Journal of Wave-Material Interaction*, Vol. 4, No. 1-3, Jan./Apr./July, 1989, pp. 11-29.
- [50] H. A. Sosa and Y. E. Pak, "Three-dimensional Eigenfunction Analysis of a Crack in a Piezoelectric Material", *International Journal of Solids Structures*, Vol. 26, No. 1, 1990, pp. 1-15.
- [51] H. S. Tzou and C. I. Tseng, "Distributed Piezoelectric Sensor/Actuator Design for Dynamic Measurement/Control of Distributed Parameter Systems : a Piezoelectric

- Finite Element Approach", *Journal of Sound and Vibration*, Vol. 138, 1990, pp. 17-34.
- [52] B. T. Wang and C. A. Rogers, "Laminate Plate Theory for Spatially Distributed Induced Strain Actuators", *Journal of Composite Materials*, Vol. 25, Apr., 1991, pp. 433-452.
- [53] D. H. Robbins and J. N. Reddy, "Analysis of Piezoelectrically Actuated Beams Using a Layer-Wise Displacement Theory", *Computers and Structures*, Vol. 41, No. 2, 1991, pp. 265-279.
- [54] R. Lammering, "The Application of a Finite Shell Element for Composites Containing Piezo-electric Polymers in Vibration Control", *Computers and Structures*, Vol. 41, No. 5, 1991, pp. 1101-1109.
- [55] H. S. Tzou and J. P. Zhong, "Adaptive Piezoelectric Shell Structures : Theory And Experiments", *32nd AIAA SDM Conference, Baltimore, Maryland, Paper No. AIAA-91-1238-CP*, Apr., 8-12, 1991, pp. 2290-2296.
- [56] Y. E. Pak, "Linear Electro-elastic Fracture Mechanics of Piezoelectric Materials", *International Journal of Fracture*, Vol. 54, 1992, pp. 79-100.
- [57] D. K. Shah, W. S. Chan and S. P. Joshi, "Response of Piezoelectric Layer in Composite Laminates Due to Electromechanical Loads", *Paper No. AIAA-91-1238-CP*, 1992, pp. 2918-2923.
- [58] P. R. Heyliger and A. Jilani, "The Free Vibrations of Inhomogeneous Elastic Cylinders and Spheres", *International Journal of Solids Structures*, Vol. 29, No. 22, 1992, pp. 2689-2708.
- [59] P. R. Heyliger, "Discrete-Layer Theories for Active Composite Laminates With Embedded Piezoelectric layers, Final Report", 1992.
- [60] P. R. Heyliger and Stephen Brooks, "Exact Solutions for Laminated Piezoelectric Plates in Cylindrical Bending", Submitted to *ASEM Journal of Applied Mechanics*, Apr, 1992.

- [61] D. H. Robbins and J. N. Reddy, "Modelling of Thick Composites Using a Layerwise Laminate Theory", *International Journal for Numerical Methods in Engineering*, Vol. 36, 1993, pp. 655-677.
- [62] P. R. Heyliger and D. A. Saravanos, "On Discrete-Layer Mechanics for Health-Monitoring Applications in Sensory/Active Composite Laminates", Submitted to *ASEM Journal of Applied Mechanics*.
- [63] W. Voight, *Lehrbuch der Kristallphysik*, 2nd edition, B. G. Teubner, Leipzig, 1928.
- [64] W. P. Mason, *Piezoelectric Crystals and Their Applications to Ultrasonics*, D. Van Nostrand Co., New York, 1950.
- [65] S. Timoshenko and S. Woinowsky-Krieger, *Theory of Plates and Shells*, 2nd edition, McGraw-Hill, New York, 1959.
- [66] W. G. Cady, *Piezoelectricity*, rev. ed., Vols I and II, Dover Publications, New York, 1964.
- [67] H. F. Tiersten, *Linear Piezoelectric Plate Vibrations*, Plenum, New York, 1969.
- [68] N. Y. Nye, *Physical Properties of Crystal : Their Representation by Tensors and Matrices*, Oxford University Press, Oxford, United Kingdom, 1972.
- [69] O. C. Zienkiewicz, *The Finite Element Method*, Third edition, McGraw-Hill, 1977.
- [70] Klaus-Jürgen Bathe, *Finite Element Procedures in Engineering Analysis*.
- [71] V. E. Bottom, *Introduction to Quartz Crystal Unit Design*, Von Nostrand Reinhold Co., 1982.
- [72] J. Zelenka, *Piezoelectric Resonators and Their Applications*, Elsevier, 1984.
- [73] J. N. Reddy, *Applied Functional Analysis and Variational Methods in Engineering*, McGraw-Hill, New York, 1986.
- [74] Thomas J.R. Hughes, *The Finite Element Method*, Prentice-Hall International, 1987.
- [75] David K. Cheng, *Field and Wave Electromagnetics*, Addison-Wesley Publishing Company, 1989.

- [76] A. T. Jones, "Exact natural frequencies for cross-ply laminates," *Journal of Composite Materials* **4**, 476-491 (1970).
- [77] A. T. Jones, "Exact natural frequencies and modal functions for a thick off-axis lamina," *Journal of Composite Materials* **5**, 504-520 (1971).
- [78] S. Srinivas, C. V. Joga Rao, and A. K. Rao, "Some results from an exact analysis of thick laminates in vibration and buckling," *ASME Journal of Applied Mechanics* **37**, 868-870 (1970).
- [79] S. Srinivas and A. K. Rao, "Bending, vibration and buckling of simply supported thick orthotropic rectangular plates and laminates," *International Journal of Solids and Structures* **6**, 1463-1481 (1970).
- [80] H. F. Tiersten, *Linear Piezoelectric Plate Vibrations* (Plenum, New York, 1969).
- [81] K. P. Pauley, *Analysis of Plane Waves in Infinite, Laminated, Piezoelectric Plates*, Ph.D. Dissertation, University of California at Los Angeles (1974).
- [82] D. Ricketts, "Transverse Vibrations of Composite Piezoelectric Polymer Plates," *Journal of the Acoustical Society of America* **77**, 1939-1945 (1985).
- [83] D. Ricketts, "The Frequency of Flexural Vibrations of Completely Free Composite Piezoelectric Polymer Plates," *Journal of the Acoustical Society of America* **80**, 723-726 (1986).
- [84] C. K. Lee, "Theory of Laminated Piezoelectric Plates for the Design of Distributed Sensors and Actuators. I. Governing Equations and Reciprocal Relationships," *Journal of the Acoustical Society of America* **87**, 1144-1158 (1990).
- [85] Y. K. Yong, J. T. Stewart, and A. Ballato, "A Laminated Plate-Theory for High-Frequency, Piezoelectric Thin-Film Resonators," *Journal of Applied Physics* **74**, 3028-3046 (1993).
- [86] Pagano, N. J., 1970, "Exact Solutions for Rectangular Bidirectional Composites and Sandwich Plates", *Journal of Composite Materials* **4**, 20-34.
- [87] P. R. Heyliger and S. P. Brooks, "Exact solutions for laminated piezoelectric plates in cylindrical bending", in review.

- [88] R. M. Jones, *Mechanics of Composite Materials*, McGraw-Hill, New York (1975).
- [89] P. R. Heyliger and D. A. Saravanos, "On discrete-layer mechanics for health-monitoring applications in sensory/active composite laminates", in *Proceedings of ASME Winter Annual Meeting*, New Orleans, LA, Nov. 28-Dec. 3 (1993).

## APPENDIX

Property	1	2	3
$E_1$ (GPa)	237.0	81.3	132.38
$E_2$	23.2	81.3	10.756
$E_3$	10.5	64.5	10.756
$\nu_{12}$	0.154	0.329	0.24
$\nu_{13}$	0.178	0.432	0.24
$\nu_{23}$	0.177	0.432	0.49
$G_{44}$	2.15	25.6	3.606
$G_{55}$	4.4	25.6	5.6537
$G_{66}$	6.43	30.6	5.6537
$e_{24}$ ( $C/m^2$ )	-0.01	12.72	0
$e_{31}$	-0.13	-5.20	0
$e_{32}$	-0.14	-5.20	0
$e_{33}$	-0.28	15.08	0
$\frac{\epsilon_{11}}{\epsilon_0}$	12.5	1475	3.5
$\frac{\epsilon_{22}}{\epsilon_0}$	11.98	1475	3.0
$\frac{\epsilon_{33}}{\epsilon_0}$	11.98	1300	3.0

Table A1. Elastic, piezoelectric, and dielectric properties of piezoelectric materials.

Definitions of coefficients used in exact solution:

$$A = -C_{55} C_{44} C_{33} \epsilon_{33} - C_{55} C_{44} e_{33}^2 \quad (291)$$

$$B = A_{11} C_{44} e_{33}^2 + A_{11} C_{44} C_{33} \epsilon_{33} - 2 A_{13} C_{44} A_{14} e_{33} + C_{55} A_{24}^2 C_{33} - C_{55} C_{44} C_{33} A_{44} - (292)$$

$$A_{13}^2 C_{44} \epsilon_{33} + 2 C_{55} C_{44} A_{34} e_{33} + C_{55} A_{22} e_{33}^2 + C_{55} C_{44} A_{33} \epsilon_{33} + C_{55} A_{22} C_{33} \epsilon_{33} +$$

$$A_{14}^2 C_{44} C_{33} - 2 C_{55} A_{23} A_{24} e_{33} - C_{55} A_{23}^2 \epsilon_{33}$$

$$C = -2 A_{12} A_{23} A_{13} \epsilon_{33} - A_{11} A_{22} e_{33}^2 - C_{55} A_{23}^2 A_{44} - C_{55} A_{24}^2 A_{33} + C_{55} C_{44} A_{33} A_{44} - (293)$$

$$A_{12}^2 e_{33}^2 - 2 C_{55} A_{22} A_{34} e_{33} - C_{55} C_{44} A_{34}^2 + 2 C_{55} A_{23} A_{24} A_{34} - A_{11} A_{22} C_{33} \epsilon_{33} -$$

$$A_{11} C_{44} A_{33} \epsilon_{33} + A_{11} C_{44} C_{33} A_{44} + C_{55} A_{22} C_{33} A_{44} - C_{55} A_{22} A_{33} \epsilon_{33} - A_{13}^2 C_{44} A_{44} +$$

$$A_{12}^2 C_{33} \epsilon_{33} + 2 A_{12} A_{24} A_{14} C_{33} - 2 A_{12} A_{24} A_{13} e_{33} - A_{11} A_{24}^2 C_{33} - 2 A_{12} A_{23} A_{14} e_{33} +$$

$$2 A_{11} A_{23} A_{24} e_{33} + A_{13}^2 A_{24}^2 + 2 A_{13} C_{44} A_{14} A_{34} - 2 A_{11} C_{44} A_{34} e_{33} + 2 A_{13} A_{22} A_{14} e_{33} +$$

$$A_{14}^2 A_{23}^2 + A_{13}^2 A_{22} \epsilon_{33} + A_{11} A_{23}^2 \epsilon_{33} - 2 A_{13} A_{24} A_{14} A_{23} - A_{14}^2 A_{22} C_{33} - A_{14}^2 C_{44} A_{33}$$

$$D = -A_{11} C_{44} A_{33} A_{44} - A_{11} A_{22} C_{33} A_{44} + 2 A_{11} A_{22} A_{34} e_{33} + A_{11} A_{22} A_{33} \epsilon_{33} + C_{55} A_{22} A_{34}^2 - (294)$$

$$C_{55} A_{22} A_{33} A_{44} + A_{13}^2 A_{22} A_{44} - 2 A_{12} A_{24} A_{14} A_{33} + 2 A_{12} A_{24} A_{13} A_{34} + 2 A_{12} A_{23} A_{14} A_{34} -$$

$$2 A_{12} A_{23} A_{13} A_{44} - 2 A_{12}^2 A_{34} e_{33} - A_{12}^2 A_{33} \epsilon_{33} + A_{12}^2 C_{33} A_{44} + A_{11} A_{24}^2 A_{33} -$$

$$2 A_{11} A_{23} A_{24} A_{34} + A_{11} A_{23}^2 A_{44} + A_{11} C_{44} A_{34}^2 + A_{14}^2 A_{22} A_{33} - 2 A_{13} A_{22} A_{14} A_{34}$$

$$E = A_{11} A_{22} A_{33} A_{44} + A_{12}^2 A_{34}^2 - A_{11} A_{22} A_{34}^2 - A_{12}^2 A_{33} A_{44} \quad (295)$$

$$D_1 = C_{44} e_{33}^2 + C_{44} C_{33} \epsilon_{33} \quad (296)$$

$$D_2 = -C_{44} A_{33} \epsilon_{33} + C_{44} C_{33} A_{44} - 2 C_{44} A_{34} e_{33} + 2 A_{23} A_{24} e_{33} - (297)$$

$$A_{22} e_{33}^2 + A_{23}^2 \epsilon_{33} - A_{22} C_{33} \epsilon_{33} - A_{24}^2 C_{33}$$



$$D_3 = A_{22} A_{33} \epsilon_{33} - A_{22} C_{33} A_{44} - 2 A_{23} A_{24} A_{34} + 2 A_{22} A_{34} e_{33} + \quad (298)$$

$$A_{23}^2 A_{44} - C_{44} A_{33} A_{44} + A_{24}^2 A_{33} + C_{44} A_{34}^2$$

$$D_4 = A_{22} A_{33} A_{44} - A_{22} A_{34}^2 \quad (299)$$

$$f_{11} = A_{12} (C_{33} \epsilon_{33} + e_{33}^2) - (A_{23} \epsilon_{33} + A_{24} e_{33}) A_{13} + (-A_{23} e_{33} + A_{24} C_{33}) A_{14} \quad (300)$$

$$f_{12} = -A_{12} (A_{33} \epsilon_{33} - C_{33} A_{44} + 2 A_{34} e_{33}) - (A_{23} A_{44} - A_{24} A_{34}) A_{13} + (A_{23} A_{34} - A_{24} A_{33}) A_{14} \quad (301)$$

$$f_{13} = -A_{12} (A_{33} A_{44} - A_{34}^2) \quad (302)$$

$$f_{21} = -C_{44} \epsilon_{33} A_{13} - C_{44} e_{33} A_{14} \quad (303)$$

$$f_{22} = (A_{22} \epsilon_{33} - C_{44} A_{44} + A_{24}^2) A_{13} - A_{12} (A_{23} \epsilon_{33} + A_{24} e_{33}) + \quad (304)$$

$$(A_{22} e_{33} + C_{44} A_{34} - A_{23} A_{24}) A_{14}$$

$$f_{23} = -A_{12} (A_{23} A_{44} - A_{24} A_{34}) - A_{22} A_{34} A_{14} + A_{22} A_{44} A_{13} \quad (305)$$

$$f_{31} = -A_{13} C_{44} e_{33} + A_{14} C_{44} C_{33} \quad (306)$$

$$f_{32} = A_{13} (A_{22} e_{33} + C_{44} A_{34} - A_{23} A_{24}) + A_{12} (-A_{23} e_{33} + A_{24} C_{33}) + \quad (307)$$

$$A_{14} (-A_{22} C_{33} - C_{44} A_{33} + A_{23}^2)$$

$$f_{33} = A_{12} (A_{23} A_{34} - A_{24} A_{33}) + A_{14} A_{22} A_{33} - A_{13} A_{22} A_{34} \quad (308)$$

# REPORT DOCUMENTATION PAGE

*Form Approved*  
OMB No. 0704-0188

Public reporting burden for this collection of information is estimated to average 1 hour per response, including the time for reviewing instructions, searching existing data sources, gathering and maintaining the data needed, and completing and reviewing the collection of information. Send comments regarding this burden estimate or any other aspect of this collection of information, including suggestions for reducing this burden, to Washington Headquarters Services, Directorate for Information Operations and Reports, 1215 Jefferson Davis Highway, Suite 1204, Arlington, VA 22202-4302, and to the Office of Management and Budget, Paperwork Reduction Project (0704-0188), Washington, DC 20503.

1. AGENCY USE ONLY (Leave blank)	2. REPORT DATE October 1994	3. REPORT TYPE AND DATES COVERED Final Contractor Report	
4. TITLE AND SUBTITLE Discrete-Layer Piezoelectric Plate and Shell Models for Active Tip-Clearance Control		5. FUNDING NUMBERS WU-505-63-5B G-NAG3-1520	
6. AUTHOR(S) P.R. Heyliger, G. Ramirez, and K.C. Pei		8. PERFORMING ORGANIZATION REPORT NUMBER E-9133	
7. PERFORMING ORGANIZATION NAME(S) AND ADDRESS(ES) Colorado State University Department of Civil Engineering Fort Collins, Colorado 80523		10. SPONSORING/MONITORING AGENCY REPORT NUMBER NASA CR-195383	
9. SPONSORING/MONITORING AGENCY NAME(S) AND ADDRESS(ES) National Aeronautics and Space Administration Lewis Research Center Cleveland, Ohio 44135-3191		11. SUPPLEMENTARY NOTES Project Manager, Dale A. Hopkins, Structures Division, NASA Lewis Research Center, organization code 5210, (216) 433-3260	
12a. DISTRIBUTION/AVAILABILITY STATEMENT Unclassified - Unlimited Subject Category 39		12b. DISTRIBUTION CODE	
13. ABSTRACT (Maximum 200 words) The objectives of this work were to develop computational tools for the analysis of active-sensory composite structures with added or embedded piezoelectric layers. The targeted application for this class of smart composite laminates and the analytical development is the accomplishment of active tip-clearance control in turbomachinery components. Two distinct theories and analytical models were developed and explored under this contract: (1) a discrete-layer plate theory and corresponding computational models, and (2) a three-dimensional general discrete-layer element generated in curvilinear coordinates for modeling laminated composite piezoelectric shells. Both models were developed from the complete electromechanical constitutive relations of piezoelectric materials, and incorporate both displacements and potentials as state variables. This report describes the development and results of these models. The discrete-layer theories imply that the displacement field and electrostatic potential through-the-thickness of the laminate are described over an individual layer rather than as a smeared function over the thickness of the entire plate or shell thickness. This is especially crucial for composites with embedded piezoelectric layers, as the actuating and sensing elements within these layers are poorly represented by effective or smeared properties. Linear Lagrange interpolation polynomials were used to describe the through-the-thickness laminate behavior. Both analytic and finite element approximations were used in the plane or surface of the structure. In this context, theoretical developments are presented for the discrete-layer plate theory, the discrete-layer shell theory, and the formulation of an exact solution for simply-supported piezoelectric plates. Finally, evaluations and results from a number of separate examples are presented for the static and dynamic analysis of the plate geometry. Comparisons between the different approaches are provided when possible, and initial conclusions regarding the accuracy and limitations of these models are given.			
14. SUBJECT TERMS Laminates; Composite structures; Piezoelectricity; Smart materials; Smart structures; Finite element method; Plates; Shells; Actuators; Sensors		15. NUMBER OF PAGES 169	
17. SECURITY CLASSIFICATION OF REPORT Unclassified		16. PRICE CODE A08	
18. SECURITY CLASSIFICATION OF THIS PAGE Unclassified	19. SECURITY CLASSIFICATION OF ABSTRACT Unclassified	20. LIMITATION OF ABSTRACT	